SOME IMPULSIVE MATHEMATICAL MODELS IN PEST MANAGEMENT

Ph.D. THESIS

by

ANJU GOEL

DEPARTMENT OF MATHEMATICS
INDIAN INSTITUTE OF TECHNOLOGY ROORKEE
ROORKEE-247667 (INDIA)
SEPTEMBER, 2018

SOME IMPULSIVE MATHEMATICAL MODELS IN PEST MANAGEMENT

A THESIS

Submitted in partial fulfilment of the requirements for the award of the degree

of

DOCTOR OF PHILOSOPHY

in

MATHEMATICS

by

ANJU GOEL

DEPARTMENT OF MATHEMATICS
INDIAN INSTITUTE OF TECHNOLOGY ROORKEE
ROORKEE-247667 (INDIA)
SEPTEMBER, 2018

INDIAN INSTITUTE OF TECHNOLOGY ROORKEE
ROORKEE

CANDIDATE'S DECLARATION

I hereby certify that the work which is being presented in the thesis entitled "**SOME IMPULSIVE MATHEMATICAL MODELS IN PEST MANAGEMENT**" in partial fulfilment of the requirements for the award of the Degree of Doctor of Philosophy and submitted in the Department of Mathematics of the Indian Institute of Technology Roorkee, Roorkee is an authentic record of my own work carried out during a period from January, 2013 to June, 2018 under the supervision of Dr. Sunita Gakkhar, Professor, Department of Mathematics, Indian Institute of Technology Roorkee, Roorkee.

The matter presented in this thesis has not been submitted by me for the award of any other degree of this or any other Institution.

(ANJU GOEL)

This is to certify that the above statement made by the candidate is correct to the best of my knowledge.

(SUNITA GAKKHAR**)**
Supervisor

The Ph.D. Viva-Voce Examination of **Ms. Anju Goel,** Research Scholar, has been held on .....

Chairman, SRC **Signature of External Examiner**

This is to certify that the student has made all the corrections in the thesis.

Signature of Supervisor **Head of the Department**
Dated:.....

Dedicated

to

My Husband (ASHWANI GARG)

&

My Son (ARNAV GARG)

Abstract

In this thesis, attempts have been made to investigate the dynamics of pest control models considering various pest management tactics with birth pulses. The mathematical models in pest management are the system of differential equation with impulsive conditions. These impulsive effects may occur due to the instantaneous killing of pest using pesticides, releasing natural enemies and harvesting pest. Dynamical behaviors of some impulsive models with time-dependent strategies as well as state-dependent strategies have been explored. Emphasis is given to exploring the factors that are responsible for pest eradication. Due to impulses in pest control systems underlying equations have complex dynamical behavior, including periodic solutions, quasi-periodic, chaotic behavior etc.. The numerical simulations are carried out to explore the dynamic complexity in impulsive models. The efforts have been made to interpret mathematical results and to explore the biological relevance of these results.

Chapter 1 includes brief introduction including basic concepts for pest control, mathematical tools, literature survey and summary of the thesis. The chapters 2, 3 and 4 are devoted to the control of pest using single pest management strategy. The next three chapters incorporate the Integrated Pest Management approach to control the pest population. The effect of pesticides on the environment is considered in chapter 8. A state dependent control is discussed in chapter 9. The conclusions and future scope are presented in the last chapter.

In particular, the second chapter deals with the dynamics of an impulsive stage-structured pest control model. In this model, birth pulses occur at regular intervals to release immature pest. The Ricker type birth function is assumed. Pest population is controlled by periodic spray killing mature as well as immature pest instantaneously. This is synchronized with birth pulses. The discrete dynamical system determined

by the stroboscopic map is analyzed. The threshold condition for pest eradication is established. It is found that if the birth rate parameter is below the critical level, then the pest can be effectively controlled. Finally, numerical simulations depict the complex dynamics of the model.

In chapter 3, birth pulse and chemical spray are no more synchronous. The pesticide is sprayed periodically before the birth at the fixed time. The effect of pesticide spray timing on threshold condition for pest eradication is studied. The pest will extinct when the time of pesticide spray exceeds the critical value. The maximum reduction in immature and mature densities will occur near the birth pulse when the basic reproduction number exceeds one. Further, asynchronous pulses reduce the complexity of the system.

A pest control model using pesticides having residual effects is discussed in chapter 4. The effect of residual pesticide can be described by kill function. Birth pulse and chemical spray are assumed to be asynchronous. The basic reproduction number for pest eradication has been computed. The effects of various model parameters on the threshold condition are investigated. It is found that the killing efficiency rate reduces the threshold below unity which is required for effective pest control. Further, the decay rate of the pesticide enhances the threshold and pest outbreak may occur. Finally, numerical simulations depict the complex dynamical behaviors.

In chapter 5, a model is developed considering the continuous mechanical effort (harvesting) to control the immature pest while mature pest is controlled impulsively by the pesticide. It is found that the pest cannot be controlled successfully in the absence of harvesting effort. The combination of harvesting effort and pesticide is needed for successful pest control. The use of pesticides can be reduced by incorporating mechanical control. It is found that when mature pest density goes beyond a critical level, then the pest-free state will be stable. Further, the rate reduces the complexity of the system with an increase in immature pest mortality rate. Due to asynchronous pulses, the harvesting reduces the complexity of the system. The chances of pest-eradication also increase with less toxic pesticides.

In chapter 6, an impulsive model with three pulses is considered where the mechanical, chemical control and birth pulse occur at three different fixed times. The increase

in time delay of chemical control reduces the mature pest density as well as the threshold for pest eradication. The threshold value of harvesting effort has been obtained for the stable pest-free state. The critical level of pulse period is obtained to control the pest population. Numerical simulations have been performed to show the complex dynamical behavior, including period-doubling bifurcation and chaotic dynamics. The Lyapunov exponent and Lyapunov dimension are computed to establish the pest outbreak in the form of chaotic attractor.

In chapter 7, integrated pest management approach comprising of the impulsive chemical as well as mechanical control is considered. The residual effect of pesticide with the delayed response is assumed. The harvesting effort and birth pulse occur asynchronously. The basic reproduction number has been computed. The bifurcation diagram with respect to birth rate has been plotted to show the stability regions of the pest-free state and interior fixed point. The harvesting effort of immature and mature pest reduces the threshold condition and thereby enhancing the stability of pest-free state. Numerical simulations reveal that increasing the delayed response may stabilize the pest-free state. It is found that the shorter delayed response rate is not sufficient for pest eradication. The combination of time delay in harvesting and the delayed response rate is required to control the pest population.

Chapter 8 investigates the toxic effects of pesticides on the environment. The sufficiently small toxicant removal from the environment may eradicate the pest successfully. Otherwise, the pest will occur in regular/irregular periodic manner. For the lower birth rate pest can be eradicated completely. Similarly, the pest outbreak will occur when toxin input into the environment is sufficiently small.

A state-dependent combined strategy for biological and chemical control is discussed in chapter 9. The Poincare map is used to explore the system dynamics. Sufficient conditions for the existence and stability of natural enemy-free and positive period-1 solutions are obtained. The positive period-1 solution bifurcates from the semi-trivial solution through a fold bifurcation. Complex dynamical behavior, including chaos is obtained. It is also observed that if more natural enemies are released, the complexity of the system increase, but the pest population will remain below the threshold level.

Acknowledgements

It is a delight to convey my gratitude, too few of the many sources of inspiration for me, to all the people who have supported me during my Ph.D. journey. Without their encouragement and constant motivation, the research in this thesis would have taken far longer to complete.

I feel it's true that:
"And, when you want something, all the universe conspires in helping you to achieve it."

I feel privileged to express my sincere regards and gratitude to my doctoral supervisor Dr. Sunita Gakkhar, Professor, Department of Mathematics, Indian Institute of Technology Roorkee for their valuable guidance throughout my research work. You have been a constant inspiration and a mentor to me. Without your valuable expertise, the idea of this research would not have become a reality. The critical comments, rendered by her during the discussion are deeply appreciated. She is helping me positively at any time without any reservations. Your advice on research as well as on my career has been precious. I hope her help will be with me all the time in the future. I would like to thank you for your continuous guidance that helped me grow both as a researcher as well as an academician.

I would also like to express my gratitude towards to Prof. N. Sukavanam, Head, Department of Mathematics, IIT Roorkee, Prof. Tanuja Srivastava, DRC Chairman, Prof. Roshan Lal, Dr. Sandip Banerjee and Prof. Bikas Mohanty for their brilliant suggestions and feedback during my research. I also thank staff members of the department for providing me the cooperation and infrastructural support for the completion of this research. My sincere thanks to the administration of Mahatma Gandhi Central Library, IIT-Roorkee for providing adequate journal sources that served a potential

vehicle in high-quality academic research.

I owe an overwhelming debt of gratitude to my parents Sh. Krishan Goel and Smt. Suman Goel, who cooperated with me at every stage and boosted my confidence and morale during the hot and cold situations. It is because of their love and encouragement, that I have been able to enjoy the educational opportunities. I would like to pay my hearty gratitude to my brothers Naveen Goel and Deepak Goel for bolstering their support and encouragement throughout my journey of doctoral education.

My special, sincere, heartfelt and indebtedness is due to I express my heartfelt thanks and deepest regards to my husband Ashwani Garg, without his support completion of my research work has been impossible. He supported me unconditionally all throughout my research. I owe my lovely, thanks to my loving son Arnav Garg. (I know you pray for me all the time. Thanks a Lot.) They understand the extreme hot and cold environment that I face in Roorkee.

Special thanks to my friends whose regular interactions, contact and encouragement helped me stay resilient and persistent during the hard times. I also extend my sincere thanks to Ridhi, Shweta, Nidhi, Teekam, Shail Dinkar and all respondents for their timely help and the moral support. My heartfelt thanks to everybody who have helped me directly or indirectly, for the successful accomplishment of the work.

Above all, I express my profound gratitude to the Almighty for all his grace and light which tilled in me the faith, strength, and courage to accomplish my goals and providing me the opportunity to pursue higher studies.

I gratefully acknowledge the financial support provided to me by *Ministry of Human Resources and Development (MHRD), India* to carry out this research.

With profound gratitude, love, and devotion, I dedicate this thesis to my Son (ARNAV GARG).

Roorkee (Anju Goel)

September , 2018

Table of Contents

List of Symbols

a :	Transformation rate from immature to mature class
b :	Birth rate
d :	Mortality rate of the total pest population
m :	Set of all non-negative integer numbers
p :	Birth rate for Beverton-Holt function
t :	Time
x :	Population density of juvenile/immature pest
y :	Population density of adult/mature pest
N :	Total population density of the pest
T :	Pulse period
$\Re$:	Real line
$\Re^n$:	n-dimensional Euclidian space over $\Re$
$\Re_+$:	Set of all non negative real numbers
C_+ :	Set of positive continuous functions
$C([a,b];\Re^n)$:	Space of continuous functions from $[a,b]$ to $\Re^n$
$C^\infty(X)$:	Set of all infinitely differentiable continuous functions X
$A(N)$:	Maturation rate function
$B(N)$:	Birth rate function
$B_i(N)$:	Birth rate functions
$D_i(N)$:	Mortality rate functions for immatrue/mature pest
R_0 :	Basic reproduction number

List of Symbols in Individual Chapters

Chapter 2

k :	Killing rate of juvenile/immature pest due to pesticide spray
T :	Time at which new births and chemical spray synchronize
d_1 :	Mortality rate of the juvenile/immature pest
d_2 :	Mortality rate of the adult/mature pest
T_1 :	Time of new births occurrence at m^{th} pulse
T_2 :	Time of pesticide spray at m^{th} pulse
μ :	Killing rate of adult/mature pest species due to pesticide spray

Chapter 3–4

d :	Mortality rate of the immature and mature pest population
lT :	Time of pesticide spray
T :	Time at which new births occur
α :	Killing rate of juvenile/immature pest species due to pesticide spray
β :	Killing rate of adult/mature pest species due to pesticide spray
a_1 :	Decay rate due to residual effect of chemicals
m_1 :	Killing efficiency rate due to residual effect of chemicals

Chapter 5

d : Mortality rate of the immature/mature pest

E : Killing rate of juvenile/mature pest species due to mechanical control

μ : Killing rate of adult/mature pest species due to pesticide

d_1 : Mortality rate of the juvenile/immature pest

d_2 : Mortality rate of the adult/mature pest

l_rT : Time of pesticide application

β_1 : Killing rate of juvenile/immature pest species due to pesticide spray

β_2 : Killing rate of adult/mature pest species due to pesticide spray

Chapter 6

d : Mortality rate of the immature/mature pest population

E : Harvesting effort for juvenile/immature pest species

α : Killing rate of adult/mature pest species due to pesticide

τ_1 : Time delay in mechanical control applications

τ_2 : Time delay in chemical control applications

τ_{m1} : Time of mechanical control applications

τ_{m2} : Time of chemical control applications

Chapter 7

d : Mortality rate of the immature and mature pest

a_1 : Decay rate

c_1 : Delayed response rate

k_1 : Kill function for immature pest

k_2 : Kill function for mature pest

m_1 : Killing efficiency rate

E_1 : Harvesting effort for juvenile/immature pest

E_2 : Harvesting effort for adult/mature pest

τ_3 : Time delay in harvesting

τ_m : Mechanical control timing

Chapter 8

c : Depuration rate of the toxicant from the environment

d : Mortality rate of the pest

g : Excretion rate of the toxicant from the pest

h : Depletion rate of the toxicant from the environment

k : Absorbing rate of the toxicant by the pest from the environment

r : Decline in growth rate associated with the uptake of toxicant

x : Population density of the pest

T : Period of the constant input of the toxicant

E : Harvesting effort

μ : Toxicant input amount in the environment

C_0 : Concentration of toxicant in pest

C_E : Concentration of toxicant in the environment

Chapter 9

a : Per capita rate of predation of natural enemy

d : Mortality rate of natural enemy

k : Half saturation constant

l : Threshold level at which control measures are applied

r : Conversion rate of pest into natural enemy

x : Population density of pest

y : Population density of natural enemy

α : Killing rate of pest due to pesticide

β : Killing rate of natural enemy due to pesticide

μ : Release of natural enemy

τ : Delay or lag parameter

List of Figures

List of Tables

Chapter 1

Introduction

1.1 General Introduction

Over the last few decades, one of the major challenges of the farmers in the agricultural field is controlling the pest. The apparently uncertain behavior of the pest may cause serious ecological and economic problems for the farmers. The pest attacks the crop and reduces the agricultural crop production since early civilization [181, 182]. The main motives of the farmers are to minimize the losses due to the pest by the most economical means and with the least impact on the environment [228]. In this context, the use of mathematical models is particularly significant. Mathematical models are applied in all scenarios of the real world [1, 15, 22, 27, 32, 34, 35, 37, 47, 48, 49, 72, 106, 108, 110, 111, 112, 122, 192, 193, 199, 212]. Mathematical modeling of pest control models has a very long history and they emphasizes on preventing pest damage [147, 214, 240]. Mathematical models can give direction to understand the implementation of different pest control mechanism [81, 190]. The main aim of the pest control modeling is to understand the life cycle of the pest, to determine the pest control methods and to predict the effectiveness of control strategies that can help in reducing pest outbreak [216, 227]. Usually, farmers implemented two schemes to prevent pest damage:

- To implement control at a fixed time for pest eradication [45, 154].
- To implement measures only when the amount of pests reaches a critical level and reduce the pest below that level not to extinct the pest [156, 169].

Most of the pest control models focus on various aspects such as the amount of the pest population killed to avoid economic damage, reduce the use of the pesticide and fraction of releasing natural enemies for pest control as well as reducing the use of pesticides. In this thesis, stage-structured mathematical models are used with single control tactic and the combination of control tactic. A system of impulsive differential equations represents the mathematical representation of pest control problem. In this, impulsive reduction in the pest population occurs after poisoning/trapping.

The aim of the present work is to study the dynamical behavior of some pest control models in which various control methods are used. The attempts are made to explore different mechanisms that may eradicate the pest population. The stability of dynamical models has been investigated and bifurcation analysis has been carried out. Emphasis is given to provide the threshold for pest elimination or keeping it below that level.

In the following sections, the brief discussion about the basic concepts, methods, and tools related to the work are described.

1.1.1 Pest Management

Pest species have been defined as unwanted organisms that disturbs human activity. Pests create a nuisance, spread disease to people, animals, and plants. It is judged by man to cause harm to himself, his crops, animals or his property. Pest includes insects, rodents, bacteria, and plants. In agricultural field, an insect may be classified as a pest. Pest cause damage directly to the products, e.g. codling moth larval damage to apples. It is well known that a variety of pest species pose a serious health risk to humans and pets, as well as causing great damage to property and crops. If the damage to crops by the pest is sufficient to reduce the yield by an amount then it is unacceptable to the farmer. Controlling insects and other arthropods are complex. Some attempts to control or manage the harm caused by insects has a long and varied history. Pest management practices which in turn will provide some ideas (economic, social and technical) to be acting in the future. Such pest control often involves chemical control. There are different approaches to get rid of agricultural pests [20, 21, 206].

- **Cultural Control** The goal of cultural control is to suppress pest problems by

minimizing the resources for their survival (water, shelter, food). More than hundred years ago, cultural methods started with the use of chalks, wood dash and neem leaves etc.. Further, tobacco extract spray and powder of chrysanthemum flowers was used to keep away from pests [88].

- **Mechanical Control** Mechanical control involves the use of machines, devices and physical methods to control pests. Traps, screens, barriers, fences, etc. are used to prevent pest activity or remove pests from the area.

- **Chemical Control** The pesticide was initially viewed as a miraculous way of controlling the pest. This is an important method to get rid of the pest. Insecticides are useful because they quickly kill a significant proportion of an insect population. Chemical control relies mainly on the use of synthetic pesticides to suppress pests. But sometimes chemical control provides an only feasible method for preventing economic loss. There are many deleterious effects associated with the use of chemicals that need to be reduced or eliminated. Pesticide pollution is also recognized as a major health hazard to human as well as to the environment. The chemicals adversely affect many other species, including the natural enemies of pests [153].

- **Biological Control** Biological control is the reduction in pest populations by other living organisms, often called natural enemies or beneficial species. Virtually all pests have some natural enemies. The key to successful biological control is to identify the pest and its natural enemy. The density of natural enemy and its times of release is critical to maintain the pest below economic injury levels. For example, Mynah bird for the control of locusts (Mauritius, 1762) and Vedalia beetle for cottony cushion scale on citrus (USA, 1889) were used to control pest population. Biological products often contain the bacterium Bacillus thuringiensis, viruses, fungi, or parasitoids. One of the first successful cases of biological control in greenhouses was the use of the parasitoid Encarsia Formosa against the greenhouse whitefly Trialeurodes vaporariorum on tomatoes and cucumbers [68, 227, 228].

1.1.2 Pest Management Goals

There are many tactics which are effective for pest control. Single or combination of tactics will give pesticide applications the best strategy for a specific goal. Prevention, suppression, and eradication are three approaches to maintain pest population below the economic injury level.

Prevention Prevention includes planting weeds, disease-free seeds. growing varieties of plant resistance to disease or insects. Sometimes, cultural controls can also use to prevent weedy plants from seeding. Pesticides and choosing harvesting times are sometimes used for pest prevention.

Suppression Suppression pest control methods are used to reduce pest population levels. The main aim of choosing method is not to eliminate all pests, but reduce their populations to a point below the economic injury level.

Eradication Eradication is the total elimination of a pest. The eradication may be very expensive over larger areas and it will be less successful.

1.1.3 Integrated Pest Management

The concept of integrates pest management(IPM) was introduced in the late 1950 [207]. It was widely practised during the 1970 and 1980 and used several tactics such as biological control, crop rotation, harvesting, and pesticide spray, etc. to reduce pest populations below economic levels [58, 224, 225, 227, 228]. Integrated pest management is a long-term, low-cost strategy that uses a combination of biological, cultural and chemical tactics that reduce pest population to tolerable levels.

Integrated pest management(IPM) strategy is proven to be more effective and less damaging to the environment than the classic tactics (such as biological control or chemical control) both experimentally [58, 225, 226] and theoretically [14, 176, 224, 233]. The main aim is to eradicate the pest or keep the pest population below a threshold for ecological damage [216].

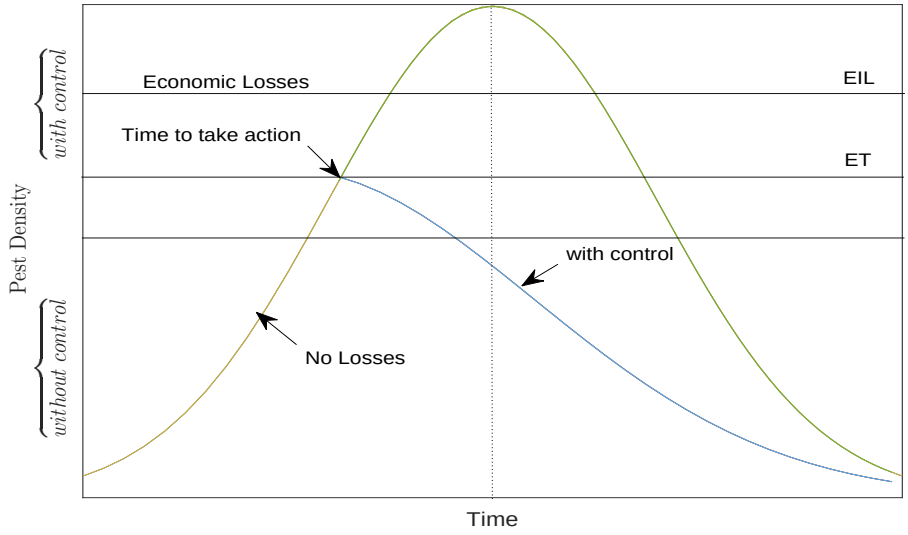

Figure 1.1: Relationship between economic threshold to the economic injury level and time of taking action

In IPM, the emphasis is given on two main concepts: economic injury level(EIL) and economic threshold(ET). The economic threshold(ET) is usually defined as the number of the pest in the field when control actions must be taken to effectively prevent the economic injury level(EIL)from being reached and exceeded (see 1.1). Economic injury level(EIL) is the lowest pest population density that will cause economic damage. The economic threshold must be less than the economic injury level [207].

Mathematical models are being used in pest management to estimate and predict economic threshold for pest populations [68, 176]. Impulsive differential equations are commonly used to model chemical [125] and biological strategies [158, 170] which are applied in pulses periodically to control pest population [137, 147, 190, 216]. These pulses are applied at a distinct time or state of the system. The mathematical techniques are vital for exploring the rapid changes in the control parameters across the threshold. This threshold can cause abrupt changes between the states of an impulsive system. Such type of changes between different states of an ecological system often accompanied by the occurrence of extinction, periodic solutions, and chaos. Few papers have been published on impulsive dynamical behavior including limit cycles, invariant sets, and attractors [183, 218]. In the next section, the attempts have been made to

study impulsive systems.

1.2 Impulsive Differential Equations

Many evolution processes are characterized by the fact that at certain moments of time they experience a change of state abruptly. These processes are subject to short-term perturbations whose duration is negligible in comparison with the duration of the process. Consequently, it is natural to assume that these perturbations act instantaneously, that is, in the form of impulses. It is known that many biological processes exhibit impulsive effects. Thus, impulsive differential equations, that is, differential equations involving impulse effects, appear as a natural description of observed evolution phenomena of several real-world problems. Equations of such type can be found in every domain of applied sciences [11, 12, 140, 187, 218, 220]. Impulsive systems have much richer dynamics than the corresponding theory of differential equations without impulses and has emerged an important area of investigation. These differential equations [11, 59, 120] have been recently used in population dynamics in relation to impulsive vaccination [2, 45, 62, 87, 201], population ecology [93, 129, 142], the chemotherapeutic treatment of disease [118, 173], birth pulses [218]. The IPM model based on combination of biological and chemical control applied impulsively were presented in [88, 138]. The host-parasitoid model with impulsive control was considered in [216]. The model considering microbial control with pathogen has also been investigated in [63, 97].

In 1960, the theory of impulsive differential equations started with the pioneering work of Mil'man and Myshkis [159]. Further, the fundamental theory of impulsive differential equations is developed in the monographs by Bainov and Simeonov [12], Lakshmikantham, Bainov and Simeonov [120], and Samoilenko and Perestyuk [194] during the 1990s. These monographs present qualitative solution properties, the existence of solutions, asymptotic properties of solutions and stability theory of impulsive differential equations.

The impulsive differential equations can be successfully used for mathematical simulation of processes and phenomena which are subject to short-term perturbations

during their evolution [12]. Impulsive differential equations undergoes rapid development in the theory of biology, economics, electronics, medicine, optimal control and population dynamics [80, 118, 120, 142, 145, 236]. Lakmeche et al. [118] transformed the problem of periodic solution into a fixed-point problem. They obtained the existence conditions of the trivial solution and the positive period-1 solution. The duration of the perturbations is negligible in comparison with the duration of the process considered, and they can be thought of as momentary. Even though the impulsive dynamical system is first formulated by Mil'man and Myshkis [159]. From a long period, it is a subject of intensive investigations [118, 120, 218, 237]. An impulsive differential equation is divided into three components:

- A continuous-time differential equation which governs the state of the system between impulses.
- An impulse equation, which models an impulsive jump defined by a jump function at the instant an impulse occurs.
- A jump criterion, which defines a set of jump events in which the impulse equation is active.

Consider the system

$$\begin{aligned} \frac{dX}{dt} &= F(X,t), \qquad t \neq nT,\ n \in 1,2,3,..., \\ \Delta X &= B(X), \qquad t = nT, \\ X(0^+) &= X(0). \end{aligned} \tag{1.2.1}$$

The system (1.2.1) is a system of impulsive differential equation. The solution $X(t)$ of the system (1.2.1) is piecewise continuous function from $\Re_+ \to \Re_+^n$. The solution $X(t)$ is continuous in the intervals $(nT \leq t < (n+1)T]$. Further, it is easy to prove that the system (1.2.1) has a positive solution for positive initial conditions.

Consider $\Re_+ = [0, \infty)$, $\Re_+^n = \{X = (X_1, X_2, X_3...X_n) \in \Re^n, X_1, X_2, X_3...X_n \geq 0\}$ and $F = \{F_1, F_2, ..., F_n\}$. Let $V : \Re_+ \times \Re_+^n \to \Re_+$, then the function V belongs to class V_0 if

1. V(t) is continuous in $(nT \leq t < (n+1)T] \times \Re_+^n$ for each $X \in \Re_+^n$, $n \in Z_+$and $\lim_{(t,X)\to(nT^+,X)} V(t,X) = V(nT^+,X)$ exist.

2. L is locally Lipschitzian in X.

Definition 1.2.1. Let $V \in V_0$, then for $(t, X) \in (nT \leq t < (n+1)T] \times \Re_+^n$, the upper right derivative of $V(t, X)$ with respect to the impulsive differential system (1.2.1) can be defined as

$$D^+V(t,X) = \lim_{h\to 0} \sup \frac{1}{h}\Big[V(t+h, X+hF(t,X)) - V(t,X)\Big].$$

Theorem 1.2.1. *If the function F is Lipschitz in X, then there exists a unique solution of the system* (1.2.1).

Theorem 1.2.2. *Let $X(t)$ be a solution of the system* (1.2.1) *with $X(0^+) \geq 0$, then $X(t) \geq 0$ for all $t \geq 0$. Further, $X(t) > 0$, for $t > 0$ if $X(0^+) > 0$.*

Let the map $X \to F(X)$ from an open subset $D \subset R^n$ toR^n be such that the solution $X(t)$ to the differential equation (1.2.1) is uniquely determined by its initial value $X(0) = X_0$ and this solution is denoted by $X(t, X_0)$. It is assumed that

1. D is simply connected,

2. $\overline{X}$ is the only equilibrium point in D and,

3. there is a compact absorbing set $\mathfrak{K} \subset D$.

Definition 1.2.2. A set $\mathfrak{K}$ is called absorbing in D if, $X(t, \mathfrak{F}) \subset \mathfrak{K}$ for each component set $\mathfrak{F} \subset D_1 \subset D$ (D_1 is an open set) for sufficiently large $t > 0$.

In the system (1.2.1), impulses are applied at the fixed time. However, in the pest management system, control strategies are applied, when the pest density reaches at economic threshold level (ET). For an IPM strategy, action must be taken once critical density of the pest is observed in the field so that the EIL is not exceeded Fig.1.1. In such case, the impulses are state dependent. For instance, impulsive reduction of the pest density is possible by trapping or by poisoning with chemicals. An impulsive increase of a controlling predator density is possible by artificial breeding and releases.

The state-dependent impulsive system is written as:

$$\left.\begin{aligned}\frac{dx}{dt} &= G(x(t))x(t) - H(x(t), y(t)) = G_1(x, y),\\ \frac{dy}{dt} &= \gamma H(x(t), y(t) - dy(t) = G_2(x, y),\end{aligned}\right\} x \neq h,$$

$$\left.\begin{aligned}\Delta x(t) &= -\epsilon_1 x(t),\\ \Delta y(t) &= -\epsilon_2 y(t) + \tau,\end{aligned}\right\} x = h, \tag{1.2.2}$$

$$x(0^+) \;=\; x_0 < h, \quad y(0^+) = y_0. \tag{1.2.3}$$

Here, $0 < \epsilon_1, \epsilon_2 < 1$ be the reduction in the pest and natural density respectively, by killing or trapping once the number of pests reaches h and $\tau > 0$ be the number of natural enemies released at this time [214].

1.3 Mathematical Modeling

Pest management is concerned with developing explanation and insight about the eradication, persistence, structure and dynamics of pest species. To portray the complicated phenomena of pest management system, mathematical model is constructed.

1.3.1 Compartmental Model

In the absence of stage-structure, consider that pest density be $N(t)$ at any time t. It changes according to the growth equation [116]:

$$\frac{dN(t)}{dt} \;=\; B(N(t))N(t) - dN(t). \tag{1.3.1}$$

Here, $d > 0$ is the mortality rate and $B(N(t))$ is the birth rate function at time t.
Assume that, the function $B(N(t))$ satisfy the following assumptions for $N \in [0, \infty)$:

A1 $B(N) > 0$.

A2 The function $B : \Re \to [0, \infty)$ is continuously differentiable with $B'(N) < 0$. Biologically, it means that the per capita birth rate for a pest is decreased due to the intra-specific competition as pest population increases. Further, $B^{-1}(N)$ exists for $N \in (B(\infty), B(0^+))$.

A3 $B(0^+) > d > B(\infty)$. Biologically, it implies the saturation effect.

In biological literature, the dependence of vital rates on pest density (birth, death and survival rates) is defined by birth functions $B(N)$ as:

Ricker Function [186] $B_1(N) = be^{-N}$, $b > d$.

Beverton-Holt Function [42, 218] $B_2(N) = p(q + N^n)^{-1}$, p, q, $n > 0$, $pq^{-1} > d$.

Deriso-Schnute Function [17] $B_3(N) = b(1 - vN)^{\frac{1}{v}}$, $b > 0$, $v \leq 0$.

Roberts and Kao [187] $B_4(N) = b - cN^{\theta}$, b, c, $\theta > 0$.

These functions and their generalizations have been discussed in [42, 53, 113, 187, 215]. $B_3(N)$ reduces to $B_1(N)$ when $v \to 0$. Further, it reduces to $B_2(N)$ if $v = -1$, $n = 1$.

1.3.2 Stage Structure

In most of the population models, it is assumed that all individuals are identical and ignore the inherent stage. Many pest species go through multiple stages in their life history as they proceed from birth to death. Some of the pest species are going through four stages: egg, larva, pupa and adult. The egg is the unborn stage of insects, the larva is a young stage, the pupa is a stage between larva and adult. There may also exist some other insects going through three stages: egg (unborn stage), nymph (young stage) and adult (final stage). Moreover, some of the birds, mammals and reptiles have a very simple life cycle: they born and then grow up. Most popularly, the population goes through two stages in their life cycle recognized as immature and mature. This stage-structured phenomenon has its own significance in the dynamics of the interacting species. However, in many situations age structure can influence population size and growth in a major way. It has been recognized that mortality and fertility depend on an individual's age and even sometimes on the size of the individuals.

In pest management, it is particularly important as all the stages of pest do not harm the crops equally. Considering the stage-structure in the pest species so that the total pest population $N(t)$ be divided in two stages: immature/juvenile stage $x(t)$ and mature/ adult stage $y(t)$, $N(t) = x(t) + y(t)$ at time t. The immature pest has

no reproductive capability. Let $A(N(t))$ be the per capita maturation rate of immatures/juveniles. Let $D_1(N(t))$ and $D_2(N(t))$ be the per capita death rate functions of immature and mature pest respectively. The dynamics of a stage-structured model with continuous birth function $B(N(t))$ is governed by the system of differential equations is given as follows [Kostara [115]]:

$$\begin{aligned} \frac{dx}{dt} &= -D_1(N(t))x(t) - A(N(t))x(t) + B(N(t))y(t) \\ \frac{dy}{dt} &= A(N(t))x(t) - D_2(N(t))y(t). \end{aligned} \tag{1.3.2}$$

The dynamics of the system (1.3.2) is characterized by the equilibria and periodic solutions in [18, 19, 115]. In most cases, ordinary differential equations are used to build stage structure models. However, the impulsive differential equations are more suitable for the mathematical simulation of evolutionary processes in which the parameters undergo relatively long periods of smooth variation followed by a short-term rapid change in their values.

1.3.3 Impulsive Differential Equations Incorporating Births in Pulses

Many species give birth in a very short time period. It means a dynamics, increase in population due to birth are assumed to be time-independent. In this thesis, the birth rate function $B(N(t))N(t)$ is assumed to be of Ricker type and Beverton-Holt Type.

Birth pulses play an important role in the ecological system. Researchers have mostly considered that the mature pest reproduces throughout the year, but almost always births are seasonal or occur in regular pulses. Hence, the term of the continuous reproduction of mature population is replaced with an annual birth pulse. This growth pattern has been termed as a birth pulse [28]. Due to birth pulses, the system may lead to chaotic behavior and a variety of complex dynamical behaviors such as the existence of quasi-periodic, period-doubling bifurcation, chaotic attractor etc. may be expected. The linear birth pulse $\Delta N(t) = B(N(t))N(t)$, was discussed in [144].

It is assumed that the mature pest reproduce periodically in the birth pulse at an interval T_1. Let $x(mT_1)^+$ and $y(mT_1)^+$ be the density of immature and mature pest after m^{th} birth pulse. The system (1.3.2) can be modified by incorporating birth pulses

using impulsive differential equations as:

$$\left.\begin{aligned}\frac{dx}{dt} &= -D_1(N(t))x(t) - A(N(t))x(t),\\ \frac{dy}{dt} &= A(N(t))x(t) - D_2(N(t))y(t),\end{aligned}\right\} t \neq mT_1, m = 1, 2, 3, ..., \tag{1.3.3}$$

$$\left.\begin{aligned}x(mT_1)^+ &= x(mT_1) + B(N(mT_1))y(mT_1),\\ y(mT_1)^+ &= y(mT_1),\end{aligned}\right\} t = mT_1. \tag{1.3.4}$$

Now to control the pest population, many pest management strategies have been applied periodically, which instantaneously kills a portion of pest. Accordingly, the instant effect of the pest management strategies will be modeled as an impulsive phenomenon which occurs periodically. As mechanical control affects the immature and mature pests differently with the differential killing rates k and μ respectively, are assumed for them under the impulsive control strategy at time $t = mT_2$, i.e.

$$\left.\begin{aligned}x(mT_2)^+ &= (1-k)x(mT_2),\\ y(mT_2)^+ &= (1-\mu)y(mT_2),\end{aligned}\right\} t = mT_2. \tag{1.3.5}$$

Chemical control has been used frequently in agricultural fields. Before pesticide control is introduced into the biological systems, there are two important things to note. First, in order to concentrate on the development of the model for pest population dynamics, it is assumed that the pest will be equally susceptible to the pesticides at different ages, such as larvae and adult stages. When the pesticide is sprayed, it kills pest instantly or it may remain in the crop or pest. On the basis, the effect of the pesticide on the pest can be formulated mathematically as:

Instantaneous Effect of Pesticides: When the pesticide is sprayed, it kills immature and mature pest instantaneously with constant killing rate α and β. Under impulsive control strategy, this phenomena can be modeled at the fixed time moments as:

$$\left.\begin{aligned}x(mT_3)^+ &= (1-\alpha)x(mT_3),\\ y(mT_3)^+ &= (1-\beta)y(mT_3),\end{aligned}\right\} t = mT_3. \tag{1.3.6}$$

Residual effect of Pesticides: In many cases, the amount of the pesticide may remain in the crop/ in the pest after it has been sprayed [155, 209, 230]. If pesticides have long-term residual effects then pesticide application frequencies can be reduced.

When the pesticides have residual effects on the pest, the impact of the pesticide on the pest population can be described by different kill functions. Kill functions incorporating residual effects can be modeled as:

- Let m_1 be the mortality rate or killing efficiency rate, $a_1 > 0$ be the decay rate. High pest mortality requires a large dosage of pesticide, then the impact of the pesticide or the kill function of the pest populations can be defined as [23]:

$$k(t)x(t) = m_1 e^{-a_1 t} x(t). \tag{1.3.7}$$

  Due to the degradation of the pesticide, the kill function incorporating decay effect of the pesticide can be defined as a negative exponential function.

- If pesticide applications have been applied repeatedly at time nT (where T is the period of pesticide application), then the kill function with residual effects can be described as follows:

$$k(t)x(t) = m_1 e^{-a_1(t-nT)} x(t), \quad nT < t < (n+1)T. \tag{1.3.8}$$

- The step function is highly useful when dealing with jump discontinuities in the pest population function. The spraying of pesticide at specific time T_4, the pesticide dosage function or kill function is [126]:

$$k(t)x(t) = \begin{cases} mx(t), & T < t < (n+T_4)T, \\ 0, & (n+T_4)T < t < (n+1)T, \end{cases} \tag{1.3.9}$$

  where, T_4 is the duration of pesticide residues.

Pesticide controls are not limited to only once during the time interval. Farmers may spray more than once and with different dosages of pesticide during the time interval. The mathematical expression with the assumption that there is more than one spray time in the time interval. Due to this, pest develops resistance to the pesticide. Hence, once there is a delayed response to the pesticide application, the pests must increase continuously. Therefore, it is necessary to involve a delayed response to pesticides into the kill function which yields the following piecewise periodic function [172, 173]:

$$k(t) = m_1(e^{-a_1(t-nT)} - e^{-c_1(t-nT)}), \quad nT < t < (n+1)T, \tag{1.3.10}$$

where, c_1 is the delayed response rate with $c_1 > a_1$. Pest-natural enemy systems to model IPM strategies have been proposed and investigated the effects of a piecewise kill function and a step kill function on the success of pest control [221]. The existence and stability of pest-free periodic solutions have been derived. The effects of parameters on the threshold values have been discussed.

1.4 Mathematical Techniques

In this section, some fundamental mathematical tools are required to investigate the dynamical behavior of impulsive pest management systems with time-dependent as well as state-dependent impulsive strategies.

The impulsive systems are a combination of continuous and discrete components. The stroboscopic map is a tool to describe the system dynamics. It is obtained in two steps: properties of the system are embodied in the discrete system. Following steps has been used to construct the stroboscopic map:

(a) The analytical solution of the continuous part of the impulsive system between the pulses is obtained using the initial conditions.

(b) The discrete condition is applied to the analytical solution. It determines the solution after n^{th} pulse in terms of the previous pulse, $n = 1, 2, 3, ...$ This represents the discrete stroboscopic map.

The dynamics of impulsive system is determined by the dynamics of the stroboscopic map. The following qualitative methods of discrete dynamical systems have been applied to analyze various impulsive dynamical models proposed in this thesis.

1.4.1 Fixed Points of the Map

Consider the following system of first order autonomous difference equations or maps:

$$X(n+1) = F(X(n)) \quad \text{or} \quad X \to F(X), \tag{1.4.1}$$

with

$$X = (X_1, X_2, X_3...X_m) \in \Re^m,$$
$$F = (F_1, F_2, F_3...F_m) \in \Re^m,$$
$$\text{and } F : \Re^m \to \Re^m.$$

Here, $X(n)$ denote the state of the system (1.4.1) at discrete time $n \in \mathbb{Z}$. Observe that, the system (1.4.1) is autonomous as it does not contain time variable explicitly. The system (1.4.1) with the initial conditions can take the form:

$$X(n+1) = F(X(n)) \text{ or } X \to F(X), \tag{1.4.2}$$

with

$$X = (X(1), X(2), X(3)...X(m)) \in \Re^m,$$
$$F = (F_1, F_2, F_3...F_m) \in \Re^m,$$
$$\text{and } F : \Re^m \to \Re^m,$$
$$X(n=0) = X(0),\ X(0) = (X(10), X(20), X(30)...X(m0)).$$

For notational compactness, to indicate the integer dependence of the equation, subscripts can be used. Now the discrete dynamical system (1.4.2) can be written as:

$$X_{n+1} = F(X_n) \text{ or } X \to F(X) \quad X(0) = X_0. \tag{1.4.3}$$

Definition 1.4.1. (Invariant Set) The set $S \subseteq \Re^m$ is said to an invariant set for the map $X \to F(X)$ (1.4.3) if

$$X_0 \in S \Rightarrow F^n(X_0) \in S,\ \forall\ n.$$

If a solution belongs to S at some time instant, then it belongs to S for all future and past time [231].

Definition 1.4.2. (Positively Invariant Set) A set S is said to be a positively invariant set if

$$X_0 \in S \Rightarrow F^n(X_0) \in S,\ \forall\ n \geq 0.$$

It means that a solution initiating in S remains in S.

Definition 1.4.3. (Fixed Points of Map) A point X^* of the system (or map)(1.4.3) is said to be a fixed point if it satisfies $F(X^*) = X^*$.

In other words, equilibrium solution does not change with time. It is also known as critical point/ equilibrium point/ singularity/ stationary point or steady state.

The analysis of the dynamical system is concerned with fixed points of the system because there is no general method available to find the analytical solutions of nonlinear systems. Therefore, qualitative analysis is very helpful to know the long-term behavior of the system. In order to describe the behavior of solutions near a fixed point, some tools will be discussed in the next section:

1.4.2 Local Stability Analysis

Stability theory is a fundamental topic in applied science, including every branch of control theory. There are many kinds of stability concepts such as absolute stability, Lyapunov stability, the stability of periodic solution etc.. The Lyapunov stability concept has been studied extensively for a long time. There is a rich literature on this topic [69, 74, 119, 120, 151, 160, 165, 194, 210, 231]. It is important to analyze the behavior of non-linear system near the possible fixed points.

Definition 1.4.4. The fixed point X^* of the system (1.4.3) is said to be locally stable(Lyapunov Stable), if for each $\epsilon > 0$ there exists a $\delta > 0$ such that

$$\| F^n(X_0) - X^* \| < \epsilon \quad \text{whenever} \quad \| X_0 - X^* \| < \delta. \tag{1.4.4}$$

According to the definition, a fixed point is said to be locally stable if any solution trajectory that starts from any point near to the point X^* then it remains close to X^*.

Definition 1.4.5. The fixed point X^* of the system (1.4.3) is said to be unstable if it is not stable.

Definition 1.4.6. The fixed point X^* of the system (1.4.3) is said to be asymptotically stable if X^* is locally stable and there exists a $\delta > 0$ such that

$$\lim_{n\to\infty} F^n(X) = X^* \quad \text{when} \ \| X_0 - X^* \| < \delta. \tag{1.4.5}$$

It means that the solution trajectories starting from the initial conditions close to the equilibrium point not only remain close to it but also converge to it asymptotically.

However, the behavior of the solution near a fixed point may be studied by the linearized system. The behavior of the nonlinear systems in the neighborhood of the fixed point will be decided by the eigenvalues of the linearized system [180]. The difference equations governing interacting populations often take the form:

$$X_{in+1} = F_i(X_{1n}, X_{2n}, ..., X_{nn}),\ X_i(0) = X_{i0} \geq 0,\ i = 1, 2, ..., n. \tag{1.4.6}$$

Let X be any solution in the neighborhood of X^* and

$$X \ = \ X^* + \vartheta$$

Consider $\vartheta = \vartheta_1, \vartheta_2, ..., \vartheta_n$ is a small perturbation from the fixed point then

$$\vartheta_{n+1} = A\vartheta_n. \tag{1.4.7}$$

The matrix $A = (a_{ij})_{X^*}(i, j = 1, 2, ...n)$ is the Variational/Jacobi matrix at the fixed point X^*. The linear system (1.4.7) with the Jacobian matrix is called linearization of non-linear system (1.4.3) at X^*. Let ϑ_0 be the initial perturbation from the fixed point X^* then

$$\vartheta_n = A^n\vartheta_0.$$

The stable or unstable behavior is decided by the eigenvalues of the linearized system (1.4.7). Let λ be the eigenvalue of A with the corresponding eigenvector ϑ then $\vartheta_n = \lambda^n\vartheta_0$. The characteristic equation is

$$det(A - \lambda I) = \lambda^n + a_1\lambda^{n-1} + ... + a_n, \quad a_0 \neq 0. \tag{1.4.8}$$

The necessary and sufficient condition for local stability is that the eigenvalues of linearized matrix lie in the unit circle [188, 231].

Stable A fixed point X^* of the system (1.4.3) is said to be stable if the maximum modulus of the eigenvalues of A is less than one.

Unstable A fixed point X^* of the system (1.4.3) is called unstable if the maximum modulus of the eigenvalues of A is not less than one.

Saddle A fixed point X^* of the system (1.4.3) is called saddle if the maximum modulus of at least one eigenvalue of A is less than one while other eigenvalue greater than one.

Definition 1.4.7. [231] A fixed point X^* is said to be a hyperbolic fixed point of the system (1.4.3) if none of the eigenvalues of A have unit modulus.
A fixed point X^* is called non-hyperbolic point of the system if

1. The linearized matrix A has at least one eigenvalue equal to 1 while remaining eigenvalues having moduli not equal to 1.

2. The linearized matrix A has at lest one eigenvalue equal to -1 while remaining eigenvalues having moduli not equal to 1.

3. The linearized matrix A has at least two complex conjugate eigenvalues having modulus 1 (which are not one of the first four roots of unity) while remaining eigenvalues having moduli not equal to 1.

In particular, for $n = 2$, the characteristic equation (1.4.8) is written as:

$$\lambda^2 - a_1\lambda + a_2 = 0, \tag{1.4.9}$$

with $a_1 > 0$ and $a_2 > 0$. Let the characteristic equation (1.4.9) in terms of trace T and determinant D be written as:

$$\lambda^2 - Tr\lambda + Det = 0. \tag{1.4.10}$$

The fixed point $X = (x, y)$ is stable when the magnitude of eigenvalues of A is less than unity. Now, the necessary and sufficient conditions under which roots of the equation (1.4.10) lie in a unit circle, are given by the Jury's condition:

$$1 - Tr + Det >, \tag{1.4.11}$$

$$1 + Tr + Det > 0, \tag{1.4.12}$$

$$1 - Det > 0. \tag{1.4.13}$$

If inequality (1.4.11) is violated, then one of the eigenvalues of A is larger than 1. If inequality (1.4.12) is violated, then one of the eigenvalues of A is less than -1. Finally, if inequality (1.4.13) is violated, then A has a complex-conjugate pair of eigenvalues lying outside the unit circle. The general result can be found in the reference [99].

Theorem 1.4.1. ***(Hartman-Grobman Theorem)*** *Wiggins[231] If X^* is a hyperbolic equilibrium point, then there is a homeomorphism from $\Re^n$ to $\Re^n$ defined in the neighborhood of X^*. That maps trajectories of nonlinear system to the trajectories of the linearized system.*

Accordingly, the behavior of a dynamical system near a hyperbolic equilibrium point is qualitatively same as the behavior of its linearized matrix near this equilibrium point provided that no eigenvalue of the linearized matrix has modulus ± 1. Also the method fails if any eigenvalue has modulus one.

Following theorems are used to get an idea regarding qualitative behavior of the system:

Theorem 1.4.2. [The Stable Manifold Theorem] *[51]: Let X^* be a hyperbolic fixed point of a map $F : \Re^m \to \Re^m$ then in the neighborhood of an open set O of X^* there exists two manifolds $W^S(X^*)$ of dimension E^S and $W^U(X^*)$ of dimension E^U such that:*

- *The stable subspace E^S is tangent to $W^S(X^*)$ at X^* and for any solution $X(n)$ of (1.4.3) with $X(0) \in W^S$, $\lim_{n\to\infty} X(n) = X^*$.*
- *The unstable subspace E^U is tangent to $W^U(X^*)$ and $X(0) \in W^u(X^*)$, then there exists a principal negative solution $x(-n)$ with $\lim_{n\to\infty} X(-n) = X^*$.*

where, S and U are the local stable and unstable manifold of the fixed point respectively.

1.4.3 Global Stability

A fixed point X^* of the system (1.4.3) is said to be globally asymptotically stable if it is asymptotically stable and for all initial values converges to the fixed point X^* [6]. A system which is stable for all initial conditions in the state space is globally stable.

The global behavior of a nonlinear difference equation can be different from its local behavior. In local stability, the system is stable at a particular point, but in global stability, the system is stable in the entire domain. A locally stable system may not be stable globally, but the globally stable system is always locally stable everywhere. Asymptotic stability is a local property, however, for linear systems, this is the same as global asymptotic stability.

There are several methods for analyzing global stability, but in analyzing difference equations, Lyapunov stability theory plays an important role. Lyapunov stability theory generally includes Lyapunov first and second methods [51, 61, 231]. In 1892, for investigating the stability of nonlinear differential equations, the Russian mathematician A.M. Lyapunov introduced a method which is known as a Lyapunovs direct method. This method is used to investigate the qualitative nature of solutions without actually determining the solutions themselves [127].

In this thesis, Lyapunovs second method has been established to analyze the global behavior of difference equations. The method is described below:

Consider X^* be a fixed point of the system (1.4.3). Let $V : \Re^n \to \Re$ be defined as a real-valued function. The variation of V relative to (1.4.3) can be defined as:

$$\Delta V_n = V(X_{n+1}) - V(X_n) \tag{1.4.14}$$

Let there exist a continuously differentiable, real-valued function $V : \Re^n \to \Re$, such that

- The function V is positive definite, i.e.

$$V(X) > 0, \quad \forall \quad X \neq 0, V(0) = 0. \tag{1.4.15}$$

- The time derivative of $V(x)$ is negative definite, i.e.

$$\dot{V}(X) < 0, \quad \forall \quad X \neq 0, \dot{V}(0) = 0. \tag{1.4.16}$$

The positive definite function V from an open subset G of $\Re^n$ into $\Re$ is a Lyapunov function on the set G if

- V is continuous on G.

- $\Delta V \leq 0$ whenever both X_n and $X_{n+1} = F(X_n)$ are in G.

According to the Lyapunov second method, if there exists a positive definite Lyapunov function for the system (1.4.3) then the fixed point is globally asymptotically stable. However, if derivative of $V(x)$ is negative semi definite, i.e.

$$\dot{V}(X) < 0, \quad \forall \quad X \neq 0. \tag{1.4.17}$$

then the fixed point is globally stable.

This method gives a sufficient condition only, which means that failure of a Lyapunov function does not mean that the equilibrium point is not stable or asymptotically stable. To apply this method for any nonzero equilibrium point, the system is to be shifted to the origin.

Definition 1.4.8. [Periodic Solutions] The fixed point X^* of the system (1.4.3) is called the periodic solution if there exists a constant ω, such that

$$\begin{aligned} F^{\omega}(X^*) &= X^*, \\ F^{i}(X^*) &\neq X^* \quad \text{for } i = 1, 2, 3, ..., \omega - 1, \end{aligned}$$

then the solution X^* is called ω-periodic solution and ω is called the period of the solution X [166].

1.4.4 Bifurcation

Consider the system (1.4.3) depending on the parameter b:

$$X_{n+1} = F(X_n, b), \ X \in \Re^m, \ b \in \Re^p. \tag{1.4.18}$$

A study of changes in the qualitative behavior of dynamical systems as parameters are varied is called bifurcation theory. Large qualitative changes in the dynamics of the system due to small quantitative changes in parameter result in bifurcations. The parameters which are responsible for qualitative changes in the behavior are called bifurcation parameter. In particular, fixed points can be created, destroyed, or can change their stability with variation in parameter b. As the parameter is varied, these qualitative changes in the behavior of the system can occur at certain critical values of the parameter.

Bifurcation analysis investigates the change in the nature of the attractor, i.e. stable to unstable, fixed point to cycle, etc. due to parameter variation. To destabilize the fixed point, one or more of the eigenvalues have to cross the unit circle as the parameter b changes its value.

In this thesis, several types of bifurcations have been studied, e.g. fold(tangent), transcritical, period halving and flip(period-doubling) bifurcations. In the following, some results related to them will be recalled.

- **Fold bifurcation**(or Saddle-node bifurcation) is the basic mechanism by which fixed points are created and destroyed. As a critical parameter is varied, two fixed points move toward each other, collide, and mutually annihilate. Saddle-node bifurcation is a bifurcation of a fixed point onto two fixed points at a critical value of a control parameter with one being of saddle type and the other being stable node. Sometimes it is called Saddle-node bifurcation or tangent bifurcation.

- **Transcritical bifurcation** is exchange or transfer of stability between two fixed points at a critical value of a control parameter. In this bifurcation, the stable node becomes a saddle and the saddle becomes a stable node. In the transcritical case, the two fixed points don't disappear after the bifurcation, instead, they just switch their stability. A fixed point must exist for all values of a parameter and can never be destroyed.

Theorem 1.4.3. [Wiggins (1990)] *Consider a one-parameter family of one-dimensional maps*

$$x \to f(x, b), \quad x \in \Re, \quad b \in \Re, \tag{1.4.19}$$

having a non-hyperbolic fixed point with an eigenvalue 1*, then the map* (1.4.19) *undergoes a fold bifurcation at* $(x, b) = (x_0, b_0)$ *provided*

$$\left.\begin{array}{l} f(x_0, b_0) = 0, \\ \dfrac{\partial f(x_0, b_0)}{\partial x} = 1, \end{array}\right\} \text{ non hyperbolic fixed point,} \tag{1.4.20}$$

$$\text{with} \quad \frac{f(x_0, b_0)}{\partial b} \neq 0, \qquad \frac{\partial^2 f(x_0, b_0)}{\partial^2 x} \neq 0. \tag{1.4.21}$$

If the condition (1.4.21) are changed to

$$\frac{f(x_0,b_0)}{\partial b}=0, \qquad \frac{f(x_0,b_0)}{\partial x \partial b}\neq 0, \qquad \frac{\partial^2 f(x_0,b_0)}{\partial^2 x}\neq 0, \tag{1.4.22}$$

then the system (1.4.19) experiences a transcritical bifurcation at the fixed point x_0 as the parameter b varies through the bifurcation value $b=b_0$.
For detailed analysis one can refer Wiggins (1990) [231], Guckenheimer and Holmes (1983)[69] and Kuznetsov (2013) [117].

- **Period-halving bifurcation** is a bifurcation in which the system switches to a new behavior with half the period of the original system. A series of period-halving bifurcations leads the system from chaos to order.

- **Flip bifurcation**(Period-doubling Bifurcation) is a bifurcation in which the system switches from a periodic solution to another periodic solution with twice the period of the original solution, i.e. a new periodic solution emerges from an existing periodic solution, and the period of the new periodic solution is twice that of the old one. Period doubling bifurcation is also called flip bifurcation.

  Consider the map (1.4.18) has a non-hyperbolic fixed point and the eigenvalue associated with the linearization of the map about the fixed point is -1 rather than 1. Now a result will be presented that ensures the flip bifurcation:

  Theorem 1.4.4. [Guckenheimer and Holmes (1983)] *Let $f_b:\Re\to\Re$ be a one-parameter family of one-dimensional maps having such that f_{b_0} has a fixed point x_0 with an eigenvalue -1. Assume that*

$$\left.\begin{aligned} &f(x_0,b_0)=0,\\ &\frac{\partial f(x_0,b_0)}{\partial x}=-1, \end{aligned}\right\} \text{ non hyperbolic fixed point,}$$

$$\begin{aligned} \frac{\partial f}{\partial b}\frac{\partial^2 f(x_0,b_0)}{\partial x^2}+2\frac{\partial^2 f(x_0,b_0)}{\partial x\partial b}&\neq 0, \qquad at(x_0,b_0),\\ \bar{a}=\frac{1}{2}\left(\frac{\partial^2 f}{\partial x^2}\right)^2+\frac{1}{3}\frac{\partial^3 f}{\partial x^3}&\neq 0, \qquad at(x_0,b_0), \end{aligned}$$

then, there exists a smooth curve of fixed points of f_b passing through (x_0,b_0), the stability of which changes at (x_0,b_0). There is also a smooth curve γ passing

through (x_0, b_0) *so that* γ-$\{(x_0, b)\}$ *is a union of hyperbolic period-*2 *orbits. The sign of* $\bar{a}$ *determines the stability and the direction of bifurcation of the orbits of period-*2*. If* $\bar{a}$ *is positive, the orbits are stable, if* $\bar{a}$ *is negative they are unstable [231].*

The **period doubling cascade** is a sequence of doubling of periods and a further doubling of the repeating period, as the bifurcation parameter is changed and so on. In a series of papers in 1958-1963, Pekka Myrberg was the first to discover the period-doubling bifurcation. After the first period-2 bifurcation, the system undergoes a series of period-doubling bifurcation in which a cycle of period 2^k losses its stability and a stable cycle of period 2^{k+1} arises. As bifurcation parameter varies, periodic orbits of periods 2, 4, 8, 16, occur [167, 168]. This is a well-known phenomenon of the period-doubling route to chaos and the hallmark of logistic and Ricker maps [150, 152]. Period-doubling bifurcation has been studied extensively in [50].

The **period-adding sequence** means the successive generation of periodic solutions with longer periods when the value of a control parameter is changed. Period-adding sequence includes chaotic states between periodic states in a 1-parameter bifurcation diagram, the phenomenon is called the alternating **periodic-chaotic sequence** [5]. These phenomena are interesting in terms of bifurcation phenomena because they can be considered as successive local bifurcations. These period-adding sequences have been observed in chemical reactions [54], electrical circuits [89]. Such type of sequences has been studied in one-dimensional difference equations [100, 101, 105]. Period adding is also present in a delay-difference equation population model with density-dependent reproduction [24] and in the density-dependent age-structured model [70].

1.4.5 Center Manifold Theorem

To analyze the behavior of hyperbolic equilibria when the maximum modulus of the eigenvalues was not unity. In cases where the equilibrium is not hyperbolic, the linearization may fail to reveal the behavior of the system on certain subspaces of the state space. These subspaces are associated with the eigenvectors of the Jacobian matrix with eigenvalue $\lambda = 1$.

The theory resulting from the analysis of these subspaces is called Center Manifold Theory. The specific case of Center Manifold Theory for the two dimensions will be expounded here.

Consider a discrete dynamical system with transition function defined from the state space $\Re^2 \rightarrow \Re^2$, with an associated parameter space a subset of $\Re^2$. This analysis will concern the qualitative changes happen to the systems fixed point due to variation in input parameters.

Denote this system as

$$X_{n+1} = F(X_n, b),\ X \in \Re^m,\ b \in \Re^p. \tag{1.4.23}$$

For the purposes of analysis, it will also assume that $F(X, b)$ has continuous derivatives at least up to the third degree. For a given value of b say b^* the point $X*$ is said to be an equilibrium of the system if

$$F(X^*, b^*) = X^*. \tag{1.4.24}$$

By the suitable change of variables, the system (1.4.23) can be represented as:

$$\begin{aligned} x &\rightarrow Ax + f(x, y), \\ y &\rightarrow By + g(x, y), \qquad (x, y) \in \Re^c \times \Re^s, \end{aligned} \tag{1.4.25}$$

or

$$\begin{aligned} x_{n+1} &\rightarrow Ax_n + f(x_n, y_n), \\ y_{n+1} &\rightarrow By_n + g(x_n, y_n). \end{aligned} \tag{1.4.26}$$

It is considered that the modulus value of all eigenvalues of the $c \times c$ matrix A is one, and all the eigenvalues of $s \times s$ matrix B are less than one in magnitude where, $c + s = m$.

$$f(0,0) = 0, \qquad Df(0,0) = 0 \qquad g(0,0) = 0 \qquad Dg(0,0) = 0. \tag{1.4.27}$$

Evidently, $(x, y) = (0, 0)$ is a fixed point of the map (1.4.23). The linear approximation is not sufficient for determining its stability. The following theorem guarantees the existence of a center manifold which is a curve $y = h(x)$ on which the dynamics of the system (1.4.25) (or (1.4.26)) is given by the map on the center manifold [231].

Theorem 1.4.5. [Existence] *There exists a center manifold for the system* (1.4.25) (or (1.4.26)) *which is tangent to* $\{(x, y) \in (\Re^c \times \Re^s) \mid y = 0\}$ *can be represented locally as a graph of a function* $h : \Re^c \to \Re^c$ *such that*

$$W^c = \{(x, y) \in \Re^c \times \Re^s \mid y = h(x), h(0) = 0, Dh(0) = 0, \mid x \mid < \delta\}, \qquad (1.4.28)$$

for a sufficiently small δ*. Further, the dynamics restricted to* W^c (1.4.28) *is given by the map:*

$$u \to Au + f(x, h(u)), \qquad u \in \Re^c. \qquad (1.4.29)$$

The next result allows to conclude that $(x, y) = (0, 0)$ is stable or unstable based on whether or not $u = 0$ is stable or unstable in (1.4.29) [231].

Theorem 1.4.6. [Stability]

- *Suppose the zero solution of* (1.4.29) *is stable (asymptotically stable) (unstable). Then the zero solution of* (1.4.25) (or (1.4.26)) *is stable (asymptotically stable) (unstable).*
- *Suppose that the zero solution of* (1.4.29) *is stable. Let* (x_n, y_n) *be a solution of* (1.4.25)*(or* (1.4.26)*) with* (x_0, y_0) *sufficiently small. Then there is a solution* u_n *of* (1.4.29) *such that* $\mid x_n - u_n \mid \leq n\beta^n$ *and* $\mid y_n - h(u_n) \mid \leq n\beta^n$ *for all* n *where* n *and* β *are positive constants with* $\beta < 1$*.*

For detailed analysis can be found in Carr (1981) [26], Elaydi (2008) [52] and Zhang (2006) [242].

1.4.6 Lyapunov Exponents

One of the characteristic of chaotic orbits is its sensitive dependence on initial conditions. This means that the orbits corresponding to nearby initial conditions eventually move apart as the system moves forward in time. Lyapunov exponent may be used to obtain a measure of the sensitive dependence upon initial conditions. The Lyapunov exponent is the important tool for chaotic solution [6, 13, 119, 171, 177]. They are similar to eigenvalues used in the local stability analysis of non-linear dynamical system [57]. Lyapunov exponents describe what happens near an entire trajectory rather than describing what happens near a fixed point.

The Lyapunov exponents provide basic stability information about the directional rates of convergence or divergence between initially neighboring trajectories, like eigenvalues in linear systems [67]. Lyapunov exponents are the measure of exponential rates of convergence or divergence of nearby trajectories in phase space [139].

Let Lyapunov exponents [119] be defined for the trajectory $X(t) = (X_1(t), X_2(t), ..., X_n(t))$ of the system (1.4.3). Two trajectories of the n-dimensional phase space starting from two nearby initial conditions X_0 and $X_0' = X_0 + \delta X_0$ are considered. They evolve with time yielding the vectors $X(t)$ and $X'(T) = X(t) + \delta X(t)$, respectively. It is measured by Euclidean norm.

$$d(X_0, t) = \| \delta X(X_0, T) \| \equiv \sqrt{\delta X_1^2 + \delta X_2^2 + ...\delta X_n^2}. \tag{1.4.30}$$

Let $d(X_0, t)$ be the distance at any time t between two trajectories $X(t)$ and $X'(t)$. By linearizing (1.4.3), the time evolution of δX

$$\delta \dot{X} = M(X(T)).\delta X, \tag{1.4.31}$$

where, M is the linearized matrix of the system (1.4.3). Then, Lyapunov Exponent is defined as the mean rate of divergence of two close trajectories

$$\lambda(X_0, \delta X) = \lim_{t \to \infty} \frac{1}{t} \log \left(\frac{d(X_0, t)}{d(X_0, 0)} \right). \tag{1.4.32}$$

Furthermore, there are $n-$ orthonormal vectors e_i of δX_i, $i = 1, 2, ..., n$ such that

$$\lambda \dot{e_i} = M(X_0) e_i, \quad M = diag(\lambda_1, \lambda_2, ..., \lambda_n). \tag{1.4.33}$$

That is, there are $n-$ Lyapunov exponents given by

$$\lambda_i(X_0) = \lambda_i(X_0, e_i), \quad i = 1, 2, ..., n. \tag{1.4.34}$$

From (1.4.32) and (1.4.34),

$$d_i(X_0, t) = d_i(X_0, 0) e^{\lambda_i t}, \quad i = 1, 2, ..., n. \tag{1.4.35}$$

To identify whether the motion is periodic or chaotic, it is sufficient to consider the nonzero Lyapunov exponent λ_m and Rearranging the other exponents in descending order $\lambda_1 \geq \lambda_2 \geq \lambda_3 \geq \lambda_4 \geq ..... \geq \lambda_n$, the attractors are classified as follows:

- $\lambda_m < 0$: Stable Equilibrium Points/ Periodic Attractors
  As it increases, $d(X_0, t)$ (or simply $d(t)$) decreases and for $t \to \infty$,$\mid d(X_0, t) \mid \to 0$. This is the case for a stable equilibrium point or a stable periodic solution where two nearby trajectories converge towards the same attractor in the limit $t \to \infty$.

  - For a stable equilibrium point $\lambda_i < 0$, $\forall i$.

  - For a stable limit cycle, $\lambda_1 = 0$ and $\lambda_i < 0$ for $i = 2, 3, 4, ..., n$.

  - For a stable torus or quasi- periodic, $\lambda_1 = \lambda_2 = 0$ and $\lambda_i < 0$ for $i = 3, 4, ..., n$.

- $\lambda_m > 0$: Chaotic Attractors

  - For strange attractor at least one Lyapunov exponent should be positive. As t increases, $\mid d(X_0, t) \mid$ grows exponentially fast, implying sensitive dependence on perturbation about initial condition. Thus, a positive Lyapunov exponent is the essence of deterministic chaos.

Thus, all negative exponents represent regular orbits, while at least one positive exponent signals the presence of chaotic motion.

1.4.7 Lyapunov Dimension

The most basic property of a strange attractor is its fractal dimension. Strange attractor generally has a non-integer dimension. There is a relationship between the Lyapunov exponents and one of the fractal dimensions, which is called the Lyapunov dimension. The appealing feature of this dimension is that it is easy to calculate if the Lyapunov exponents are known.

There are several ways to compute the attractor dimension: the capacity dimension, information dimension, correlation dimension and Lyapunov exponent. Only the Lyapunov dimension is presented here, for other types [177].

Let $\lambda_1 \geq \lambda_2 \geq \lambda_3 \geq \lambda_4 \geq ..... \geq \lambda_n$ be the Lyapunov exponents of a dynamical system. Let j be the largest integer for which the sum of the j largest Lyapunov exponent is non-negative i.e. $\sum_{i=1}^{j} \lambda_i \geq 0$. The Lyapunov dimension D_L as

suggested by Kaplan and Yorke [104] is defined:

$$D_L = \begin{cases} j + \dfrac{\sum_{i=1}^{j} \lambda_i}{|\lambda_{j+1}|}, & j < n, \\ n, & j = n, \\ 0, & \text{otherwise.} \end{cases} \tag{1.4.36}$$

For the $n-$dimensional system, the Lyapunov dimension D_L is defined by Eq. (1.4.36). Therefore, according to the classification of the attractors with respect to its Lyapunov exponents, $D_L = 0$ for stable fixed point, $D_L = 1$ in case of periodic solution, $D_L = 2$ for a quasi-periodic attractor. For the strange attractor the Lyapunov dimension is non-integer. For example, in 2D chaotic dynamics with Lyapunov exponents λ_- and λ_+, the Lyapunov dimension is non-integer numbers between 1 and 2.

1.4.8 Chaos

Chaos is the phenomenon of occurrence of bounded non-periodic evolution in completely deterministic nonlinear dynamical systems with high sensitive dependence on initial conditions.

- Deterministic means their future dynamics are fully defined by their initial conditions. That is, the system has no random or noisy inputs or parameters.
- Non-periodic means that there are trajectories which do not settle down to fixed points, periodic orbits, or quasi-periodic orbits as $t \to \infty$.
- The irregular behavior arises from the system's nonlinearity, rather than from noisy driving forces.
- Sensitive dependence on initial conditions means that nearby trajectories separate exponentially fast, i.e., the system has a positive Lyapunov exponent.

The effect of nonlinearity often renders a periodic solution unstable for certain parametric choices. While nonlinearity does not guarantee chaos, its make the chaotic existence possible [38, 39, 51].

The positive Lyapunov exponent is the spirit of deterministic chaos.

1.4.9 Mathematical Tools for State-Dependent System

In this section, basic concepts of the state-dependent impulsive theory are reviewed.

Definition 1.4.9. (Poincare Map): Consider $\widehat{x}(t)$ be a periodic solution through the point x^* of the system

$$\frac{dx(t)}{dt} = F(x)$$

If $\prod$ be a hyperplane perpendicular to $\widehat{x}(t)$ at the point x^*, then for any point x near x^*, the solution curve through x will cross $\prod$ again at a point $M(x)$, near x^*. The map $M : N \subset \prod \to \prod$.

$$x \to M(x)$$

is called the Poincare map for the periodic orbit. Further, x^* is a fixed point for M, when $M(x^*) = x^*$.

Definition 1.4.10. (Stability of Periodic Orbits): The periodic solution $\widehat{x}(t)$ of the system $(1.2.2) - (1.2.3)$ is stable if for each $\epsilon > 0$, there exists a δ such that

$$|| \, x - x^* \, || < \delta \Longrightarrow || \, M^n(x) - x^* \, || < \epsilon.$$

Definition 1.4.11. (Asymptotic Stability of Periodic Orbits): The periodic solution $\widehat{x}(t)$ of the system $(1.2.2) - (1.2.3)$ is asymptotically stable if it is stable and there exists a $\delta > 0$ such that

$$|| \, x - x^* \, || < \delta \Longrightarrow \lim_{n \to \infty} M^n(x) = x^*.$$

The periodic solution is called asymptotic orbitally stable.

Definition 1.4.12. A trajectory of the system $(1.2.2) - (1.2.3)$ is said to be of order k-periodic if there exists a positive integer $k \geq 1$ such that k is the smallest integer for $y_0 = y_k$.

Definition 1.4.13. A solution $(x(t), y(t))$ of the system $(1.2.2) - (1.2.3)$ is said to be semi-trivial solution if one of its components is zero and another is nonzero.

1.4.10 Analogue of Poincare Criterion

The state dependent impulsive system (1.2.2) − (1.2.3) can be rewritten as:

$$\begin{cases} \dfrac{dx}{dt} = G_1(x,y), & \dfrac{dy}{dt} = G_2(x,y) \quad \text{if } \Phi(x,y) \neq 0, \\ \Delta x(t) = \alpha_1(x,y), & \Delta y(t) = \beta_1(x,y) \quad \text{if } \Phi(x,y) = 0 \end{cases} \tag{1.4.37}$$

The function $\Phi(x,y)$ is a sufficiently smooth function on a neighborhood of the points $\psi(t_k), \phi(t_k)$ such that grad$\Phi(x,y) \neq 0$ and t_k is the moment of the k^{th} jump, where $k \in \aleph$. Let the suffix k demotes the evaluation at the point $\psi(t_k^+), \phi(t_k^+)$.

Let system admits a $T-$ periodic solution $x = \psi(t)$, $y = \phi(t)$,$\psi(t+T) = \psi(t)$ and $\phi(t+T) = \phi(t)$. Define Δ_k as:

$$\Delta_k = \frac{G_{1+}\left(\frac{\partial\beta_1}{\partial y}\frac{\partial\Phi}{\partial x} - \frac{\partial\beta_1}{\partial x}\frac{\partial\Phi}{\partial y} + \frac{\partial\Phi}{\partial x}\right) + G_{2+}\left(\frac{\partial\alpha_1}{\partial x}\frac{\partial\Phi}{\partial y} - \frac{\partial\alpha_1}{\partial y}\frac{\partial\Phi}{\partial x} + \frac{\partial\Phi}{\partial y}\right)}{G_1\frac{\partial\psi}{\partial x} + G_2\frac{\partial\phi}{\partial y}}$$

The multiplier λ is defined as:

$$\lambda = \prod_{k=1}^{q} \Delta_k exp\left[\int_0^T \left(\frac{\partial G_1}{\partial x}(\psi(t),\phi(t)) + \frac{\partial G_2}{\partial y}(\psi(t),\phi(t))\right) dt\right],$$

The T-periodic solution $x = \psi(t)$, $y = \phi(t)$ of the system (1.2.2) − (1.2.3) is orbitally asymptotically stable if the multiplier λ satisfies the condition $\mid \lambda \mid < 1$. The proofis referred to [202].

Let $\phi(t)$ be a fundamental matrix of impulsive system (1.2.2) − (1.2.3), then there exists a unique non-singular matrix $B \in C^{n\times n}$ such that

$$\phi(t+nT) = \phi(t)B, \quad t \in R, \tag{1.4.38}$$

The matrix B is the monodromy matrix [120] of the impulsive system (1.2.2) − (1.2.3) (corresponding to the fundamental matrix). A monodromy matrix is the inverse of the fundamental matrix of a system of ODEs evaluated at zero times the fundamental matrix evaluated at the period of coefficients of the system. All monodromy matrices of the system (1.2.2) − (1.2.3) are similar and have the same eigenvalues. The eigenvalues $\mu_j, j = 1, 2, ..., n$ of the monodromy matrices are called the Floquet multipliers of the system (1.2.2) − (1.2.3) [120].

Floquet Theory: The stability of periodic solution can also be studied in terms of characteristic or Floquet multiplier. Then, the T-periodic impulsive system (1.2.2) − (1.2.3) is

- Stable if and only if all multipliers μ_j, $j = 1, 2, ..., n$ satisfy the inequality $\mid \mu_j \mid \leq 1$.
- Asymptotically stable if and only if all multipliers μ_j, $j = 1, 2, ..., n$ satisfy the inequality $\mid \mu_j \mid < 1$.
- Unstable if $\mid \mu_j \mid > 1$ for some $j = 1, 2, ..., n$.

1.5 Literature Survey

A brief literature survey is presented that includes the studies of those articles which are related to the research work of this thesis.

Several mathematical models have been investigated in literature by considering different aspects such as stage structure [3, 4, 10, 78, 79, 121, 124, 164, 191], residual effect [126, 221], integrated pest management strategy [14, 84, 233], state dependent [214, 229] etc. which are helpful for pest control.

This thesis is mainly focused on pest control. The success of any pest management regime depends on the control methods, their timings and the dynamics of biological species. Many mathematical models are developed to predict the success of a pest management plan using different mechanisms for controlling pests. The chemical control is a common and more effective method for pest control. When the pesticide is sprayed, the pest density abruptly reduces to a lower level [92, 225]. For the process of effective pest control, excessive use of a single control strategy is undesirable. Therefore, different pest-control techniques should work together rather than alone. Also, to reduce the use of chemical, non-chemical control strategies should be combined with it [31, 58]. Some mathematical models incorporate the dynamics of pest when chemical control /biological controls are applied continuously [30, 158, 184, 185, 206] or impulsively [8, 97, 170, 189, 216, 234]. Tang et al. [222] proposed an impulsive pest-natural enemy model in which periodically spraying pesticides and releasing natural enemies were considered. They investigated three cases in terms of different patterns of insecticide applications.

As most of the pest species go through many life stages: immature stage and mature stage. Their vital rates depend on age, size, or development stage which can have

a significant influence on the dynamics at the population level. In order to understand the dynamics of pests, it is necessary to consider this diversity adequately into account [157]. The stage structure of pest population is critical as different stages of pest respond differently to chemical / biological controls. For example, Saltcedar leaf beetle is such a pest for which eggshell, pathogens may not be effective against pest eggs. Another example is pesticides are not effective against the immature stage of the pest. Therefore, incorporation of the stage-structured pest population is necessary for the implementation of control strategies. Stage-structured population models are widely used to examine the importance of different life stages. The concept of compartmental models have been received much attention because such type of models are simpler than the models governed by partial differential equations. Also, these models can exhibit similar phenomena as the models based on partial differential equations [16]. The delayed ODE juvenile-adult models [78, 79], compartmental ODE models without delay [10, 218, 219] and difference equation models [51] have been investigated.

The mathematical, as well as biological approach of a single-species growth model with stage-structured has been discussed by Aiello and Freedman [3]. The effect of impulsive harvesting of the pest on a stage-structured pest-natural enemy model has been discussed [204]. Some stage-structured predator-prey systems for pest control have been addressed with the impulse to model the process of periodically releasing natural enemies [175, 196].

In some models, the continuous reproduction of population is removed from the models and replaced with a birth pulse. The effect of density-dependent birth pulses and stage-structured has been considered by Sanyi Tang and Lansun Chen [218]. The author analyzed the dynamics of the system by using the stroboscopic map for different density-dependent birth pulses. Many authors have investigated harvesting models with stage-structured and birth pulse [86, 96, 220]. Roberts and Kao et al. [187] investigated a model for the dynamics of a fatal infectious disease with the birth pulse. They discussed the existence and the stability of periodic solutions. Several single-species models have also been proposed with impulsive control strategies and birth pulses [61, 131, 149, 219]. Some work of integrated pest management model with birth pulses have also been done for pest control [86, 96]

Sometimes chemical pesticides have a residual effect on pest control, that is, the amount of pesticide may remain on or in a crop/pest after it has been applied [155, 209, 230]. Some examples of pesticides with residual effects can be found in [114, 195, 221]. To model the effect of the pesticides, Panetta et al. [172, 174] addressed continuous or piecewise-continuous periodic functions. The threshold value is obtained. Very few mathematical models on pest control with residual effect have been available in literature [103, 126, 221]. Liang et al. [126] have considered the effect of delayed response to the pesticides on the pest and natural enemy. They have used the continuous periodic function to model the residual effect with a delayed response of the pesticide.

These models assume that the pest population killed instantaneously. However, real scenario is not always the same. In particular, pesticide appears in the environment first, after that it is absorbed by the pest, and then the pest is affected which is the toxicity of pesticide. It does not affect the pest immediately, it will remain for a short-time period in the field before toxins are capable of decreasing the growth rate of the pest [136]. Therefore, it is necessary to introduce the effect of toxicant input to model the pest-control system.

Most toxicant-population models are based on the work of Hallam and his coworkers [75, 76, 77]. Some continuous mathematical population models with toxicant effect have been studied [66, 162, 197, 198]. Some of the single/multiple population systems with toxicant effect have been investigated [98, 128, 133, 134, 135, 136]. However, the majority of these studies has been emphasized on the effects of toxicant emitted into the environment from industrial and household resources on biological species. But very few literature is found for pest-control problems with pesticide toxin input [31, 133, 136]. Recently, Liu et al. [133] have also investigated a stage-structured model for pest control. They have modeled the impulsive system by introducing a constant periodic pesticide input and releasing natural enemies at the different fixed moment. They impulsive pest control models have also been proposed with birth pulses in the polluted environment [148]. The effects of pulse harvesting time on the maximum annual-sustainable yield has been analyzed. Liu et al. [144] employed two species system in a polluted environment with a birth pulse and obtained the conditions for a

positive periodic solution.

Biological control is the reduction in the pest populations from the releasing of natural enemies or beneficial species [40, 41]. Many authors have employed impulsive pest-natural enemy systems to investigate the dynamics of pest control model [7, 9, 137, 138, 142, 147]. Liu et al. [142] investigated the predator-prey system by periodic impulsive immigration of natural enemies and establish the conditions for pest extinction. Liu et al. [138] ignored the side effects of pesticide on natural enemies. Also, they assumed that the time of spraying pesticide and releasing natural enemies is synchronous. Further, the effects of pesticide on natural enemies have been incorporated and a predator-prey impulsive system with integrated pest strategies at the different fixed time has been discussed [137]. Lu et al. [147] analyzed the pest-predator model under insecticides used impulsively. They have focused on the effects of the fraction of population which died due to the pesticide. They concluded that different pest control techniques should work together rather than a single tactic.

However, these studies only consider impulsive control at fixed time intervals to eradicate the pest population. Such control measure of pest management is called fixed-time control strategy, modeled by impulsive differential equations. Although this control measure is better than the classical one, it has shortcomings. In recent years, in order to overcome such drawbacks, several researchers have started paying attention to another control measure based on the state feedback control strategy, which is taken only when the amount of the monitored pest population reaches a threshold value [92, 93, 94, 95]. Obviously, this control measure is more effective and economical for pest control [179, 237, 244]. The impulsive stage-structured system has been discussed with state feedback control [93]. Many mathematical models have been studied for interactions between pest, natural enemy, and pesticides in the last decades. The interactions between pest and the natural enemy is a predator-prey interaction.

The population dynamics of predator-prey interactions can be modeled by using the Lotka-Volterra equations [210, 211]. Several investigations have been carried out for two species, ecological models incorporating species interactions and non-linear functional responses [33, 46, 56, 71, 73, 82, 83, 107, 109, 123, 161, 208, 232]. Several mathematical models have incorporated pest-natural systems (prey-predator) using

state dependent impulsive effects [92, 95, 169, 223, 229]. Jiang et al. [92, 95] obtained the sufficient conditions of existence and stability of semi-trivial solution, and positive periodic solution by using the Poincar map.

Time delay plays an important role in the ecological system. The delay may occur due to gestation time of natural enemy and maturation time of pest. Delay-induced destabilization and oscillations can be observed in predator-prey models [36, 60, 163]. Therefore, consideration of delay effect in the pest-natural enemy model is realistic. In recent years, significant progress has been made in the theory of impulsive ordinary differential equations and delayed differential equations. However, a number of difficulties are realized while dealing with delay differential equations [143]. Difficulty level may be elevated when delay incorporated in impulsive systems.

Few researchers study dynamical systems with delay and state-dependent impulses [43, 44] and they tend to focus more on a purely mathematical point of view. Moreover, the stability of the system is usually investigated by constructing a Lyapunov function which is complex and not easy to get [141].

In the next section, summary of the thesis is presented.

1.6 Organization of the Thesis

The thesis includes total ten chapters, organized as follows:

Chapter 1 is the introductory part of the thesis in which all basic components regarding pest control models are discussed. It is followed by the literature survey. Furthermore, thesis summary has also been incorporated.

Chapter 2 employs an impulsive pest control system with single tactics. The stage-structured system consists of the mature and immature pest. Birth pulses occur at regular intervals to release immature pest. The Ricker type birth function is assumed. The pest population is controlled by the periodic spray of chemical pesticides killing mature as well as immature pest instantaneously. This is synchronized with birth pulses. The discrete dynamical system determined by the stroboscopic map is analyzed. The threshold condition for the stability of the pest-free state is obtained and the existence of a period-1 solution is established. Finally, numerical simulations

show the complex dynamics of the model. There exists a characteristic sequence of bifurcations above the threshold value of birth rate leading to chaos. Periodic halving bifurcations are also observed in some cases.

In **chapter** 3, the birth pulses and chemical spray are no more synchronous. It is assumed that both are used with the same periodicity. The problem of finding a non-trivial periodic solution is reduced to the existence of a non-trivial fixed point of the associated stroboscopic map. The effect of pesticide spray timing on the threshold condition of pest eradication is studied. It is shown that once a threshold condition is reached, a stable a non-trivial periodic solution emerges via bifurcation. More complex dynamical behaviors are observed in this case as compared to synchronous pesticide spray.

In **chapter** 4, a stage-structured pest control model using pesticides with residual effects is discussed. Birth pulses and chemical sprays are assumed to be asynchronous. The pesticide is considered to have residual effects on immature as well as a mature pest. The residual pesticide has a long-time continuous effect on the pest which can be described by the kill function. The conditions for the existence of pest eradication as well as a non-trivial period-1 solution are obtained and their stabilities are discussed. The conditions of transcritical and flip bifurcation are established. The effects of various model parameters on the threshold conditions are investigated. Finally, numerical simulations depict the complex dynamical behaviors of the model. There exists a characteristic sequence of bifurcations above the threshold value of parameter leading to chaos. Periodic halving bifurcations are also observed in some cases.

In **chapter** 5, integrated pest management approach comprising of chemical and mechanical control is investigated. It is assumed that chemical control and birth pulse occur at same fixed times. The pesticide is assumed to kill the only mature pest. Further, the continuous mechanical effort (harvesting) is applied to control the immature pest. The Beverton-Holt type of birth function and the differential death rates for mature and immature pest are considered. The discrete system obtained from the stroboscopic map is analyzed for the dynamical behavior of the system. The existence of the pest-free state and positive period-1 solution is investigated. The threshold conditions for the stability of pest-free state as well as a period-1 solution

are investigated. The effect of killing rate due to mechanical and chemical control on the basic reproduction number is shown. Numerical simulations have been performed to show complex dynamical behavior. Another model incorporates asynchronous pulses. The harvesting reduces the complexity of the system. The chances of pest eradication also increase with less toxic pesticides.

In **chapter** 6, an impulsive model with three pulses of the same periodicity is introduced. Mechanical control, chemical control, and birth pulse occur at different fixed times. Discrete system obtained from the stroboscopic map is analyzed. The conditions for the stability of pest-free state as well as a period-1 solution are investigated. The effect of harvesting and pesticide spray timing on pest is shown. The existence of transcritical bifurcation has been established. Numerical simulations are performed to show the complex dynamical behavior. The period-doubling bifurcation is observed. Also, above the threshold level, there is a characteristics sequence of bifurcation leading to chaotic dynamics.

In **chapter** 7, integrated pest management approach comprising the chemical as well as mechanical control is considered. The delayed response of residual pesticide is incorporated. Mechanical control and birth pulse occur at different fixed times. However, the periodic mechanical effort is applied asynchronously. The discrete system obtained from the stroboscopic map is analyzed for the dynamical behavior of the system. The existence of the pest-free solution and positive period-1 solution are investigated. The threshold conditions for the stability of pest-free state as well as a period-1 solution are investigated. Due to a delayed response, the threshold value for pest eradication decreases.

Chapter 8 deals with a single species stage-structured impulsive pest control model with birth pulses. In this model, the pest density is controlled by spraying toxic pesticides and cultural control. Also, the effect of pesticide's toxicity to the environment as well as to the pest is considered. The discrete dynamical system determined by the stroboscopic map is analyzed. Sufficient conditions for the stability of pest-free State as well as the non-trivial period-one solution are obtained. Numerical simulations are carried out to illustrate our theoretical results and facilitate their interpretation.

Chapter 9 describes delay differential pest-natural enemy system with impulsive

state feedback control. Chemical and biological controls are applied to control the pest. Boundedness of solution is analyzed using the comparison theorem. The Poincare map is used to discuss the dynamics of an impulsive system. Sufficient conditions for the existence and stability of natural enemy-free positive period-1 solution are obtained. When semi-trivial periodic solution loses its stability, the existence and stability of the non-trivial period solution are also established. Complex dynamical behavior, including chaos is obtained. Numerical simulations substantiate the analytical results.

Chapter 10 incorporates the conclusions and the future scope of the work.

Chapter 2

An Impulsive Stage-Structured Pest Control Model Using Chemical Control Synchronized with Birth Pulse

2.1 Introduction

In agricultural systems, chemical pesticides are commonly used for controlling pest as they are relatively cheap and instantaneously reduce the pest load. In most instances, pesticide spray occurs in pulses and is modeled as impulsive systems. Generally, pest responds differently to pesticides depending on their life stages. This makes the incorporation of stage-structure in the pest control models inevitable.

Many pest management models without stage-structure have been developed assuming continuous growth of pest [63, 88, 97, 138, 216]. Some impulsive models have also been investigated incorporating stage structure [93, 196, 238]. Very few models for pest control are available incorporating birth pulses [131]. However, impulsive models with birth pulses have been discussed in other contexts [86, 144, 187, 219]. A single-species stage-structured model with birth pulses has been studied by Sanyi Tang and Lansun Chen [218]. Stage-structured harvesting model with birth pulses have been discussed [96, 148, 220]. In most of the stage-structured models, death rates

for immature and mature populations are considered to be the same which may not be realistic.

In the present chapter, a stage-structured pest control model with a birth pulse is proposed and analyzed. Different mortality rates are considered for the immature and mature pest. Further, different killing rates due to pesticides are also considered. The spray timing is synchronized with the birth pulse.

2.2 Model Formulation

Let a be the constant maturation rate and d_i, $i = 1, 2$ be the constant mortality rates of immature and mature pest. The system (1.3.2) is written as:

$$\begin{aligned} \frac{dx}{dt} &= B(N(t))y(t) - d_1x(t) - ax(t), \\ \frac{dy}{dt} &= ax(t) - d_2y(t). \end{aligned} \tag{2.2.1}$$

In this chapter, the birth rate function $B(N(t))N(t)$ is assumed to be of Ricker type.

$$B(N) = be^{-N}. \tag{2.2.2}$$

It is assumed that the mature pest reproduce in pulses periodically with period T_1. Let the density of immature and mature pest after m^{th} birth pulse be $x(mT_1)^+$ and $y(mT_1)^+$, respectively. The system (2.2.1) incorporating birth pulses is given as:

$$\left.\begin{aligned} \frac{dx}{dt} &= -d_1x(t) - ax(t), \\ \frac{dy}{dt} &= ax(t) - d_2y(t), \end{aligned}\right\} t \neq mT_1, m = 1, 2, 3, ..., \tag{2.2.3}$$

$$\left.\begin{aligned} x(mT_1)^+ &= (1-k)x(mT_1) + B(N(mT_1))y(mT_1), \\ y(mT_1)^+ &= (1-\mu)y(mT_1), \end{aligned}\right\} t = mT_1. \tag{2.2.4}$$

The pesticide is sprayed on the pest periodically, which instantaneously kills a portion of pest. No residual effect is considered for pesticide. Accordingly, the pesticide spray is modeled as impulsive phenomenon which occurs periodically. As pesticides affect immature and mature pests differently, therefore the differential killing rates k and μ respectively are assumed. Accordingly, periodic pesticide spray at time $t = mT_2$ gives

the following jump conditions:

$$\left.\begin{aligned} x(mT_2)^+ &= (1-k)x(mT_2), \\ y(mT_2)^+ &= (1-\mu)y(mT_2), \end{aligned}\right\} t = mT_2. \tag{2.2.5}$$

Here, the densities of immature and mature pest are $x(mT_2)^+$ and $y(mT_2)^+$ respectively just after pesticide spray. For simplicity, it is further assumed that new births and chemical spray of pesticide are synchronized, i.e. $T_1 = T_2 = T$. Accordingly, the impulsive conditions (2.2.4) and (2.2.5) can be combined as:

$$\left.\begin{aligned} x(mT)^+ &= (1-k)x(mT) + B(N(mT))y(mT), \\ y(mT)^+ &= (1-\mu)y(mT), \end{aligned}\right\} t = mT.$$

The dynamics of stage-structured impulsive pest control system defined on the set $\Re^2_+ = \{(x,y) \in \Re^2 \mid x \geq 0, y \geq 0\}$ with positive model parameters is written as:

$$\left.\begin{aligned} \frac{dx}{dt} &= -d_1 x(t) - a x(t), \\ \frac{dy}{dt} &= a x(t) - d_2 y(t), \end{aligned}\right\} t \neq mT, \tag{2.2.6}$$

$$\left.\begin{aligned} x(mT)^+ &= (1-k)x(mT) + B(N(mT))y(mT), \\ y(mT)^+ &= (1-\mu)y(mT), \end{aligned}\right\} t = mT, \tag{2.2.7}$$

$$x(0) = x_0 > 0, \qquad y(0) = y_0 > 0. \tag{2.2.8}$$

Equations (2.2.7) represent the synchronous birth pulses and chemical spray at times $t = mT$, T being the periodicity of the two pulses. The system (2.2.6) − (2.2.8) is associated with the initial conditions (2.2.8).

2.3 Model Analysis

Let the immature and mature pest densities be $x = x_{m-1}$ and $y = y_{m-1}$ at $t = (m-1)T$ respectively. The analytical solution of the differential equations (2.2.6) between the birth pulses $(m-1)T \leq t < mT$ is obtained as:

$$\begin{aligned} x(t) &= e^{-(a+d_1)(t-(m-1)T)} x_{m-1}, \\ y(t) &= \left(\frac{a(1 - e^{(\epsilon - a)(t-(m-1)T)})}{a - \epsilon} x_{m-1} + y_{m-1} \right) e^{-d_2(t-(m-1)T)}, \\ \epsilon &= d_2 - d_1. \end{aligned} \tag{2.3.1}$$

The following map can be obtained from (2.3.1) by applying impulsive condition (2.2.7):

$$\begin{aligned} x_m &= f(x_{m-1}, y_{m-1}), \quad y_m = g(x_{m-1}, y_{m-1}), \\ f(x_{m-1}, y_{m-1}) &= (1-k)e^{-(a+d_1)T}x_{m-1} + b \times exp[-(e^{-(a+d_1)T} + \hat{\beta})x_{m-1} + e^{-d_2T}y_{m-1}] \\ &\quad \times[\hat{\beta}x_{m-1} + e^{-d_2T}y_{m-1}], \\ g(x_{m-1}, y_{m-1}) &= (1-\mu)(\hat{\beta}x_{m-1} + e^{-d_2T}y_{m-1}), \\ \hat{\beta} &= \frac{ae^{-d_2T}(1-e^{(\epsilon-a)T})}{a-\epsilon}. \end{aligned} \tag{2.3.2}$$

The map (2.3.2) constitutes difference equations. These equations describe the densities of immature and mature pest at m^{th} pulse in terms of values at previous pulse. This is stroboscopic sampling at the time when the birth pulse (chemical spray) occurs. For the Ricker Function, the dynamical behavior of the system (2.2.6) − (2.2.8) will be given by the dynamical behavior of the map (2.3.2) coupled with the system (2.3.1).

Let R_0 be the intrinsic net reproductive number denoting the average number of offspring that an individual produces over the period of its lifetime [146]. Define

$$b_0 = \hat{\beta}^{-1}[(1-(1-k)e^{-(d_1+a)T})(1-(1-\mu)e^{-d_2T})],$$

$$R_0 = b\ b_0^{-1}. \tag{2.3.3}$$

2.3.1 Existence of Fixed Points

The fixed points of the map (2.3.2) are obtained by solving the system $x = f(x, y)$, $y = g(x, y)$. Accordingly, the stroboscopic map (discrete dynamical system) (2.3.2) admits the following two fixed points:

1. The unique pest-free state $E_0 = (0, 0)$ exists without any parametric restriction.

2. The non-trivial fixed point $E^* = (x^*, y^*)$ is obtained as:

$$\begin{aligned} x^* &= \frac{(\epsilon-a)(1-(1-\mu)e^{-d_2T})\log(R_0)}{a(R+1)e^{-d_2T}(e^{(\epsilon-a)T}-1)}, \\ y^* &= \frac{(1-\mu)\log(R_0)}{R+1}, \\ R &= \frac{be^{-(d_1+a)T}}{R_0(1-(1-k)e^{-(d_1+a)T})}. \end{aligned}$$

Consequently, the interior point exists for $R_0 > 1$, for biological feasible choices of ϵ and a. If $R_0 = 1$ then interior fixed point collides with the pest-free state, i.e. $E^* = E_0$.

2.3.2 Local Stability Analysis of Fixed Points

Let $X = (x, y)$ be any arbitrary fixed point. The local stability about the fixed point is based upon the standard linearization technique. The linearized system corresponding to (2.3.2) about $X = (x, y)$ is given by:

$$X_m = AX_{m-1}. \tag{2.3.4}$$

The coefficients of the matrix $A = (a_{ij})_{2\times 2}$ are:

$$\left.\begin{aligned} a_{11} &= (1-k)e^{-(d_1+a)T} + b \times exp[-(e^{-(d_1+a)T} + \hat{\beta})x - e^{-d_2T}y] \times \{\hat{\beta} \\ &\quad - (\hat{\beta}x + e^{-d_2T}y) \times (e^{-(d_1+a)T} + \hat{\beta})\}, \\ a_{12} &= b \times exp[-d_2T - xe^{-(d_1+a)T} - \hat{\beta}x - e^{-d_2T}y] \times \{1 - (\hat{\beta}x + e^{-d_2T}y)\}, \\ a_{21} &= (1-\mu)\hat{\beta}, \\ a_{22} &= (1-\mu)e^{-d_2T}. \end{aligned}\right\} \tag{2.3.5}$$

The characteristic equation in terms of trace Tr and determinant Det be written as:

$$\lambda^2 - Tr\lambda + Det = 0$$

Theorem 2.3.1. *The fixed point $E_0 = (0, 0)$ of the map (2.3.2) is locally asymptotically stable if*

$$R_0 < 1. \tag{2.3.6}$$

Proof. Using (2.3.5), coefficients of the linearized matrix $A = (a_{ij})_{2\times 2}$ are evaluated about the pest-free state $(0, 0)$ as:

$$\begin{aligned} a_{11} &= (1-k)e^{-(d_1+a)T} + b\hat{\beta}, \qquad a_{12} = be^{-d_2T}, \\ a_{21} &= (1-\mu)\hat{\beta}, \qquad\qquad\quad a_{22} = (1-\mu)e^{-d_2T}. \end{aligned}$$

Accordingly, the trace Tr and determinant Det are computed as:

$$\begin{aligned} Tr &= (1-k)e^{-(d_1+a)T} + b\hat{\beta} + (1-\mu)e^{-d_2T}, \\ Det &= (1-k)(1-\mu)e^{-(d_1+d_2+a)T}. \end{aligned}$$

In the following, it is observed that Jury's conditions (1.4.12) and (1.4.13) are always satisfied:

$$\begin{aligned} 1 + Tr + Det &= (1 + (1-k)e^{-(d_1+a)T})(1 + (1-\mu)e^{-d_2T}) + b\hat{\beta} > 0, \\ 1 - Det &= 1 - (1-k)(1-\mu)e^{-(d_1+d_2+a)T} > 0. \end{aligned}$$

The expression $1 - Tr + Det$ simplifies to:

$$\begin{aligned} 1 - Tr + Det &= 1 - (1-k)e^{-(d_1+a)T} - b\hat{\beta} - (1-\mu)e^{-d_2T} \\ &\quad +(1-k)(1-\mu)e^{-(d_1+a+d_2)T} \\ &= (1-(1-k)e^{-(d_1+a)T})(1-(1-\mu)e^{-d_2T}) - b\hat{\beta}. \end{aligned}$$

Accordingly, the Jury's condition (1.4.11), that is $1 - Tr + Det > 0$ gives:

$$(1-(1-k)e^{-(d_1+a)T})(1-(1-\mu)e^{-d_2T}) \;>\; b\hat{\beta}.$$

i.e.

$$b < (1-(1-k)e^{-(d_1+a)T})(1-(1-\mu)e^{-d_2T})\hat{\beta}^{-1} = b_0. \tag{2.3.7}$$

Using (2.3.3) and (2.3.7), the stability condition (2.3.6) is obtained. □

Thus, the pest eradication is possible when $R_0 < 1$ and the trajectories of the map (2.3.2) in the neighborhood of $(0,0)$ tend to origin. The existence of non-trivial fixed point is overruled in this case. From (2.3.3) and (2.3.6), the fixed point $(0,0)$ is locally stable for $b \in (0, b_0)$.

When $R_0 > 1$, the fixed point $(0,0)$ is unstable and non-trivial fixed point E^* exists in this case. The next theorem establishes the local stability of E^*.

Theorem 2.3.2. *Let us denote*

$$\begin{aligned} C &= 2[\epsilon(e^{d_2T} - (1-\mu)) + ae^{2(a-\epsilon)T}((1-\mu) - e^{(d_1+a)T})](1 + (1-k)(1-\mu)e^{-(d_1+d_2+a)T}), \\ F &= [\epsilon(e^{d_2T} + (1-\mu)) - ae^{2(a-\epsilon)T}((1-\mu) + e^{(d_1+a)T})](1-(1-k)e^{-(d_1+a)T}) \\ &\quad \times(1-(1-\mu)e^{-d_2T}). \end{aligned}$$

The non-trivial fixed point $E^* = (x^*, y^*)$ is locally asymptotically stable provided

$$b_0 < b < b_0\ exp(CF^{-1})(= b_c). \tag{2.3.8}$$

Proof. Using (2.3.5), coefficients of linearized matrix A are computed around E^* as:

$$\begin{aligned} a_{11} &= (1-k)e^{-(d_1+a)T} + b_0[\hat{\beta} - (\hat{\beta}x^* + y^*e^{-d_2T})(e^{-(d_1+a)T} + \hat{\beta})], \\ a_{12} &= b_0e^{-d_2T}[1 - (\hat{\beta}x^* + e^{-d_2T}y^*)], \quad a_{21} = (1-\mu)\hat{\beta}, \quad a_{22} = (1-\mu)e^{-d_2T}. \end{aligned}$$

The trace Tr and determinant Det are computed as:

$$\begin{aligned} Tr &= (1-k)e^{-(d_1+a)T} + b_0[\hat{\beta} - (\hat{\beta}x^* + e^{-d_2T}y^*)(e^{-(d_1+a)T} + \hat{\beta})] + (1-\mu)e^{-d_2T}, \\ Det &= e^{-(d_1+d_2+a)T}[(1-k)(1-\mu) - b_0y^*]. \end{aligned}$$

It is observed that Jury's conditions (1.4.11) and (1.4.13) are always satisfied:

$$\begin{aligned} 1 - Tr + Det &= 1 - (1-k)e^{-(d_1+a)T} - b_0[(\hat{\beta} - (\hat{\beta}x^* + e^{-d_2T}y^*)(e^{-(d_1+a)T} + \hat{\beta})] \\ &\quad -(1-\mu)e^{-d_2T} + e^{-(d_1+d_2+a)T}[(1-k)(1-\mu) - b_0y^*] \\ &= (1-(1-k)e^{-(d_1+a)T})(1-(1-\mu)e^{-d_2T}) - b_0[\hat{\beta} - (\hat{\beta}x^* + e^{-d_2T}y^*) \\ &\quad \times(e^{-(d_1+a)T} + \hat{\beta}) - e^{-(d_1+d_2+a)T}y^*] \\ &= (1-(1-k)e^{-(d_1+a)T})(1-(1-\mu)e^{-d_2T})(1 - \log(R_0) > 0, \\ 1 - Det &= 1 - e^{-(d_1+d_2+a)T}[(1-k)(1-\mu) - b_0y^*] > 0. \end{aligned}$$

The expression $1 + Tr + Det$ simplifies to:

$$\begin{aligned} 1 + Tr + Det &= 1 + (1-k)e^{-(d_1+a)T} + b_0[(\hat{\beta} - (\hat{\beta}x^* + e^{-d_2T}y^*)(e^{-(d_1+a)T} + \hat{\beta})] \\ &\quad +(1-\mu)e^{-d_2T} + e^{-(d_1+d_2+a)T}[(1-k)(1-\mu) - b_0y^*] \\ &= (1+(1-k)e^{-(d_1+a)T})(1+(1-\mu)e^{-d_2T}) + b_0[\hat{\beta} - (\hat{\beta}x^* + e^{-d_2T}y^*) \\ &\quad \times(e^{-(d_1+a)T} + \hat{\beta}) + e^{-(d_1+d_2+a)T}y^*] \\ &= (1+(1-k)e^{-(d_1+a)T})(1+(1-\mu)e^{-d_2T}) \\ &\quad +(1-(1-k)e^{-(d_1+a)T})(1-(1-\mu)e^{-d_2T}) \\ &\quad \times\left[1 - \frac{\epsilon(e^{d_2T} + (1-\mu)) - ae^{2(a-\epsilon)T}((1-\mu) + e^{(d_1+a)T})}{\epsilon(e^{d_2T} - (1-\mu)) + ae^{2(a-\epsilon)T}((1-\mu) - e^{(d_1+a)T})}\log(R_0)\right]. \end{aligned}$$

Accordingly, Jury's condition (1.4.12), $1 + Tr + Det > 0$, gives

$$R_0 < exp\left(\frac{2[\epsilon(e^{d_2T} - (1-\mu)) + H](1 + (1-k)(1-\mu)e^{-(d_1+d_2+a)T})}{[\epsilon(e^{d_2T} + (1-\mu)) - H](1-(1-k)e^{-(d_1+a)T})}\right), \tag{2.3.9}$$

where $H = ae^{2(a-\epsilon)T}((1-\mu) - e^{(d_1+a)T})$.

Therefore, using (2.3.9) and (2.3.3) with the existence condition $b_0 < b$ gives the required condition (2.3.8). □

Since the fixed point E^* is locally stable, the trajectories of the system (2.2.6) – (2.2.8) approach to the following period-1 solution $(x_e(t), y_e(t))$ for $b_0 < b < b_c$:

$$\begin{aligned} x_e(t) &= e^{-(a+d_1)(t-(m-1)T)}x^*, \qquad (2.3.10) \\ y_e(t) &= \left(\frac{a(1-e^{(\epsilon-a)(t-(m-1)T)})}{(a-\epsilon)}x^* + y^*\right)e^{-d_2(t-(m-1)T)}, \qquad (m-1)T < t < mT. \end{aligned}$$

Consequently, periodic solution (2.3.10) of the system $(2.2.6)-(2.2.8)$ is locally asymptotically stable in the range $b_0 < b < b_c$.

Further increasing the value of b beyond b_c, the fixed point E^* losses its stability and the system $(2.2.6)-(2.2.8)$ may exhibit complex dynamics. The bifurcation analysis at $b = b_0$ and $b = b_c$ is carried out in the next section.

2.3.3 Bifurcation Analysis

It is observed that the pest-free state $E_0 = (0, 0)$ becomes non-hyperbolic as one of the eigenvalues becomes 1 at $b = b_0$ ($R_0 = 1$). At $R_0 = 1$, the interior fixed point E^* collides with E_0. Thus, as b increases through b_0, interior fixed point $E^* = (x^*, y^*)$ passes through the fixed point at $(0, 0)$ and exchange their stabilities at $b = b_0$. Theorem 1.4.3 and Center Manifold Theorem 1.4.5 are used to characterize the nature of bifurcation point $b = b_0$ in the following theorem:

Theorem 2.3.3. *The map* (2.3.2) *undergoes transcritical bifurcation at* $b = b_0$.

Proof. Consider the map

$$\begin{pmatrix} x \\ \\ y \end{pmatrix} \to \begin{pmatrix} b \times (\hat{\beta}x + e^{-d_2T}y) \times exp[-e^{-(d_1+a)T}x - \hat{\beta}x - e^{-d_2T}y] \\ +(1-k)e^{-(d_1+a)T}x \\ (1-\mu)(\hat{\beta}x + e^{-d_2T}y) \end{pmatrix}. \quad (2.3.11)$$

Let $x = u$, $y = v$, $b = b_0 + b_1$. The fixed point E_0 of the map (2.3.2) is transformed to (u, v) and the map (2.3.11) becomes:

$$\begin{pmatrix} u \\ \\ v \end{pmatrix} \to \begin{pmatrix} (1-k)e^{-(d_1+a)T}u + (\hat{\beta}u + e^{-d_2T}v) \times (b_1 + b_0) \\ \times exp[-e^{-(a+d_1)T}u - \hat{\beta}u - e^{-d_2T}v] \\ (1-\mu)(\hat{\beta}u + e^{-d_2T}v) \end{pmatrix}. \quad (2.3.12)$$

The map (2.3.12) can be rewritten as:

$$\begin{pmatrix} u \\ \\ v \end{pmatrix} \to M \begin{pmatrix} u \\ \\ v \end{pmatrix} + \begin{pmatrix} -b_0[e^{-2d_2T}v^2 + (\hat{\beta}^2 + \hat{\beta}e^{-(d_1+a)T})u^2 \\ +e^{-d_2T}uv(2\hat{\beta} + e^{-(d_1+a)T})] + e^{-d_2T}b_1v + \hat{\beta}b_1u \\ 0 \end{pmatrix} \quad (2.3.13)$$

The matrix M is obtained as:

$$M = \begin{pmatrix} (1-k)e^{-(d_1+a)T} + b_0\hat{\beta} & b_0e^{-d_2T} \\ (1-\mu)\hat{\beta} & (1-\mu)e^{-d_2T} \end{pmatrix}.$$

The eigenvalues of M are 1 and $(1-k)(1-\mu)e^{-(a+d_1+d_2)T}$.

The corresponding eigenvectors V_1 and V_2 are $\{v_1, 1\}^T$ and $\{v_2, 1\}^T$ respectively where $v_1 = (1-(1-\mu)e^{-d_2T})(1-\mu)^{-1}\hat{\beta}^{-1}$ and $v_2 = [-e^{-d_2T}(1-(1-k)e^{-(d_1+a)T})]\hat{\beta}^{-1}$.

Consider the transformation

$$\begin{pmatrix} u \\ v \end{pmatrix} = J \begin{pmatrix} \bar{x} \\ \bar{y} \end{pmatrix}, \qquad J = (V_1 \;\; V_2).$$

Using (2.3.13) and further, simplification gives:

$$\begin{pmatrix} \bar{x} \\ \bar{y} \end{pmatrix} \to \begin{pmatrix} 1 & 0 \\ 0 & (1-k)(1-\mu)e^{-(d_1+d_2+a)T} \end{pmatrix} \begin{pmatrix} \bar{x} \\ \bar{y} \end{pmatrix} + \begin{pmatrix} f_1(\bar{x}, \bar{y}, b_1) \\ f_2(\bar{x}, \bar{y}, b_1) \end{pmatrix}, \quad (2.3.14)$$

where

$$\begin{aligned} f_1(\bar{x}, \bar{y}, b_1) &= a_1 b_1 \bar{x} + a_2 b_1 \bar{y} + a_3 \bar{x}\bar{y} + a_4 \bar{x}^2 + a_5 \bar{y}^2, \\ f_2(\bar{x}, \bar{y}, b_1) &= -f_1(\bar{x}, \bar{y}, b_1), \end{aligned}$$

$$\begin{aligned}
a_1 &= \psi^{-1}[e^{-d_2T} + (1-(1-\mu)e^{-d_2T})(1-\mu)^{-1}], \\
a_2 &= \psi^{-1}[e^{-d_2T} - (1-(1-k)e^{-(d_1+a)T})e^{-d_2T}], \\
a_3 &= \psi^{-1}\Bigg[-2e^{-d_2T} - 2\left(\frac{(1-(1-k)e^{-(d_1+a)T})(1-(1-\mu)e^{-d_2T})}{(1-\mu)\hat{\beta}^2}\right)(\hat{\beta}^2 + e^{-2(d_1+a)T}) \\
&\quad -(2\hat{\beta} + e^{-(d_1+a)T})\left(\frac{(1-(1-\mu)e^{-d_2T})}{(1-\mu)\hat{\beta}} - \frac{e^{-d_2T}(1-(1-k)e^{-(d_1+a)T})}{\hat{\beta}}\right)\Bigg] b_0 e^{-d_2T}, \\
a_4 &= \psi^{-1}\Bigg[-e^{-d_2T} - \left(\frac{(1-(1-\mu)e^{-d_2T})^2}{(1-\mu)\hat{\beta}}\right)(\hat{\beta}^2 + \beta e^{-2(d_1+a)T}) - e^{-d_2T}(2\hat{\beta} + e^{-(d_1+a)T}) \\
&\quad \times(1-(1-\mu)e^{-d_2T})(1-\mu)^{-1}\hat{\beta}^{-1}\Bigg)\Bigg] b_0, \\
a_5 &= \psi^{-1}\Bigg[-1 - e^{-d_2T}(1-(1-k)e^{-(d_1+a)T})^2\hat{\beta}^{-2}(\hat{\beta}^2 + \beta e^{-2(d_1+a)T}) \\
&\quad +(2\hat{\beta} + e^{-(d_1+a)T}) \times (1-(1-k)e^{-(d_1+a)T})\hat{\beta}^{-1}\Bigg] b_0 e^{-d_2T}, \\
\psi &= [1-(1-\mu)(1-k)e^{-(d_1+d_2+a)T}](1-\mu)^{-1}\hat{\beta}^{-1}.
\end{aligned}$$

The center manifold $w^c(0)$ for the map (2.3.11) can be represented as:

$$w^c(0) = \{(\bar{x}, \bar{y}, b_1) \in \Re^3 | \bar{y} = f(\bar{x}, b_1), f(0,0) = 0, Df(0,0) = 0\}.$$

Let $\bar{y} = f(\bar{x}, b_1) = B_0 b_1 + B_1 b_1 \bar{x} + B_2 \bar{x}^2 + O(|b_1|^2 + |\bar{x}|^3)$.

Computation for Center Manifold gives:

$$\begin{aligned} B_0 &= 0, \quad B_1 = \frac{a_1}{1-(1-\mu)(1-k)exp[-(a+d_1+d_2)T]}, \\ B_2 &= \frac{a_4}{(1-\mu)(1-k)exp[-(a+d_1+d_2)T]-1}. \end{aligned}$$

The map restricted to the center manifold is given by:

$$\bar{f} : \bar{x} \to \bar{x} + f(\bar{x}, \bar{y}, b_1) = \bar{x} + a_1 b_1 \bar{x} + a_2 b_1 \bar{y} + a_3 \bar{x}\bar{y} + a_4 \bar{x}^2 + a_5 \bar{y}^2,$$

$$= \bar{x} + a_1 b_1 \bar{x} + a_3 \frac{a_4}{(1-k)(1-\mu)e^{-(a+d_1+d_2)T}} \bar{x}^3 + a_4 \bar{x}^2 + O(|b_1|^2 + |b_1 \bar{x}^2| + |\bar{x}|^4).$$

Using Theorem 1.4.3, it can be calculated that

$$\frac{\partial \bar{f}(0,0)}{\partial b_1} = 0, \quad \frac{\partial^2 \bar{f}(0,0)}{\partial x \partial b_1} = a_1 \neq 0, \quad \frac{\partial^2 \bar{f}(0,0)}{\partial^2 x} = 2a_4 \neq 0.$$

Note that, all the conditions of Theorem 1.4.3 are satisfied at $(\bar{x}, b_1) = (0, 0)$. Further, E^* becomes E_0 at $b = b_0$. Hence, the map (2.3.2) undergoes to transcritical bifurcation at $b = b_0$. □

Similarly, the non-trivial fixed point $E^* = (x^*, y^*)$ becomes non-hyperbolic at $b = b_c$ as one of the eigenvalues of A becomes -1. The associated bifurcation is called flip bifurcation (period-doubling bifurcation). The following theorem characterizes flip bifurcation at $b = b_c$.

Theorem 2.3.4. *The map* (2.3.2) *undergoes to flip bifurcation about* E^* *at* $b = b_c$. *Moreover, if* $\bar{a} > 0$ *(*$\bar{a} < 0$*), then period-*2 *solutions that bifurcate from this fixed point are stable (unstable).*

Proof. Consider the map

$$\begin{pmatrix} x \\ \\ y \end{pmatrix} \to \begin{pmatrix} b \times (\hat{\beta} x + e^{-d_2 T} y) \times exp[-e^{-(d_1+a)T} x - \hat{\beta} x - e^{-d_2 T} y] \\ +(1-k)e^{-(d_1+a)T} x \\ (1-\mu)(\hat{\beta} x + e^{-d_2 T} y) \end{pmatrix}. \quad (2.3.15)$$

Let $x = x^* + U$, $y = y^* + V$, $b = b_c + b_{c1}$. The fixed point E^* of the map is transformed to (U, V) and the map (2.3.15) becomes:

$$\begin{pmatrix} U \\ V \end{pmatrix} \to \begin{pmatrix} c_{11}U + c_{12}V + c_{13}U^2 + c_{14}UV + c_{15}V^2 + c_{16}b_{c1}U + c_{17}b_{c1}V \\ c_{21}U + c_{22}V \end{pmatrix} \quad (2.3.16)$$

where

$$
\begin{aligned}
c_{11} &= (1-k)e^{-(d_1+a)T} + b_c \times exp[-e^{-(d_1+a)T}x^* - \hat{\beta}x^* - e^{-d_2T}y^*]\{\hat{\beta} - (\hat{\beta}x^* + e^{-d_2T}y^*) \\
&\quad \times (e^{-(d_1+a)T} + \hat{\beta})\}, \\
c_{12} &= b_c \times exp[-e^{-(d_1+a)T}x^* - \hat{\beta}x^* - e^{-d_2T}y^*]\{e^{-d_2T} - (\hat{\beta}x^* + e^{-d_2T}y^*)e^{-d_2T}\}, \\
c_{13} &= b_c \times exp[-e^{-(d_1+a)T}x^* - \hat{\beta}x^* - e^{-d_2T}y^*]\{(-\hat{\beta}(e^{-(d_1+a)T} + \hat{\beta}) + \frac{1}{2}(e^{-d_2T}y^* + \hat{\beta}x^*) \\
&\quad \times (e^{-(d_1+a)T} + \hat{\beta})^2)\}, \\
c_{14} &= b_c \times exp[-e^{-(d_1+a)T}x^* - \hat{\beta}x^* - e^{-d_2T}y^*]\{(-e^{-d_2T}(e^{-(d_1+a)T} + 2\hat{\beta}) + e^{-d_2T} \\
&\quad \times (e^{-d_2T}y^* + \hat{\beta}x^*)(e^{-(d_1+a)T} + \hat{\beta}))\}, \\
c_{15} &= b_c \times exp[-e^{-(d_1+a)T}x^* - \hat{\beta}x^* - e^{-d_2T}y^*]\{-e^{-2d_2T} + \frac{1}{2}(e^{-d_2T}y^* + \hat{\beta}x^*)e^{-2d_2T}))\}, \\
c_{16} &= exp[e^{-(d_1+a)T} - x^* - \hat{\beta}x^* - e^{-d_2T}y^*](\hat{\beta} - (e^{-d_2T}y^* + \hat{\beta}x^*)(e^{-(d_1+a)T} - \hat{\beta})), \\
c_{17} &= exp[-e^{-(d_1+a)T}x^* - \hat{\beta}x^* - e^{-d_2T}y^*](e^{-d_2T} - e^{-d_2T}(e^{-d_2T}y^* + \hat{\beta}x^*)), \\
c_{21} &= (1-\mu)\hat{\beta}, \\
c_{22} &= (1-\mu)e^{-d_2T}.
\end{aligned}
$$

The map (2.3.16) can be written as:

$$
\begin{pmatrix} U \\ V \end{pmatrix} \to C \begin{pmatrix} U \\ V \end{pmatrix} + \begin{pmatrix} c_{13}U^2 + c_{14}UV + c_{15}V^2 + c_{16}b_{c1}U + c_{17}b_{c1}V \\ 0 \end{pmatrix}. \quad (2.3.17)
$$

The eigenvalues of $C = (C_{ij})_{2\times 2}$ are -1 and λ.

The corresponding eigenvectors V_3 and V_4 are $\{v_3, 1\}^T$ and $\{\{v_4, 1\}^T$ respectively where $v_3 = -(1 + (1-\mu)e^{-d_2T})(1-\mu)^{-1}\hat{\beta}^{-1}$ and $v_4 = (\lambda - (1-\mu)e^{-d_2T})(1-\mu)^{-1}\hat{\beta}^{-1}$.

Consider the transformation

$$
\begin{pmatrix} U \\ V \end{pmatrix} = J' \begin{pmatrix} \bar{x} \\ \bar{y} \end{pmatrix}, \quad J' = (V_3 \;\; V_4).
$$

Using (2.3.17) and simplification gives:

$$
\begin{pmatrix} \bar{x} \\ \bar{y} \end{pmatrix} \to \begin{pmatrix} -1 & 0 \\ 0 & \lambda \end{pmatrix} \begin{pmatrix} \bar{x} \\ \bar{y} \end{pmatrix} + \begin{pmatrix} f_1(\bar{x}, \bar{y}, b_{c1}) \\ f_2(\bar{x}, \bar{y}, b_{c1}) \end{pmatrix}. \quad (2.3.18)
$$

The functions in the above map are obtained as:

$$
\begin{aligned}
f_1(\bar{x}, \bar{y}, b_{c1}) &= g_1 b_1 \bar{x} + g_2 b_1 \bar{y} + g_3 \bar{x}\bar{y} + g_4 \bar{x}^2 + g_5 \bar{y}^2, \\
f_2(\bar{x}, \bar{y}, b_{c1}) &= -f_1(\bar{x}, \bar{y}, b_1),
\end{aligned}
$$

$$\begin{aligned} g_1 &= [c_{16}v_3 + c_{17}]\psi_1^{-1}, & g_2 &= [c_{16}v_4 + c_{17}]\psi_1^{-1}, \\ g_3 &= [c_{15} - c_{14}(v_3 + v_4) - 2c_{13}v_3v_4]\psi_1^{-1}, & g_4 &= [c_{15} - c_{14}v_3 + v_3^2]\psi_1^{-1}, \\ g_5 &= [c_{15} + c_{14}v_4 + v_4^2]\psi_1^{-1}, & \psi_1 &= -(1+\lambda)(1-\mu)^{-1}\hat{\beta}^{-1}. \end{aligned}$$

The center manifold theorem [69] is used to determine the nature of bifurcation about E_0 at $b_{c1} = 0$. The center manifold of the map (2.3.15) can be represented as:

$$w^c(0) = \{(\bar{x}, \bar{y}, b_{c1}) \in \Re^3 | \bar{y} = h(\bar{x}, b_{c1}), h(0,0) = 0, Dh(0,0) = 0\}.$$

Let $\bar{y} = h(\bar{x}, b_{c1}) = M_0 b_{c1} + M_1 b_{c1}\bar{x} + M_2\bar{x}^2 + O(|b_{c1}|^2 + |\bar{x}|^3)$.

Computation for center manifold gives:

$$\begin{aligned} M_0 &= 0, \quad M_1 = \psi_1^{-1}[c_{17} - (1 + (1-\mu)e^{-d_2T})(1-\mu)^{-1}\hat{\beta}^{-1}](1+\lambda)^{-1}, \\ M_2 &= \psi_1^{-1}\left[c_{15} - c_{14}\frac{(1 + (1-\mu)e^{-d_2T})}{(1-\mu)\hat{\beta}} + \left(\frac{-(1 + (1-\mu)e^{-d_2T})}{\hat{\beta}(1-\mu)}\right)^2\right](1-\lambda)^{-1}. \end{aligned}$$

Thus, the map restricted to the center manifold is given by:

$$\bar{h} : \bar{x} \to -\bar{x} + h(\bar{x}, \bar{y}, b_{c1}) = -\bar{x} + g_1 b_{c1}\bar{x} + g_2 b_{c1}\bar{y} + g_3\bar{x}\bar{y} + g_4\bar{x}^2 + g_5\bar{y}^2,$$

$$\begin{aligned} \bar{h} : \bar{x} \to -\bar{x} + h(\bar{x}, \bar{y}, b_{c1}) &= -\bar{x} + g_1 b_{c1}\bar{x} + g_3\psi_1^{-1}(1-\lambda)^{-1}\bar{x}^3 \\ &\times \left[c_{15} - c_{14}\frac{(1 + (1-\mu)e^{-d_2T})}{(1-\mu)\hat{\beta}} + \left(\frac{(1 + (1-\mu)e^{-d_2T})}{\hat{\beta}(1-\mu)}\right)^2\right] \\ &+ g_4\bar{x}^2 + O(|b_{c1}|^2 + |b_{c1}\bar{x}^2| + |\bar{x}|^4). \end{aligned}$$

From Theorem 1.4.4, it can be observed that

$$\frac{\partial\bar{h}(0,0)}{\partial b_{c1}}\frac{\partial^2\bar{h}(0,0)}{\partial x^2} + 2\frac{\partial^2\bar{h}(0,0)}{\partial x\partial b_{c1}} = 0 + 2g_1 \neq 0,$$

$$\begin{aligned} \bar{a} &= \frac{1}{2}\left(\frac{\partial^2\bar{h}(0,0)}{\partial x^2}\right)^2 + \frac{1}{3}\frac{\partial^3\bar{h}(0,0)}{\partial x^3} \\ &= 2g_4^2 + 2g_3\psi_1^{-1}\left[c_{15} - c_{14}\frac{(1 + (1-\mu)e^{-d_2T})}{(1-\mu)\hat{\beta}} + \left(\frac{(1 + (1-\mu)e^{-d_2T})}{\hat{\beta}(1-\mu)}\right)^2\right](1-\lambda)^{-1} \\ &\neq 0. \end{aligned}$$

Note that, all the conditions of Theorem 1.4.4 are satisfied at $(\bar{x}, b_{c1}) = (0,0)$. The map (2.3.2) undergoes to flip bifurcation at $b = b_c$. Accordingly, there exist, period-2 solutions. These bifurcating period-2 solutions will be stable if $\bar{a} > 0$ and unstable if $\bar{a} < 0$. □

There exist a series of bifurcations that lead to chaotic dynamic when b increases from b_c. This will be explored through numerical simulation in the next section later.

For the global stability of two fixed points, the following theorems are concluded:

2.3.4 Global Stability Analysis

In this section, Lyapunov Second Method will be used to establish the global stability of various fixed points.

Theorem 2.3.5. *The locally asymptotically stable pest-free point E_0 of the map* (2.3.2) *is globally asymptotically stable in the interior of a positive quadrant of $x-y$ plane.*

Proof. Observe that, $R_0 < 1$, means that $b < b_0$. Also, $0 < 1-(1-k)e^{-(a+d_1)T}) < 1$ and $0 < (1-(1-\mu)e^{-d_2T}) < 1$.

Similarly, $0 < b\hat{\beta} < 1-(1-k)e^{-(a+d_1)T}) < 1$ and $0 < b\hat{\beta} < (1-(1-\mu)e^{-d_2T}) < 1$ also hold.

Consider the positive definite function

$$V_1(x_m, y_m) \;=\; x_m + y_m.$$

Computation of ΔV_1 and its simplification gives

$$\begin{aligned}
\Delta V_1(x_m,y_m) &= f(x_m,y_m)+g(x_m,y_m)-x_m-y_m \\
&= (1-k)e^{-(a+d_1)T}x_m + b[\hat{\beta}x_m + e^{-d_2T}y_m]exp[-(e^{-(a+d_1)T}+\hat{\beta})x_m \\
&\quad -e^{-d_2T}y_m] + [(1-\mu)(\hat{\beta}x_m + y_m e^{-d_2T})] - x_m - y_m \\
&\leq [(1-k)e^{-(a+d_1)T} + b\hat{\beta} + (1-\mu)\hat{\beta} - 1]x_m + [(b+(1-\mu))e^{-d_2T} - 1]y_m \\
&\leq [-(1-k)(1-\mu)e^{-(a+d_1+d_2)T} + (1-k)e^{-(a+d_1)T} + b\hat{\beta} + (1-\mu)e^{-d_2T} \\
&\quad -1]x_m + [be^{-d_2T} + (1-\mu)e^{-d_2T} - 1]y_m \\
&< [b\hat{\beta}(1-(1-k)e^{-(a+d_1)T})^{-1}(1-(1-\mu)e^{-d_2T})^{-1} - 1]x_m \\
&\quad +[b\hat{\beta}(1-(1-\mu)e^{-d_2T})^{-1} - 1]y_m \\
&< [b\hat{\beta}(1-(1-k)e^{-(a+d_1)T})^{-1}(1-(1-\mu)e^{-d_2T})^{-1} - 1]x_m \\
&\quad +[b\hat{\beta}(1-(1-k)e^{-(a+d_1)T})^{-1}(1-(1-\mu)e^{-d_2T})^{-1} - 1]y_m \\
\Delta V_1(x_m,y_m) &< -(1-R_0)(x_m+y_m).
\end{aligned}$$

It is observed that $V_1(x_m, y_m)$ is negative definite when $R_0 < 1$. Therefore, $V_1(x_m, y_m)$ is a Lyapunov function. Hence, the pest-free point E_0 is globally asymptotically stable.

□

Theorem 2.3.6. *The local asymptotically stable interior fixed point E^* of the map (2.3.2) is globally asymptotically stable in the interior of a positive quadrant of $x - y$ plane.*

Proof. Observe that, the interior fixed point E^* exists if $b > b_0(R_0 > 1)$. Consider the positive definite function:

$$V_2(x_m, y_m) \;=\; \mid x_m - x^* \mid + \mid y_m - y^* \mid .$$

Computation of ΔV_2 and its simplification gives

$$\begin{aligned}
\Delta V_2 &= \mid [(1-k)e^{-(a+d_1)T}x_m + b[\hat{\beta}x_m + e^{-d_2T}y_m] \times exp[-\{e^{-(a+d_1)T} + \hat{\beta}\}x_m - e^{-d_2T}y_m] \\
&\quad -(1-k)e^{-(a+d_1)T}x^* + b[\hat{\beta}x^* + e^{-d_2T}y^*] \times exp[-\{e^{-(a+d_1)T} + \hat{\beta}\}x^* - e^{-d_2T}y^*] \mid \\
&\quad + \mid (1-\mu)(\hat{\beta}x_m + y_m e^{-d_2T}) - (1-\mu)(\hat{\beta}x^* + y^* e^{-d_2T}) \mid - \mid x_m - x^* \mid - \mid y_m - y^* \mid \\
&= \mid [(1-k)e^{-(a+d_1)T}x_m + b[\hat{\beta}x_m + e^{-d_2T}y_m] \times exp[-\{e^{-(a+d_1)T} + \hat{\beta}\}x_m - e^{-d_2T}y_m] \\
&\quad -(1-k)e^{-(a+d_1)T}x^* - b_0(R+1)^{-1}\log(R_0) \mid - \mid (x_m - x^*) \mid - \mid (y_m - y^*) \mid \\
&\quad + \mid [(1-\mu)(\hat{\beta}x_m + y_m e^{-d_2T}) - (1-\mu)(R+1)^{-1}\log(R_0)] \mid \\
&\leq \mid [(1-k)e^{-(a+d_1)T}x_m + b[\hat{\beta}x_m + e^{-d_2T}y_m] - x^* \mid - \mid (x_m - x^*) \mid - \mid (y_m - y^*) \mid \\
&\quad + \mid [(1-\mu)(\hat{\beta}x_m + y_m e^{-d_2T}) - y^*] \mid \\
&< - \mid [b\hat{\beta}(1-(1-k)e^{-(a+d_1)T})^{-1}(1-(1-\mu)e^{-d_2T})^{-1} - 1]x_m \mid \\
&\quad - \mid [b\hat{\beta}(1-(1-\mu)e^{-d_2T})^{-1}(1-(1-k)e^{-(a+d_1)T})^{-1} - 1]y_m \mid \\
\Delta V_2 &< - \mid b - b_0 \mid \times \mid x_m \mid - \mid b - b_0 \mid \times \mid y_m \mid \\
\Delta V_2 &< - \mid R_0 - 1 \mid \times \mid x_m \mid - \mid R_0 - 1 \mid \times \mid y_m \mid .
\end{aligned}$$

Since $V_2(x_m, y_m)$ is negative if the condition (2.3.8) holds. Thus, V_2 is a Lyapunov function and interior fixed point E^* is globally asymptotically stable. □

2.4 Numerical Simulations

To study the dynamical behavior, numerical simulations have been carried out for the set of parameters. The threshold R_0 is analyzed with respect to model parameters.

The objective is not limited to local stability, but to explore the existence of complex dynamical behavior, including periodic solutions and chaos in the system (2.2.6) − (2.2.8). Consider the set of parameters as:

$$a = 0.4, b = 4, k = 0.6, \mu = 0.8, d_1 = 0.5. \tag{2.4.1}$$

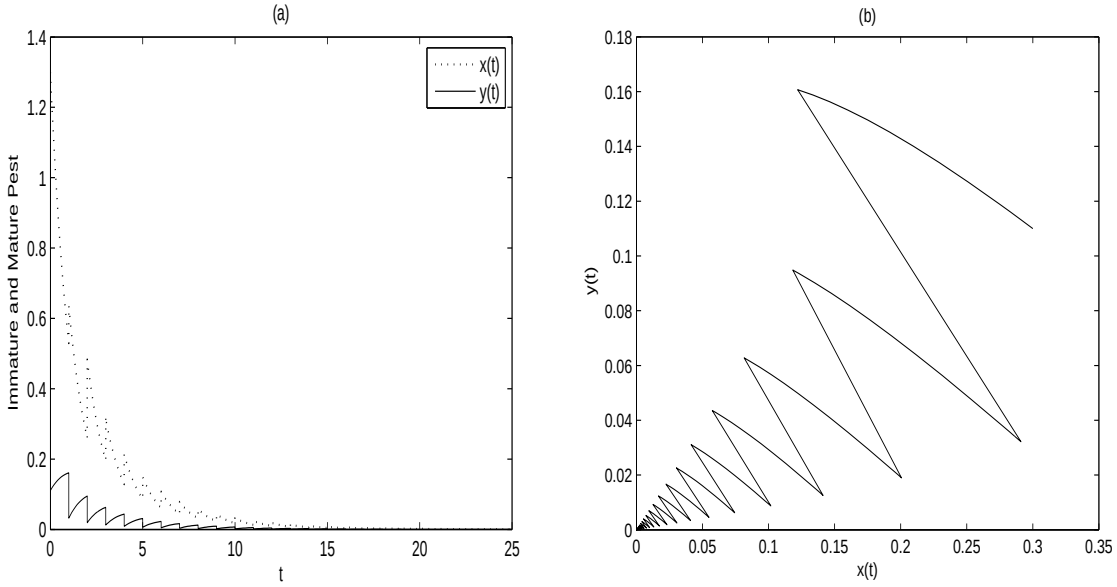

Figure 2.1: (a) Time series (b) Phase portrait in $x - y$ plane depicting stability of the pest-free state in the system (2.2.6) − (2.2.8) at $b = 2$, $d_2 = 0.2$.

Considering $T = 1.0$ and $d = d_1 = d_2 = 0.5$, the constant b_0 is computed as $b_0 = 3.6797$. For $b = 3.0$, the basic reproduction number R_0 is less than 1 ($R_0 = bb_0^{-1} = 0.8153$). According to Theorem 2.3.1, the pest-free state of the map (2.3.2) is locally asymptotically stable. Taking $b = 4$, ($R_0 = 1.087 > 1$), the pest-free state becomes unstable and the non-trivial fixed point $E^* = (0.1316, 0.0060)$ is stable as $b_0 < b < 38.7733$ (Theorem 2.3.2). The transcritical bifurcation occurs at $b = 3.6797$.

Considering, the case $d_1 > d_2$, $d_2 = 0.2$, while keeping other parameters unchanged, the threshold for the stability of E_0 is reduced to $b_0 = 2.9732$. Accordingly, the pest-free state of the map (2.3.2) is locally asymptotically stable for $b < 2.9732$ and unstable for $b > b_0$. The non-trivial fixed point $E^* = (0.4310, 0.0202)$ of the map (2.3.2) is locally stable for $2.9732 < b < 31.51$. The transcritical bifurcation occurs at $b = 2.9732$.

For, $d_1 > d_2$, $d_2 = 0.2$, Fig. 2.1 and Fig. 2.2 shows the stability of the pest-free state and period-1 solution (x_e, y_e) of the system (2.2.6) – (2.2.8) respectively.

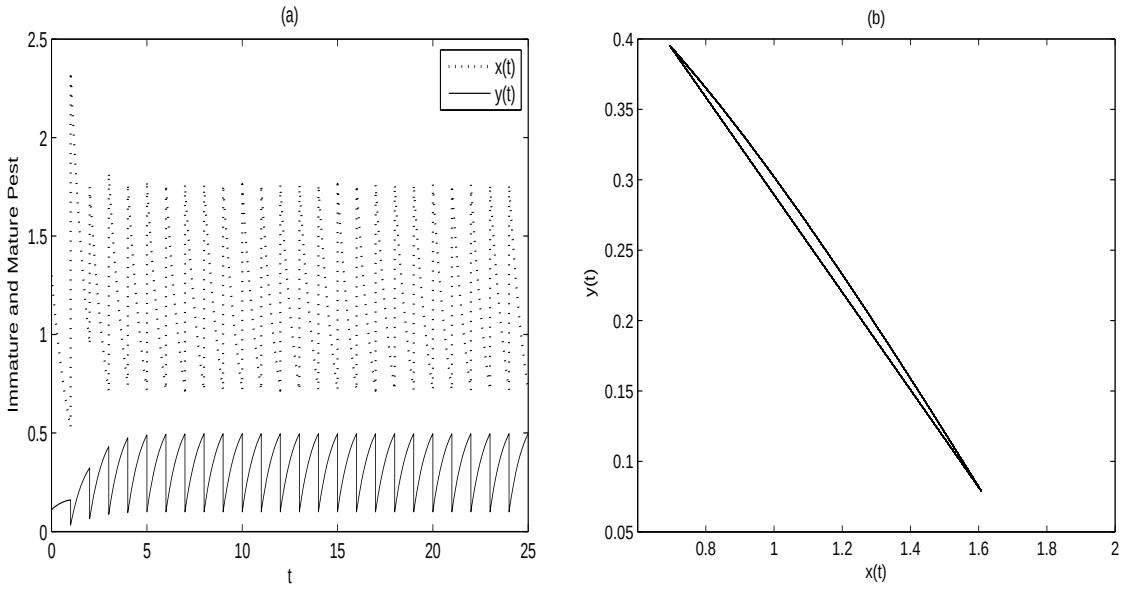

Figure 2.2: (a) Time series (b) Phase portrait in $x - y$ plane depicting stability of Period-1 solution of the system (2.2.6) – (2.2.8) at $b = 10$, $d_2 = 0.2$.

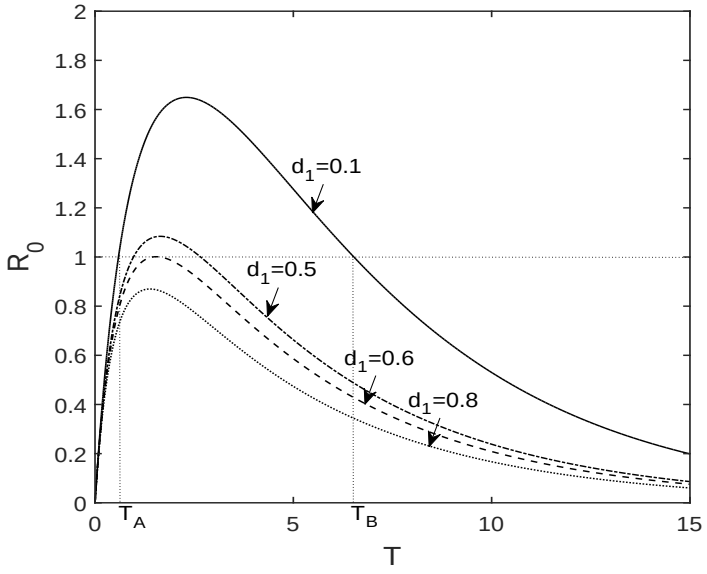

Figure 2.3: Variation of R_0 with T at $d_2 = 0.2$.

Fig. 2.3 shows the variation of R_0 with pulse period T for $d_2 = 0.2$ and different

values of d_1. E_0 is stable in the range $0 < T < T_A \cup T_B < T < 1$ for $d_1 = 0.1$. The non-monotonic behavior of R_0 with respect to pulse period T is observed. As the value of T increases, R_0 first increases and attains a peak and then it decreases with increase in T. It can be easily observed that as d_1 increases, the domain of stability of E_0 with respect to T increases and pest eradication may occur. Observe that, $R_0 < 1$, for all values of T when $d_1 = 0.8$. Thus, E_0 remains stable irrespective of T for $d_1 = 0.8$ and $d_2 = 0.2$.

In Fig. 2.4, the curve $R_0 = 1$ corresponding to equation (2.3.3) is drawn on $T - d_2$ plane, keeping other parameters as in (2.4.1). This curve bifurcates the $T - d_2$ domain into pest eradication (green) and coexistence (red) regions. It is observed that there exists a critical value of d_2 (say d_{2c}), for which pest eradication is possible irrespective of pulse period T. For the given data set, it is obtained as $d_{2c} = 0.6271$. For smaller values of d_2, eradication is still possible depending upon the pulse period T.

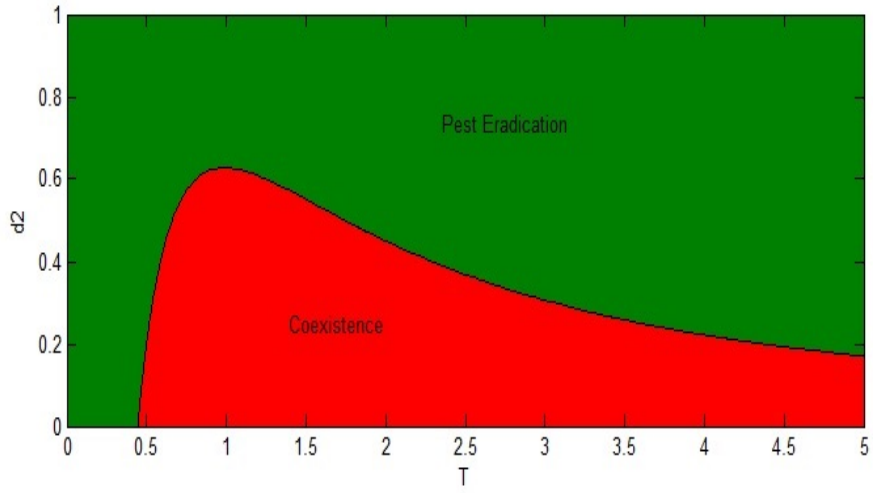

Figure 2.4: Two-parameter bifurcation diagram on $T - d_2$ plane.

Similarly, two-parameter bifurcation diagrams with respect to T and d_1 are drawn in Fig. 2.5 for $d_2 = 0.2, 0.5$ and 0.6. It is clear that the region of pest eradication increases with increasing d_2. For $d_2 = 0.2$, the critical d_1 may exist for $d_2 > 1$ outside the domain (see Fig. 2.5(a)). Further, the critical d_1 decreases with increase in d_2. Accordingly, the pest will be eradicated when $d_1 > d_{1c}$ irrespective of T. The eradication

is still possible for a suitable choice of T in $d_1 < d_{1c}$.

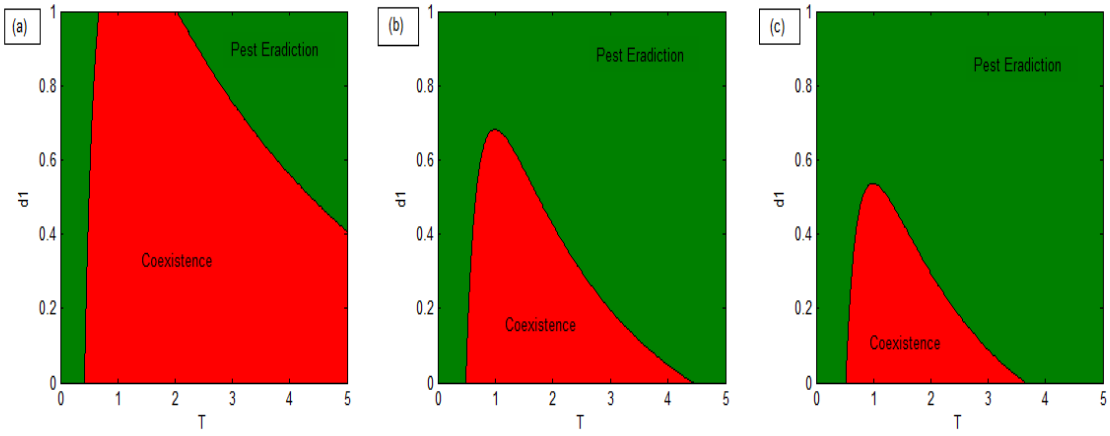

Figure 2.5: Two-parameter bifurcation diagrams on $T - d_1$ plane at (a) $d_2 = 0.2$ (b) $d_2 = 0.5$ (c) $d_2 = 0.6$.

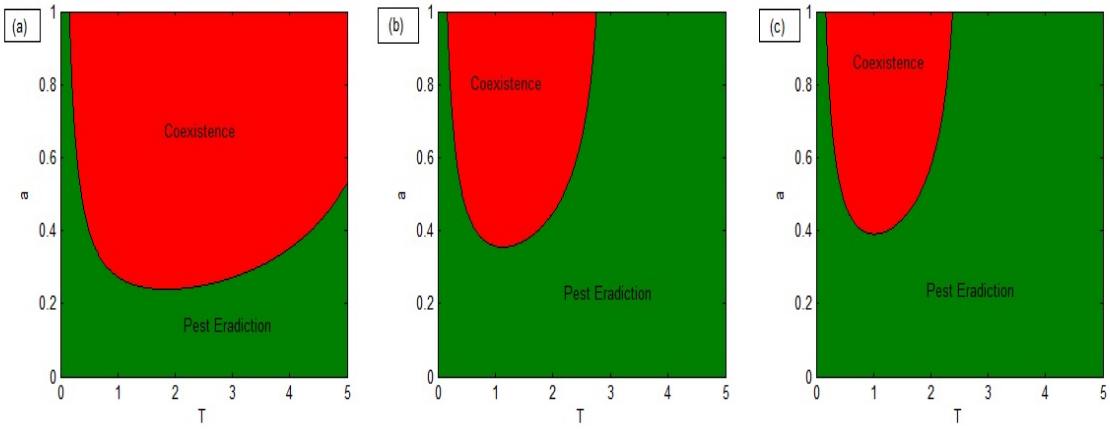

Figure 2.6: Two-parameter bifurcation diagrams on $T-a$ Plane at (a) $d_1 = 0.5$ $d_2 = 0.2$ (b) $d_1 = d_2 = 0.5$ (c) $d_1 = 0.5$, $d_2 = 0.6$.

Another set of two-parameter bifurcation diagrams with respect to T and a is shown in Fig. 2.6 in three cases: $d_1 > d_2$, $d_1 = d_2$ and $d_1 < d_2$. The pest eradication

will occur when $a < a_c$ irrespective of T. For $a > a_c$, the eradication is possible for a suitable choice of T. The eradication of pest is most probable for $d_1 < d_2$ for the choice of a and T as the corresponding region is biggest out of the three cases.

To study the complex dynamical behavior, typical bifurcation diagrams are drawn for total pest population in Fig. 2.7 with respect to critical parameter b which is involved in $R_0 = b\, b_0^{-1}$ as well as in $R_c = b\, b_c^{-1}$. The three diagrams are drawn for the cases: (a) $d_1 = d_2$, (b) $d_1 > d_2$ and (c) $d_1 < d_2$. The case (a) is idealized and mostly considered by the investigators. The case (b) is more realistic while case (c) is rarely observed in nature. The case (c) is considered only for completeness. The diagrams show the existence of chaos through period-doubling route. The comparison of Fig. 2.7(b) with Fig. 2.7(a) clearly shows that the dynamics is more complex in the case $d_1 > d_2$ than $d_1 = d_2$.

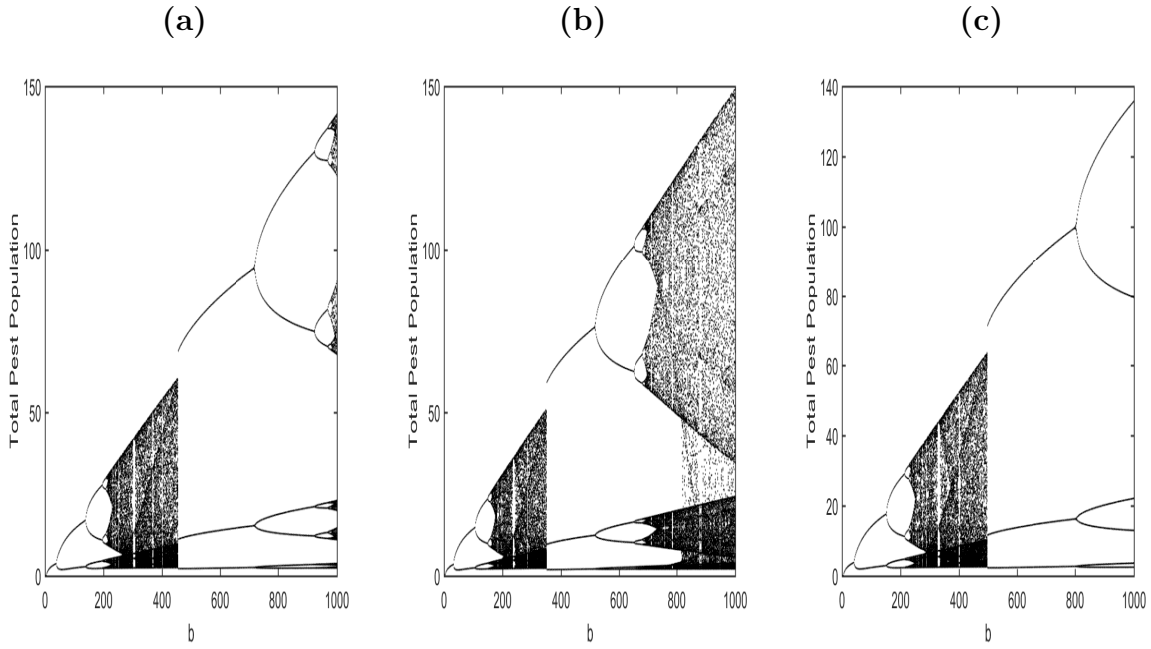

Figure 2.7: Bifurcation diagrams of the map (2.3.2) for total pest population with respect to b (a) $d_1 = d_2 = 0.5$ (b) $d_1 = 0.5$, $d_2 = 0.2$ (c) $d_1 = 0.5$, $d_2 = 0.6$.

The critical value for the period-doubling bifurcation parameter is $b_c = 31.51$ as obtained from equation (2.3.8) is confirmed from the diagram. The period-2 solution occurs in the range $b \in (31.51, 106.1)$. As the parameter value of b increases further, the successive period-doubling with period-4, period-8 and period-16 occur in the intervals $(106.1, 149.16)$,$(149.16, 160)$ and $(160, 163)$ respectively. Typical periodic attractors are

drawn in these intervals in Fig. 2.8 for $b = 50, 110, 150$ and 162. It ultimately leads to chaos in the interval $(163, 350.55)$. This chaotic region is followed by a region of the period-3 solution in the interval $(350, 516)$ which again becomes chaotic through period-doubling for $b > 749$. The pest coexists in periodic solution/chaotic attractor for these domains. The cascades of period-doubling is observed in the bifurcation diagram, which is the route to chaos in the system (2.2.6) − (2.2.8).

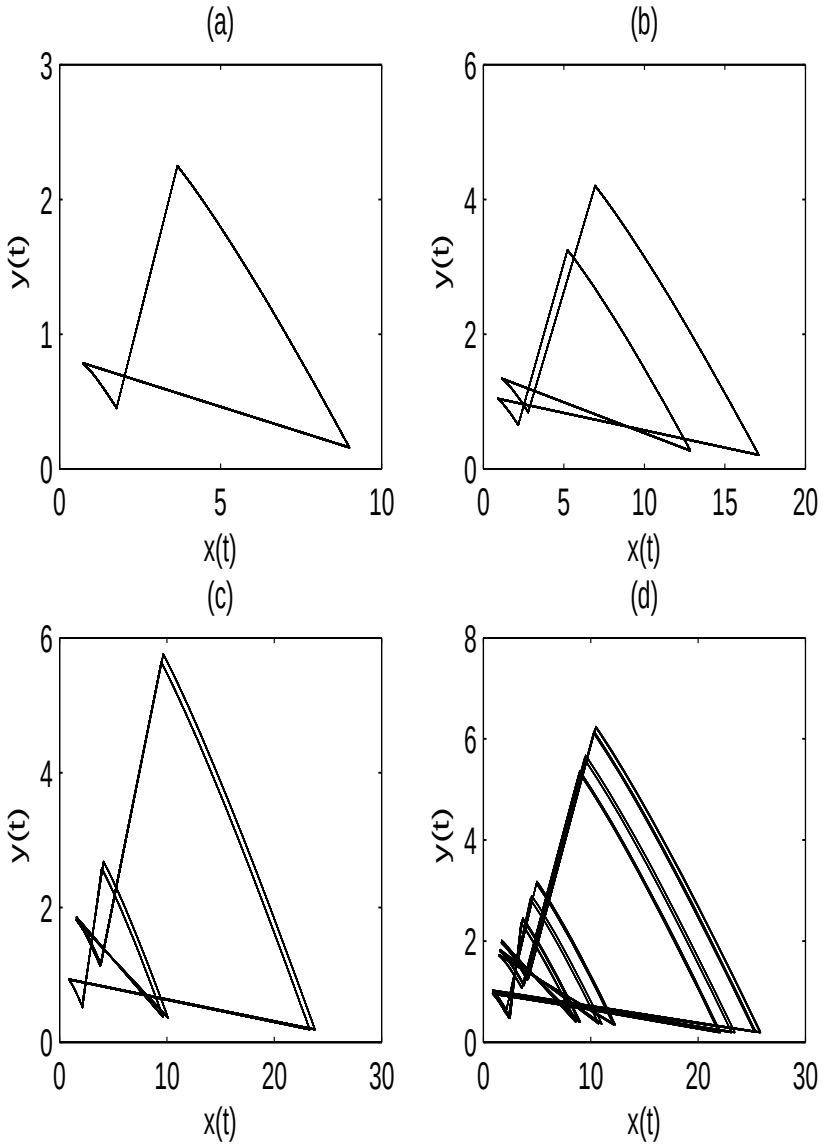

Figure 2.8: Periodic attractors of the system (2.2.6) − (2.2.8): (a) Period-2 at $b = 50$ (b) Period-4 at $b = 110$ (c) Period-8 at $b = 150$ (d) Period-16 at $b = 162$.

The chaotic regions of Fig. 2.7(b) are separately blown up in Fig. 2.9. The rich

dynamical behavior is clearly visible, including crises, chaos, periodic windows, stability and period-doubling. It is known that Lyapunov exponents quantify the exponential divergence of initially close trajectories and identify a chaotic behavior.

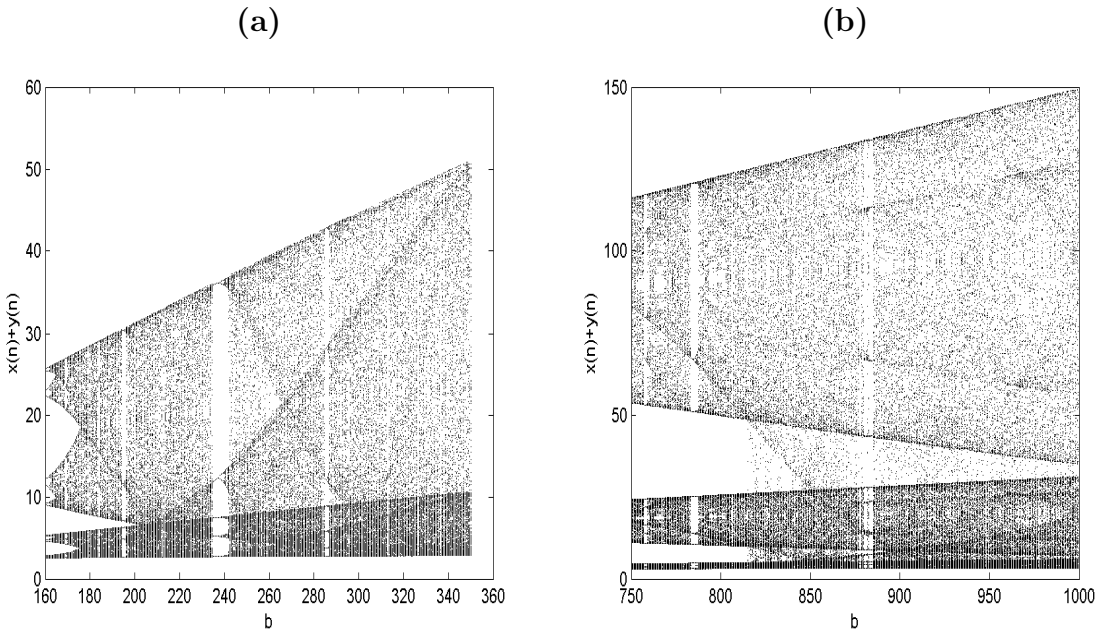

Figure 2.9: Magnified parts of bifurcation diagram 2.7(b) (a) $b \in (160, 350)$ (b) $b \in (750, 1000)$.

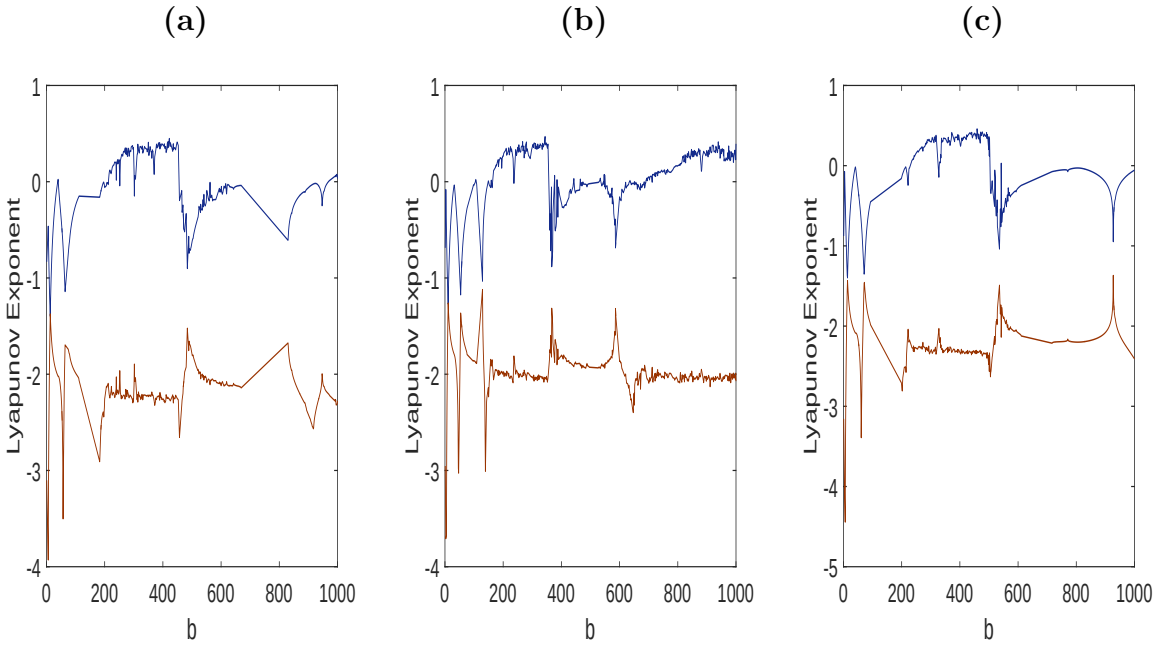

Figure 2.10: Two Lyapunov exponents of the map (2.3.2) for total pest population with respect to b (a) $d_1 = d_2 = 0.5$ (b) $d_1 = 0.5$, $d_2 = 0.2$ (c) $d_1 = 0.5$, $d_2 = 0.6$.

Lyapunov exponents drawn in Fig. 2.10 further confirm the existence of chaos. Accordingly, attractors drawn in Fig. 2.11(a) and Fig. 2.11(b) at $b = 200$ and $b = 900$ are strange attractors. Crisis is shown in the neighborhood of $b = 757$ in Fig. 2.12.

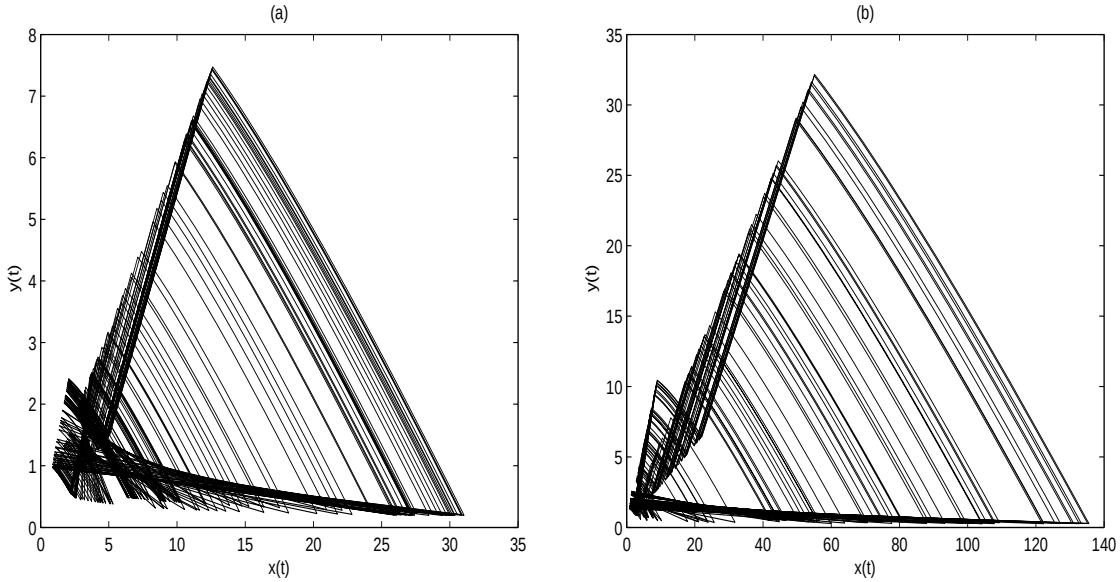

Figure 2.11: Chaotic attractors of the system (2.2.6)−(2.2.8) at (a) $b = 200$ (b) $b = 900$.

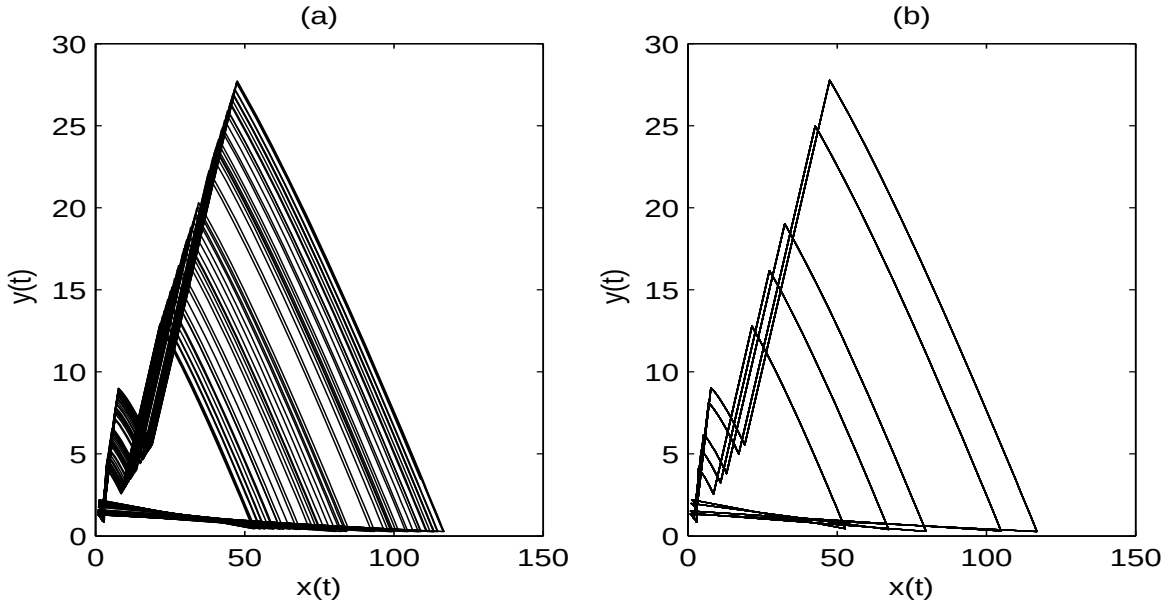

Figure 2.12: Emergence of crises of the system (2.2.6) − (2.2.8) at (a) $b = 757$ (b) $b = 758$.

Fig. 2.13 shows the bifurcation diagrams with respect to maturation rate $a \in (0, 1)$ with $b = 500$. The existence of chaos is observed in all the three cases through

repeated period-doubling with an increase in maturation rate a. However, the smallest chaotic region is obtained for the case $d_1 > d_2$. Period-3 solutions appear beyond the chaotic region in all the cases. Further, period-doubling occurs only in the case $d_1 > d_2$.

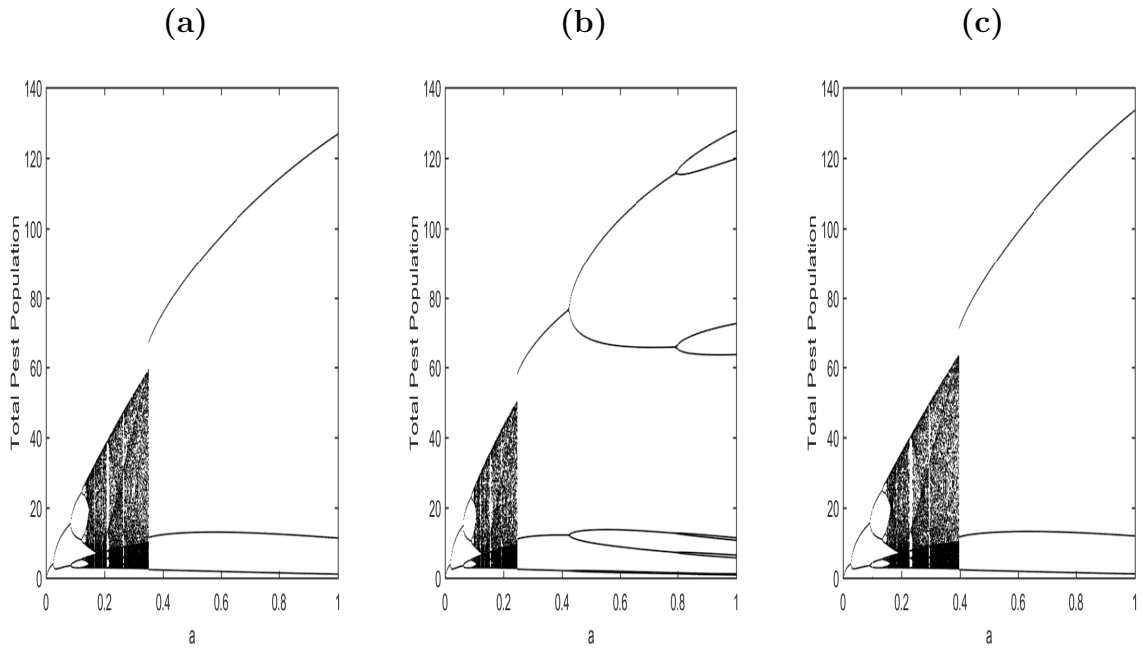

Figure 2.13: Bifurcation diagrams of the map (2.3.2) for total pest population with respect to a (a) $d_1 = d_2 = 0.5$ (b) $d_1 = 0.5$, $d_2 = 0.2$ (c) $d_1 = 0.5$, $d_2 = 0.6$.

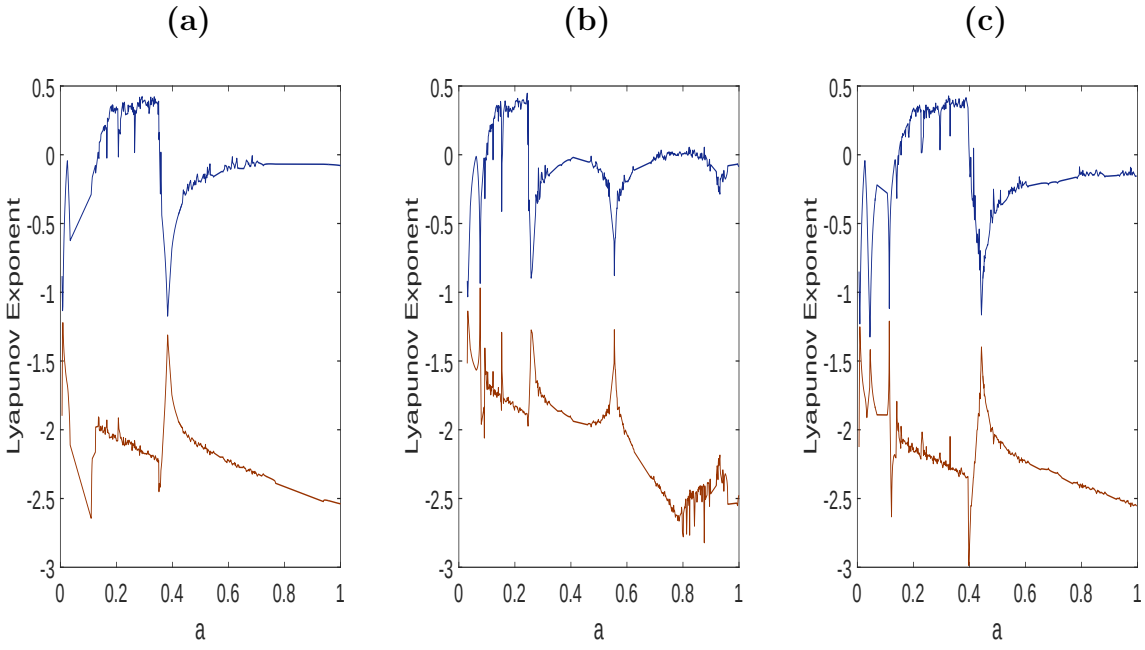

Figure 2.14: Two Lyapunov exponents of the map (2.3.2) for total pest population with respect to a (a) $d_1 = d_2 = 0.5$ (b) $d_1 = 0.5$, $d_2 = 0.2$ (c) $d_1 = 0.5$, $d_2 = 0.6$.

To further confirm the chaotic nature of the map (2.3.2), two Lyapunov exponents are drawn in Fig. 2.14. The negative Lyapunov exponents confirm the complex dynamics for certain range of parameter a.

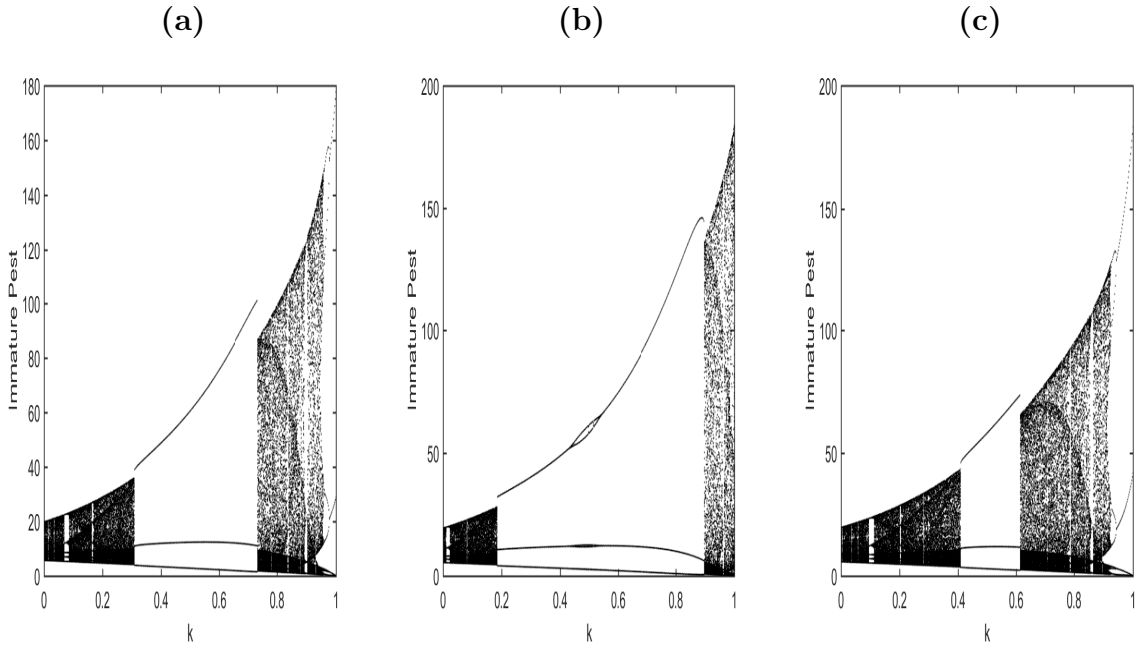

Figure 2.15: Bifurcation diagrams of the map (2.3.2) for total pest population with respect to k (a) $d_1 = d_2 = 0.5$ (b) $d_1 = 0.5$, $d_2 = 0.2$ (c) $d_1 = 0.5$, $d_2 = 0.6$.

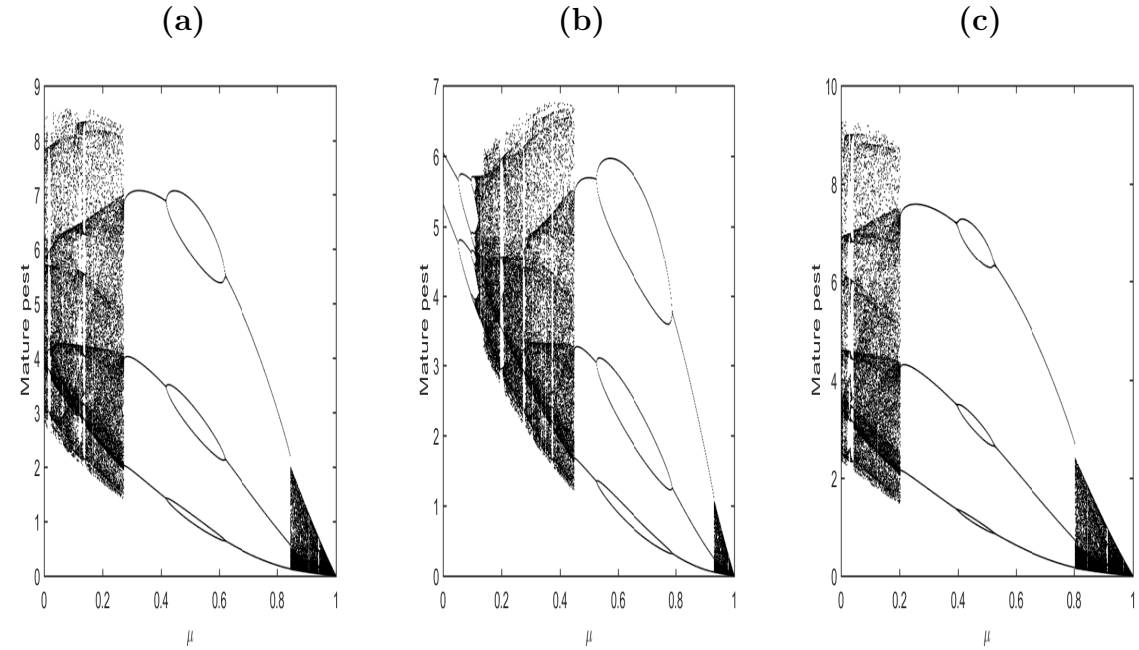

Figure 2.16: Bifurcation diagrams of the map (2.3.2) for total pest population with respect to μ (a) $d_1 = d_2 = 0.5$ (b) $d_1 = 0.5$, $d_2 = 0.2$ (c) $d_1 = 0.5$, $d_2 = 0.6$.

Similarly, bifurcation diagrams with respect to killing rates k and μ are drawn in Fig. 2.15 and Fig. 2.16 respectively. Chaotic region is again found to be the smallest when $d_1 > d_2$. Two chaotic regions are separated by a region of the period-3 solution.

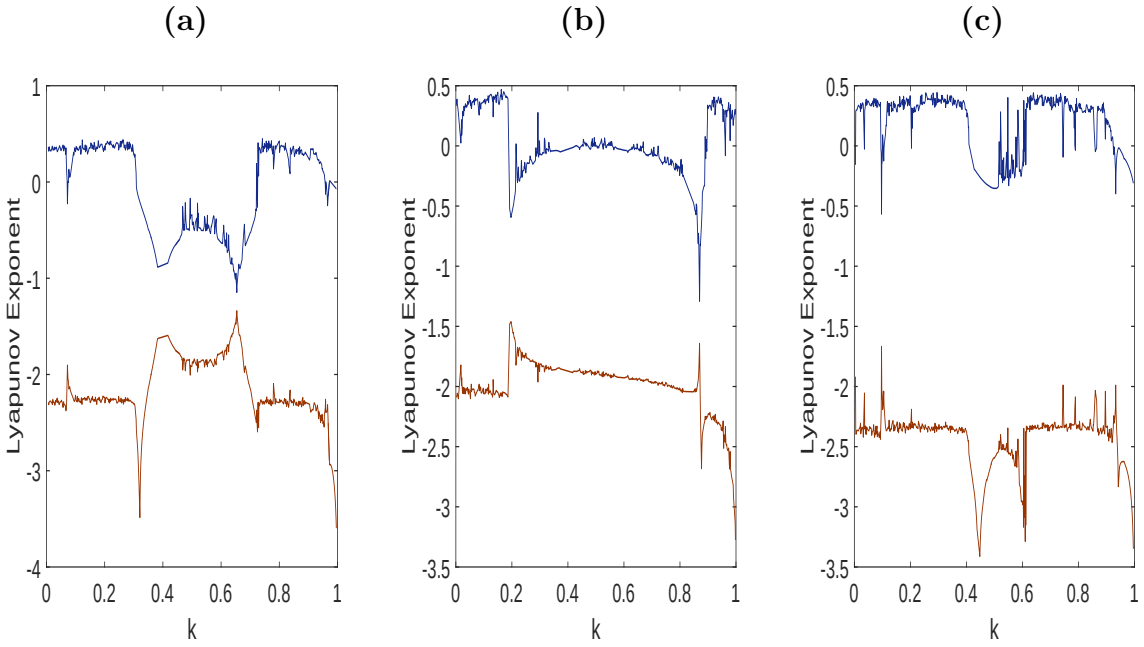

Figure 2.17: Two Lyapunov exponents of the map (2.3.2) for total pest population with respect to k (a) $d_1 = d_2 = 0.5$ (b) $d_1 = 0.5$, $d_2 = 0.2$ (c) $d_1 = 0.5$, $d_2 = 0.6$.

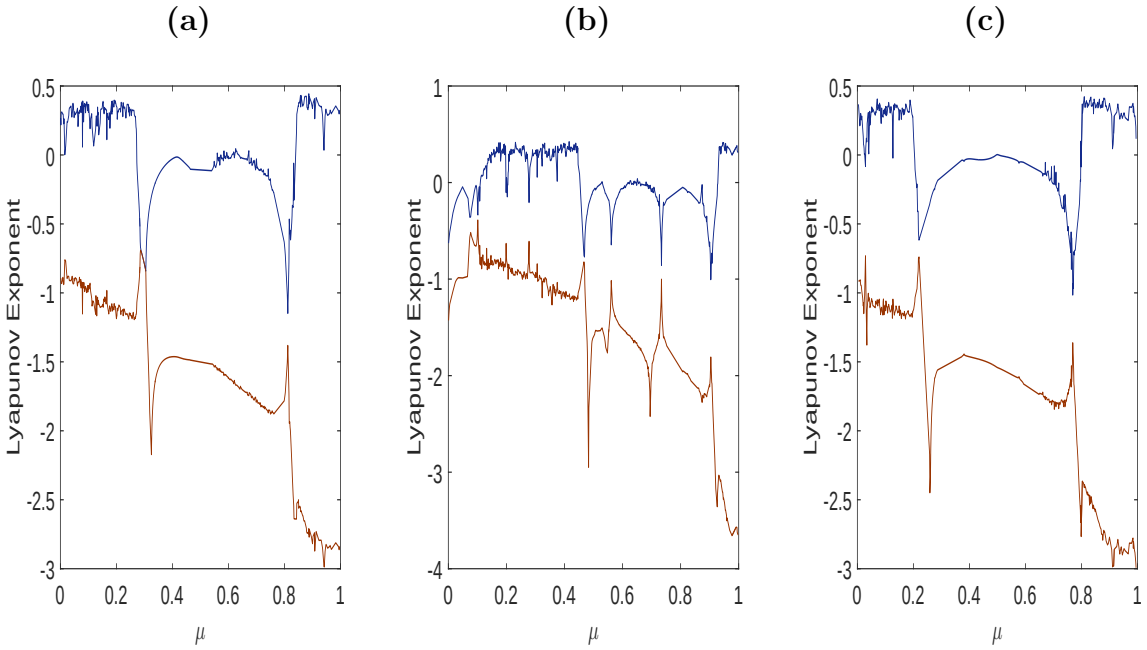

Figure 2.18: Two Lyapunov exponents of the map (2.3.2) for total pest population with respect to μ (a) $d_1 = d_2 = 0.5$ (b) $d_1 = 0.5$, $d_2 = 0.2$ (c) $d_1 = 0.5$, $d_2 = 0.6$.

Lyapunov exponents corresponding to bifurcation diagram are plotted in Fig. 2.17 and Fig. 2.18. The map (2.3.2) has at least one zero Lyapunov exponent at some values of k and μ which shows the existence of periodic orbits. The sum of two Lyapunov exponent is negative for the smaller values of k and μ indicating the presence of chaos.

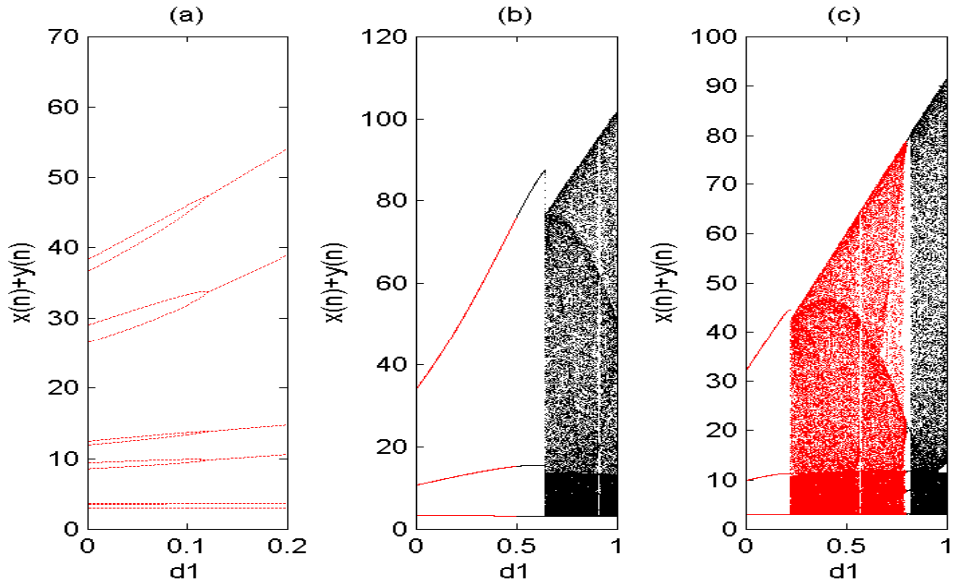

Figure 2.19: Bifurcation diagrams of the map (2.3.2) for total pest population with respect to d_1 (a) $d_2 = 0.2$ (b) $d_2 = 0.5$ (c) $d_2 = 0.8$.

Now, to see the effects of variation in mortality rate of the pest on the dynamics of the map (2.3.2), bifurcation diagrams and the corresponding spectrum of Lyapunov exponents are drawn in Fig. 2.19 and Fig. 2.20 respectively.

Lyapunov exponent confirms the existence of chaotic regions and periodic windows in the parametric space. For some parameter values, one of the Lyapunov exponents is obtained to be higher than zero such that the sum of exponents is still less than zero. This confirms the existence of chaos. It can be observed from Fig. 2.19 and Fig. 2.20 that, there exist stable periodic windows in the chaotic region. No chaos is observed when $d_2 = 0.2$. The chaotic region exists for higher values of d_1 when $d_2 = 0.5$. It occurs in the region $d_1 > d_2$. However, when $d_2 = 0.8$, it occurs even for $d_1 < d_2$. The chaotic region increases with increasing d_2.

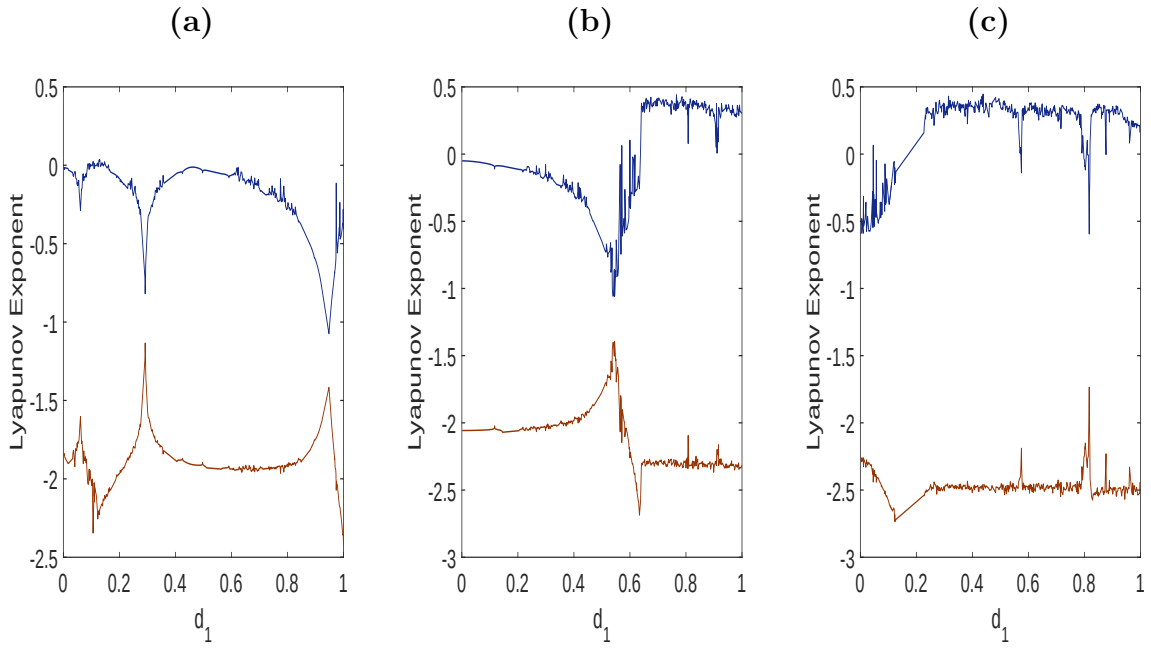

Figure 2.20: Two Lyapunov exponents of the map (2.3.2) for total pest population with respect to d_1 (a) $d_2 = 0.2$ (b) $d_2 = 0.5$ (c) $d_2 = 0.8$.

2.5 Discussion

In this chapter, a stage-structured pest control model with birth pulses is considered. A time-dependent impulsive control strategy for chemical control is used. Pesticide spray timing is synchronized with birth pulse. Discrete dynamical system (2.3.2) determined by the stroboscopic map, possesses two fixed points, corresponding to wash out of pest and coexistence. Stability analysis has been carried out about two fixed points. Threshold conditions which guarantee the existence and stability of pest extinction as well as positive period-1 solution are obtained about the birth parameter. The conditions for transcritical and flip bifurcation are also obtained and analyzed. It reveals that the period-1 solution bifurcates from the pest-free state through a transcritical bifurcation.

The behavior of net reproductive number with respect to model parameters has been investigated numerically. When the mortality rates of the immature and mature pest are smaller, the threshold value for pest extinction reduces. Numerical results show that the rich dynamics of the system (2.2.6) − (2.2.8) including stable period-1,

period-n and chaotic solutions. Bifurcation diagrams and Lyapunov exponents show the range of parameters for which the map (2.3.2) has a chaotic solution. The solution may tend to stable point or strange attractor depending upon the parameter values.

Chapter 3

An Impulsive Pest Control Model with Birth Pulse Using Asynchronous Pesticide Spray

3.1 Introduction

In most impulsive models, different kinds of impulsive effect are assumed to be synchronized. Some impulsive models incorporating asynchronous pulses have been discussed [63, 65, 130, 169, 239, 243]. In [131], stage-structured pest control model with asynchronous pulses has been investigated. They have considered that pesticide spray kills the only mature pest. Some pesticides for e.g., Tetrachlorvinphos is effective against both stages of the pest Rhizopertha in Sorghum. Zhongjun et al. have proposed a stage-structured impulsive pest control model incorporating birth pulses [149]. They have assumed that pesticide effects both immature and mature pest with same killing efficiency rate.

This chapter extends stage-structured pest control model when the birth pulses are not synchronized with pulses of chemical spray. The simplifying assumption of the previous chapter is relaxed. The purpose of this chapter is to examine the effect of pesticide spray timing on the threshold and the dynamics of the system.

3.2 The Mathematical Model

In this section, a stage-structured impulsive pest control model is developed considering periodic pesticide spray asynchronous with birth pulses. To formulate the model following assumptions have been made:

- For simplicity, mortality rates of immature and mature pest are assumed to be the same, i.e. $d_1 = d_2 = d$.
- Birth pulse take places periodically at $t = mT$, $m = 1, 2, 3...$.
- The pesticide is sprayed between two successive (say $(m-1)^{th}$ and m^{th}) birth pulses at time $t = (m + l - 1)T, 0 < l < 1$. The periodicity of chemical spray T is the same as that of the birth pulse.
- The mature and immature pests are killed instantaneously at rates α and β, $0 < \alpha, \beta < 1$, respectively.

$$\left.\begin{aligned} x((m+l-1)T)^+ &= (1-\beta)x((m+l-1)T), \\ y((m+l-1)T)^+ &= (1-\alpha)y((m+l-1)T), \end{aligned}\right\} t = (m+l-1)T.$$

Using these assumptions, the model is written as:

$$\left.\begin{aligned} \frac{dx}{dt} &= -dx(t) - ax(t), \\ \frac{dy}{dt} &= ax(t) - dy(t), \end{aligned}\right\} t \neq (m+l-1)T, t \neq mT, \tag{3.2.1}$$

$$\left.\begin{aligned} x((m+l-1)T)^+ &= (1-\beta)x((m+l-1)T), \\ y((m+l-1)T)^+ &= (1-\alpha)y((m+l-1)T), \end{aligned}\right\} t = (m+l-1)T, \tag{3.2.2}$$

$$\left.\begin{aligned} x(mT)^+ &= x(mT) + B(N(mT))y(mT), \\ y(mT)^+ &= y(mT), \end{aligned}\right\} t = mT, \tag{3.2.3}$$

$$x(0) \;=\; x_0 > 0,\ y(0) = y_0 > 0. \tag{3.2.4}$$

The biomass of the immature and mature pest just after the m^{th} birth pulse are $x(mT)^+$ and $y(mT)^+$ respectively. All parameters of the model (3.2.1) – (3.2.4) are assumed

to be positive. The initial densities of immature and mature pests are x_0 and y_0 respectively. Equations (3.2.2) and (3.2.3) represent the asynchronous pesticide spray with birth pulse at times $t = (m+l-1)T$ and $t = mT$, T being the periodicity of two pulses. The birth rate function $B(N(t))N(t)$ is assumed to be of Ricker type:

$$B(N) = be^{-N}.$$

The dynamics of stage-structured impulsive pest control system (3.2.1) − (3.2.4) is defined on the set:

$$\Re^2_+ \;=\; \{(x,y) \in \Re^2 \mid x \geq 0, y \geq 0\}.$$

3.3 Model Analysis

Let, the immature and mature pest densities be $x = x_{m-1}$ and $y = y_{m-1}$ at $t = (m-1)T$ respectively. Then the analytical solution of differential equations (3.2.1) between the pulses $(m-1)T \leq t < (m+l-1)T$ is obtained as:

$$\left.\begin{aligned} x(t) &= e^{-(a+d)(t-(m-1)T)}x_{m-1}, \\ y(t) &= e^{-d(t-(m-1)T)}[(1-e^{-a(t-(m-1)T)})x_{m-1} + y_{m-1}], \end{aligned}\right\} (m-1)T \leq t < (m+l-1)T.$$

Similarly, the analytical solution of differential equations (3.2.1) and applying impulsive conditions (3.2.2) at $(m+l-1)T$ gives the solution:

$$\left.\begin{aligned} x(t) &= (1-\beta)e^{-(a+d)(t-(m-1)T)}x_{m-1}, \\ y(t) &= [\check{\epsilon}x_{m-1} + (1-\alpha)y_{m-1}] \times e^{-d(t-(m-1)T)} \\ &\quad - (1-\beta)e^{-(a+d)(t-(m-1)T)}x_{m-1}, \\ \check{\epsilon} &= [(\alpha-\beta)e^{-alT} + (1-\alpha)], \end{aligned}\right\} (m+l-1)T \leq t < mT. \quad (3.3.1)$$

The application of impulsive condition (3.2.3) in (3.3.1) gives the solution of the system (3.2.1) − (3.2.4) at $t = mT$ as:

$$\begin{aligned} x_m &= F_1(x_{m-1}, y_{m-1}),\ y_m = G_1(x_{m-1}, y_{m-1}), \\ F_1(x_{m-1}, y_{m-1}) &= (1-\beta)e^{-(a+d)T}x_{m-1} + b \times exp[-(\check{\epsilon}x_{m-1} + (1-\alpha)y_{m-1})e^{-dT}] \\ &\quad \times [\check{\epsilon}e^{-dT}x_{m-1} + (1-\alpha)e^{-dT}y_{m-1} - (1-\beta)e^{-(d+a)T}x_{m-1}], \\ G_1(x_{m-1}, y_{m-1}) &= \check{\mu}e^{-dT}x_{m-1} + (1-\alpha)e^{-dT}y_{m-1}, \qquad (3.3.2) \\ \check{\mu} &= \check{\epsilon} - (1-\beta)e^{-aT}. \end{aligned}$$

The difference equations (3.3.2) describe the stroboscopic sampling of the immature and mature pest at m^{th} birth pulse in terms of previous pulse.

The intrinsic net reproductive number R_{10} can be computed as:

$$R_{10} = b\ b_{10}^{-1}, \tag{3.3.3}$$

where

$$b_{10} = (1-(1-\beta)e^{-(d+a)T})(1-(1-\alpha)e^{-dT})e^{dT}\check{\mu}^{-1}.$$

Remark 3.3.1. $R_{10} > 0$ is positive provided

$$\check{\mu} \;=\; (\alpha-\beta)e^{-alT} + (1-\alpha) - (1-\beta)e^{-aT} > 0.$$

3.4 Equilibria and Stability Analysis

In this section, analysis is carried out regarding the fixed points of the map (3.3.2).

Proposition 3.4.1. *The pest-free state $E_0 = (0,0)$ always exists.*

Proposition 3.4.2. *Let*

$$\begin{aligned} x^* &= \frac{(1-(1-\alpha)e^{-dT})\log(R_{10})}{e^{-dT}(\check{\epsilon}-(1-\alpha)(1-\beta)e^{-(d+a)T})}, \\ y^* &= \frac{(\check{\epsilon}-(1-\beta)e^{-aT})\log(R_{10})}{\check{\epsilon}-(1-\alpha)(1-\beta)e^{-(d+a)T}}, \\ R_{10} &= \frac{b((\alpha-\beta)e^{-alT}+(1-\alpha)-(1-\beta)e^{-aT})}{(1-(1-\beta)e^{-(d+a)T})(1-(1-\alpha)e^{-dT})e^{dT}}. \end{aligned}$$

A non-trivial interior fixed point $E^* = (x^*, y^*)$ exists when $\check{\epsilon}-(1-\alpha)(1-\beta)e^{-(d+a)T} > 0$ and $R_{10} > 1$.

Remark 3.4.1. It may be noted that $E^* = E_0$ if $R_{10} = 1$.

Remark 3.4.2. The unique interior fixed point is feasible if the birth rate of the pest is more than a critical value b_{10} which depends upon all model parameters.

The local stability analysis for various feasible fixed points has been performed. The linearized system about any arbitrary fixed point $X = (x, y)$ can be written as:

$$X_m = AX_{m-1}. \tag{3.4.1}$$

The coefficients of linearized matrix A are:

$$\begin{aligned}
a_{11} &= (1-\beta)e^{-(d+a)T} + b[\check{\mu} - (\check{\mu}x + (1-\alpha)y)\check{\epsilon}] \times exp[-dT - (\check{\epsilon}x + (1-\alpha)y)e^{-dT}], \\
a_{12} &= b(1-\alpha) \times [1 - \check{\mu}xe^{-dT} - (1-\alpha)ye^{-dT}] \times exp[-dT - \check{\epsilon}xe^{-dT} - (1-\alpha)ye^{-dT}], \\
a_{21} &= \check{\epsilon}e^{-dT} - (1-\beta)e^{-(d+a)T}, a_{22} = (1-\alpha)e^{-dT}.
\end{aligned}$$

The characteristic equation corresponding to (3.4.1) is:

$$\lambda^2 - Tr\lambda + Det = 0.$$

For the stability of the pest-free state, the following theorem is established:

Theorem 3.4.3. *The pest-free state $E_0 = (0, 0)$ is locally asymptotically stable if*

$$R_{10} < 1, \tag{3.4.2}$$

and unstable for $R_{10} > 1$.

Proof. The coefficients of the linearized matrix A at the pest-free fixed point are:

$$\begin{aligned}
a_{11} &= (1-\beta)e^{-(d+a)T} + b\check{\mu} \times e^{-dT}, \quad a_{12} = b(1-\alpha) \times e^{-dT}, \\
a_{21} &= \check{\epsilon}e^{-dT} - (1-\beta)e^{-(d+a)T}, \quad a_{22} = (1-\alpha)e^{-dT}.
\end{aligned}$$

The eigenvalues are given by the following quadratic equation:

$$\lambda^2 - ((1-\beta)e^{-(d+a)T} + b\check{\mu}e^{-dT} + (1-\alpha)e^{-dT})\lambda + (1-\alpha)(1-\beta)e^{-(2d+a)T} = 0.$$

The two Jury's conditions (1.4.12) and (1.4.13) that is $1+Tr+Det > 0$ and $1-Det > 0$ are always satisfied.

By applying Jury's condition (1.4.11) that is $1 - Tr + Det > 0$ gives:

$$1 - ((1-\beta)e^{-(d+a)T} + b\check{\mu}e^{-dT} + (1-\alpha)e^{-dT}) + (1-\alpha)(1-\beta)e^{-(2d+a)T} > 0,$$

i.e.

$$b < (1 - (1-\beta)e^{-(d+a)T})(1 - (1-\alpha)e^{-dT})e^{dT}\check{\mu}^{-1} = b_{10}. \tag{3.4.3}$$

It is observed that, the condition (3.4.3) with the condition (3.3.3) establish the local stability condition (3.4.2) of the pest-free state. Hence, the threshold condition for stability is $R_{10} < 1$. However, for $R_{10} > 1$, then one of the eigenvalues will be greater than 1. Hence, the pest-free state will be unstable for $R_{10} > 1$. □

Remark 3.4.3. The pest eradication is possible when $R_{10} < 1$ or b lies in the range $b \in (0, b_{10})$. For this range of b, trajectories of the map (3.3.2) approach to the origin and the pest will be eradicated.

Remark 3.4.4. When $R_{10} > 1$, the pest outbreak can occur as it is the existence condition for the interior non-trivial fixed point.

Remark 3.4.5. It is found that one of the eigenvalues of A about E_0 is one at $R_{10} = 1$. Therefore, the pest-free point becomes non-hyperbolic. To analyze the behavior of E_0 at $R_{10} = 1$, the center manifold theory has been performed in the next section.

For the stability of interior fixed point, the following theorem is concluded:

Theorem 3.4.4. *Let us assume the constants P and Q as:*

$$\begin{aligned} P &= 2(\check{\epsilon} - (1-\alpha)(1-\beta)e^{-(d+a)T}) \times (1 + (1-\beta)(1-\alpha)e^{-(2d+a)T}), \\ Q &= (1 - (1-\alpha)e^{-dT}) \times (\check{\epsilon} + (1-\alpha)(1-\beta)e^{-(d+a)T}) \times (1 - (1-\beta)e^{-(d+a)T}). \end{aligned}$$

The non-trivial fixed point $E^* = (x^*, y^*)$ is locally asymptotically stable provided

$$b < b_{10} \exp(P/Q) (= b_{1c}). \tag{3.4.4}$$

Proof. Coefficient of linearized matrix $A[E^*]$ are computed around $E^* = (x^*, y^*)$ as:

$$\begin{aligned} a_{11} &= (1-\beta)e^{-(d+a)T} + b_{10}e^{-dT}[\check{\epsilon} - (1-\beta)e^{-aT} - \check{\epsilon}y^*], \\ a_{12} &= b_{10}(1-\alpha)[1-y^*]e^{-dT}, \quad a_{21} = \check{\epsilon}e^{-dT} - (1-\beta)e^{-(d+a)T}, \quad a_{22} = (1-\alpha)e^{-dT}. \end{aligned}$$

Accordingly, the trace Tr and determinant Det are computed as:

$$\begin{aligned} Tr &= (1-\beta)e^{-(d+a)T} + b_{10}e^{-dT}[\check{\epsilon} - (1-\beta)e^{-aT} - \check{\epsilon}y^*] + (1-\alpha)e^{-dT}, \\ Det &= (1-\beta)(1-\alpha)e^{-(2d+a)T}[1 - b_{10}y^*]. \end{aligned}$$

It is observed that Jury's conditions (1.4.11) and (1.4.13) are always satisfied:

$$\begin{aligned} 1 - Tr + Det &= 1 - (1-\beta)e^{-(d+a)T}b_{10}e^{-dT}[\check{\epsilon} - (1-\beta)e^{-aT} - \check{\epsilon}y^*] - (1-\alpha)e^{-dT} \\ &\quad -(1-\beta)(1-\alpha)e^{-(2d+a)T}[1 - b_{10}y^*] \\ &= (1 - (1-\beta)e^{-(d+a)T})(1 - (1-\alpha)e^{-dT}) - b_{10}[(\alpha-\beta)e^{-alT} \\ &\quad +(1-\alpha) - (1-\beta)e^{-aT}](1-y^*)e^{-dT} \\ &= (1 - (1-\beta)e^{-(d_+a)T})(1 - (1-\alpha)e^{-dT})y^* > 0. \\ 1 - Det &= 1 - (1-\beta)(1-\alpha)e^{-(d+a)T}[1 - b_{10}y^*] > 0. \end{aligned}$$

The expression $1 + Tr + Det$ simplifies to:

$$\begin{aligned}
1 + Tr + Det &= 1 + (1-\beta)e^{-(d+a)T} + b_{10}[(\alpha-\beta)e^{-(d+al)T} + (1-\alpha)e^{-dT} \\
&\quad -(1-\beta)e^{-(d+a)T} - \{(\alpha-\beta)e^{-(d+al)T} + (1-\alpha)e^{-dT}\}y^*] \\
&\quad +(1-\alpha)e^{-dT} + (1-\beta)(1-\alpha)e^{-(2d+a)T}[1 - b_{10}y^*] \\
&= (1 + (1-\beta)e^{-dT-aT})(1 + (1-\alpha)e^{-dT}) + b_{10}[(\alpha-\beta)e^{-alT} \\
&\quad +(1-\alpha) - (1-\beta)e^{-aT} - \{(\alpha-\beta)e^{-alT} + (1-\alpha) \\
&\quad +(1-\beta)(1-\alpha)e^{-(d+a)T}\}y^*]e^{-dT} \\
&= (1 + (1-\beta)e^{-dT-aT})(1 + (1-\alpha)e^{-dT}) \\
&\quad +(1 - (1-\beta)e^{-dT-aT})(1 - (1-\alpha)e^{-dT}) \\
&\quad \times[1 - \frac{(\alpha-\beta)e^{-alT} + (1-\alpha) + (1-\beta)(1-\alpha)e^{-(d+a)T}}{(\alpha-\beta)e^{-alT} + (1-\alpha) - (1-\beta)(1-\alpha)e^{-(d+a)T}} \log(R_{10})].
\end{aligned}$$

Further, simplifying the Jury's condition (1.4.12), $1 + Tr + Det > 0$,

$$R_{10} < \exp \frac{2(\check{\epsilon} - (1-\alpha)(1-\beta)e^{-(d+a)T}) \times (1 + (1-\beta)(1-\alpha)e^{-(2d+a)T})}{(1-(1-\alpha)e^{-dT})(\check{\epsilon} + (1-\alpha)(1-\beta)e^{-(d+a)T})(1-(1-\beta)e^{-(d+a)T})} \quad (3.4.5)$$

Accordingly, the condition (3.4.5) and (3.3.3) together with the existence condition $b_{10} < b$ yields the stability condition (3.4.4). □

The trajectories of the system $(3.2.1) - (3.2.4)$ tend to following period-1 solution $(x_e(t), y_e(t))$:

$$\begin{aligned}
x_e(t) &= x^* e^{-(a+d)(t-(m-1)T)}, \qquad (3.4.6) \\
y_e(t) &= [(1 - e^{-a(t-(m-1)T)})x^* + y^*]e^{-d(t-(m+l-1)T)}, \qquad (m-1)T \le t < (m+l-1)T.
\end{aligned}$$

$$\begin{aligned}
x_e(t) &= (1-\beta)x^* e^{-(a+d)(t-(m-1)T)}, \qquad (m+l-1)T \le t < mT, \qquad (3.4.7) \\
y_e(t) &= [\check{\epsilon}x^* e^{-al(t-(m-1)T)} + (1-\alpha)y^* - (1-\beta)x^* e^{-a(t-(m-1)T)}]e^{-d(t-(m+l-1)T)}.
\end{aligned}$$

Remark 3.4.6. Since E^* is locally stable, the periodic solution $(3.4.6) - (3.4.7)$ of the system $(3.2.1) - (3.2.4)$ is locally stable in the range $b_{10} < b < b_{1c}$.

Remark 3.4.7. The interior fixed point become non-hyperbolic at $b = b_{1c}$ and one of the eigenvalues becomes 1. So, there is a possibility of flip bifurcation.

3.5 Bifurcation Analysis

First, transcritical bifurcation is carried out at $b = b_{10}$. The flip bifurcation at $b = b_{1c}$ is established in the next subsection. The behavior of bifurcation will be analyzed using Center Manifold Theorem 1.4.5.

3.5.1 Transcritical Bifurcation Analysis

Theorem 3.5.1. [Transcritical Bifurcation] *The map* (3.3.2) *exhibits transcritical bifurcation at* $R_{10} = 1$ $(b = b_{10})$.

Proof. Considering b to be the bifurcation parameter, $b = b_{10}$ corresponds to $R_{10} = 1$:

$$b_{10} = (1-(1-\beta)e^{-(d+a)T})(1-(1-\alpha)e^{-dT})e^{dT}\breve{\mu}^{-1}.$$

Consider the map

$$\begin{pmatrix} x \\ \\ y \end{pmatrix} \to \begin{pmatrix} b\times[\breve{\mu}x+(1-\alpha)y]\times exp[-dT-\breve{\epsilon}e^{-dT}x+(1-\alpha)e^{-dT}y] \\ +(1-\beta)xe^{-(a+d)T} \\ \breve{\mu}xe^{-dT}+(1-\alpha)ye^{-dT} \end{pmatrix}. \quad (3.5.1)$$

Let us introduce $x = u$, $y = v$, $b = b_{10} + b_1$. The fixed point E_0 of the map (3.3.2) is transformed to (u, v) and the map (3.5.1) becomes:

$$\begin{pmatrix} u \\ \\ v \end{pmatrix} \to \begin{pmatrix} (b_1+b_{10})(\breve{\mu}u+(1-\alpha)v)\times exp[-dT-(\breve{\epsilon}u+(1-\alpha)v)e^{-dT}] \\ +(1-\beta)e^{-(a+d)T}u \\ \breve{\mu}ue^{-dT}+(1-\alpha)ve^{-dT} \end{pmatrix} \quad (3.5.2)$$

Now, the map (3.5.2) can be rewritten as:

$$\begin{pmatrix} u \\ v \end{pmatrix} \to M\begin{pmatrix} u \\ v \end{pmatrix} + \begin{pmatrix} c_{11}u^2+c_{12}uv+c_{13}v^2+c_{14}b_1u+c_{15}b_1v \\ 0 \end{pmatrix}. \quad (3.5.3)$$

The coefficients of the matrix $M = m_{ij_{2\times 2}}$ and coefficients $c_{ij_{1\times 5}}$ are obtained as:

$$\begin{aligned}
m_{11} &= (1-\beta)e^{-(d+a)T}+b_{10}(\breve{\epsilon}e^{-dT}-(1-\beta)e^{-(d+a)T}), \quad m_{12} = b_{10}(1-\alpha)e^{-dT}, \\
m_{21} &= \breve{\epsilon}e^{-dT}-(1-\beta)e^{-(d+a)T}, \quad m_{22} = (1-\alpha)e^{-dT}, \\
c_{11} &= -b_{10}e^{-2dT}[(\alpha-\beta)^2e^{-2alT}+2(1-\alpha)(\alpha-\beta)e^{-alT}+(1-\alpha)^2 \\
&\quad -\breve{\epsilon}(1-\beta)e^{-aT}], \\
c_{12} &= -b_{10}(1-\alpha)e^{-2dT}[2(\alpha-\beta)e^{-alT}+2(1-\alpha)-(1-\beta)e^{-aT}], \\
c_{13} &= -b_{10}(1-\alpha)^2e^{-2dT}, \quad c_{14} = \breve{\epsilon}e^{-dT}-(1-\beta)e^{-(d+a)T}, \quad c_{15} = (1-\alpha)e^{-dT}.
\end{aligned}$$

The eigenvalues of M are 1 and $(1-\alpha)(1-\beta)e^{-(a+2d)T}$.

The corresponding eigenvectors are $V_5 = \{v_5, 1\}^T$ and $V_6 = \{v_6, 1\}^T$ respeectively where $v_5 = (1-(1-\alpha)e^{-dT})\breve{\mu}^{-1}e^{dT}$ and $v_6 = (1-\alpha)((1-\beta)e^{-(d+a)T}-1)\breve{\mu}^{-1}$.

Consider the transformation

$$\begin{pmatrix} u \\ v \end{pmatrix} = J_{E_0}\begin{pmatrix} \bar{x} \\ \bar{y} \end{pmatrix}, \quad J_{E_0} = (V_5 \;\; V_6)\,. \tag{3.5.4}$$

Using the transformation (3.5.4), the map (3.5.3) can be written as:

$$\begin{pmatrix} \bar{x} \\ \bar{y} \end{pmatrix} \to \begin{pmatrix} 1 & 0 \\ 0 & (1-\alpha)(1-\beta)e^{-(a+2d)T} \end{pmatrix}\begin{pmatrix} \bar{x} \\ \bar{y} \end{pmatrix} + \begin{pmatrix} f_1(\bar{x},\bar{y},b_1) \\ f_2(\bar{x},\bar{y},b_1) \end{pmatrix} \tag{3.5.5}$$

where

$$\begin{aligned}
f_1(\bar{x},\bar{y},b_1) &= d_1b_1\bar{x} + d_2b_1\bar{y} + d_3\bar{x}\bar{y} + d_4\bar{x}^2 + d_5\bar{y}^2,\\
f_2(\bar{x},\bar{y},b_1) &= -f_1(\bar{x},\bar{y},b_1),\\
d_1 &= (1-(1-\alpha)(1-\beta)e^{-(a+2d)T}) \times (\check{\epsilon} - (1-\beta)e^{-aT})^{-1}e^{dT},\\
d_2 &= (1-\alpha)(1-\beta)(1-(1-\alpha)(1-\beta)e^{-(a+2d)T})(\check{\epsilon} - (1-\beta)e^{-aT})^{-1}e^{-(a+d)T},\\
d_3 &= \Big(2c_{13} + 2c_{11}e^{dT} \times \breve{\mu}^{-2}(1-\alpha)((1-\beta)e^{-(d+a)T}-1)(1-(1-\alpha)e^{-dT}),\\
&\quad + c_{12}e^{dT}\breve{\mu}^{-1}(1-2(1-\alpha)e^{-dT} + (1-\alpha)(1-\beta)e^{-(2d+a)T})\Big)\\
&\quad \times e^{dT}\breve{\mu}^{-1}(1-(1-\alpha)(1-\beta)e^{-(a+2d)T}),\\
d_4 &= \Big(c_{11}\breve{\mu}^{-2}e^{2dT}(1-(1-\alpha)e^{-dT})^2 + c_{12}\breve{\mu}^{-1}e^{dT}(1-(1-\alpha)e^{-dT}) + c_{13}\Big)\\
&\quad \times (1-(1-\alpha)(1-\beta)e^{-(a+2d)T})e^{dT}\breve{\mu}^{-1},\\
d_5 &= (1-(1-\alpha)(1-\beta)e^{-(a+2d)T})e^{dT}\Big(c_{11}(1-\alpha)^2((1-\beta)e^{-(d+a)T}-1)^2\breve{\mu}^{-2}\\
&\quad + c_{12}(1-\alpha)((1-\beta)e^{-(d+a)T}-1)\breve{\mu}^{-1} + c_{13}\Big) \times \breve{\mu}^{-1}.
\end{aligned}$$

Applying, the center manifold for the map (3.5.1) can be represented as:

$$w^c(0) = \{(\bar{x},\bar{y},b_1) \in \Re^3 | \bar{y} = f(\bar{x},b_1), f(0,0) = 0, Df(0,0) = 0\}.$$

Let $\bar{y} = f(\bar{x},b_1) = B_0b_1 + B_1b_1\bar{x} + B_2\bar{x}^2 + O(|b_1|^2 + |b_1\bar{x}^2| + |\bar{x}|^3)$. The coefficients in $\bar{y}$ can be computed as:

$$B_0 = 0, \qquad B_1 = \frac{d_1}{(1-(1-\alpha)(1-\beta)e^{-(a+2d)T})}, \qquad B_2 = \frac{d_4}{(1-\alpha)(1-\beta)e^{-(a+2d)T}-1}.$$

The map restricted to the center manifold is given by:

$$\begin{aligned}\bar{f}:\bar{x}\to\bar{x}+f_1(\bar{x},\bar{y},b_1) &= \bar{x}+d_1b_1\bar{x}+d_2b_1\bar{y}+d_3\bar{x}\bar{y}+d_4\bar{x}^2+d_5\bar{y}^2\\ &= \bar{x}+d_1b_1\bar{x}+d_3\frac{d_4}{(1-\alpha)(1-\beta)e^{-(a+2d)T}-1}\bar{x}^3+d_4\bar{x}^2\\ &\quad +O(|b_1|^2+|b_1\bar{x}^2|+|\bar{x}|^4).\end{aligned}$$

From the conditions 1.4.22, it can be observed that

$$\frac{\partial\bar{f}(0,0)}{\partial b_1} = 0, \quad \frac{\partial^2\bar{f}(0,0)}{\partial x\partial b_1}=d_1\neq 0, \quad \frac{\partial^2\bar{f}(0,0)}{\partial^2 x}=2d_4\neq 0.$$

Note that, all conditions of transcritical bifurcation are satisfied at $(\bar{x},b_1)=(0,0)$. Further, E^* becomes E_0 as $b=b_{10}$. Hence the map (3.3.2) undergoes to a transcritical bifurcation between $E_0=(0,0)$ and $E^*=(x^*,y^*)$ at $b=b_{10}$. □

3.5.2 Flip Bifurcation Analysis

Theorem 3.5.2. [Flip Bifurcation] *The map* (3.3.2) *undergoes flip bifurcation at* $b=b_{1c}$.

Proof. Consider the map

$$\begin{pmatrix} x\\ \\ y\end{pmatrix}\to\begin{pmatrix} b\times[\check{\mu}x+(1-\alpha)y]\times exp[-dT-(\check{\epsilon}x+(1-\alpha)y)e^{-dT}]\\ +(1-\beta)xe^{-(a+d)T}\\ \check{\mu}e^{-dT}x+(1-\alpha)e^{-dT}y\end{pmatrix}. \quad (3.5.6)$$

Let $x=x^*+u, y=y^*+v, b=b_{1c}+b_{c1}$. The fixed point E^* of the map (3.3.2) is transformed to (u,v) and the map (3.5.6) becomes:

$$\begin{pmatrix} u\\ v\end{pmatrix}\to\begin{pmatrix} s_{11}u+s_{12}v+s_{13}u^2+s_{14}uv+s_{15}v^2+s_{16}b_{c1}u+s_{17}b_{c1}v\\ s_{21}u+s_{22}v\end{pmatrix}. \quad (3.5.7)$$

where

$$\begin{aligned}s_{11} &= (1-\beta)e^{-(d+a)T}+b_{1c}exp[-dT-\check{\epsilon}e^{-dT}x^*+(1-\alpha)e^{-dT}y^*]\times\{\check{\epsilon}-(1-\beta)e^{-aT}\\ &\quad -\check{\epsilon}e^{-dT}\times(\check{\epsilon}x^*+(1-\alpha)y^*-(1-\beta)e^{-aT}x^*)\},\\ s_{12} &= b_{1c}(1-\alpha)exp[-dT-\check{\epsilon}e^{-dT}x^*-(1-\alpha)e^{-dT}y^*]\times\{1-(\check{\mu}x^*+(1-\alpha)y^*)e^{-dT}\},\\ s_{13} &= \check{\epsilon}b_{1c}\times exp[-2dT-\check{\epsilon}e^{-dT}x^*-(1-\alpha)e^{-dT}y^*]\times\left\{\frac{1}{2}(\check{\mu}x^*+(1-\alpha)y^*)\times\check{\epsilon}e^{-dT}\right.\\ &\quad \left.-(\check{\epsilon}-(1-\beta)e^{-aT})\right\},\\ s_{14} &= b_{1c}(1-\alpha)exp[-2dT-(\check{\epsilon}x^*+(1-\alpha)y^*)e^{-dT}]\{\check{\epsilon}(\check{\mu}x^*+(1-\alpha)y^*)e^{-dT}-\check{\mu}-\check{\epsilon}\},\end{aligned}$$

$$
\begin{aligned}
s_{15} &= b_{1c}(1-\alpha)^2 exp[-2dT-(\check{\epsilon}x^*+(1-\alpha)y^*)e^{-dT}]\left\{\frac{1}{2}(\check{\mu}x^*+(1-\alpha)y^*)e^{-dT}-1\right\},\\
s_{16} &= exp[-dT-(\check{\epsilon}x^*+(1-\alpha)y^*)e^{-dT}]\{\check{\epsilon}-(1-\beta)e^{-aT}-\check{\epsilon}e^{-dT}(\check{\mu}x^*+(1-\alpha)y^*)\},\\
s_{17} &= (1-\alpha)\times exp[-dT-(\check{\epsilon}+(1-\alpha)y^*)e^{-dT}]\times\{1-e^{-dT}\check{\mu}x^*-(1-\alpha)e^{-dT}y^*\},\\
s_{21} &= \check{\epsilon}e^{-dT}-(1-\beta)e^{-(d+a)T}, \qquad s_{22}=(1-\alpha)e^{-dT}.
\end{aligned}
$$

The map (3.5.7) can be rewritten as:

$$
\begin{pmatrix} u \\ v \end{pmatrix} \to S \begin{pmatrix} u \\ v \end{pmatrix} + \begin{pmatrix} s_{13}u^2+s_{14}uv+s_{15}v^2+s_{16}b_{c1}u+s_{17}b_{c1}v \\ 0 \end{pmatrix}. \tag{3.5.8}
$$

The eigenvalues of $S=(s_{ij})_{2\times 2}$ are 1 and λ.

The corresponding eigenvectors are $V_7=\{v_7,1\}^T$ and $V_8=\{v_8,1\}^T$ respectively where $v_7=-e^{dT}(1+(1-\alpha)e^{-dT})\check{\mu}^{-1}$ and $v_8=e^{dT}(\lambda-(1-\alpha)e^{-dT})\check{\mu}^{-1}$.

Consider the transformation

$$
\begin{pmatrix} u \\ v \end{pmatrix} = J' \begin{pmatrix} \bar{x} \\ \bar{y} \end{pmatrix}, \qquad J'=(V_7 \;\; V_8). \tag{3.5.9}
$$

Using the transformation (3.5.9) in the map (3.5.8):

$$
\begin{pmatrix} \bar{x} \\ \bar{y} \end{pmatrix} \to \begin{pmatrix} -1 & 0 \\ 0 & \lambda \end{pmatrix} \begin{pmatrix} \bar{x} \\ \bar{y} \end{pmatrix} + \begin{pmatrix} f_1(\bar{x},\bar{y},b_{c1}) \\ f_2(\bar{x},\bar{y},b_{c1}) \end{pmatrix}. \tag{3.5.10}
$$

The functions in the above map are obtained as:

$$
\begin{aligned}
f_1(\bar{x},\bar{y},b_{c1}) &= g_1 b_{c1}\bar{x}+g_2 b_{c1}\bar{y}+g_3\bar{x}\bar{y}+g_4\bar{x}^2+g_5\bar{y}^2,\\
f_2(\bar{x},\bar{y},b_{c1}) &= -f_1(\bar{x},\bar{y},b_{c1}),\\
g_1 &= g_6^{-1}\times[s_{17}-(1+(1-\alpha)e^{-dT})\check{\mu}^{-1}e^{dT}s_{16}],\\
g_2 &= g_6^{-1}\times[s_{17}+(\lambda-(1-\alpha)e^{-dT})\check{\mu}^{-1}e^{dT}s_{16}],\\
g_3 &= g_6^{-1}\times[2s_{15}+s_{14}(\lambda-1-2(1-\alpha)e^{-dT})(\check{\epsilon}e^{-dT}-(1-\beta)e^{-(d+a)T})^{-1}\\
&\quad -2s_{13}(1+(1-\alpha)e^{-dT})(\lambda-(1-\alpha)e^{-dT})(\check{\epsilon}e^{-dT}-(1-\beta)e^{-(d+a)T})^{-2}],\\
g_4 &= [s_{13}-s_{14}(1+(1-\alpha)e^{-dT})(\check{\epsilon}-(1-\beta)e^{-aT})^{-1}e^{dT}\\
&\quad +(1+(1-\alpha)e^{-dT})^2\check{\mu}^{-2}e^{2dT}]\times g_6^{-1},\\
g_5 &= [s_{13}+s_{14}(\lambda-(1-\alpha)e^{-dT})(\check{\epsilon}-(1-\beta)e^{-aT})^{-1}e^{dT}\\
&\quad +(\lambda-(1-\alpha)e^{-dT})^2\check{\mu}^{-2}e^{2dT}]\times g_6^{-1},\\
g_6 &= -(1+\lambda)[\check{\epsilon}e^{-dT}-(1-\beta)e^{-(d+a)T}]^{-1}.
\end{aligned}
$$

The center manifold theorem is used to determine the nature of the bifurcation of the fixed point $(0,0)$ at $b_{c1}=0$. The center manifold of the map (3.5.6) can be represented as:

$$w^c(0) = \{(\bar{x},\bar{y},b_{c1})\in\Re^3|\bar{y}=h(\bar{x},b_{c1}), h(0,0)=0, Dh(0,0)=0\}.$$

Let $\bar{y}=h(\bar{x},b_{c1})=M_0b_{c1}+M_1b_{c1}\bar{x}+M_2\bar{x}^2+O(|b_{c1}|^2+|b_{c1}\bar{x}^2|+|\bar{x}|^3)$. The coefficients in $\bar{y}$ can be computed as:

$$\begin{aligned}
M_0 &= 0,\\
M_1 &= g_6^{-1}(1-\lambda)^{-1}\times[s_{17}-(1+(1-\alpha)e^{-dT})\breve{\mu}^{-1}e^{dT}s_{16}],\\
M_2 &= g_6^{-1}(\lambda-1)^{-1}[s_{13}-s_{14}(e^{dT}+(1-\alpha))(\breve{\epsilon}-(1-\beta)e^{-aT})^{-1}+(e^{dT}+(1-\alpha))^2\breve{\mu}^{-2}].
\end{aligned}$$

The map restricted to the center manifold is:

$$\bar{h}:\bar{x}\to-\bar{x}+h(\bar{x},\bar{y},b_{c1}) = -\bar{x}+g_1b_{c1}\bar{x}+g_2b_{c1}\bar{y}+g_3\bar{x}\bar{y}+g_4\bar{x}^2+g_5\bar{y}^2,$$

$$\begin{aligned}
\bar{h}:\bar{x}\to-\bar{x}+h(\bar{x},\bar{y},b_{c1}) &= -\bar{x}+g_1b_{c1}\bar{x}+g_3g_6^{-1}(\lambda-1)^{-1}[s_{13}-s_{14}(e^{dT}+(1-\alpha))\\
&\quad\times(\breve{\epsilon}-(1-\beta)e^{-aT})^{-1}+(e^{dT}+(1-\alpha))^2\breve{\mu}^{-2}]\bar{x}^3+g_4\bar{x}^2\\
&\quad+O(|b_{c1}|^2+|b_{c1}\bar{x}^2|+|\bar{x}|^4).
\end{aligned}$$

Using Theorem 1.4.4:

$$\frac{\partial\bar{h}(0,0)}{\partial b_{c1}}\frac{\partial^2\bar{h}(0,0)}{\partial x^2}+2\frac{\partial^2\bar{h}(0,0)}{\partial x\partial b_{c1}} = 0+2g_1\neq 0.$$

$$\begin{aligned}
\bar{a} &= \frac{1}{2}(\frac{\partial^2\bar{h}(0,0)}{\partial x^2})^2+\frac{1}{3}\frac{\partial^3\bar{h}(0,0)}{\partial x^3}\\
&= 2g_4^2-2g_3\frac{(1-\lambda)^2}{\breve{\epsilon}e^{-dT}-(1-\beta)e^{-(d+a)T}}\left(s_{13}+\frac{s_{14}(1+(1-\alpha)e^{-dT})}{\breve{\epsilon}e^{-dT}-(1-\beta)e^{-(d+a)T}}+s_{17}\right)\\
&\neq 0.
\end{aligned}$$

Since all conditions for flip bifurcation are satisfied at $(\bar{x},b_{c1})=(0,0)$. There exist, period-2 solutions. These bifurcating period-2 solutions will be stable if $\bar{a}>0$ and unstable if $\bar{a}<0$. □

Further, increasing the parameter value $b>b_{1c}$, the fixed point E^* losses its stability and the map (3.3.2) may exhibit complex dynamics. The complex dynamical behavior will be shown in a later section.

3.6 Effect of Pesticide Spray Timing and Killing Rate

The primary concern associated with the eradication of the pest is the minimum use of pesticides with maximum reduction of the pest population. This reduces the cost of pest control with minimal effect on the environment. This can be achieved by suitably selecting the spray time l.

3.6.1 Effect of Pesticide Spray Timing l

The threshold depends on pesticide spray timing l. The derivative of R_{10} with respect to l is computed:

$$\frac{dR_{10}}{dl} = -\frac{abT(\alpha-\beta)e^{-dT-alT}}{(1-(1-\alpha)e^{-dT})(1-(1-\beta)e^{-(d+a)T})}.$$

Accordingly, the threshold R_{10} is a monotonic decreasing function with respect to l when $\alpha > \beta$ and monotonic increasing function when $\alpha < \beta$. This indicates that if killing (poisoning) rate of mature pest is greater than immature pest then threshold R_{10} decreases. Once, the threshold R_{10} becomes less than unity, the pest will be eradicated.

The expression of y^* involves killing rate of immature and mature pest is affected by pesticide spray timing. Taking the first order derivative of the mature pest density with respect to parameter l:

$$\begin{aligned}\frac{dy^*}{dl} &= -\frac{aT(1-\beta)(\alpha-\beta)(1-(1-\alpha)e^{-dT})e^{-alT-a\log(R_{10})}}{(\check{\epsilon}-(1-\alpha)(1-\beta)e^{-(d+a)T})^2} \\ &- \frac{aT(\alpha-\beta)e^{-alT}}{(\check{\epsilon}-(1-\alpha)(1-\beta)e^{-(d+a)T}}.\end{aligned}$$

Further, it can be easily seen that the equilibrium density of mature pest is a decreasing function with respect to pesticide spraying time parameter l for $\alpha > \beta$. Accordingly, bigger the value of l, lower will be the mature pest density at equilibrium.
Similarly, it can be proved that the equilibrium density of immature pest is a monotonic function with respect to parameter l.

3.6.2 Effect of Killing Rate α and β on Threshold R_{10}

The killing efficiency rates α and β also affect the threshold R_{10}. The effects of pesticide spray on threshold R_{10} will be analyzed by taking first order derivatives of the threshold R_{10} defined by (3.3.3) with respect to β and α respectively and these are obtained as:

$$\frac{dR_{10}}{d\beta} = -\frac{be^{-dT}((1-\alpha)e^{-(d+a)T}(1-e^{-alT})+e^{-alT}-e^{-aT})}{(1-(1-\alpha)e^{-dT})(1-(1-\beta)e^{-(d+a)T})^2} < 0.$$

$$\frac{dR_{10}}{d\alpha} = -\frac{be^{-dT}[(1-\beta)e^{-dT}(e^{-alT}-e^{-aT})+1-e^{-alT}]}{(1-(1-\alpha)e^{-dT})^2(1-(1-\beta)e^{-(d+a)T})} < 0.$$

It can be easily observed that increasing killing (or poisoning) rate β or α reduces the threshold value R_{10}. Accordingly, with sufficient large values of killing rates α and β, the pest eradication may be possible.

3.7 Numerical Simulations

In this section, numerical analysis of the system (3.2.1)−(3.2.4) and the map (3.3.2) are performed based on the analytical results. The critical parameters for the investigation are identified as a, d, l, T, α and β that are involved in R_{10} which affect the dynamics of the system (3.2.1) − (3.2.4). Consider the following parameter set

$$a = 0.4, d = 0.2, \alpha = 0.8, \beta = 0.4. \tag{3.7.1}$$

The positive equilibrium of the map (3.3.2) depends on pesticide spray timing l. Fig. 3.1 shows the variation of the equilibrium level of pest density versus l for different killing rates $\beta, \alpha \in (0, 1)$ of immature and mature pest. It is observed that the lowest equilibrium level of the pest is possible when $l = 1$. Fig. 3.1(a) shows that when $\alpha < \beta$, immature pest equilibrium density increases, which is not effective for pest control. From a biological point of view, the aim is to reduce the pest to the lower level not to eliminate it.

From Table 3.1, it can be observed that pesticide spray timing l reduce the pest density. If pesticide will be sprayed at time $l = 0.1$, the reduction in immature and mature pest equilibrium densities are 6.4% and 83.30% respectively. The reduction is 83.82% and 98.26% of immature and mature pest respectively if the pesticide is sprayed

just before the birth pulse. The maximum reduction in the immature and mature pest is 95.83% and 99.59% if the time of spraying pesticide is the same with that of birth pulse ($l = 1$). Therefore, the best timing of pesticide spray is just before the births.

l	x^*	Percent decrease in x	y^*	Percent decrease in y	R_{10}	b_{1c}	b_{10}	E^*
0.0	2.5106	0	2.2574	0	39.6040	9233.60	0.3030	stable
0.1	2.3500	6.40	0.3769	83.30	2.9243	75.3061	3.7616	stable
0.2	2.1694	13.59	0.3274	85.49	2.6824	80.6293	4.1009	stable
0.3	1.9690	21.57	0.2796	87.61	2.4499	86.6899	4.4900	stable
0.4	1.7491	30.33	0.2337	89.65	2.2265	93.6580	4.9404	stable
0.5	1.5106	39.83	0.1898	91.59	2.0119	101.7607	5.4674	stable
0.6	1.2550	50.01	0.1481	93.44	1.8057	111.3072	6.0917	stable
0.7	0.9841	60.80	0.1089	95.18	1.6076	122.7296	6.8424	stable
0.8	0.7003	72.11	0.0725	96.79	1.4173	136.6512	7.7613	stable
0.9	0.4062	83.82	0.0392	98.26	1.2344	154.0045	9.9110	stable
1	0.1048	95.83	0.0094	99.59	1.0587	176.2511	10.3899	stable

Table 3.1: Effect of impulsive pesticide spraying time on pest density and stability of positive fixed point for $b = 11$, $\beta = 0.4$, $\alpha = 0.8$.

From Fig. 3.1(b), it is concluded that when $\alpha = 0.8$, the pest will remain below the threshold level. Also, for $\alpha = 0.9$, the pest will be totally eradicated. But, highly toxic pesticides are needed to reduce the pest which may not be environmentally friendly.

Considering $T = 1.0$, $l = 0.5$ and data set (3.7.1), the constant b_{10} is computed as $b_{10} = 5.4674$. For $b = 5$, the basic reproduction number is obtained as ($R_{10} = 0.9145 < 1$). According to Theorem (3.4.3), the pest-free state is locally asymptotically stable and coexistence is not possible. Taking $b = 11$, the pest-free fixed point becomes unstable. The non-trivial fixed point $E^* = (1.5106, 0.1898)$ is stable as $b_{10} < b < 101.7607$ (Theorem (3.4.4)). Further, transcritical bifurcation occurs at $b = 5.4674$.

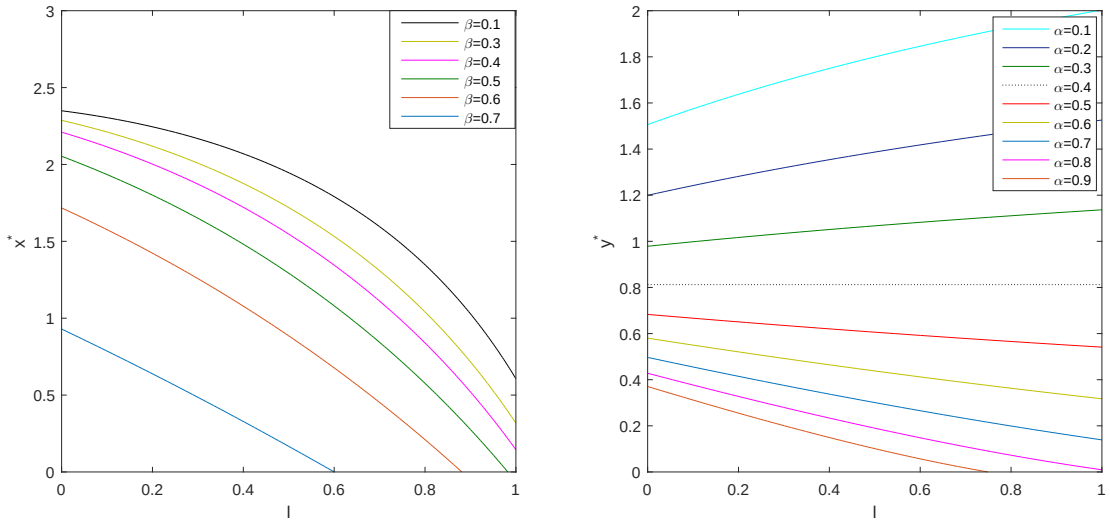

(a) **(b)**

Figure 3.1: Equilibrium density versus l for data set (3.7.1).

Fig. 3.2 is drawn to show the variation of R_{10} with β in the range $0 < \beta < 1$ for fixed $\alpha = 0.2$, 0.3, 0.4, 0.6 and 0.8 and $l = 0.5$. It is observed that the threshold R_{10} is monotonic decreasing function with respect to β. It is concluded that when $\alpha < \beta = 0.8$, the threshold R_0 is less than 1 and the pest eradication will occur.

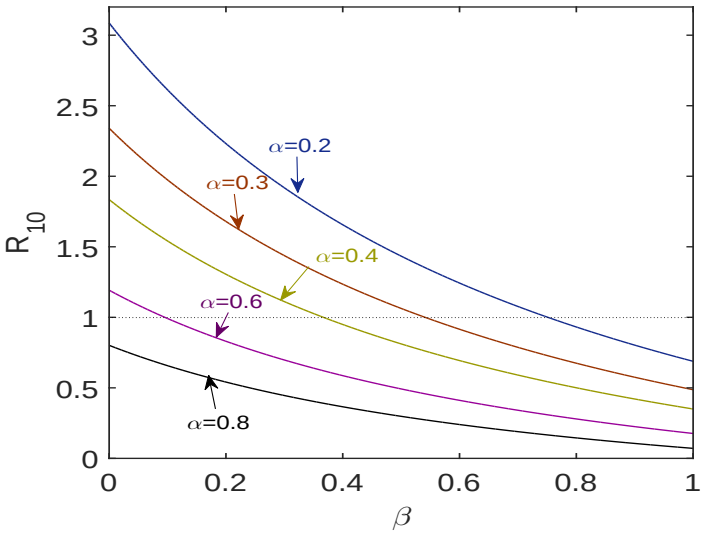

Figure 3.2: Variation of R_{10} versus β.

Fig. 3.3(a) shows the variation of R_{10} with pulse period T for $l = 0.5$. The non-monotonic behavior of R_{10} with respect to impulsive period T is observed. As

the values of T increases, R_{10} first increases and attains a peak, then it decreases with increase in T. Once the threshold value R_{10} becomes less than 1, the pest go to extinction.

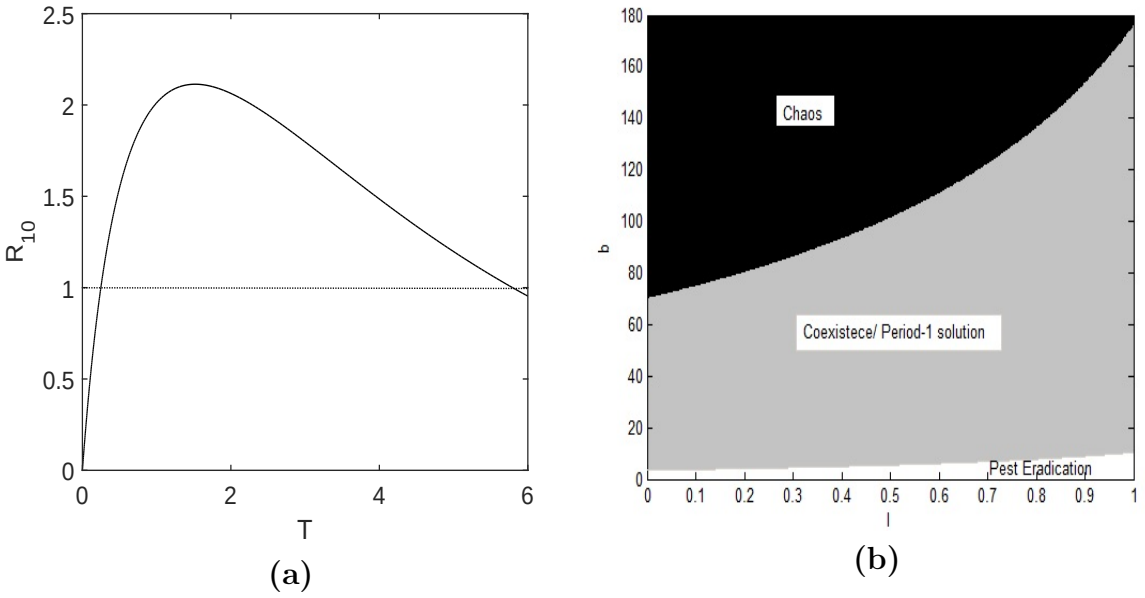

Figure 3.3: (a) Variation of R_{10} with T (b) Two-parameter bifurcation diagram in $l-b$ plane.

To see complexity due to pesticide spray timing and birth rate, two-parameter bifurcation diagram is drawn in the $l-b$ plane. In Fig. 3.3(b), region of the pest extinction is shown by white, while the region of the stable period-1 solution is shown by light-grey. For higher birth rates of the pest, the map (3.3.2) becomes chaotic, which is shown in the black region. At lower birth rates, the pest will be eradicated for all values of pesticide spray time. It has been observed that the pest will go to extinction in a small neighborhood of $(0,0)$. The period doubling leads to chaos for the higher birth rate.

In Fig. 3.4, the line $R_{10}=1$ separates the region of the pest-free state and interior fixed point stability. The region below the line $R_{10}=1$ is the region of stability of the pest-free state. On the other hand, the region above the line $R_{10}=1$ is the region of the instability of the pest-free state. For a fixed value of pesticide spray timing l, the corresponding killing rate of mature pest is needed to clear the pest population.

Fig. 3.5 is drawn to show the importance of incorporating asynchronous pulses. The threshold R_{10} is plotted with the killing efficiency of immature pest β in the range

$\beta \in (0,1)$ for the data set (3.7.1) and $l = 0.5$. For synchronous pulses, R_{10} is greater than 1 and pest outbreak will occur. Further, the threshold R_{10} becomes less than unity for $\beta > 0.10936$ for asynchronous pulses. Accordingly, the pest-free state remains stable for $\beta > 0.10936$ ($0.10936 < \beta < \alpha = 0.8$) and the pest will be eradicated. Therefore, incorporation of asynchronous pulses is a better choice to achieve the pest-free solution.

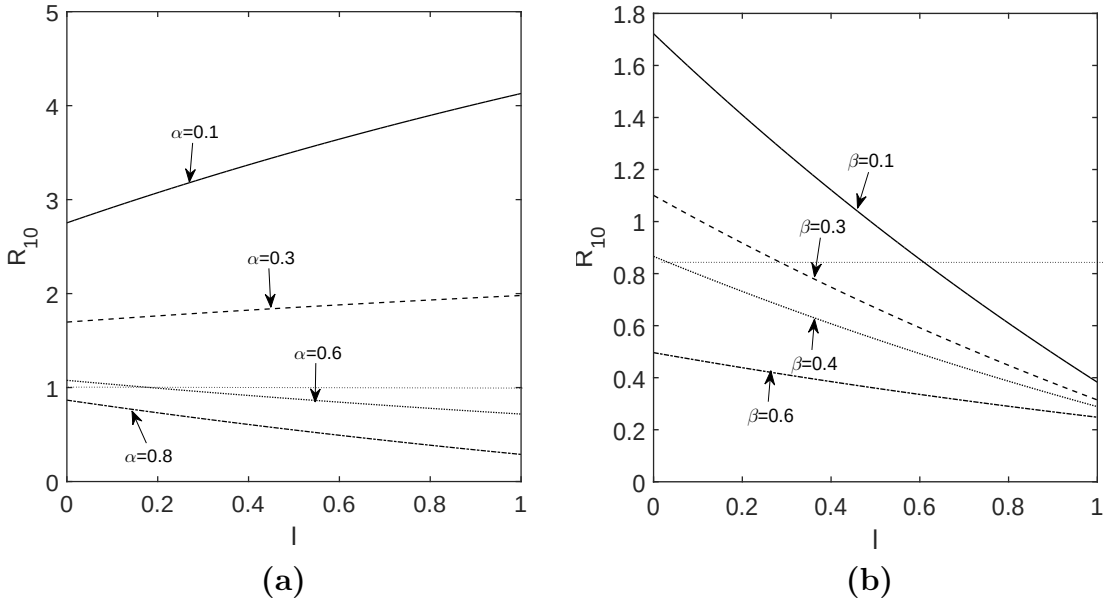

Figure 3.4: Two-parameter bifurcation diagram in $R_{10} - l$ plane for (a) Different values of α (b) Different values of β.

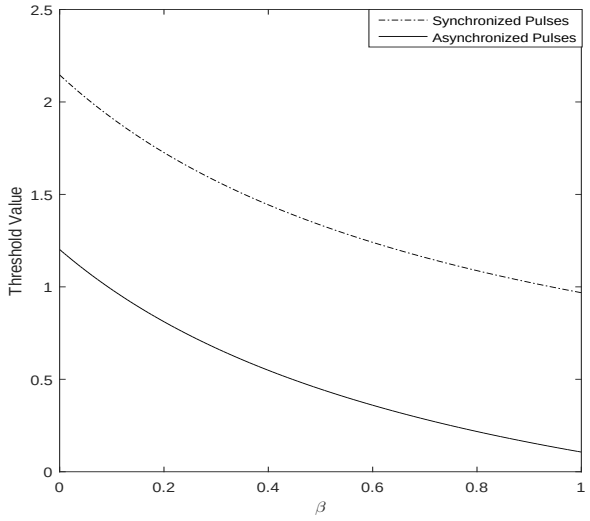

Figure 3.5: Effect of synchronous and asynchronous pulses.

The typical bifurcation diagram is drawn for total pest population in Fig. 3.6(a) with respect to critical parameter b which is involved in $R_{10} = bb_{10}^{-1}$ as well as in $R_c = bb_{1c}^{-1}$. The bifurcation diagram of the system (3.2.1) − (3.2.4) shows the existence of chaos through period-doubling route. For $l = 0.5$, the critical value obtained from equation (3.4.4) for a flip bifurcation parameter is $b_{1c} = 101.7607$. Period-doubling bifurcation is confirmed from Fig. 3.6(a). The stable period-1 solution occurs in the range $b \in (5.4674, 101.7607)$. As the parameter value of b increases beyond b_{1c}, the period-1 solutions destabilize and successive period-doubling with period-2, period-4, period-8 and period-16 occur in the intervals $(101.7607, 296.841)$, $(296.841, 406.783)$, $(406.783, 434.8518)$ and $(434.8518, 441.16)$ respectively. The cascades of period-doubling are observed in the bifurcation diagram, which is the route to chaos in the system. Several periodic windows are visible in the interval $(500, 700)$. For more clarity, a region of Fig. 3.6(a) is separately blown up in Fig. 3.6(b) in the interval $(690, 720)$ and a periodic window is clearly visible.

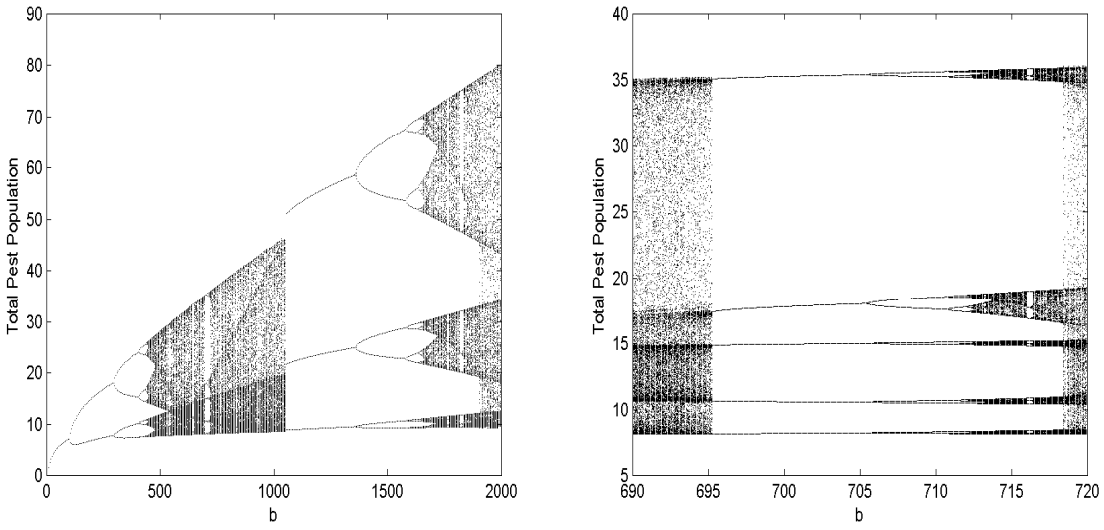

(a) **(b)**

Figure 3.6: (a) Bifurcation diagram of the system (3.2.1) − (3.2.4) for total pest population with respect to parameter b (b) Blown up in $(690, 720)$.

Fig. 3.7 shows bifurcation diagrams of the system (3.2.1) − (3.2.4) with respect to pesticide spray time $l \in (0, 1)$ with $b = 450$. The system (3.2.1) − (3.2.4) depicts the very complex dynamical behavior if the pesticide is sprayed just before birth pulse.

As parameter l increases, chaotic behavior is followed by a period-halving bifurcation. From an ecological point of view, it can be observed that immature and mature pest decreases as pesticide spray timing l increases. It is noted that pesticide spray time may reduce complexity with increasing l and may stabilize the system.

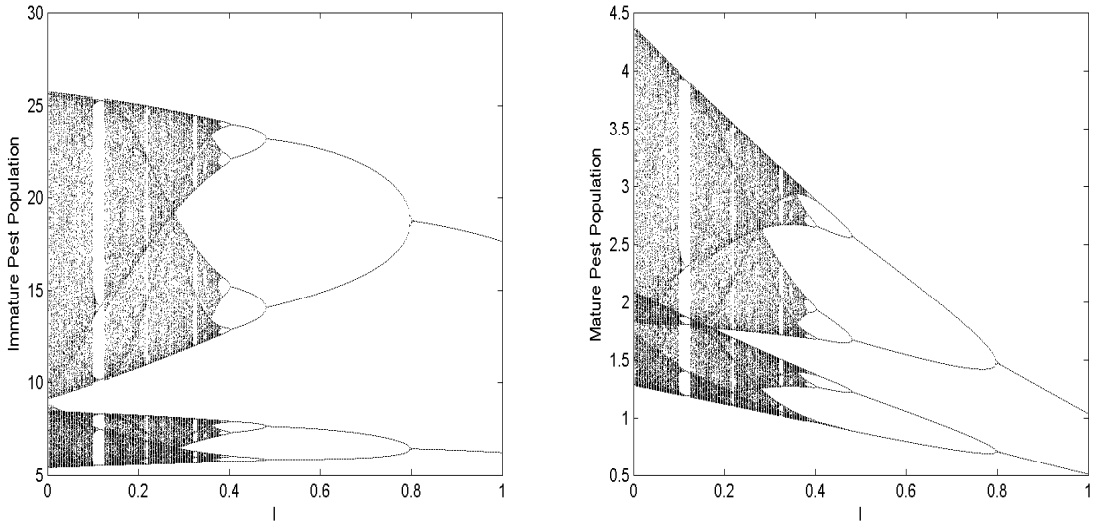

(a) **(b)**

Figure 3.7: Bifurcation diagrams of the system (3.2.1) – (3.2.4) for (a) Immature pest (b) Mature pest with respect to l.

3.8 Discussion

In this chapter, a stage-structured pest model is considered with the birth pulse and impulsive pesticide spray at a fixed time. By using the stroboscopic map, the complete expression for a periodic solution with period-1 is obtained. Also, the threshold conditions for the stability of two fixed points are obtained. The effects of pesticide spray timing on the immature and mature pest are considered. The results show that the best time of pesticide spray is towards the end of the season, i. e. before and near the next birth pulse. The system with Ricker type birth function shows a very complex dynamical behavior. As the parameter l increases, period-halving bifurcations followed by chaotic behavior. The mature pest density decreases with respect to pesticide spray timing l provided $\alpha > \beta$. Also, there exists a cascade of period-halving bifurcations from chaos to cycles.

Chapter 4

An Impulsive Pest Control Model with Birth Pulse Using Pesticide Having Instantaneous and Residual Effects

4.1 Introduction

Most of the pesticides are assumed to be of non-residual nature, that is, they kill the pest instantaneously and have no residual effects. For example, Pyrethrum is widely used non-residual insecticide. However, some pesticides are residual pesticides which remain effective on or in a crop/pest after the pesticide spray for some length of time [209, 230]. Some residual pesticides control the pest for weeks, months or even years. The biological pesticides are environmentally friendly, but they have a short-term residual effect. On the other hand, Organochlorine insecticides have a long-term residual effect. The instantaneous effect of chemicals on the pest is assumed in most of the impulsive models. The instantaneous killing efficiency of the pesticides on the pest (i.e. without residual effect) has been extensively discussed [216, 217, 218, 219, 222].

Residual effects of pesticides play a vital role in successful pest control. This residual pesticide may affect the pest continuously. The residual pesticide effects are modeled by continuous or piecewise-continuous periodic functions which affect the growth

rate of pest [172]. In the absence of stage-structure and birth pulses, very few pest control models are available which incorporate residual effects of pesticides [126, 221]. In previous chapters, 2 and 3, the only instantaneous effect of the pesticide has been incorporated.

In this chapter, a pest control nonlinear dynamical model has been proposed and analyzed. The stage-structured model incorporates asynchronous chemical spray and birth pulses. It considers the residual effect of pesticides on both immature and mature pest. The effects of residual pesticide on threshold condition will be investigated.

4.2 The Mathematical Model

For the stage-structured pest control model following assumptions have been made:

- The deaths of immature and mature pests are assumed to be proportional to their densities x and y respectively. Their death rates are constant.
- The maturation rate of immature pest is constant a.
- The mature pest reproduce periodically and birth occurs in pulses at an interval T. The birth function $B(N(t))$ is considered of Ricker type.
- The pesticide spray occurs impulsively at the time $t = \tau_{mp} = (m-1)T + \tau_p$ where $\tau_p = lT$, $(0 < l < 1)$ between two successive birth pulses which occur at $t = (m-1)T$ and $t = mT$, $m = 1, 2, 3...$. The pesticide has instantaneous as well as residual effect on the pest.
- The pesticide kills both immature and mature pest population instantaneously at different rates β and α respectively, $0 < \alpha, \beta < 1$:

$$x(\tau_{mp})^+ = (1-\beta)x(\tau_{mp}), \quad y(\tau_{mp})^+ = (1-\alpha)y(\tau_{mp}), \quad t = \tau_{mp}. \tag{4.2.1}$$

- The residual pesticide has long-time continuous effect on the pest. Its effect on the pest is described by the kill rate function $k(t)$ [126]. Let m_1 be the killing efficiency and a_1 be its decay rate. Then

$$k(t) = m_1 e^{-a_1(t-\tau_p)}, \qquad t > \tau_p. \tag{4.2.2}$$

The impulsive stage-structured pest control model with birth pulse using a pesticide spray that have residual effect is defined on the set $\Re^2_+ = \{(x, y) \in \Re^2 \mid x \geq 0, y \geq 0\}$. Considering all parameters to be constant and positive, the complete model can be formulated as:

$$\left.\begin{aligned} \frac{dx}{dt} &= -(d + a + m_1 e^{-a_1(t-\tau_p)})x(t), \\ \frac{dy}{dt} &= ax(t) - (d + m_1 e^{-a_1(t-\tau_p)})y(t), \end{aligned}\right\} t \neq \tau, t \neq mT, \tag{4.2.3}$$

$$\left.\begin{aligned} x(\tau_{mp})^+ &= (1-\beta)x(\tau_{mp}), \\ y(\tau_{mp})^+ &= (1-\alpha)y(\tau_{mp}), \end{aligned}\right\} t = \tau_{mp}, \tag{4.2.4}$$

$$\left.\begin{aligned} x(mT)^+ &= x(mT) + be^{-x(mT)-y(mT)}y(mT), \\ y(mT)^+ &= y(mT), \end{aligned}\right\} t = mT, \tag{4.2.5}$$

$$x(0) \;=\; x_0 > 0, y(0) = y_0 > 0. \tag{4.2.6}$$

4.3 Model Analysis

Theorem 4.3.1. *The system* (4.2.3) − (4.2.6) *is ultimately bounded.*

Proof. Define a positive definite continuous function

$$V(t) = x(t) + y(t).$$

Let $D^+V(t, X)$ denotes Dini's derivative [120]. Using (4.2.3), it is computed as:

$$D^+V(t, X) \;=\; -(d + m_1 e^{-a_1(t-\tau_p)})(x(t) + y(t)), \qquad t \neq mT, \quad t \neq \tau_{mp}.$$

Considering $0 < d + m_1 < d_1$, it simplifies to yields:

$$D^+V(t, X) \leq -d_1 V(t, X), \qquad t \neq mT, \quad t \neq \tau_{mp}. \tag{4.3.1}$$

Using condition (4.2.4) at $t = \tau_{mp}$ and choosing $\gamma = \min\{\beta, \alpha\}$ gives:

$$\begin{aligned} V(\tau_{mp})^+ &= (1-\beta)x(\tau_{mp}) + (1-\alpha)y(\tau_{mp}), \\ &\leq (1-\gamma)V(\tau T). \end{aligned} \tag{4.3.2}$$

Applying birth pulses (4.2.5) at $t = mT$:

$$V(mT^+) = x(mT) + be^{-x(mT)-y(mT)}y(mT) + y(mT) \leq V(mT) + b. \quad (4.3.3)$$

Using Lemma 2.5 in [8], it can be obtained that

$$V(t) \leq V(0^+)e^{-d_1 t} + b\left(\frac{e^{-d_1(t-mT)} - e^{-d_1 T}}{(1-e^{-d_1 T})}\right) \to b\frac{e^{-d_1 T}}{(1-e^{-d_1 T})}, \quad as\ t \to \infty.$$

Therefore, the solution $(x(t), y(t))$ of the system (4.2.3) − (4.2.6) is bounded by a constant $b > 0$, $x(t) \leq b$ and $y(t) \leq b\ \forall$ large values of t. Hence, $V(t)$ is uniformly ultimately bounded. □

4.3.1 Stroboscopic Map

Let $x = x_{m-1}$ and $y = y_{m-1}$ be the immature and mature pest density respectively at $t = (m-1)T$. The analytical solution of differential equations (4.2.3) after the birth pulse and before the chemical spray can be obtained as:

$$\begin{aligned} x(t) &= x_{m-1}e^{-(a+d)(t-(m-1)T)+\phi}, && (m-1)T \leq t < \tau_{mp}, \\ y(t) &= e^{-d(t-(m-1)T)+\phi}[y_{m-1} + x_{m-1}(1-e^{-a(t-(m-1)T)})]. \end{aligned}$$

The analytical solution of the equations (4.2.3) with after the chemical spray and before the birth pulse (4.2.4) is:

$$\begin{aligned} x(t) &= (1-\beta)x_{m-1}e^{-(a+d)(t-(m-1)T)+\phi}, && \tau_{mp} \leq t < mT, \\ y(t) &= [(\alpha-\beta)x_{m-1}e^{-(d+a)lT} + (1-\alpha)(y_{m-1}+x_{m-1})e^{-dlT}]e^{-d(t-\tau_p)+\phi} \\ &\quad -(1-\beta)x_{m-1}e^{-(a+d)(t-(m-1)T)+\phi}, && (4.3.4) \\ a_1\phi &= m_1[e^{-a_1(t-(m-1)T)} - 1]. \end{aligned}$$

After the chemical spray, the solution (4.3.4) with impulsive conditions (4.2.5) gives the following map after each successive birth pulse at $t = mT$:

$$\begin{aligned} x_m &= b \times exp[-(\alpha-\beta)x_{m-1}e^{-(d+al)T+\theta} - (1-\alpha)(y_{m-1}+x_{m-1})e^{-dT+\theta}] \\ &\quad \times[(\alpha-\beta)x_{m-1}e^{-alT} + (1-\alpha)(y_{m-1}+x_{m-1}) - (1-\beta)x_{m-1}e^{-aT}] \times e^{-dT+\theta} \\ &\quad +(1-\beta)x_{m-1}e^{-(a+d)T+\theta}, && (4.3.5) \\ y_m &= [(\alpha-\beta)x_{m-1}e^{-alT} + (1-\alpha)(y_{m-1}+x_{m-1}) - (1-\beta)x_{m-1}e^{-aT}]e^{-dT+\theta}, \\ a_1\theta &= m_1[(e^{-a_1 T} - 1)] < 0. \end{aligned}$$

The discrete system of equations (4.3.5) is the stroboscopic sampling of the immature and mature pest. The dynamical behavior of the system (4.2.3) – (4.2.6) will be given by the dynamical behavior of the map (4.3.5) coupled with the system (4.3.4).

The intrinsic net reproductive number R_0 is computed as:

$$R_0 = b\ b_0^{-1}, \tag{4.3.6}$$

$$b_0 = \frac{(1-(1-\beta)e^{-dT-aT+\theta})(1-(1-\alpha)e^{-dT+\theta})}{((\alpha-\beta)e^{-alT}+(1-\alpha)-(1-\beta)e^{-aT})}e^{-dT+\theta}.$$

Remark 4.3.1. Since the numerator in b_0 should be always positive. Therefore, the basic reproduction number R_0 will be positive provided

$$(\alpha-\beta)e^{-alT}+(1-\alpha)-(1-\beta)e^{-aT}) > 0.$$

4.3.2 Fixed Points of Stroboscopic Map

The stroboscopic map (4.3.5) admits the following two equilibrium states:

- The unique pest-free fixed point $E_0 = (0, 0)$ exists without any parametric restriction.

- The unique non-trivial interior fixed point $E^* = (x^*, y^*)$ exists for $R_0 > 1$ and is obtained as

$$\begin{aligned} x^* &= \frac{(1-(1-\alpha)e^{-dT+\theta})\log(R_0)}{e^{-dT+\theta}((\alpha-\beta)e^{-alT}+(1-\alpha)-(1-\alpha)(1-\beta)e^{-(d+a)T+\theta})}, \\ y^* &= \frac{((\alpha-\beta)e^{-alT}+(1-\alpha)-(1-\beta)e^{-aT})\log(R_0)}{(\alpha-\beta)e^{-alT}+(1-\alpha)-(1-\alpha)(1-\beta)e^{-(d+a)T+\theta}}. \end{aligned}$$

Thus, E^* is biologically feasible if the birth rate of the pest is more than a critical value b_0 which depends upon all model parameters.

Remark 4.3.2. For $R_0 = 1$, the interior fixed point E^* collides to the pest-free point E_0.

4.3.3 Stability Analysis about the Fixed Points

For the local stability of any fixed point $E = (x, y)$ of the map (4.3.5), the coefficients of linearized matrix A are given as:

$$\left.\begin{aligned} a_{11} &= b\Psi[\check{\epsilon} - (1-\beta)e^{-aT} - \check{\epsilon}\{\check{\epsilon}x + (1-\alpha)y - (1-\beta)e^{-aT}x\}e^{-dT+\theta}]e^{-dT+\theta} \\ &\quad + (1-\beta)e^{-(d+a)T+\theta}, \\ a_{12} &= b(1-\alpha)\Psi[1 - e^{-dT+\theta}((1-\alpha)y + \check{\epsilon}x - (1-\beta)e^{-aT}x)]e^{-dT+\theta}, \\ a_{21} &= [\check{\epsilon} - (1-\beta)e^{-aT}]e^{-dT+\theta}, \quad a_{22} = (1-\alpha)e^{-dT+\theta}, \\ \Psi &= exp[-\check{\epsilon}e^{-dT+\theta}x - (1-\alpha)ye^{-dT+\theta}], \quad \check{\epsilon} = (1-\alpha) + (\alpha-\beta)e^{-alT}. \end{aligned}\right\} \quad (4.3.7)$$

For the local stability of the pest-free state, the following theorem establishes:

Theorem 4.3.2. *The pest-free state $E_0 = (0, 0)$ of the map (4.3.5) is locally asymptotically stable if*

$$R_0 < 1. \quad (4.3.8)$$

Proof. Using (4.3.7), the linearized matrix $A[E_0]$ about $(0, 0)$ is computed as:

$$A[E_0] = \begin{pmatrix} [(1-\beta)e^{-aT} + b(\check{\epsilon} - (1-\beta)e^{-aT})]e^{-dT+\theta} & (\check{\epsilon} - (1-\beta)e^{-aT})e^{-dT+\theta} \\ b(1-\alpha)e^{-dT+\theta} & (1-\alpha)e^{-dT+\theta} \end{pmatrix}.$$

Accordingly, the trace Tr and determinant Det are computed as:

$$\begin{aligned} Tr &= (1-\beta)e^{-(d+a)T+\theta} + b(\check{\epsilon} - (1-\beta)e^{-aT})e^{-dT+\theta} + (1-\alpha)e^{-dT+\theta}, \\ Det &= (1-\beta)(1-\alpha)e^{-(2d+a)T+2\theta}. \end{aligned}$$

It is observed that Jury's conditions (1.4.12) and (1.4.13) are always satisfied:

$$\begin{aligned} 1 + Tr + Det &= 1 + (1-\beta)e^{-(d+a)T+\theta} + b(\check{\epsilon} - (1-\beta)e^{-aT})e^{-dT+\theta} \\ &\quad + (1-\alpha)e^{-dT+\theta} + (1-\beta)(1-\alpha)e^{-(2d+a)T+2\theta} > 0, \\ 1 - Det &= 1 - (1-\beta)(1-\alpha)e^{-(2d+a)T+2\theta} > 0. \end{aligned}$$

The expression $1 - Tr + Det$ simplifies to:

$$\begin{aligned} 1 - Tr + Det &= 1 - (1-\beta)e^{-(d+a)T+\theta} - be^{-dT+\theta}[(1-\alpha) + (\alpha-\beta)e^{-alT} \\ &\quad - (1-\beta)e^{-aT}] + (1-\alpha)e^{-dT+\theta} + (1-\beta)(1-\alpha)e^{-(2d+a)T+2\theta} \\ &= (1 - (1-\beta)e^{-(d+a)T+\theta})(1 - (1-\alpha)e^{-dT+\theta}) \\ &\quad - b[(1-\alpha)e^{-dT+\theta} + (\alpha-\beta)e^{-(d+al)T+\theta} - (1-\beta)e^{-(d+a)T+\theta}]. \end{aligned}$$

Accordingly, the Jury's condition (1.4.11), $1 - Tr + Det > 0$ gives

$$(1-(1-\beta)e^{-(d+a)T+\theta})(1-(1-\alpha)e^{-dT+\theta}) > be^{-dT+\theta}[\check{\epsilon}-(1-\beta)e^{-aT}],$$

i.e.

$$b < \frac{(1-(1-\beta)e^{-(d+a)T+\theta})(1-(1-\alpha)e^{-dT+\theta})}{e^{-dT+\theta}((1-\alpha)+(\alpha-\beta)e^{-alT}-(1-\beta)e^{-aT})} = b_0. \tag{4.3.9}$$

The stability condition (4.3.8) is obtained using (4.3.9) and (4.3.6). This completes the proof. □

The solution trajectories in the neighborhood of $(0,0)$ tend to origin and the pest will be eradicated for $b \in (0, b_0)$. When the condition $R_0 < 1$ is not satisfied, the pest-free state is locally unstable.

Remark 4.3.3. In the absence of residual effect, i.e. $(m_1 = 0, \theta = 0)$, the threshold R_0^N is obtained as:

$$R_0^N = b\frac{((\alpha-\beta)e^{-alT}+(1-\alpha)-(1-\beta)e^{-aT})}{(1-(1-\beta)e^{-dT-aT})(1-(1-\alpha)e^{-dT})}e^{-dT}.$$

Observe that, $R_0 < R_0^N$. Note that, R_0^N is the same as R_0 computed in the chapter 3. The threshold R_0 reduces to R_0^N when only the instantaneous effect of pesticide is considered. Therefore, inclusion of residual effect of pesticide increases the possibility of stable the pest-free state as compared to instantaneous effect.

Remark 4.3.4. The model parameters m_1 and a_1 are involved in the threshold R_0. The first order derivatives of the threshold R_0 defined by (4.3.6) with respect to m_1 and a_1 respectively are obtained as:

$$\begin{aligned}
\frac{dR_0}{dm_1} &= \frac{b(1-(1-\beta)(1-\alpha)e^{-(2d+a)T+2\theta})((\alpha-\beta)e^{-alT}+(1-\alpha)-(1-\beta)e^{-aT})}{(1-(1-\alpha)e^{-dT+\theta})^2(1-(1-\beta)e^{-(d+a)T+\theta})^2} \\
&\quad \times e^{-dT+\theta}(e^{-a_1T}-1)a_1 < 0, \\
\frac{dR_0}{da_1} &= \frac{b(1-(1-\beta)(1-\alpha)e^{-(2d+a)T+2\theta})((\alpha-\beta)e^{-alT}+(1-\alpha)-(1-\beta)e^{-aT})}{(1-(1-\alpha)e^{-dT+\theta})^2(1-(1-\beta)e^{-(d+a)T+\theta})^2} \\
&\quad \times m_1e^{-a_1T}(e^{a_1T}-1-a_1T)a_1^{-2}e^{-dT+\theta} > 0.
\end{aligned}$$

This indicates that R_0 is monotonic decreasing with respect to m_1 and monotonic increasing with respect to a_1. Therefore, a sufficient increase in the killing efficiency rate m_1 may reduce the threshold R_0 below unity and eradicate the pest from the field. This is due to the stability of the pest-free state (Theorem 4.3.2). Increasing the decay rate a_1, enhances the threshold and the pest may persist in the field.

Remark 4.3.5. The basic reproduction number R_0 depends upon killing rates α and β due to pesticide spray. The first order derivatives of R_0 with respect to α and β are found to be negative:

$$\frac{dR_0}{d\alpha} = -\frac{be^{-dT+\theta}((1-\beta)e^{-dT+\theta}(e^{-aT}-e^{-a_1lT})+1-e^{-alT})}{(1-(1-\alpha)e^{-dT+\theta})^2(1-(1-\beta)e^{-(d+a)T+\theta})} < 0.$$

$$\frac{dR_0}{d\beta} = -\frac{be^{-dT+\theta}((1-\alpha)e^{-(d+a)T+\theta}(1-e^{-a_1lT})+e^{-aT}-e^{-alT})}{(1-(1-\alpha)e^{-dT+\theta})(1-(1-\beta)e^{-(d+a)T+\theta})^2} < 0.$$

Accordingly, a sufficient increase in any of these two parameters may reduce the threshold value R_0 and once $R_0 < 1$, the pest population can be eradicated successfully.

The pest-free state is stable if $R_0 < 1$. Since E_0 is only fixed point when $R_0 < 1$, it is possible that it may be globally stable. The next theorem proves its global stability.

Theorem 4.3.3. *The locally asymptotically stable pest-free state E_0 of the map* (4.3.5) *is globally asymptotically stable in the interior of positive quadrant of $x-y$ plane.*

Proof. Consider the positive definite function

$$V_1(x_m, y_m) = x_m + y_m.$$

Now, computation of ΔV_1 and its simplification gives

$$\begin{aligned}
\Delta V_1(x_m, y_m) &= f(x_m, y_m) + g(x_m, y_m) - x_m - y_m \\
&= (1-\beta)e^{-(d+a)T+\theta}x_m + be^{-dT+\theta}[(\alpha-\beta)e^{-alT}x_m + (1-\alpha)(y_m+x_m) \\
&\quad -(1-\beta)e^{-aT}x_m]exp[-e^{-dT+\theta}(\check{\epsilon}x_m - (1-\alpha)y_m)] \\
&\quad +[\check{\epsilon}x_m + (1-\alpha)y_m - (1-\beta)e^{-aT}x_m]e^{-dT+\theta} - x_m - y_m \\
&\leq [\{(1-\beta)e^{-aT} + b\{\check{\epsilon} - (1-\beta)e^{-aT}\} + (1-\beta)e^{-aT} + (1-\alpha) \\
&\quad -(\alpha-\beta)e^{-alT}\}e^{-dT+\theta} - 1]x_m + [(1-\alpha)\{b+1\}e^{-dT+\theta} - 1]y_m.
\end{aligned}$$

Further simplification of ΔV_1 yields:

$$\Delta V_1 < -(1-R_0)V_1(x_m, y_m) < 0.$$

Further, $\Delta V_1(0,0) = 0$. Therefore, $V_1(x_m, y_m)$ is negative definite when $R_0 < 1$. Thus, $V_1(x_m, y_m)$ is a Lyapunov function and the pest-free state E_0 is globally asymptotically stable in the positive quadrant of $x-y$ plane. □

Remark 4.3.6. The pest-free state E_0 of the map (4.3.5) will become non-hyperbolic at $R_0 = 1$ (or $b = b_0$) and there is a possibility of transcritical bifurcation. Also, at this point E^*=E_0.

To analyze the stability about E_0 at $R_0 = 1$, the center manifold theory is used. The following theorem explores the existence of transcritical bifurcation:

4.3.4 Transcritical Bifurcation Analysis

Theorem 4.3.4. *The map* (4.3.5) *undergoes a transcritical bifurcation at* $b = b_0$.

Proof. Let $\Upsilon = e^{-dT+\theta}((\alpha-\beta)e^{-alT} + (1-\alpha) - (1-\beta)e^{-aT})$. Consider the map

$$\begin{pmatrix} x \\ \\ y \end{pmatrix} \to \begin{pmatrix} b \times exp[-(\alpha-\beta)xe^{-(alT+d)T+\theta} - (1-\alpha)(y+x)e^{-dT+\theta}] \\ \times[\Upsilon x + (1-\alpha)e^{-dT+\theta}y] + (1-\beta)xe^{-(a+d)T+\theta} \\ \Upsilon x + (1-\alpha)e^{-dT+\theta}y \end{pmatrix}. \quad (4.3.10)$$

Let $x = u$, $y = v$, $b = b_1 + b_0$, $b_0 = \Upsilon^{-1}(1-(1-\beta)e^{-dT-aT+\theta})(1-(1-\alpha)e^{-dT+\theta})$. The pest-free point E_0 of the map (4.3.5) is transformed to (u, v) and the map (4.3.10) becomes:

$$\begin{pmatrix} u \\ v \end{pmatrix} \to \begin{pmatrix} (b_1+b_0)\Theta(\Upsilon u + (1-\alpha)ve^{-dT+\theta}) + (1-\beta)ue^{-(a+d)T+\theta} \\ \Upsilon u + (1-\alpha)ve^{-dT+\theta} \end{pmatrix}, \quad (4.3.11)$$

where $\Theta = exp[-(\alpha-\beta)ue^{-(d+al)T+\theta} - (1-\alpha)(v+u)e^{-dT+\theta}]$.

The map (4.3.11) can be rewritten as:

$$\begin{pmatrix} u \\ v \end{pmatrix} \to M \begin{pmatrix} u \\ v \end{pmatrix} + \begin{pmatrix} c_{11}u^2 + c_{12}uv + c_{13}v^2 + c_{14}b_1u + c_{15}b_1v \\ 0 \end{pmatrix}.$$

The coefficients of the matrix $M = (m_{ij})_{2\times 2}$ and coefficients $(c_{ij})_{1\times 5}$ are computed as:

$$\begin{aligned} m_{11} &= (1-\beta)e^{-(d+a)T+\theta} + b_0\Upsilon, \quad m_{21} = \Upsilon, \quad m_{12} = b_0(1-\alpha)e^{-dT+\theta}, \\ m_{22} &= (1-\alpha)e^{-dT+\theta}, c_{11} = -b_0\Upsilon[(\alpha-\beta)+(1-\alpha)]e^{-dT+\theta}, \\ c_{12} &= -b_0(1-\alpha)[\Upsilon + (\alpha-\beta)e^{-(d+al)T+\theta} + (1-\alpha)e^{-dT+\theta}]e^{-dT+\theta}, \\ c_{13} &= -b_0(1-\alpha)^2e^{-2(dT+\theta)}, \quad c_{14} = \Upsilon, \quad c_{15} = (1-\alpha)e^{-dT+\theta}. \end{aligned}$$

The eigenvalues of M are 1 and $(1-\alpha)(1-\beta)e^{-(a+2d)T+2\theta}$.

The corresponding eigenvectors V_9 and V_{10} are $\{v_9, 1\}^T$ and $\{v_{10}, 1\}^T$ respectively where

$v_9 = \Upsilon^{-1}(1-(1-\alpha)e^{-dT+\theta})$ and $v_{10} = \Upsilon^{-1}e^{-dT+\theta}(1-\alpha)((1-\beta)e^{-(d+a)T+\theta}-1)$.

Consider the transformation

$$\begin{pmatrix} u \\ v \end{pmatrix} = J \begin{pmatrix} \bar{x} \\ \bar{y} \end{pmatrix}, \quad J' = (V_9 \;\; V_{10}).$$

Now, the map (4.3.11) can be simplified as:

$$\begin{pmatrix} \bar{x} \\ \bar{y} \end{pmatrix} \to \begin{pmatrix} 1 & 0 \\ 0 & (1-\alpha)(1-\beta)e^{-(a+2d)T+2\theta} \end{pmatrix} \begin{pmatrix} \bar{x} \\ \bar{y} \end{pmatrix} + \begin{pmatrix} f_1(\bar{x},\bar{y},b_1) \\ f_2(\bar{x},\bar{y},b_1) \end{pmatrix},$$

where

$$\begin{aligned}
f_1(\bar{x},\bar{y},b_1) &= d_1b_1\bar{x} + d_2b_1\bar{y} + d_3\bar{x}\bar{y} + d_4\bar{x}^2 + d_5\bar{y}^2,\\
f_2(\bar{x},\bar{y},b_1) &= -f_1(\bar{x},\bar{y},b_1),\\
d_1 &= [1-(1-\alpha)(1-\beta)e^{-(a+2d)T+2\theta}]\Upsilon^{-1},\\
d_2 &= (1-\alpha)(1-\beta)[1-(1-\alpha)(1-\beta)e^{-(a+2d)T+2\theta}]\Upsilon^{-1}e^{-(a+2d)T+\theta},\\
d_3 &= [2c_{13} + 2c_{11}\Upsilon^{-2}e^{-dT+\theta}(1-\alpha)((1-\beta)e^{-(d+a)T+\theta}-1)(1-(1-\alpha)e^{-dT+\theta})\\
&\quad + c_{12}\Upsilon^{-1}(1-2(1-\alpha)e^{-dT+\theta}+(1-\alpha)(1-\beta)e^{-(d+a)T+\theta})]\\
&\quad \times(1-(1-\alpha)(1-\beta)e^{-(a+2d)T+2\theta})\Upsilon^{-1},\\
d_4 &= [c_{11}\Upsilon^{-1}(1-(1-\alpha)e^{-dT+\theta})^2 + c_{12}\Upsilon^{-1}(1-(1-\alpha)e^{-dT+\theta}) + c_{13}]\\
&\quad \times(1-(1-\alpha)(1-\beta)e^{-(a+2d)T+2\theta})\Upsilon^{-1},\\
d_5 &= (1-(1-\alpha)(1-\beta)e^{-(a+2d)T+2\theta})[c_{12}(1-\alpha)((1-\beta)e^{-(d+a)T+\theta}-1)\Upsilon^{-1}\\
&\quad e^{-dT+\theta} + c_{11}(1-\alpha)^2((1-\beta)e^{-(d+a)T+\theta}-1)^2\Upsilon^{-2}e^{-2dT+2\theta} + c_{13}]\Upsilon^{-1}.
\end{aligned}$$

The center manifold theorem [69] is used to determine the nature of bifurcation about E_0 at $b_1 = 0$. The center manifold for the map (4.3.10) can be represented as:

$$w^c(0) = \{(\bar{x},\bar{y},b_1) \in \Re^3 | \bar{y} = f(\bar{x},b_1), f(0,0) = 0, Df(0,0) = 0\}.$$

Let $\bar{y} = f(\bar{x},b_1) = B_0b_1 + B_1b_1\bar{x} + B_2\bar{x}^2 + O(|b_1|^2 + |b_1\bar{x}^2| + |\bar{x}|^3)$. Coefficients in $\bar{y}$ can be computed as:

$$B_0 = 0,\; B_1 = \frac{-d_1}{1-(1-\alpha)(1-\beta)e^{-(a+2d)T+2\theta}},\; B_2 = \frac{d_4}{(1-\alpha)(1-\beta)e^{-(a+2d)T+2\theta}-1}.$$

The map restricted to the center manifold is given by:

$$\begin{aligned}
\bar{f} &: \bar{x} \to \bar{x} + f_1(\bar{x},\bar{y},b_1) = \bar{x} + d_1b_1\bar{x} + d_2b_1\bar{y} + d_3\bar{x}\bar{y} + d_4\bar{x}^2 + d_5\bar{y}^2\bar{x}^2| + |\bar{x}|^4)\\
&= \bar{x} + d_1b_1\bar{x} + \frac{d_3d_4\bar{x}^3}{(1-\alpha)(1-\beta)e^{-(a+2d)T+2\theta}-1} + d_4\bar{x}^2 + O(|b_1|^2 + |b_1\bar{x}^2| + |\bar{x}|^4).
\end{aligned}$$

Using Theorem 1.4.3, it can be calculated that

$$\frac{\partial \bar{f}(0,0)}{\partial b_1} = 0, \quad \frac{\partial^2 \bar{f}(0,0)}{\partial x \partial b_1} = d_1 \neq 0, \quad \frac{\partial^2 \bar{f}(0,0)}{\partial^2 x} = 2d_4 \neq 0.$$

Note that, all conditions of transcritical bifurcation are satisfied at $(\bar{x}, b_1) = (0,0)$. Further, E^* becomes E_0 as $b = b_0$. Hence, the map (4.3.5) undergoes to transcritical bifurcation about $E_0 = (0,0)$ and $E^* = (x^*, y^*)$ at $b = b_0$. □

Note 1: The expression

$$b = \frac{(1-(1-\beta)e^{-dT-aT+\theta})(1-(1-\alpha)e^{-dT+\theta})}{((\alpha-\beta)e^{-alT}+(1-\alpha)-(1-\beta)e^{-aT})}e^{-dT+\theta} = b_0.$$

can be used to obtain the transcritical bifurcation with respect to α, β and l also.

Note 2: The map (4.3.5) neither admits saddle-node nor pitchfork bifurcation about E_0 and E^*.

Note 3: The survival state E^* exists if the pest-free state is unstable.

Remark 4.3.7. There exists no periodic solution of the map (4.3.5) in $x-y$ plane when $R_0 < 1$ and period-1 solution exists when $R_0 > 1$. To analyze the stability of period-1 solution, following theorem has been established.

Theorem 4.3.5. *Let us define the constants C and F as:*

$$\begin{aligned} C &= 2(\check{\epsilon}-(1-\beta)(1-\alpha)e^{-(d+a)T+\theta})(1+(1-\beta)(1-\alpha)e^{-2(d+a)T+2\theta}), \\ F &= (1-(1-\beta)e^{-(d+a)T+\theta})(1-(1-\alpha)e^{-dT+\theta})(\check{\epsilon}+(1-\beta)(1-\alpha)e^{-(d+a)T+\theta}). \end{aligned}$$

The non-trivial interior fixed point $E^* = (x^*, y^*)$ of the map (4.3.5) is locally asymptotically stable provided

$$b < b_0 exp(CF^{-1})(= b_c). \tag{4.3.12}$$

Proof. Using (4.3.7), the coefficients of the matrix $A[E^*]$ are computed around E^* as:

$$\begin{aligned} a_{11} &= (1-\beta)e^{-(d+a)T+\theta} + b[\check{\epsilon}-(1-\beta)e^{-aT} - (\check{\epsilon}x^* + (1-\alpha)y^* \\ &\quad -(1-\beta)e^{-aT}x^*)\check{\epsilon}e^{-dT+\theta}]e^{-dT+\theta}\Psi, \\ a_{12} &= b[1-e^{-dT+\theta}((1-\alpha)y^* + \check{\epsilon}x^* - (1-\beta)e^{-aT}x^*)] \times (1-\alpha)e^{-dT+\theta}\Psi, \\ a_{21} &= [(\alpha-\beta)e^{-alT} + (1-\alpha) - (1-\beta)e^{-aT}]e^{-dT+\theta}, \quad a_{22} = (1-\alpha)e^{-dT+\theta}, \\ \Psi &= exp[-e^{-dT+\theta}((\alpha-\beta)x^*e^{-alT} + (1-\alpha)(x^*+y^*))]. \end{aligned}$$

The trace Tr and determinant Det are computed as:

$$\begin{aligned} Tr &= b[(1-\alpha)+(\alpha-\beta)e^{-alT}-(1-\beta)e^{-aT}-((\alpha-\beta)x^*e^{-alT}+(1-\alpha)(x^*+y^*) \\ &\quad -(1-\beta)e^{-aT}x^*)\check{\epsilon}e^{-dT+\theta}]e^{-dT+\theta}\Psi+(1-\beta)e^{-(d+a)T+\theta}+(1-\alpha)e^{-dT+\theta}, \\ Det &= (1-\beta)(1-\alpha)e^{-(2d+a)T+2\theta}[1-b_0y^*]. \end{aligned}$$

It is observed that the inequalities (1.4.11) and (1.4.13) are always satisfied:

$$\begin{aligned} 1-Tr+Det &= 1-(1-\alpha)e^{-dT+\theta}-(1-\beta)e^{-(d+a)T+\theta}-b\Psi[\check{\epsilon}-(1-\beta)e^{-aT} \\ &\quad -e^{-dT+\theta}(\check{\epsilon}x^*e^{-alT}+(1-\alpha)y^*-(1-\beta)e^{-aT}x^*)\times\check{\epsilon}]e^{-dT+\theta} \\ &\quad +(1-\beta)(1-\alpha)e^{-(2d+a)T+2\theta}[1-b_0y^*] \\ &= (1-(1-\beta)e^{-(d+a)T+\theta})(1-(1-\alpha)e^{-dT+\theta})\log R_0>0. \\ 1-Det &= 1-(1-\beta)(1-\alpha)e^{-(2d+a)T+2\theta}[1-b_0y^*]>0. \end{aligned}$$

The expression $1+Tr+Det$ simplifies to:

$$\begin{aligned} 1+Tr+Det &= 1+(1-\alpha)e^{-dT+\theta}+(1-\beta)e^{-(d+a)T+\theta}+b\Psi e^{-dT+\theta}[\check{\epsilon} \\ &\quad -(1-\beta)e^{-aT}-e^{-dT+\theta}(\check{\epsilon}x^*+(1-\alpha)y^*-(1-\beta)e^{-aT}x^*)\times\check{\epsilon}] \\ &\quad +(1-\beta)(1-\alpha)e^{-(2d+a)T+2\theta}[1-b_0y^*] \\ &= (1+(1-\beta)e^{-(d+a)T+\theta})(1+(1-\alpha)e^{-dT+\theta})+b_0[(\alpha-\beta)e^{-alT} \\ &\quad +(1-\alpha)-(1-\beta)e^{-aT}-((\alpha-\beta)e^{-alT}+(1-\alpha))y^*e^{-dT+\theta} \\ &\quad +(1-\beta)(1-\alpha)e^{-(2d+a)T+2\theta}y^*] \\ &= (1+(1-\beta)e^{-(d+a)T+\theta})(1+(1-\alpha)e^{-dT+\theta}) \\ &\quad +(1-(1-\beta)e^{-(d+a)T+\theta})(1-(1-\alpha)e^{-dT+\theta}) \\ &\quad \times[1-\frac{(\alpha-\beta)e^{-alT}+(1-\alpha)+(1-\beta)(1-\alpha)e^{-(d+a)T+\theta}}{(\alpha-\beta)e^{-alT}+(1-\alpha)-(1-\beta)(1-\alpha)e^{-(d+a)T+\theta}}\log(R_0)]. \end{aligned}$$

Accordingly, Jury's condition (1.4.12), $1+Tr+Det>0$, gives:

$$\log(R_0)<\frac{2(\check{\epsilon}-(1-\beta)(1-\alpha)e^{-(d+a)T+\theta})(1+(1-\beta)(1-\alpha)e^{-2(d+a)T+2\theta})}{(1-(1-\beta)e^{-(d+a)T+\theta})(1-(1-\alpha)e^{-dT+\theta})(\check{\epsilon}+(1-\beta)(1-\alpha)e^{-(d+a)T+\theta})}. \tag{4.3.13}$$

The condition (4.3.13) with the existence condition $b_0<b$ gives the stability condition (4.3.12). Hence, if $b\in(b_0,b_c)$ then E^* is locally asymptotically stable. □

Accordingly, the fixed point E^* of the map (4.3.5) is locally asymptotically stable if $b \in (b_0, b_c)$. The trajectories of the system (4.2.3) − (4.2.6) tend to asymptotically stable period-1 solution $(x_e(t), y_e(t))$:

$$\begin{aligned} x_e(t) &= x^* e^{-(a+d)(t-(m-1)T)+\phi}, \qquad (m-1)T \leq t < \tau_{mp}, \\ y_e(t) &= e^{-d(t-(m-1)T)+\phi}[y^* + x^*(1 - e^{-a(t-(m-1)T)})]. \end{aligned}$$

$$\begin{aligned} x_e(t) &= (1-\beta)x^* e^{-(a+d)(t-(m-1)T)+\phi}, \qquad \tau_{mp} \leq t < (m-1)T, \\ y_e(t) &= [(1-\alpha)y^* + \check{\epsilon}x^* - (1-\beta)e^{-a(t-(m-1)T)})x^*] \times e^{-d(t-(m-1)T)+\phi}. \end{aligned}$$

It may be observed that violation of condition (4.3.12) will lead to instability of interior fixed point. It can be concluded that if there is a small increase in the birth rate beyond the critical value b_0, the map (4.3.5) has a positive period-1 solution until birth rate parameter b reaches the critical point $b = b_c$.

Theorem 4.3.6. *The locally asymptotically stable positive interior fixed point E^* of the map* (4.3.5) *is globally asymptotically stable.*

Proof. Consider the positive definite function:

$$V_2(x_m, y_m) = \mid x_m - x^* \mid + \mid y_m - y^* \mid .$$

Computing ΔV_2 on the same lines as in Theorem 4.3.3 proves that V_2 is a Lyapunov function. This proves the theorem. □

Note 4: The fixed point E^* loses its stability with increase in b (i.e. beyond $b > b_c$). If the stability condition of E^* is violated, then flip bifurcation occurs at $b = b_c$. Further, a stable Period-1 solution losses its stability and period-2 solution occurs.

Remark 4.3.8. The interior fixed point become non-hyperbolic at $b = b_c$. So, there is a possibility of flip bifurcation. Therefore, period-doubling can occur at $b = b_c$.

The following theorem characterizes the flip bifurcation at $b = b_c$.

4.3.5 Flip Bifurcation Analysis

Theorem 4.3.7. *The map* (4.3.5) *undergoes a flip bifurcation about* $E^* = (x^*, y^*)$ *at* $b = b_c$. *Moreover, if* $\bar{a} > 0$*(resp.* $\bar{a} < 0$*), then period-2 solutions that bifurcate from this fixed point are stable (resp. unstable).*

Proof. Consider the map

$$\begin{pmatrix} x \\ \\ y \end{pmatrix} \to \begin{pmatrix} b \times exp[-(\alpha-\beta)xe^{-(alT+d)T+\theta} - (1-\alpha)(y+x)e^{-dT+\theta}] \\ \times[\Upsilon x + (1-\alpha)e^{-dT+\theta}y] + (1-\beta)xe^{-(a+d)T+\theta} \\ \Upsilon x + (1-\alpha)e^{-dT+\theta}y \end{pmatrix}, \quad (4.3.14)$$

where,$\Upsilon = e^{-dT+\theta}((\alpha-\beta)e^{-alT} + (1-\alpha) - (1-\beta)e^{-aT})$.

Let $x = x^* + U$, $y = y^* + V$, $b = b_{c1} + b_c$. The fixed point E^* of the map (4.3.5) is perturbed to (U, V). The map (4.3.14) is transformed into:

$$\begin{pmatrix} U \\ V \end{pmatrix} \to \begin{pmatrix} s_{11}U + s_{12}V + s_{13}U^2 + s_{14}UV + s_{15}V^2 + s_{16}b_{c1}U + s_{17}b_{c1}V \\ s_{21}U + s_{22}V \end{pmatrix} (4.3.15)$$

where,

$$\begin{aligned}
s_{11} &= b_c\Psi_1 e^{-dT+\theta}[\Upsilon - \{\Upsilon x^* + (1-\alpha)y^* e^{-dT+\theta}\}\{(\alpha-\beta)e^{-alT} + (1-\alpha)\}] \\
&\quad +(1-\beta)e^{-(d+a)T+\theta}, \\
s_{12} &= b_c(1-\alpha)e^{-dT+\theta}\Psi_1[1-(1-\alpha)y^* e^{-dT+\theta} - \Upsilon x^*], \\
s_{13} &= b_c\Psi_1 e^{-dT+\theta}\left\{ -\Upsilon + \left(\frac{\Upsilon e^{-dT+\theta}}{2}x^* + \frac{(1-\alpha)}{2}y^*\right)\{(\alpha-\beta)e^{-alT} + (1-\alpha)\}\right\} \\
&\quad \times((\alpha-\beta)e^{-alT} + (1-\alpha)), \\
s_{14} &= b_c(1-\alpha)e^{-dT+\theta}\Psi_1\{(\Upsilon x^* - 1)((\alpha-\beta)e^{-(d+al)T+\theta} + (1-\alpha)e^{-dT+\theta}) \\
&\quad +((\alpha-\beta)e^{-(d+al)T+\theta} + (1-\alpha)e^{-dT+\theta})(1-\alpha)e^{-dT+\theta}y^* - \Upsilon\}, \\
s_{15} &= b_c(1-\alpha)^2\Psi_1 e^{-2dT+2\theta}\left\{ -1 + \frac{1}{2}\left((1-\alpha)y^* e^{-dT+\theta} + \Upsilon\right)\right\}, \\
s_{16} &= \Psi_1[\Upsilon - e^{-dT+\theta}\{(\alpha-\beta)e^{-alT} + (1-\alpha)\}\{(1-\alpha)e^{-dT+\theta}y^* + \Upsilon x^*\}\Upsilon], \\
s_{17} &= (1-\alpha)\Psi_1[1-(1-\alpha)e^{-dT+\theta}y^* - \Upsilon x^*]e^{-dT+\theta}, \quad s_{21} = \Upsilon, \quad s_{22} = (1-\alpha)e^{-dT+\theta}, \\
\Psi_1 &= exp[-(\alpha-\beta)x^* e^{-(al+d)T+\theta} + (1-\alpha)(x^*+y^*)e^{-dT+\theta}].
\end{aligned}$$

The map (4.3.15) can be rewritten as:

$$\begin{pmatrix} U \\ V \end{pmatrix} \to T\begin{pmatrix} U \\ V \end{pmatrix} + \begin{pmatrix} s_{13}U^2 + s_{14}UV + s_{15}V^2 + s_{16}b_{c1}U + s_{17}b_{c1}V \\ 0 \end{pmatrix}. (4.3.16)$$

The eigenvalues of $T = (s_{ij})_{2\times 2}$ are -1 and λ.

The corresponding eigenvectors are V_{11} and V_{12} are $\{v_{11}, 1\}^T$ and $\{v_{12}, 1\}^T$ respectively where, $v_{11} = -(1 + (1-\alpha)e^{-dT+\theta})\Upsilon^{-1}$ and $v_{12} = (\lambda - (1-\alpha)e^{-dT+\theta})\Upsilon^{-1}e^{-dT+\theta}$.

Consider the transformation

$$\begin{pmatrix} U \\ V \end{pmatrix} = J' \begin{pmatrix} \bar{x} \\ \bar{y} \end{pmatrix}, \qquad J' = (V_{11} \quad V_{12}).$$

Now, the map (4.3.16) can be transformed as:

$$\begin{pmatrix} \bar{x} \\ \bar{y} \end{pmatrix} \to \begin{pmatrix} -1 & 0 \\ 0 & \lambda \end{pmatrix} \begin{pmatrix} \bar{x} \\ \bar{y} \end{pmatrix} + \begin{pmatrix} f_1(\bar{x}, \bar{y}, b_{c1}) \\ f_2(\bar{x}, \bar{y}, b_{c1}) \end{pmatrix}.$$

The functions $f_1(\bar{x}, \bar{y}, b_{c1})$ and $f_2(\bar{x}, \bar{y}, b_{c1})$ are obtained as:

$$f_1(\bar{x}, \bar{y}, b_{c1}) = g_1 b_{c1}\bar{x} + g_2 b_{c1}\bar{y} + g_3\bar{x}\bar{y} + g_4\bar{x}^2 + g_5\bar{y}^2, \quad f_2(\bar{x}, \bar{y}, b_{c1}) = -f_1(\bar{x}, \bar{y}, b_{c1}),$$

$$\begin{aligned}
g_1 &= -(1+\lambda)\Upsilon^{-1}(-s_{16}(1 + (1-\alpha)e^{-dT+\theta})\Upsilon^{-1} + s_{17}),\\
g_2 &= -(1+\lambda)\Upsilon^{-1}(s_{16}(\lambda - (1-\alpha)e^{-dT+\theta})\Upsilon^{-1} + s_{17}),\\
g_3 &= -(1+\lambda)\Upsilon^{-1}(2s_{15} - s_{14}(1 - \lambda + 2(1-\alpha)e^{-dT+\theta})\Upsilon^{-1}\\
&\quad -2s_{13}(1 + (1-\alpha)e^{-dT+\theta})(\lambda - (1-\alpha)e^{-dT+\theta})\Upsilon^{-2},\\
g_4 &= -(1+\lambda)\Upsilon^{-1}[s_{13} + s_{14}(1 + (1-\alpha)e^{-dT+\theta})\Upsilon^{-1} + (1 + (1-\alpha)^2 e^{-2dT+2\theta})\Upsilon^{-2}),\\
g_5 &= -(1+\lambda)\Upsilon^{-1}[(s_{13} + s_{14}(\lambda - (1-\alpha)e^{-dT+\theta})\Upsilon^{-1} + (\lambda - (1-\alpha)e^{-dT+\theta})^2\Upsilon^{-2}].
\end{aligned}$$

The center manifold $w^c(0)$ for the map (4.3.14) can be represented as:

$$w^c(0) = \{(\bar{x}, \bar{y}, b_{c1}) \in \Re^3 | \bar{y} = h(\bar{x}, b_{c1}), h(0,0) = 0, Dh(0,0) = 0\}.$$

Let $\bar{y} = h(\bar{x}, b_{c1}) = M_0 b_{c1} + M_1 b_{c1}\bar{x} + M_2\bar{x}^2 + O(|b_{c1}|^2 + |b_{c1}\bar{x}^2| + |\bar{x}|^3)$.

Coefficients in $\bar{y}$ can be computed as:

$$\begin{aligned}
M_0 &= 0, \quad M_1 = -(1-\lambda)^{-1}\Upsilon^{-1}([-s_{16}(1 + (1-\alpha)e^{-dT+\theta})\Upsilon^{-1} + s_{17}]),\\
M_2 &= (1-\lambda)^{-1}\Upsilon^{-1}[s_{14}(1 + (1-\alpha)e^{-dT+\theta})\Upsilon^{-1} + (1 + (1-\alpha)^2 e^{-2dT+2\theta})\Upsilon^{-2} - s_{13}].
\end{aligned}$$

The map restricted to the center manifold is given by:

$$\begin{aligned}
\bar{h} : \bar{x} \to -\bar{x} + h(\bar{x}, \bar{y}, b_{c1}) &= -\bar{x} + g_1 b_{c1}\bar{x} + g_2 b_{c1}\bar{y} + g_3\bar{x}\bar{y} + g_4\bar{x}^2 + g_5\bar{y}^2,\\
\bar{h} : \bar{x} \to -\bar{x} + h(\bar{x}, \bar{y}, b_{c1}) &= -\bar{x} + g_1 b_{c1}\bar{x} - \Upsilon^{-1}[s_{13} - s_{14}(1 + (1-\alpha)e^{-dT+\theta})\Upsilon^{-1}\\
&\quad +(1 + (1-\alpha)^2 e^{-2dT+2\theta})\Upsilon^{-2}]g_3(1-\lambda)^{-1}\bar{x}^3 + g_4\bar{x}^2\\
&\quad +O(|b_{c1}|^2 + |b_{c1}\bar{x}^2| + |\bar{x}|^4).
\end{aligned}$$

The conditions of flip bifurcation are computed below:

$$\frac{\partial \bar{h}(0,0)}{\partial b_{c1}}\frac{\partial^2 \bar{h}(0,0)}{\partial x^2} \quad + \quad 2\frac{\partial^2 \bar{h}(0,0)}{\partial x \partial b_{c1}} = 0 + 2g_1 \neq 0.$$

$$\begin{aligned} \bar{a} &= \frac{1}{2}\left(\frac{\partial^2 \bar{h}(0,0)}{\partial x^2})^2 + \frac{1}{3}\frac{\partial^3 \bar{h}(0,0)}{\partial x^3}\right) \\ &= 2g_3(1-\lambda^2)\Upsilon^{-1}((s_{13}+s_{14})(1+(1-\alpha)e^{-dT+\theta})\Upsilon^{-1} - s_{17}) + 2g_4^2 \neq 0. \end{aligned}$$

Accordingly, conditions of the Theorem 1.4.4 are satisfied at $(\bar{x}, b_{c1}) = (0,0)$. Accordingly, there exist period-2 solutions. These bifurcating period-2 solutions will be stable if $\bar{a} > 0$ and unstable if $\bar{a} < 0$. □

It is noted that -1 is the eigenvalues of $A[E^*]$ at $b = b_c$. If b increases beyond b_c, there exist a variety of dynamical behaviors, including a series of bifurcations that lead to chaotic dynamic. This will be explored through numerical simulation in the next section.

4.4 Numerical Simulations

In the last sections, the qualitative analysis of the map (4.3.5) has been performed. Numerical simulation of stroboscopic map is performed to illustrate the analytical results. Further, objective is to explore the possibility of complex dynamical behavior. Extensive numerical simulation is carried out for various values of parameters. The controlling parameter is taken as b and keeping others parameter fixed as:

$$a = 0.4, d = 0.2, l = 0.5, \alpha = 0.6, \beta = 0.4, a_1 = 0.9, m_1 = 1. \tag{4.4.1}$$

Considering $T = 1.0$, the dynamical behavior of the map (4.3.5) in the positive quadrant is shown in Table 4.1 for different choices of parametric values. The column 2 depicts the linear stability behavior of positive equilibrium point and the results in column 3 are obtained by solving the system (4.2.3) − (4.2.6) numerically.

Choosing $b = 10$, the basic reproduction number can be computed as $R_0 = 0.9926 < 1 (b < 10.0746)$. Accordingly, the pest-free state is locally asymptotically stable (Theorem 4.3.2) and interior fixed point does not exist. Further, transcritical bifurcation occurs at $b = b_0 = 10.0746$ (Theorem 4.3.4). As b increases beyond b_0,

choosing $b = 12$, E_0 becomes unstable and $E^* = (0.8516, 0.0701)$ exists. E^* is stable as $b_0 < b < 104.7929$ (Theorem 4.3.5) or period-1 solution occurs. The map (4.3.5) undergoes a flip bifurcation at $b = b_c = 107.7929$ (Theorem 4.3.7).

Table 4.1: Behavior of the map (4.3.5) for the data set (4.4.1).

Parameter varied	Analytical behavior	Numerical behavior
$b < 10.0746$	E_0 stable, E^* not exists	Stable pest-free state
$b = 10.0746$	E_0 Non-Hyperbolic, $E_0 = E^*$	Transcritical Bifurcation
$10.0746 < b < 107.7929$	E_0 unstable, E^* exists, stable	Period-1 solution
$b = 107.7929$	Flip Bifurcation	Period-2 solution
$b > 107.7929$	E^* does not exists	Complex dynamics

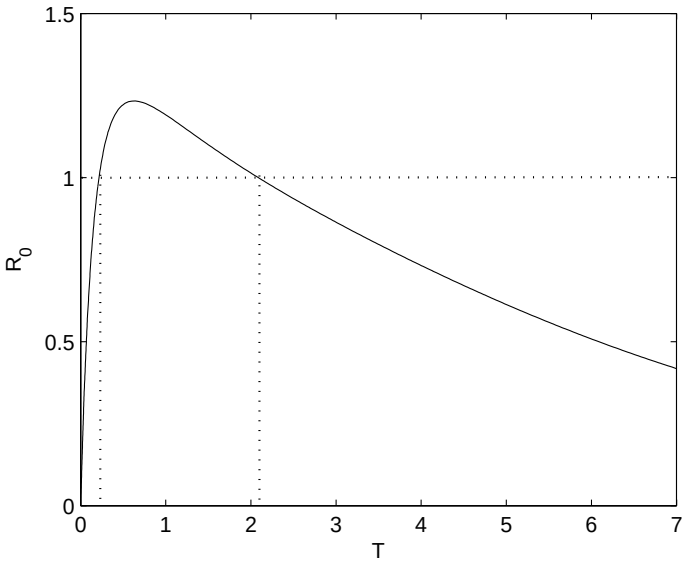

Figure 4.1: Plot of R_0 with respect to T.

Fig. 4.1 shows the variation of the threshold R_0 with pulse period T for $b = 12$. The non-monotonic behavior of R_0 with respect to impulsive period T is observed. As the value of T increases, R_0 first increases and attains a peak. It decreases with further increase in T. The pest eradication solution is stable in the region where $R_0 < 1$. The pest-free solution is unstable in the region $T \in (0.216, 2.085)$. The pest outbreak can occur for $R_0 > 1$.

The effects of pesticide spray time l on the thresholds R_0 and R_0^N are shown in Fig. 4.2. It illustrates that $R_0 < R_0^N$. So, it is better to choose pesticide having a residual effect rather than instantaneous effect only and the pest will be controlled easily. However, residual pesticide may have adverse effects on the environment/human beings. This aspect should also be incorporated.

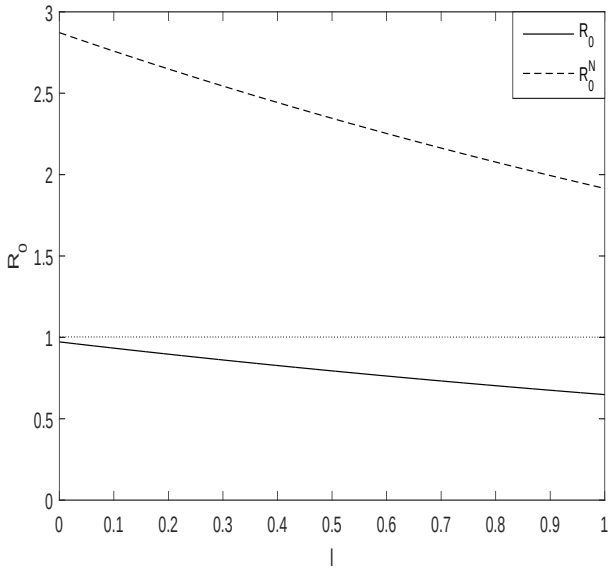

Figure 4.2: Effect of pesticide spray timing on threshold.

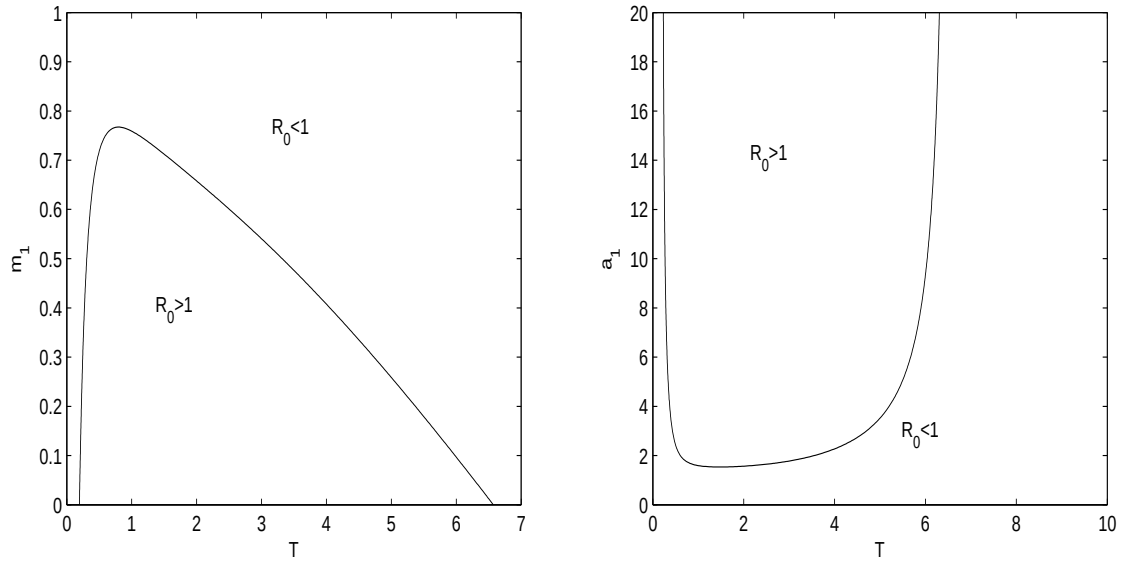

(a) **(b)**

Figure 4.3: Two-parameter bifurcation diagram in (a) $T - m_1$ plane (b) $T - a_1$ plane.

Two-parameter bifurcation diagram with respect to T and m_1 is drawn in Fig. 4.3(a) for $b = 8$. The curve $R_0 = 1$ bifurcates the $T - m_1$ plane into two regions of pest eradication ($R_0 < 1$) and pest existence ($R_0 > 1$). The pest will be eradicated when $m_1 > 0.7673$ irrespective of T. The eradication is still possible for a suitable choice of T where, $m_1 < 0.7673$.

Similarly, Fig. 4.3(b) , the curve $R_0 = 1$ corresponding to equation (4.3.6) is drawn on $T - a_1$ plane keeping other parameters as in (4.4.1) and $b = 8$. This curve also bifurcates the $T - a_1$ domain into pest eradication and coexistence regions. For smaller values of a_1, eradication may be possible depending upon the pulse period T. Further, for larger values of $T(T > 6.3065)$ eradication is possible for any choice of a_1.

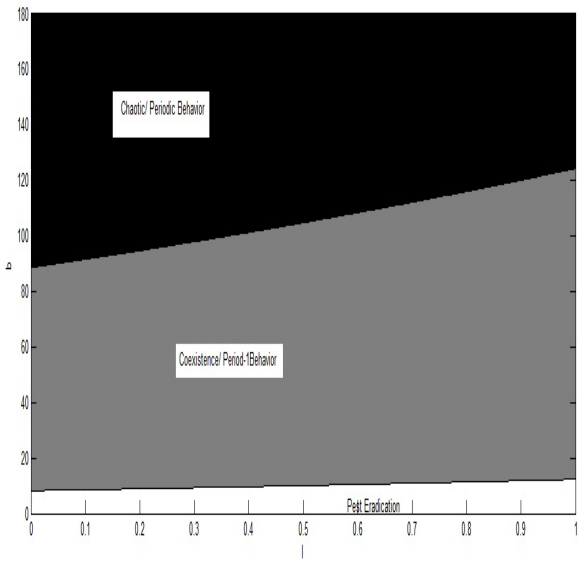

Figure 4.4: Two-parameter bifurcation diagram in $l - b$ plane.

Another, two-parameter bifurcation diagram is drawn in $l - b$ plane see Fig. 4.4. In this figure, a region of pest extinction is shown in white color, while the region of the stable period-1 solution is shown in light-grey color. For higher birth rates of the pest, the system (4.2.3) − (4.2.6) becomes chaotic, which is shown in the black color. At lower birth rates, the pest will be eradicated for all values of pesticide spray time. It has been observed that the pest will go to extinction in a small neighborhood of $(0, 0)$. The periodic doubling is the route to the chaos in the system (4.2.3) − (4.2.6) for the higher birth rate. This is shown in the next diagram.

To study the complex dynamical behavior, the typical bifurcation diagram is

drawn for total pest population in Fig. 4.5(a) with respect to parameter b. The bifurcation diagram shows the existence of chaos through period-doubling route. The critical value for a period-doubling bifurcation parameter is $b_c = 104.7929$ which is confirmed from the diagram. The rich dynamical behavior is clearly visible, including stability, period-doubling, narrow and wide periodic windows, crises and chaos. The Table 4.2 summarized the different dynamical behaviors in different domains of b.

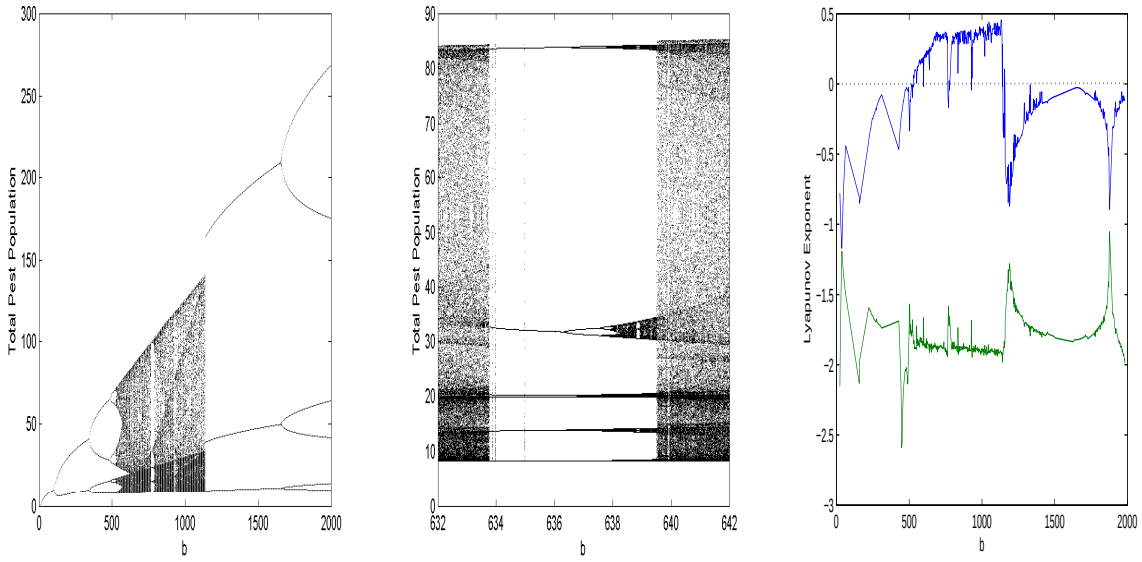

(a) **(b)** **(c)**

Figure 4.5: (a) Bifurcation diagram with respect to parameter b (b) Blown up of the bifurcation diagram for $b \in (632, 642)$ (c) Two Lyapunov exponents of the map (4.3.5) for total pest population.

Table 4.2: Behavior of the map (4.3.5) for the data set (4.4.1) about E^*.

Parameter varied	Analytical behavior	Numerical behavior
$b \in (10.0746, 104.7929)$	E_0 unstable, E^* stable	Period-1 solution
$b \in (104.7929, 343.814)$	E^* unstable	Period-2
$b \in (343.814, 486.163)$	E^* unstable	Period-4
$b \in (486.163, 424.8518)$	E^* unstable	Period-8
$b \in 424.8518, 525.16)$	E^* unstable	Period-16
$b \in (525.16, 1137.8)$	E^* unstable	Chaotic
$b \in (632, 642)$	E^* unstable	Periodic Windows

The chaotic region of Fig. 4.5(a) is separately blown up in Fig. 4.5(b) and a periodic window is clearly visible. Sudden changes in attractors can be observed easily. These sudden changes are usually related to periodic-windows in the middle of the chaotic range of attractors (see Fig. 4.5(b)).

Fig. 4.5(c) shows two Lyapunov exponents with respect to birth parameter b. The existence of the chaotic regions in the parametric space is clearly visible for one of the Lyapunov exponents is positive and other is negative. Further, two Lyapunov exponents corresponding to $b = 630$ are $\lambda_1 = 0.2205$ and $\lambda_2 = -1.8537$ such that their sum is negative. Therefore, the map (4.3.5) admits a strange attractor for this choice of b.

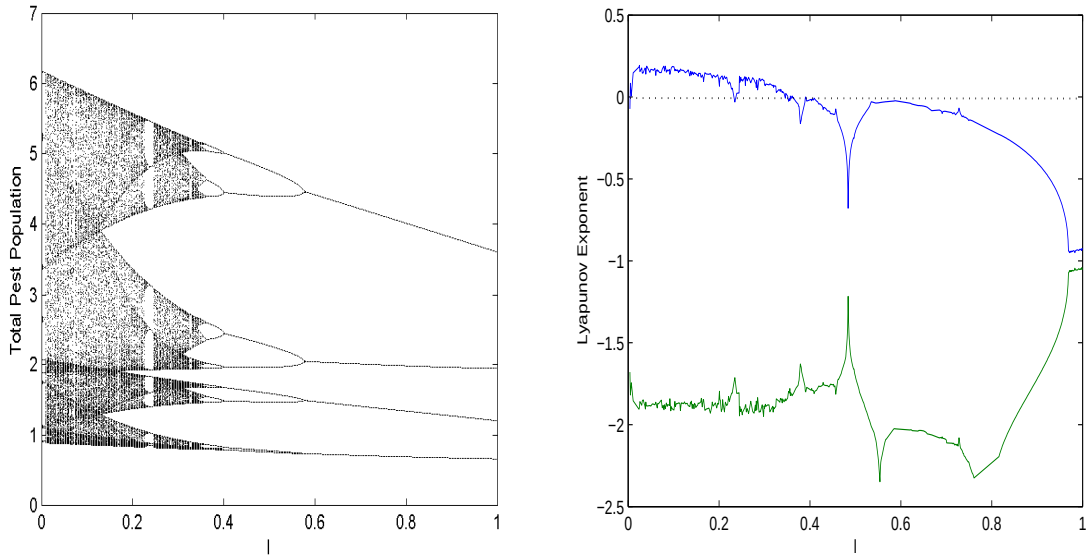

(a) **(b)**

Figure 4.6: (a) Bifurcation diagram (b) Two Lyapunov exponents of the map (4.3.5) for total pest population with respect to l.

The Fig. 4.6(a) shows bifurcation diagrams with respect to $l \in (0, 1)$ with $b = 500$. As parameter l increases, chaotic behavior is followed by a period-halving bifurcation. Note that, pesticide spray time may reduce complexity with increasing l. To further confirm chaotic nature, two Lyapunov exponents are drawn in Fig. 4.6(b).

The Fig. 4.7(a) shows the bifurcation diagram with respect to maturation rate $a \in (0, 1)$ with $b = 500$. The existence of chaos is observed through period-doubling. To further confirm the chaotic nature, two Lyapunov exponents are drawn in Fig. 4.7(b).

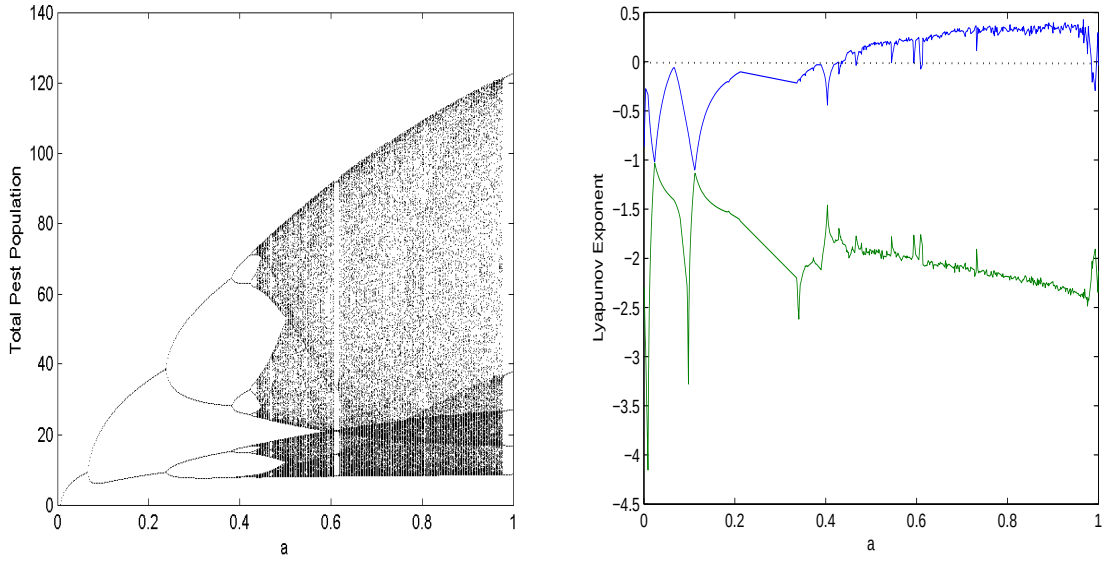

(a) **(b)**

Figure 4.7: (a) Bifurcation diagram (b) Two Lyapunov exponents of the map (4.3.5) for total pest population with respect to a.

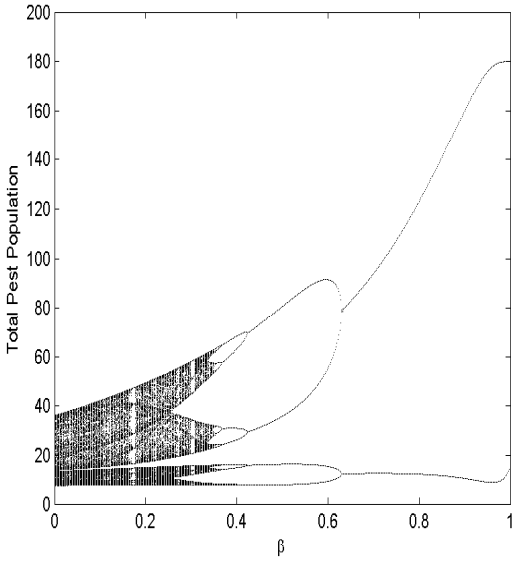

Figure 4.8: Bifurcation diagram of the map (4.3.5) for total pest population with respect to β.

Bifurcation diagram with respect to killing rate β for total pest population is drawn in Fig. 4.8 for $b = 500$. Initially, chaotic behavior is observed. Further, for a higher kill rate periodic behavior is obtained.

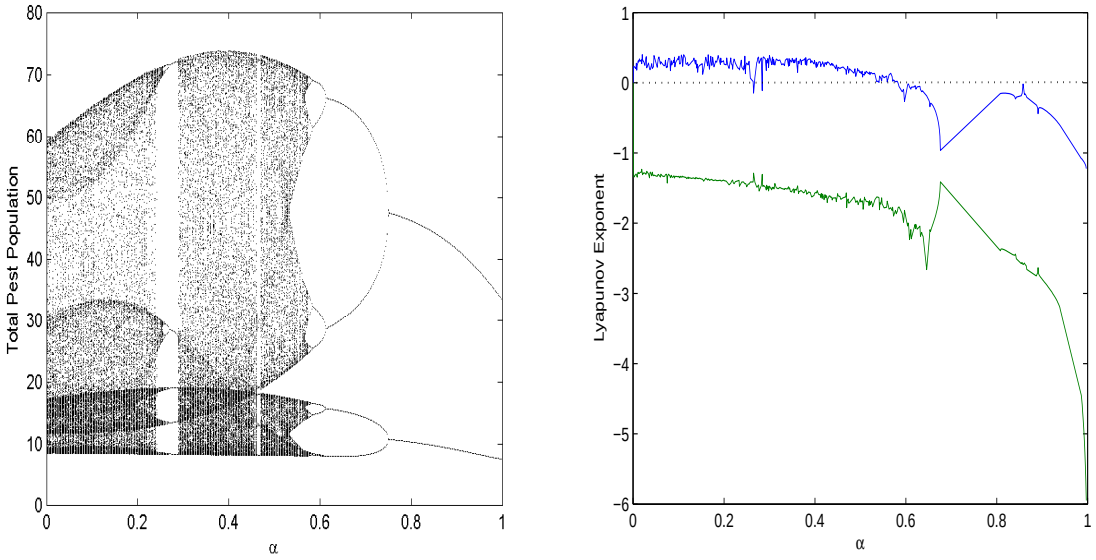

(a) **(b)**

Figure 4.9: (a) Bifurcation diagram (b) Two Lyapunov exponents of the map (4.3.5) for total pest population with respect to α.

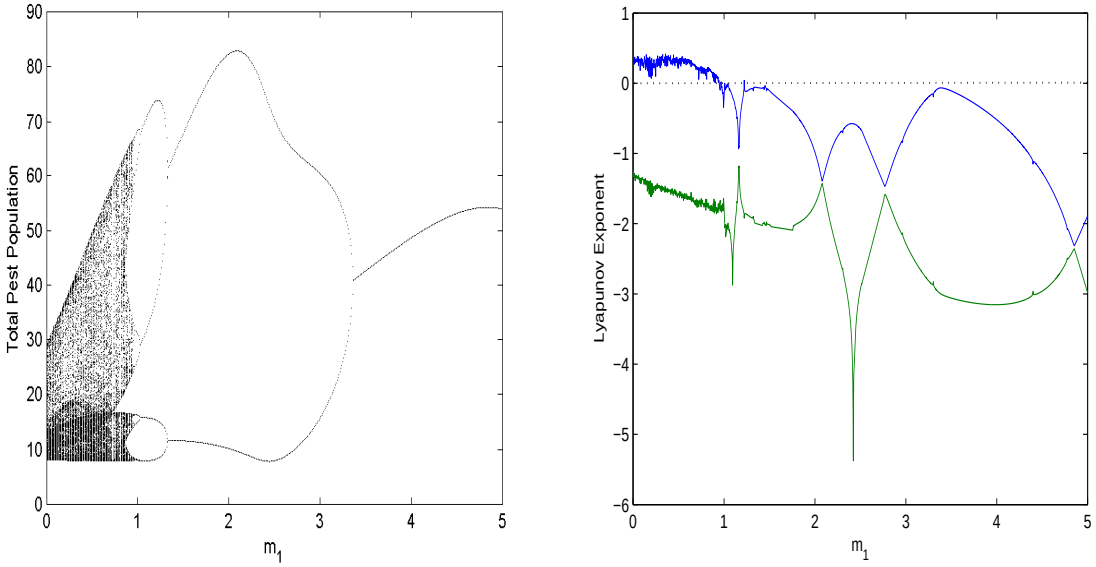

(a) **(b)**

Figure 4.10: (a) Bifurcation diagram (b) Two Lyapunov exponents of the map (4.3.5) for total pest population with respect to m_1.

Similar behavior is obtained with respect to killing rate α of the mature pest, killing efficiency rate m_1 and decay rate a_1 in Fig. 4.9, Fig. 4.10. and Fig. 4.11.

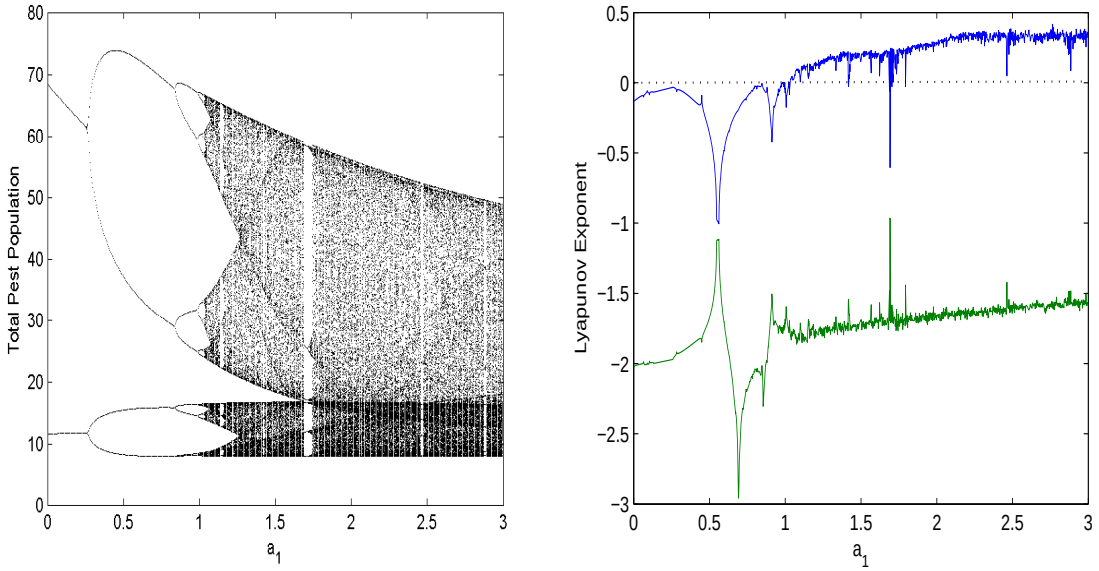

(a) **(b)**

Figure 4.11: (a) Bifurcation diagram (b) Two Lyapunov exponents of the map (4.3.5) for total pest population with respect to a_1.

4.5 Discussion

The stage-structured pest control model with birth pulses and an impulsive pesticide spray has been formulated and analyzed for studying the effects of chemical control on the pest. The period of pesticide spray timing and birth pulse is same but not synchronized. The threshold R_0 is obtained which is the basic reproduction number for the pest-free state. When the threshold is less than unity, the stability analysis of the pest-free fixed point has been established. Accordingly, the pest can be eradicated for $R_0 < 1$. The existence and stability of the interior fixed point have been obtained. The conditions for existence of the period-1 solution is $R_0 > 1$. The combined effects of pesticide (i.e. instantaneous as well as residual effects) are required to control the pest. The residual effect not only affects the stability but also has desirable effects on equilibrium densities. The conditions for transcritical and flip bifurcation have been obtained and analyzed analytically. Due to the residual effect of pesticide threshold condition reduces. The increase in the killing efficiency rate and decay rate reduces the threshold condition. Numerical results show that the system (4.2.3) – (4.2.6) has complex dynamical behavior. The bifurcation diagrams and Lyapunov exponents show the range of parameters for which the system (4.2.3) – (4.2.6) has a chaotic solution.

Chapter 5

A Mathematical Model for Integrated Pest Management Incorporating Birth Pulse

5.1 Introduction

In previous chapters, some pest control models have been investigated that involve single control strategy (impulsive use of pesticide). However, pesticides are not environmentally friendly and harmful to human beings. To preserve the quality of the environment Integrated Pest Management (IPM) strategies (i.e. combination of two or more control tactics) should be applied [58, 207, 225, 226, 227, 228]. It has been proved that IPM has been more effective rather than single tactics [14, 233]. Several mathematical models of Integrated Pest Management have been investigated to control the pest by the chemical control/biological control [88, 126, 138, 216, 221, 222, 223]. They have not incorporated stage structure and birth pulses.

Sometimes pesticides are effective against the specific stage of the pest life cycle. For example, pesticides are ineffective against the immature stage of Pest Fly. A stage-structured impulsive model incorporating integrated pest management assuming continuous growth of pest has been discussed [241]. The impulsive models with the birth pulse and integrated pest management using microbial control have been discussed [238].

In some cases, the pest may hide in the soil or crops, etc. to avoid exposure to pesticides. In such cases, the harvesting may be an effective approach for control of the pest. It may reduce the use of pesticides. Several stage-structured pest control model with birth pulses and impulsive harvesting have been discussed [29, 96].

In this chapter, a stage-structured pest control model has been proposed using Integrated Pest Management Strategies considering impulsive chemical control and cultural control (harvesting). Pesticide affects only the mature pest. Harvesting effort is applied to control the immature pest. The chemical spray is synchronized with birth pulses.

5.2 Model I: An Impulsive Stage-Structured IPM Model with Chemical Control and Birth Pulses

Let the total pest population at any time t be $N(t)$ such that $N(t) = x(t) + y(t)$. The model is formulated under following assumptions:

- Different mortality rates d_1 and d_2 are considered for immature and mature pest respectively.
- To reduce the immature pest load, physical effort is applied with harvesting rate $E > 0$.
- It is assumed that the mature pest can reproduce in a single birth pulse which occur periodically at time $t = mT_1$, $m = 1, 2, ...$
- Pesticide is sprayed to control the pest population impulsively at time $t = mT_2$, $m = 1, 2, ...$ It affects only the mature pest with killing rate μ.
- For simplicity, it is assumed new births and chemical spray of pesticide is synchronized at time $t = mT, m = 1, 2, ..., T = T_1 = T_2$.

The dynamics of stage-structured impulsive pest control system defined on the set $\Re^2_+ = \{(x, y) \in \Re^2 \mid x \geq 0, y \geq 0\}$ with positive model parameters is written as:

$$\left.\begin{aligned} \frac{dx}{dt} &= -d_1 x(t) - ax(t) - Ex(t), \\ \frac{dy}{dt} &= ax(t) - d_2 y(t), \end{aligned}\right\} t \neq mT, \tag{5.2.1}$$

$$\left.\begin{aligned} x(mT)^+ &= x(mT) + B(N(mT))y(mT), \\ y(mT)^+ &= (1-\mu)y(mT), \end{aligned}\right\} t = mT, \tag{5.2.2}$$

$$x(0) = x_0 > 0, \quad y(0) = y_0 > 0. \tag{5.2.3}$$

The birth function is assumed to be of Beverton-Holt function as:

$$B(N) = p\ (q + N^n)^{-1}. \tag{5.2.4}$$

5.2.1 Stroboscopic Map

Let $x = x_{m-1}$ and $y = y_{m-1}$ be the densities of immature and mature pest respectively at $t = (m-1)T$. The analytical solution of differential equations (5.2.1) between the pulses $(m-1)T \leq t < mT$ can be written as:

$$\begin{aligned} x(t) &= x_{m-1}e^{-(a+d_1+E)(t-(m-1)T)}, \\ y(t) &= [a(a-\epsilon)^{-1}(1-e^{(\epsilon-a)(t-(m-1)T)})x_{m-1} + y_{m-1}]e^{-d_2(t-(m-1)T)}, \\ \epsilon &= d_2 - d_1 - E. \end{aligned} \tag{5.2.5}$$

The following stroboscopic map of the system (5.2.1) − (5.2.3) can be obtained from (5.2.5) by applying impulsive condition (5.2.2)

$$\begin{aligned} x_m &= x_{m-1}e^{-(a+E+d_1)T} + \frac{p[\beta x_{m-1} + y_{m-1}e^{-d_2T}]}{q + (x_{m-1}e^{-(a+E+d_1)T} + \beta x_{m-1} + y_{m-1}e^{-d_2T})^n}, \\ y_m &= (1-\mu)(\beta x_{m-1} + y_{m-1}e^{-d_2T}), \\ \beta &= ae^{-d_2T}(1-e^{(\epsilon-a)T})(a-\epsilon)^{-1}. \end{aligned} \tag{5.2.6}$$

The difference equations (5.2.6) describe the stroboscopic sampling of the immature and mature pest population. For the Beverton-Holt Function, the dynamical behavior of the system (5.2.1) − (5.2.3) will be given by the dynamical behavior of the map (5.2.6) associated with the system (5.2.5).

The basic reproduction number R_0 is computed as:

$$\begin{aligned} R_0 &= pp_0^{-1}, \\ p_0 &= q(1-e^{-d_1T-aT-ET})(1-(1-\mu)e^{-d_2T}))\beta^{-1}. \end{aligned} \tag{5.2.7}$$

5.2.2 Existence of Fixed Points

For the map (5.2.6), the following fixed points are obtained:

(i) A unique pest-free fixed point $E_0 = (0, 0)$ exists without any parametric restriction.

(ii) The non-trivial fixed point $E^* = (x^*, y^*)$ exists for $R_0 > 1$ and is obtained as:

$$\begin{aligned} x^* &= \frac{(1-(1-\mu)e^{-d_2T})\sqrt[n]{q(R_0-1)}}{(e^{-(d_1+a+E)T}-(1-\mu)e^{-(d_2+d_1+a+E)T}+\beta)}, \\ y^* &= \frac{\beta(1-\mu)\sqrt[n]{q(R_0-1)}}{(e^{-(d_1+a+E)T}-(1-\mu)e^{-(d_2+d_1+a+E)T}+\beta)}. \end{aligned}$$

5.2.3 Local Stability Analysis of Fixed Points

To discuss the local stability about feasible fixed point (x, y) the linearized system about $X = (x, y)$ is obtained as:

$$X_m = AX_{m-1}. \tag{5.2.8}$$

The coefficients of the matrix $A = (a_{ij})_{2\times 2}$ are:

$$\left.\begin{aligned} a_{11} &= e^{-(d_1+a+E)T} + p\ \beta\ D_1^{-1} - npa(xe^{-(a+E+d_1)T} + \beta x + ye^{-d_2T})^{n-1} \\ &\quad \times (e^{-(a+E+d_1)T} + \beta)[\beta x + ye^{-d_2T}]D_1^{-2}, \\ a_{12} &= -pan(xe^{-(a+E+d_1)T} + \beta x + ye^{-d_2T})^{n-1}e^{-d_2T}[\beta x + ye^{-d_2T}]D_1^{-2} \\ &\quad pe^{-d_2T}D_1^{-1}, \\ a_{21} &= (1-\mu)\beta, \qquad a_{22} = (1-\mu)e^{-d_2T}, \\ D_1 &= q + (xe^{-(a+E+d_1)T} + \beta x + ye^{-d_2T})^n, \end{aligned}\right\}. \tag{5.2.9}$$

Theorem 5.2.1. *The fixed point $E_0 = (0, 0)$ of the map (5.2.6) is locally asymptotically stable provided*

$$R_0 < 1. \tag{5.2.10}$$

Proof. The coefficients of the linearized matrix evaluated about the pest-free state E_0 are:

$$a_{11} = e^{-(d_1+a+E)T} + p\ \beta\ q^{-1}, \quad a_{12} = pe^{-d_2T}\ q^{-1}, \quad a_{21} = (1-\mu)\beta, \quad a_{22} = (1-\mu)e^{-d_2T}.$$

The trace Tr and determinant Det are computed as:

$$\begin{aligned} Tr &= e^{-(d_1+a+E)T} + p\ \beta\ q^{-1} + (1-\mu)e^{-d_2T}, \\ Det &= (1-\mu)e^{-(d_1+d_2+a+E)T}. \end{aligned}$$

It is observed that Jury's conditions (1.4.12) and (1.4.13) are always satisfied:

$$\begin{aligned} 1 + Tr + Det &= 1 + e^{-(d_1+a+E)T} + p\beta q^{-1} + (1-\mu)(e^{-d_2T} + e^{-(d_1+d_2+a+E)T}) > 0, \\ 1 - Det &= 1 - (1-\mu)e^{-(d_1+d_2+a+E)T} > 0. \end{aligned}$$

The expression $1 - Tr + Det$ simplifies to:

$$\begin{aligned} 1 - Tr + Det &= 1 - e^{-(d_1+a+E)T} - p\ \beta\ q^{-1} - (1-\mu)e^{-d_2T} - (1-\mu)e^{-(d_1+d_2+a+E)T} \\ &= (1 - e^{-(d_1+a+E)T})(1 - (1-\mu)e^{-d_2T}) - p\ \beta\ q^{-1}. \end{aligned}$$

The Jury's condition (1.4.11), $1 - Tr + Det > 0$ gives the condition for stability

$$(1 - e^{-(d_1+a+E)T})(1 - (1-\mu)e^{-d_2T}) \ > \ p\ \beta\ q^{-1}.$$

$$p < q(1 - e^{-(d_1+a+E)T})(1 - (1-\mu)e^{-d_2T})\beta^{-1} = p_0. \tag{5.2.11}$$

Using (5.2.7) and (5.2.11), the stability condition (5.2.10) is obtained. □

Accordingly, the fixed point $(0, 0)$ is locally stable for $p \in (0, p_0)$. The trajectories in the neighborhood of $(0, 0)$ tend to origin and the pest is eradicated. The existence of non-trivial fixed point is overruled in this case.

When $R_0 > 1$, the fixed point $(0, 0)$ is unstable. Bifurcation occurs at $R_0 = 1$ and further, analysis is required, which is carried out later.

Derivative of R_0 with respect to killing rate μ is found to be negative

$$\frac{dR_0}{d\mu} = -p\beta e^{-d_2T} q^{-1} (1 - e^{-d_1T - aT - ET})^{-1} (1 - (1-\mu)e^{-d_2T}))^{-2} < 0.$$

Therefore, the killing (or poisoning) rate μ reduces the threshold value R_0 and once $R_0 < 1$, the pest can be eradicated successfully.

Theorem 5.2.2. *Let us define constants S and C as*

$$\begin{aligned} S &= n(1 - e^{-(d_1+a+E)T})(e^{-(a+E+d_1)T} + \beta + (1-\mu)e^{-(d_2+d_1+a+E)T}) \\ &\quad \times (1 - (1-\mu)e^{-d_2T}), \\ C &= 2(1 + (1-\mu)e^{-(d_1+d_2+a+E)T})(e^{-(d_1+a+E)T} - (1-\mu)e^{-(d_2+d_1+a+E)T} + \beta). \end{aligned}$$

The non-trivial fixed point $E^* = (x^*, y^*)$ of the map (5.2.6) is locally asymptotically stable provided

$$p_0 < p \ < \ \frac{S\ p_0}{S - C} = p_c. \tag{5.2.12}$$

Proof. Let us define

$$D_2 = (e^{-(d_1+a+E)T} - (1-\mu)e^{-(d_2+d_1+a+E)T} + \beta)qR_0.$$

Using (5.2.9) coefficients of the linearized matrix $A = (a_{ij})_{2\times 2}$, the trace Tr and determinant Det are evaluated about the interior fixed point (x^*, y^*) as:

$$\begin{aligned}
a_{11} &= e^{-(d_1+a+E)T} + p_0\ \beta\ q^{-1} - p_0 n\beta(R_0-1)(e^{-(a+E+d_1)T} + \beta)D_2^{-1},\\
a_{12} &= p_0\ e^{-d_2T}\ q^{-1} - n\beta p_0 D_2^{-1}(R_0-1)e^{-d_2T},\\
a_{21} &= (1-\mu)\beta, \qquad a_{22} = (1-\mu)e^{-d_2T},\\
Tr &= e^{-(d_1+a+E)T} + p_0\ \beta\ q^{-1} + (1-\mu)e^{-d_2T} - p_0 n\beta(R_0-1)(e^{-(a+E+d_1)T} + \beta)D_2^{-1},\\
Det &= (1-\mu)e^{-(d_1+d_2+a+E)T} - (1-\mu)p_0 n\beta(R_0-1)e^{-(a+E+d_1+d_2)T}D_2^{-1}.
\end{aligned}$$

In the following it is observed that condition (1.4.11) and (1.4.13) are always satisfied:

$$\begin{aligned}
1 - Tr + Det &= 1 - e^{-(d_1+a+E)T} + p_0\ \beta\ q^{-1} + (1-\mu)e^{-(d_1+d_2+a+E)T}\\
&\quad + p_0 n\beta(R_0-1)q^{-1}R_0^{-1} > 0,\\
1 - Det &= 1 + [n\beta p_0(R_0-1)D_2^{-1} - 1](1-\mu)e^{-(d_1+d_2+a+E)T} > 0.
\end{aligned}$$

The expression $1 + Tr + Det$ simplifies to:

$$\begin{aligned}
1 + Tr + Det &= 1 + e^{-(d_1+a+E)T} - p_0 n\beta(R_0-1)(e^{-(a+E+d_1)T} + \beta)D_2^{-1}\\
&\quad + (1-\mu)e^{-d_2T} + p_0\ \beta\ q^{-1} + (1-\mu)e^{-(d_1+d_2+a+E)T}\\
&\quad - (1-\mu)p_0 n\beta(R_0-1)e^{-(a+E+d_1+d_2)T}D_2^{-1}\\
&= (1 + e^{-(d_1+a+E)T})(1 + (1-\mu)e^{-d_2T}) + p_0\ \beta\ q^{-1}\\
&\quad [1 - n(R_0-1)(e^{-(a+E+d_1)T} + \beta + (1-\mu)e^{-(d_2+d_1+a+E)T})D_2^{-1}]\\
&= (1 + e^{-(d_1+a+E)T})(1 + (1-\mu)e^{-d_2T})\\
&\quad + (1 - e^{-(d_1+a+E)T})(1 - (1-\mu)e^{-d_2T})\\
&\quad \times [1 - n(R_0-1)(e^{-(a+E+d_1)T} + \beta + (1-\mu)e^{-(d_2+d_1+a+E)T})D_2^{-1}].
\end{aligned}$$

For the condition (1.4.13), that is, $1 + Tr + Det > 0$, further simplification yields

$$R_0 < \frac{S}{S-C}. \tag{5.2.13}$$

The stability condition (5.2.12) is obtained with the existence condition $p > p_0$ and using (5.2.13). Hence, if $p < p_c$ then E^* is locally asymptotically stable. □

Further, increasing the parameter value p, the fixed point E^* losses its stability and the system may exhibit complex dynamics.

Accordingly, when $p_0 < p < p_c$, the interior fixed point E^* exists and is locally asymptotically stable. The trajectories of the system (5.2.1) − (5.2.3) tend to asymptotically stable period-1 solution $(x_e(t), y_e(t))$:

$$\begin{aligned} x_e(t) &= x^* e^{-(a+d_1+E)(t-mT)}, \\ y_e(t) &= \left(\frac{ax^*(1-e^{(\epsilon-a)(t-mT)})}{a-\epsilon} + y^*\right) e^{-d_2(t-mT)}. \end{aligned} \tag{5.2.14}$$

The trivial fixed point $E_0 = (0, 0)$ of the map (5.2.6) becomes non-hyperbolic at $p = p_0$ and one of the eigenvalues is 1. Note that, when $R_0 = 1$, then $E^* = (0, 0)$. It is observed that at $p = p_0$, $E_0 = (0, 0)$ and $E^* = (x^*, y^*)$ exchange their stability. The system (5.2.1) − (5.2.3) undergoes a transcritical bifurcation at $p = p_0$.

The interior fixed point $E^* = (x^*, y^*)$ of the map (5.2.6) becomes non-hyperbolic at $p = p_c$ where one of the eigenvalues is -1. The associated bifurcation is called flip bifurcation. The system (5.2.1) − (5.2.3) undergoes a flip bifurcation about $E^* = (x^*, y^*)$ at $p = p_c$.

There exist a series of bifurcations that lead to chaotic dynamic when p increases from p_c. This will be explored through numerical simulation in the next section.

5.3 Numerical Simulations

In this section, some numerical experiments are presented to discuss various dynamical aspects of the system (5.2.1) − (5.2.3) and the map (5.2.6). The following set of parameters is considered to illustrate the theoretical results obtained in previous sections:

$$a = 0.8, c = 1, y = 14, E = 0.3, d_2 = 0.6, \mu = 0.5. \tag{5.3.1}$$

For $T = 1.0$ and $d = d_1 = d_2 = 0.6$, the constant p_0 is obtained as $p_0 = 2.2272$. The basic reproduction number can be computed as ($R_0 = 0.8980 < 1$) when $p = 2$. Accordingly, the pest-free state is locally asymptotically stable (Theorem (5.2.1)) and coexistence is impossible in this case. Further, choosing $p = 2.5$, the fixed point E_0 becomes unstable as ($R_0 = 1.1225 > 1$). The non-trivial fixed point can be computed

as $E^* = (1.5659, 0.2873)$ and it is stable as $p_0 < p < 2.7915$ (Theorem (5.2.2)). Further, transcritical bifurcation occurs at $p \approx 2.3688$ and flip bifurcation occurs at $p \approx 2.7915$ respectively.

For data set (5.3.1) with $T = 1.0$ and $d_1 = 0.2(d_1 < d_2)$. The constant p_0 is evaluated as $p_0 = 1.6717$. For $p = 1$, the pest-free state is stable and E^* does not exist as $R_0 = 0.5982(< 1)$ (Theorem (5.2.1)). Also, for $p = 2$, the fixed point E_0 is unstable and interior fixed point E^* exists as $R_0 = 1.1964 > 1$. The interior fixed point E^* is computed as $(1.2579, 0.2737)$ and stable in the parametric range $p \in (1.6717, 2.1578)$. The transcritical and flip bifurcation occurs at $p \approx 1.6717$ and $p \approx 2.1578$ respectively.

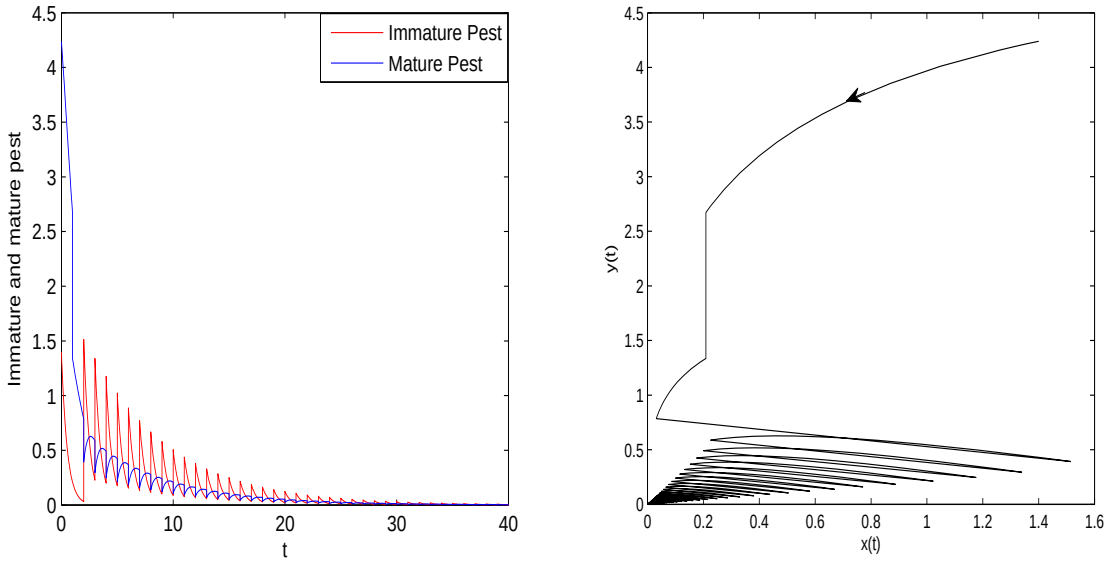

(a) **(b)**

Figure 5.1: (a) Time series (b) Phase plot depicting stable behavior of pest-free state of the system (5.2.1) – (5.2.3) at $p = 2$, $d_1 = 0.8$.

Considering the case $d_1 > d_2$. The threshold for the stability of pest-free state E_0 is computed as $p_0 = 2.5116$ for $T = 1.0$, $d_1 = 0.8$. The pest-free fixed point of the map (5.2.6) is locally asymptotically stable for $p < 2.5116$. For $p = 2$, the threshold R_0 is obtained as $R_0 = 0.79631 < 1$. Accordingly, when $p = 3$, the fixed point E_0 is unstable for $p > p_0(R_0 = 1.1945 > 1)$ and the interior fixed point $E^* = (1.8223, 0.3085)$ is locally stable for $2.5116 < p < 3.1226$. The transcritical bifurcation occurs at $p = 2.5116$.

For, $d_1 = 0.8(d_1 > d_2)$ the Fig. 5.1 and Fig. 5.2 shows the stability of pest-free

state and period-1 solution, respectively for the system (5.2.1) – (5.2.3).

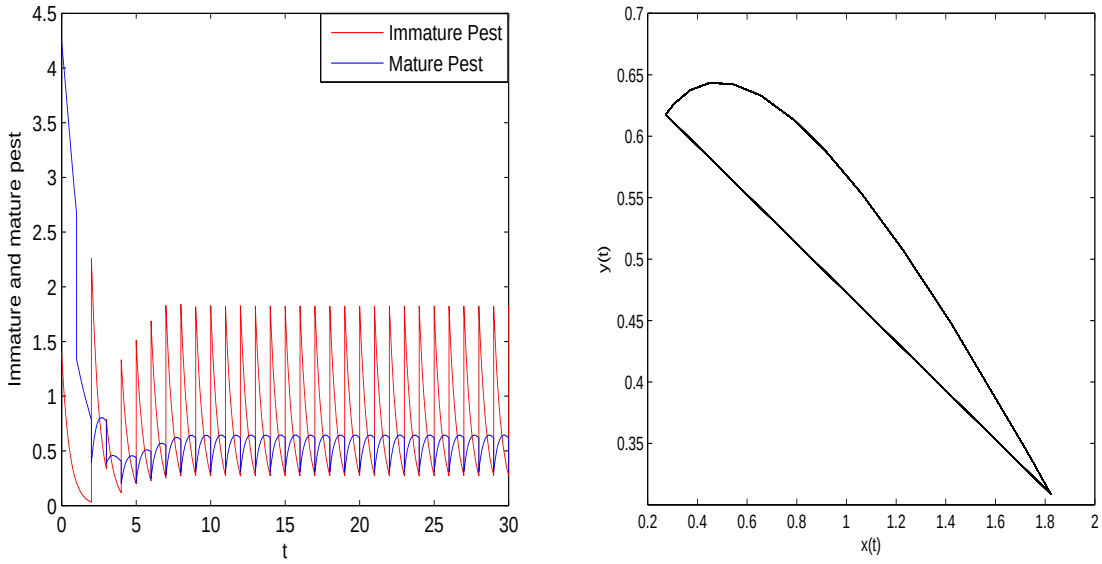

(a) **(b)**

Figure 5.2: (a) Time series (b) Phase plot depicting stable behavior of interior fixed point of the system (5.2.1) – (5.2.3) at $p = 3$, $d_1 = 0.8$.

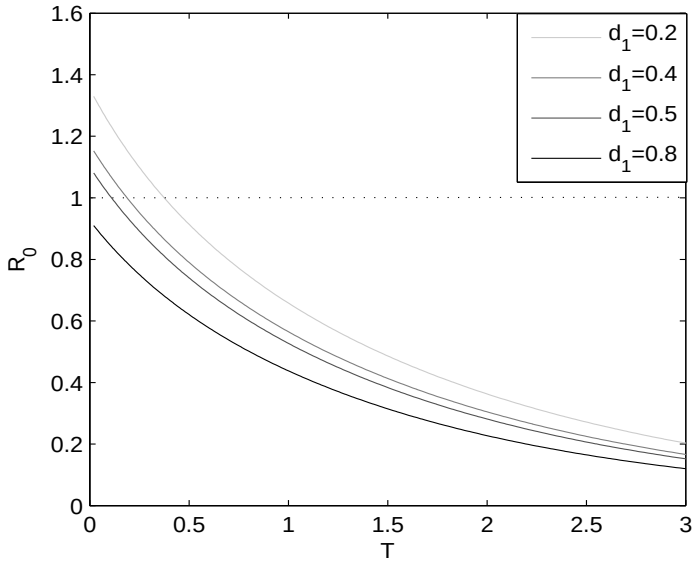

Figure 5.3: Variation of R_0 with T.

The Fig. 5.3 is drawn to show the variation of R_0 with pulse period T in the

range $0 \leq T \leq 3$ and for fixed values of $d_1 = 0.2(2)0.8$. For $d_1 = 0.2$ and $T \in (0, 0.78)$, R_0 is greater than 1 and for $T \in (0.78, 3)$ R_0 is less than 1. Further, R_0 remains greater than one for given choices of d_1 and T. Accordingly, $R_0 < 1$ for all values of T when $d_1 = 0.8$. Therefore, the pest can be controlled.

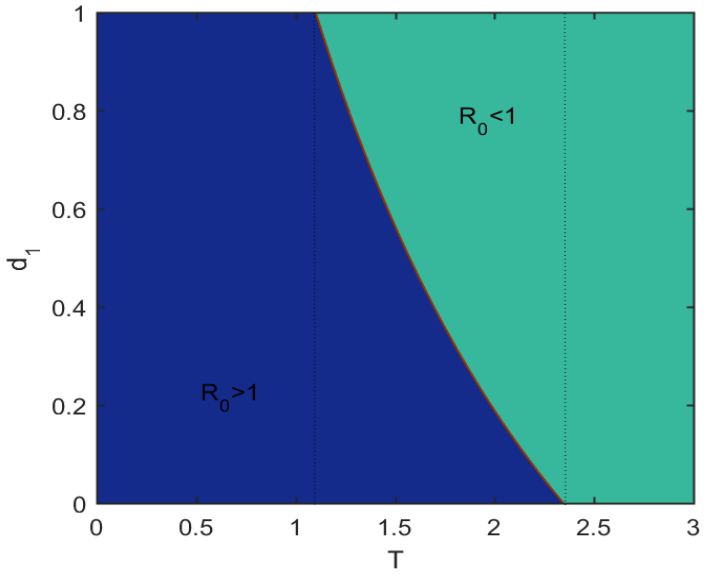

Figure 5.4: Plot of $R_0(T, d_1) = 1$ in $T - d_1$ plane.

Two-parameter bifurcation diagram with respect to T and d_1 is drawn in Fig. 5.4. The curve $R_0 = 1$(in red color) bifurcates the $T - d_1$ plane in pest eradication ($R_0 < 1$)(in green color) and pest outbreak ($R_0 > 1$)(in blue color) regions. For pest eradication, pulse period becomes smaller as d_1 increases. Accordingly, the pest will be eradicated when $T > 2.3460988$ for all values of d_1. If $T < 1.1003955$, the pest eradication is not possible irrespective of d_1 for fixed d_2. Note that, combination of pulse period and the mortality rate of immature pest is needed to control the pest.

In Fig. 5.5, the region of stability and instability for the pest-free state is drawn on $T - d_2$ plane, keeping other parameters as in (5.3.1). The aqua green color corresponding to the $R_0 < 1$(i.e all eigenvalues lies inside the unit circle) is the region of stability. On the other hand, at least one eigenvalue will lie outside the unit circle about E_0 in the navy blue region. Therefore, for $R_0 > 1$, the pest population will vary periodically. For a fixed value of mortality rate d_2, the corresponding pulse period $T > T_c$ is required to eradicate the pest. In Fig. 5.5(c), for $d_2 < 0.271855$, the pest will

survive for all values of the pulse period. Further, for $d_2 > 0.271855$, the fixed points E_0 and E^* may exist depending on the pulse period T.

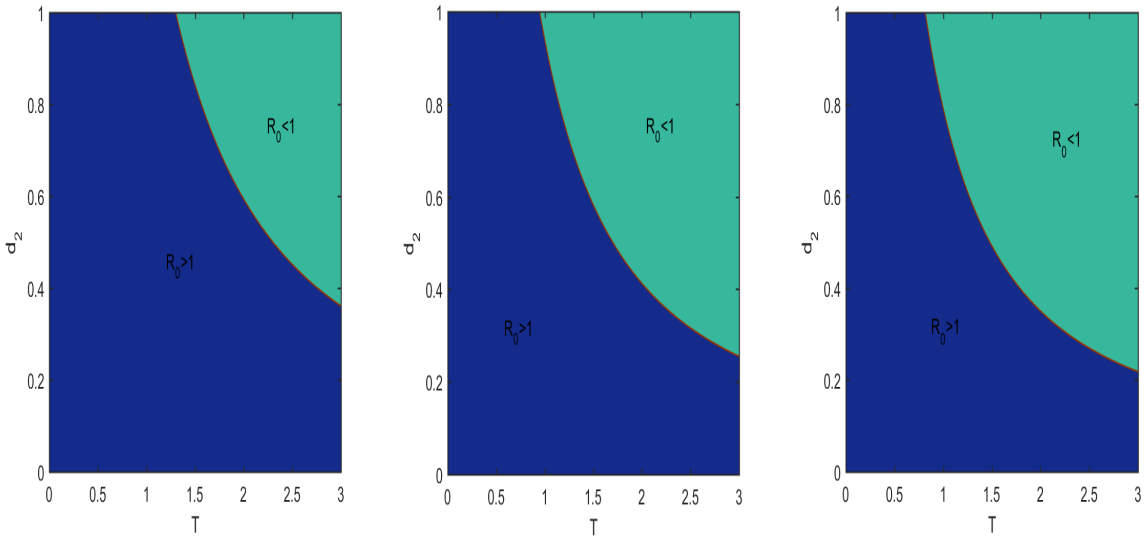

(a) **(b)** **(c)**

Figure 5.5: Plot of $R_0(T, d_2) = 1$ in $T - d_2$ plane at (a) $d_1 = 0.2$ (b) $d_1 = 0.6$ (c) $d_1 = 0.8$.

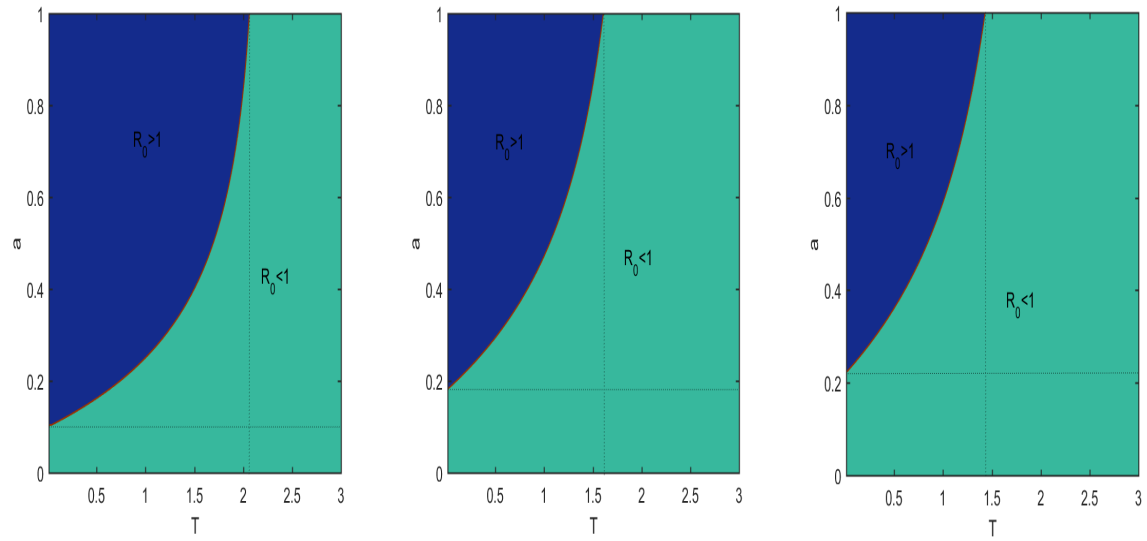

(a) **(b)** **(c)**

Figure 5.6: Two-parameter bifurcation diagrams in $T - a$ plane at (a) $d_1 = 0.2$ (b) $d_1 = 0.6$ (c) $d_1 = 0.8$.

Another set of two-parameter bifurcation diagrams with respect to T and a has been drawn in Fig. 5.6 in three cases: $d_1 < d_2$, $d_1 = d_2$ and $d_1 > d_2$. The stability of the pest-free state depends upon the threshold R_0. The critical parameters T and a are involved in R_0. The parameter space is divided into two regions by the curve $R_0 = 1$. On the right side of red curve only the pest-free state is stable and the pest can be controlled effectively. However, on the left side, the survival state E^* may exist depending on the pulse period T and maturation rate a. For $a < .2228635$, the pest eradication is possible for all values of T. If maturation rate $a > .2228635$, the pest will survive irrespective of pulse period T.

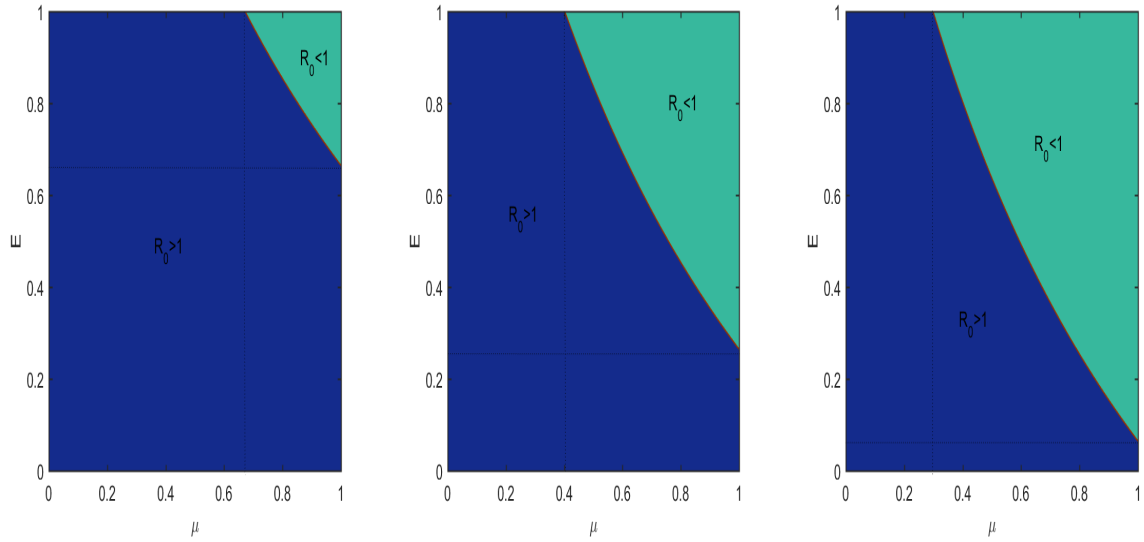

(a) **(b)** **(c)**

Figure 5.7: Two-parameter bifurcation diagrams in $\mu - E$ plane for (a) $d_1 = 0.2$ (b) $d_1 = 0.6$ (c) $d_1 = 0.8$.

Again in Fig. 5.7, a set of two-parameter bifurcation diagram has been plotted in $\mu - E$ plane showing the relationship between harvesting effort and the killing rate due to chemical control. The influence of the harvesting effort E and killing rate μ on the stability of the pest-free state E_0 has been shown. The region with aqua green color corresponds to eigenvalues inside the unit circle. It is the region of stability about the pest-free state E_0. The region below the red curve shows the pest-free state is unstable. Also, it can be observed that domain of pest eradication increases with an increase in mortality rate d_1. It can be observed that the maximum pest eradication region occurs

in Fig. 5.7(c) for $d_2 < d_1$. If harvesting effort increases, then killing rate of immature pest decreases. By applying mechanical control, use of pesticides can be decreased, which can be beneficial for the environment.

Note that, if no harvesting effort is applied (i.e. $E = 0$), the pest eradication is not possible irrespective of μ see Fig. 5.7. Also, in Fig. 5.7 the pest population will persist when chemical control is not applied. Therefore, the single strategy is not effective for pest control. In Fig. 5.7(c) it can be observed that for lower harvesting effort ($E < .06424$) or lower killing rate due to pesticide spray ($\mu <.298731$), the pest population cannot be controlled. It is concluded that the combination of harvesting effort and the killing rate is needed to control the pest population. Therefore, integrated pest management strategy is more effective rather than the single tactic. Also, from the Fig. 5.7(c), it can be concluded that for higher harvesting effort, low toxic pesticide should be used which is environmentally friendly.

In Fig. 5.8, three bifurcation diagrams are drawn with respect to key parameter b for the set of parameters (5.3.1) in the cases: $(a)d_1 < d_2$ in Fig. 5.8(a) $(b)d_1 = d_2$ in Fig. 5.8(b) and $(c)d_1 > d_2$ in Fig. 5.8(c). The case (b) is idealized and mostly considered by the investigators. The case (c) is more realistic while case (a) is rarely observed in nature. The case (a) is considered only for completeness. By comparison, it is clear that the dynamical behaviors of the map (5.2.6) are less complex in the case $d_1 > d_2$ rather than in the cases $d_1 = d_2$ or $d_1 < d_2$. The diagrams show the period-doubling phenomena which is route to chaos.

Table 5.1: Behavior of impulsive system about fixed points.

Parameter varied	Parameter Value	Dynamical behavior	Figure
$p < 2.5116$	$p = 2$	Pest-free Solution	Fig. 5.1
$p = 2.5116 < p < 3.1226$	$p = 3$	Period-1 Solution	Fig. 5.2
$3.1226 < p < 3.53$	$p = 3.3$	Period-2 solution	Fig. 5.9(a)
	$p = 3.45$	Period-4 solution	Fig. 5.9(b)
	$p = 3.5$	Period-8 solution	Fig. 5.9(c)
$3.53 < p < 3.682$	$p = 3.6$	Chaotic solution	Fig. 5.9(d)

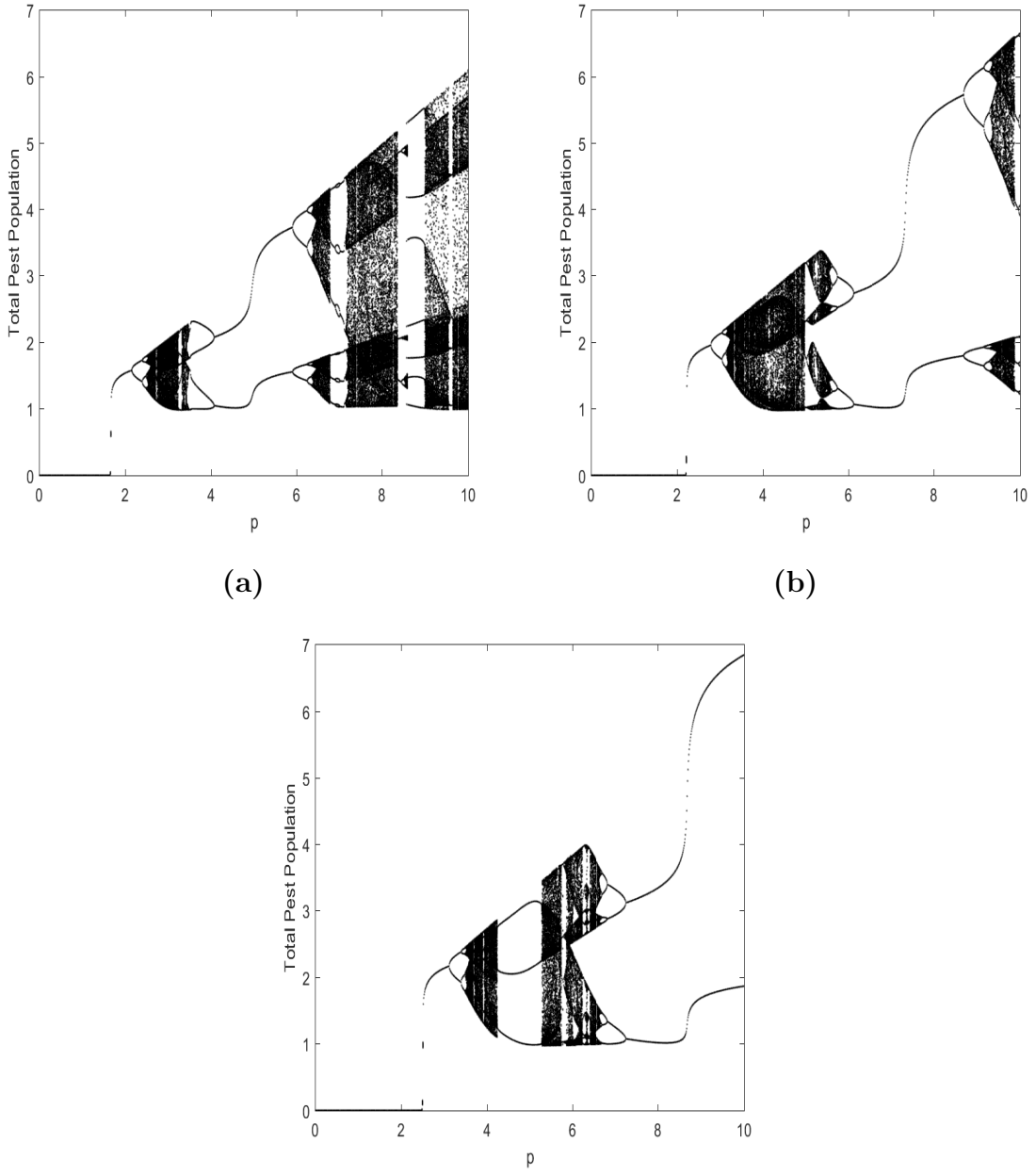

Figure 5.8: Bifurcation diagrams of the map (5.2.6) for total pest population with respect to p (a) $d_1 = 0.2$, $d_2 = 0.6$ (b) $d_1 = d_2 = 0.6$ (c) $d_1 = 0.8$, $d_2 = 0.6$.

The map (5.2.6) exhibits stability of the pest-free state up to $p = 2.51160$ in Fig. 5.8(c). The map (5.2.6) has period-1 solution in the range $p = 2.5116 < p < 3.1226$. More complex periodic solutions are observed in the range $3.1226 < p < 3.53$. A stable periodic window is also visible in the range $3.682 < p < 3.701$. The system exhibits complex dynamical behavior in the range $3.53 < p < 3.682$ including chaos.

The system (5.2.1)−(5.2.3) dynamical behaviors are further explored for different values of p while other parameters kept fixed. Also, it is shown that the systems (5.2.1) − (5.2.3) and the map (5.2.6) have same dynamical behavior. The results are discussed in the table 6.3.

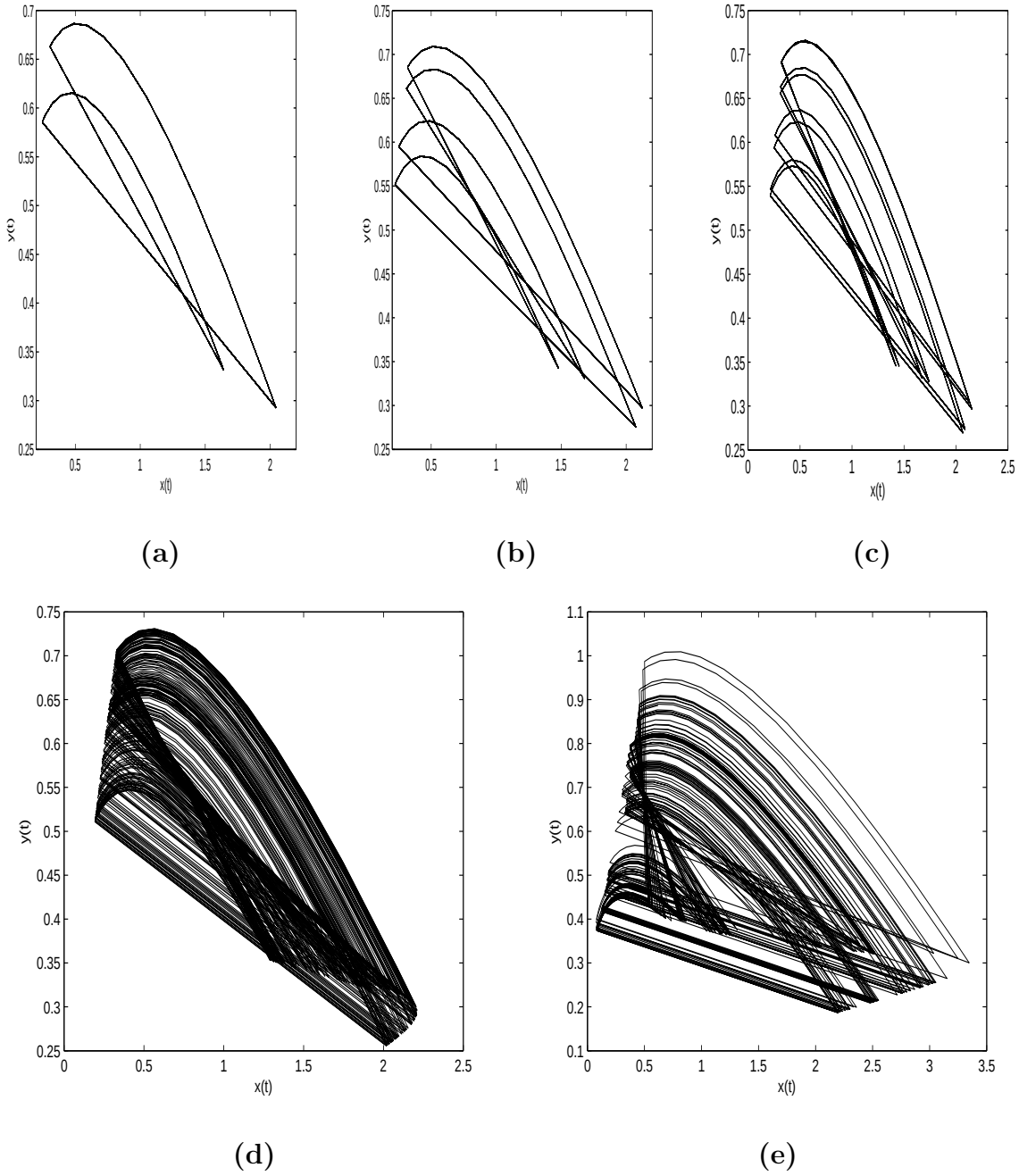

Figure 5.9: The attractors of the system (5.2.1) − (5.2.3) (a) Period-2 at $p = 3.3$ (b) Period-4 at $p = 3.45$ (c) Period-8 at $p = 3.5$ (d) Strange attractor at $p = 3.6$ (e) Strange attractor at $p = 5.65$.

The critical value for a flip bifurcation parameter is $b_c = 3.1226$ as obtained from equation (5.2.12) is confirmed from the Fig. 5.8.

The chaotic regions of Fig. 5.8(c) are separately blown up in Fig. 5.10 for (a) $p \in (3.68, 3.71)$ (b) $b \in (6.2, 6.5)$. Clearly, the rich dynamical behavior is visible including, periodic solutions/period-doubling/narrow and wide periodic windows/crises and chaos.

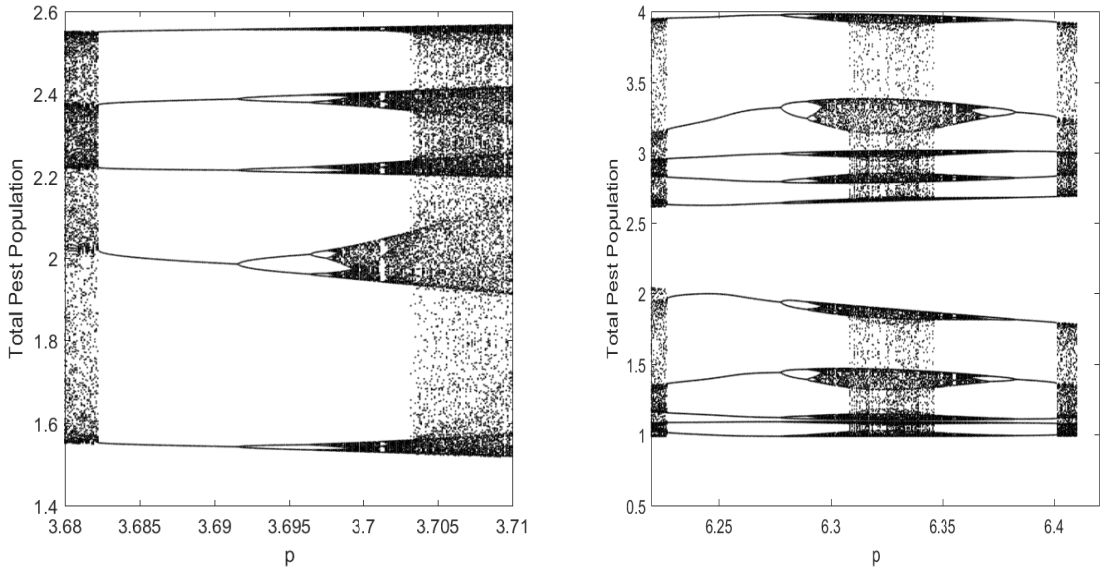

(a) **(b)**

Figure 5.10: The bifurcation diagrams for (a) $p \in (3.68, 3.71)$ (b) $p \in (6.22, 6.41)$.

The two Lyapunov exponents for $d_2 = 0.6$, drawn in Fig. 5.11 further confirms that the attractor is chaotic. Accordingly, Fig. 5.9(d) shows a typical attractor for the data set (5.3.1) with $p = 3.6$. Another, typical strange attractor is shown at $p = 5.65$ in Fig. 5.9(e).

Fig. 5.12(a) is the time series plot for $p = 4$. Here, green and red curves are drawn with respect to initial conditions $x = 1.4, y = 4.24$ and $x = 1.4001$ and $y = 4.24001$ respectively. The solution is found to be sensitive to initial conditions which indicates the presence of chaos at $p = 4$. Fig. 5.12(b) shows a strange attractor at $p = 4$.

In Fig. 5.13 chaotic attractor is drawn for $p = 4$. Here, blue and black curves show the strange attractor of impulsive system (5.2.1) – (5.2.3) and phase portrait of stroboscopic map (5.2.6) for the data set (5.3.1). It is observed that both the system

behaves alike.

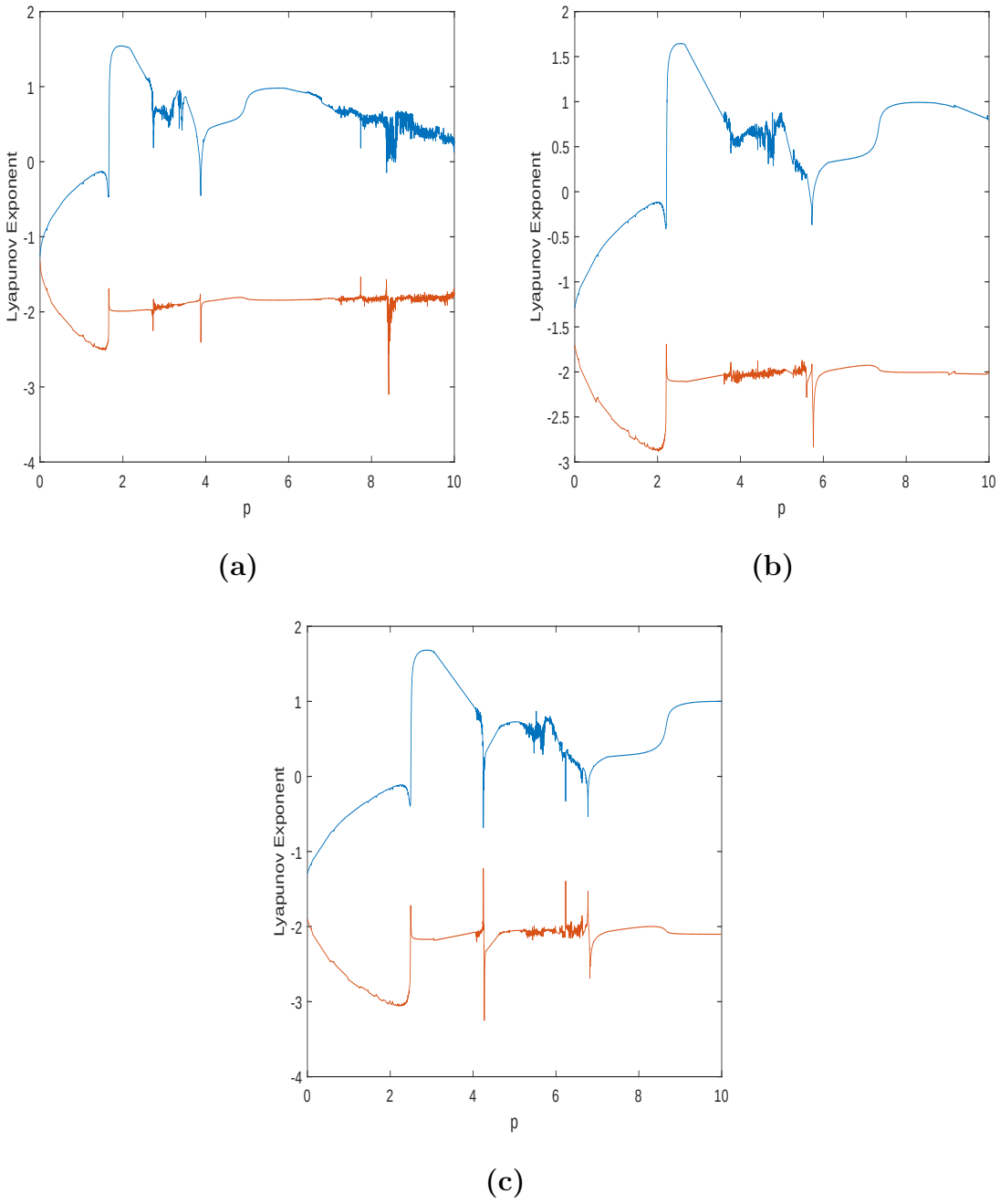

Figure 5.11: Lyapunov exponents of the map (5.2.6) for total pest population with respect to p at (a) $d_1 = 0.2$, $d_2 = 0.6$ (b) $d_1 = d_2 = 0.6$ (c) $d_1 = 0.8$, $d_2 = 0.6$.

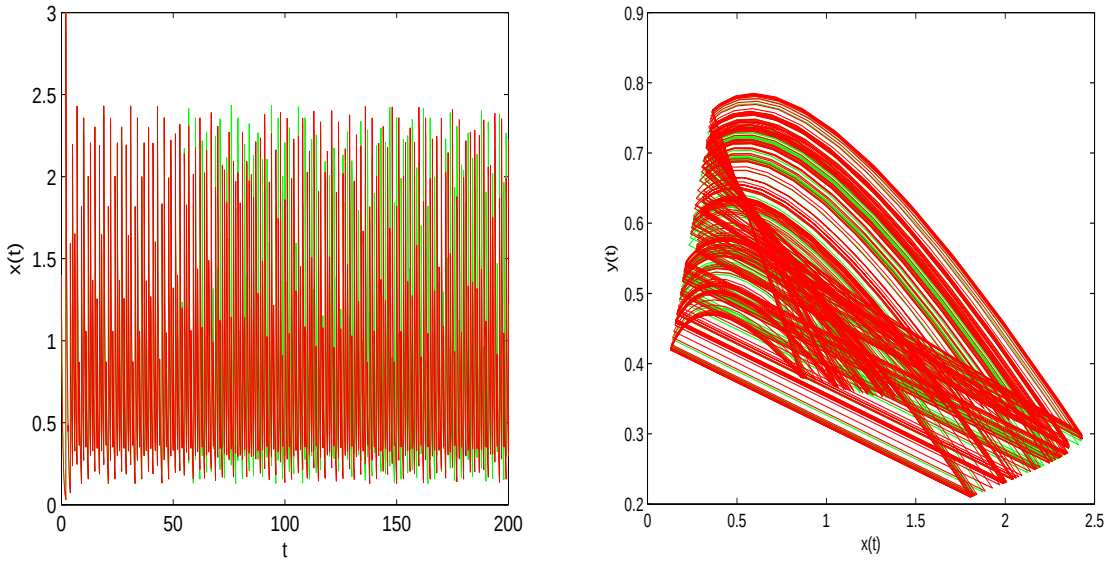

(a) **(b)**

Figure 5.12: (a) Time series to show sensitive dependence to initial condition (b) Phase plot at $p = 4$ of the system (5.2.1) – (5.2.3).

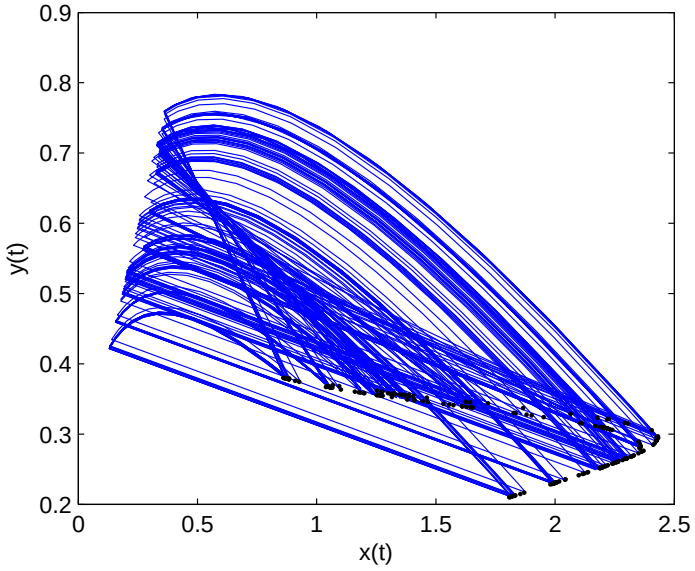

Figure 5.13: Chaotic attractor of the system (5.2.1) – (5.2.3) at $p = 4$.

A set of the bifurcation diagrams is plotted against maturation rate $a \in (0, 1)$ with $p = 3$ in Fig. 5.14. In these figures it can be observed that overall complexity

decreases with increase in parameter d_1. The existence of chaos is observed in the first two cases through repeated period-doubling with increase in a. No chaotic region is obtained for the case $d_1 > d_2$. For $d_1 > d_2$, the pest will be eradicated for $a < 0.58$ in 5.14(c). Further, transcritical bifurcation occurs at $a \approx 0.58$ and period-1 and period-2 solution occurs for $a > 0.58$ in Fig. 5.14(c).

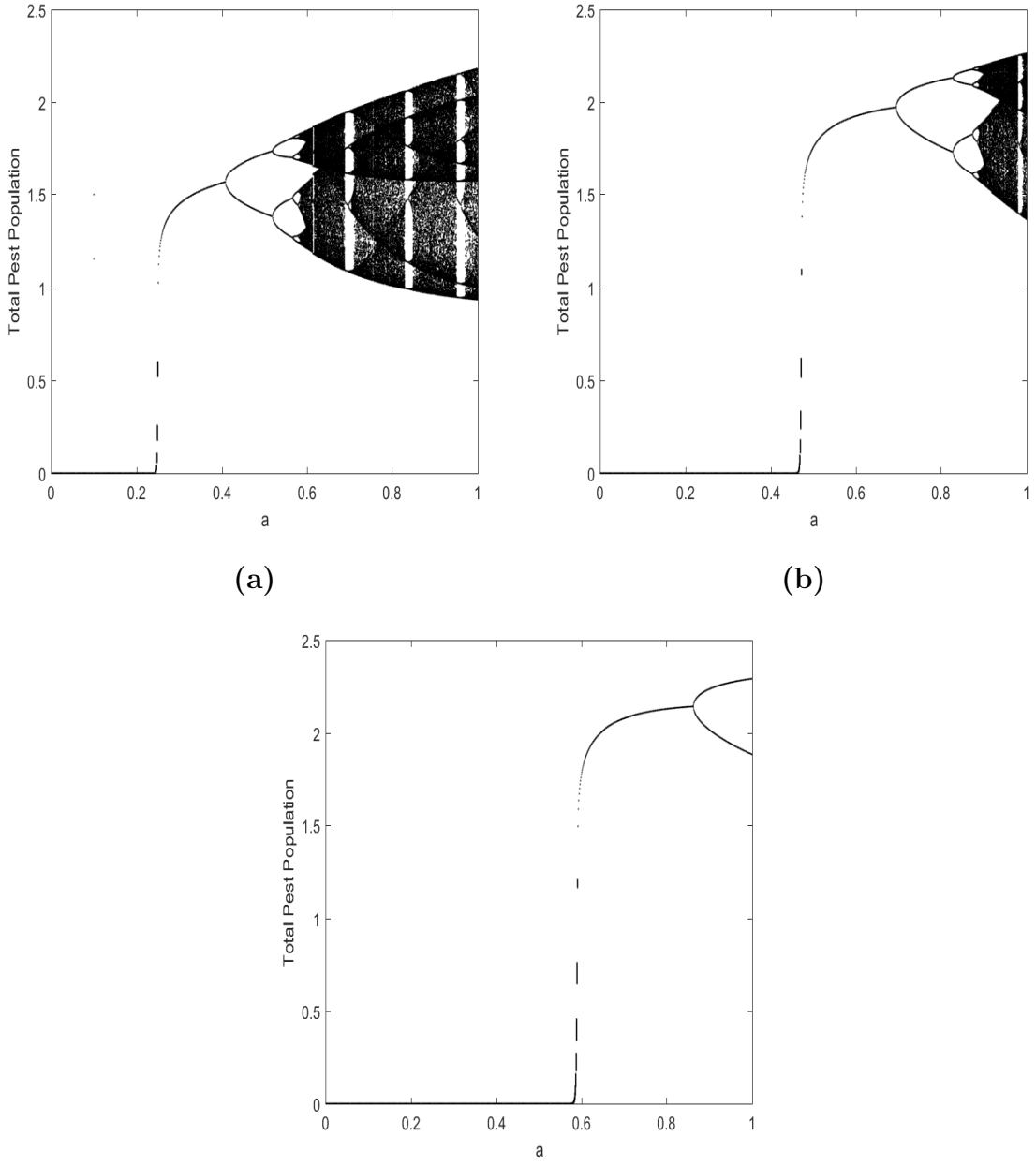

Figure 5.14: Bifurcation diagrams of the map (5.2.6) for total pest population with respect to a at $p = 3$ (a) $d_1 = 0.2$, $d_2 = 0.6$ (b) $d_1 = d_2 = 0.6$ (c) $d_1 = 0.8$, $d_2 = 0.6$.

Similarly, A set of bifurcation diagrams have been plotted with respect to the killing rates μ in the Fig. 5.15. It can be observed that overall complexity reduces with increase in parameter d_1. There period-doubling and period-halving behavior occurs with the chaotic region in between. Further, the solution settles down to the pest-free state with increase in the killing rate of the mature pest μ in Fig. 5.15(b) and in Fig. 5.15(c).

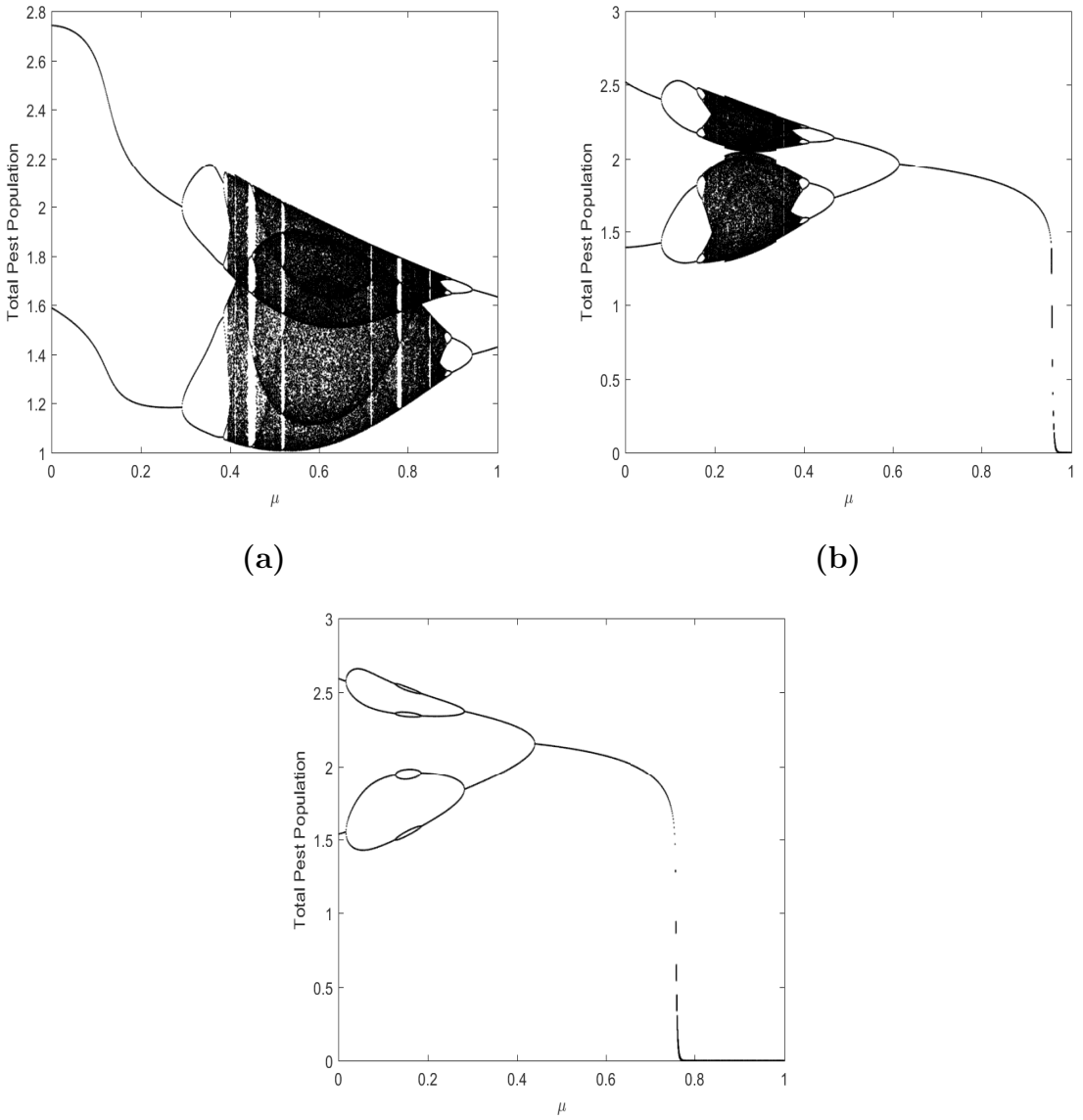

Figure 5.15: Bifurcation diagrams of the map (5.2.6) for total pest population with respect to μ at $p = 3$ (a) $d_1 = 0.2$, $d_2 = 0.6$ (b) $d_1 = d_2 = 0.6$ (c) $d_1 = 0.8$, $d_2 = 0.6$.

When the $d_1 = d_2$, the pest will be eliminated for a certain value of $\mu > 0.989$ in Fig. 5.15(b). For $d_1 > d_2$, only periodic behavior is observed and for $\mu > 0.786$ pest eradication will be possible in the Fig. 5.15 (c). Very narrow periodic windows can also be observed in the Fig. 5.15(a) and Fig. 5.15(b).

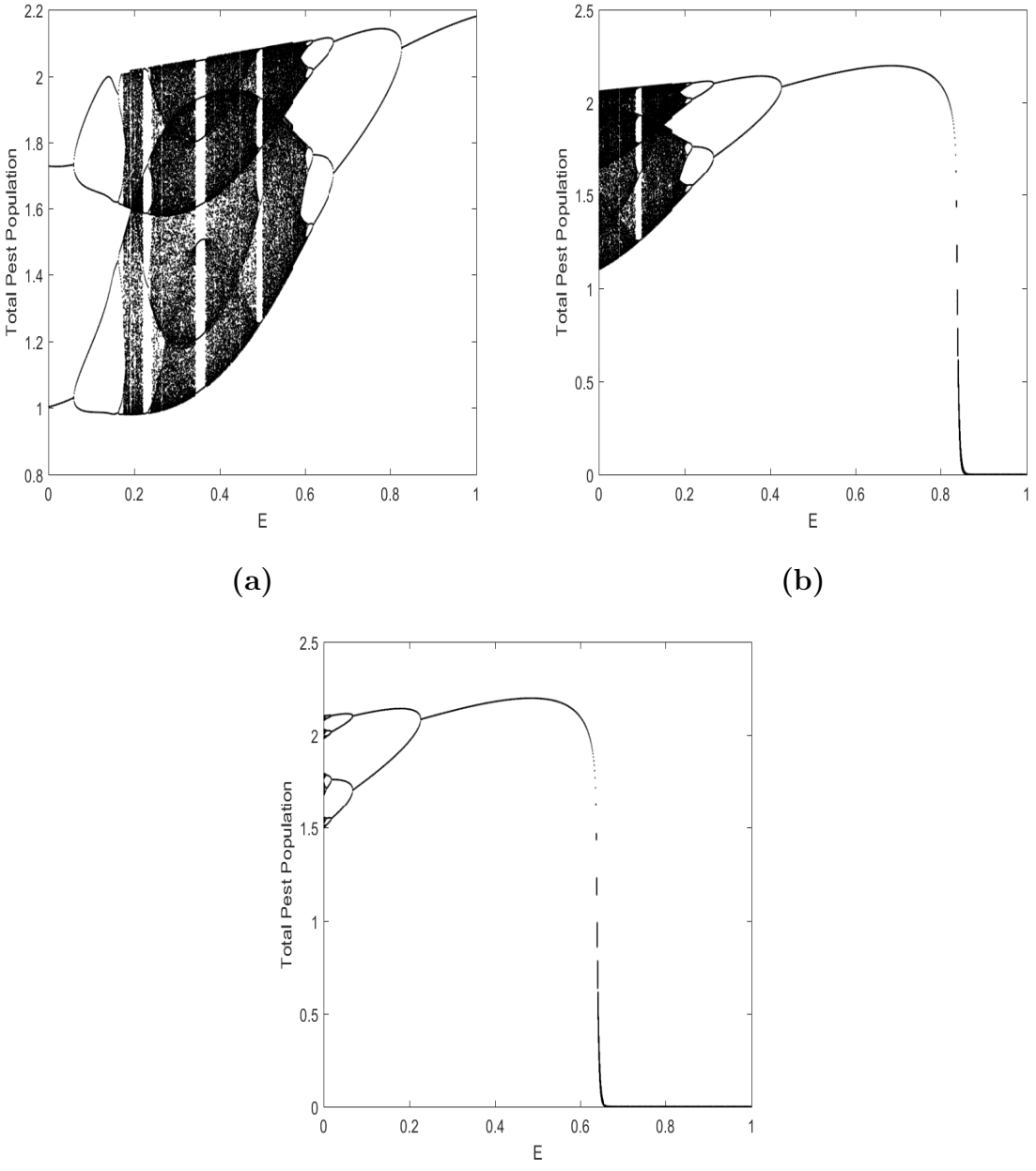

Figure 5.16: Bifurcation diagrams of the map (5.2.6) for total pest population with respect to E at $p = 3$ (a) $d_1 = 0.2$, $d_2 = 0.6$ (b) $d_1 = d_2 = 0.6$ (c) $d_1 = 0.8$, $d_2 = 0.6$.

Another set of bifurcation diagrams is plotted for pest population with respect to harvesting rate E for $p = 3$ in Fig. 5.16. From these figures it can be observed that complexity decreases with the increase of parameter d_1. A period-doubling and period halving cascade can be observed with chaotic regions in between in Fig. 5.16(a) but only period-halving behavior will appear in Fig. 5.16(b) and Fig. 5.16(c). The chaotic behavior will become periodic after a certain value of E. No chaotic behavior will appear in Fig. 5.16. Further, in Fig. 5.16, the periodic solutions become stable the pest-free solution after a critical value of the harvesting rate say E_c. The pest will be eradicated for $E > 0.856 \approx E_c$ and $E > 0.656 \approx E_c$ in Fig. 5.16. Further, in Fig. 5.16 respectively. Therefore, by indicating a critical value of the harvesting rate, pest eradication is possible. These observations suggest that harvesting rate can play a crucial role in eliminating pest.

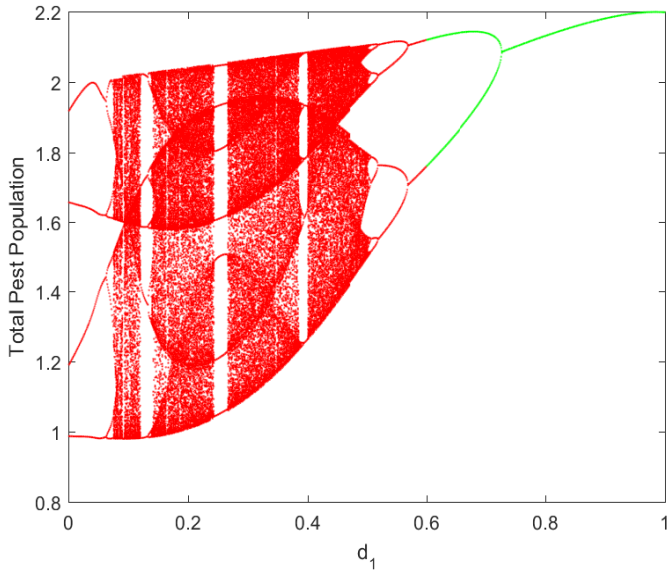

Figure 5.17: Bifurcation diagram of the map (5.2.6) for total pest population with respect to d_1 at $p = 3$.

Fig. 5.17 shows another bifurcation diagram as a function of the mortality rate of immature pest d_1 in the range $(0, 1)$ keeping the rest of the parameters fixed as in the data set (5.3.1). The figure demonstrates an abundance of period and chaotic regions. The green color shaded region is drawn for $d_1 > d_2$ and periodic behavior is observed. For $d_1 < d_2$, the red color region is drawn and the solution is more complex.

The period-halving occurs in the range $0 < d_1 < 0.6$.

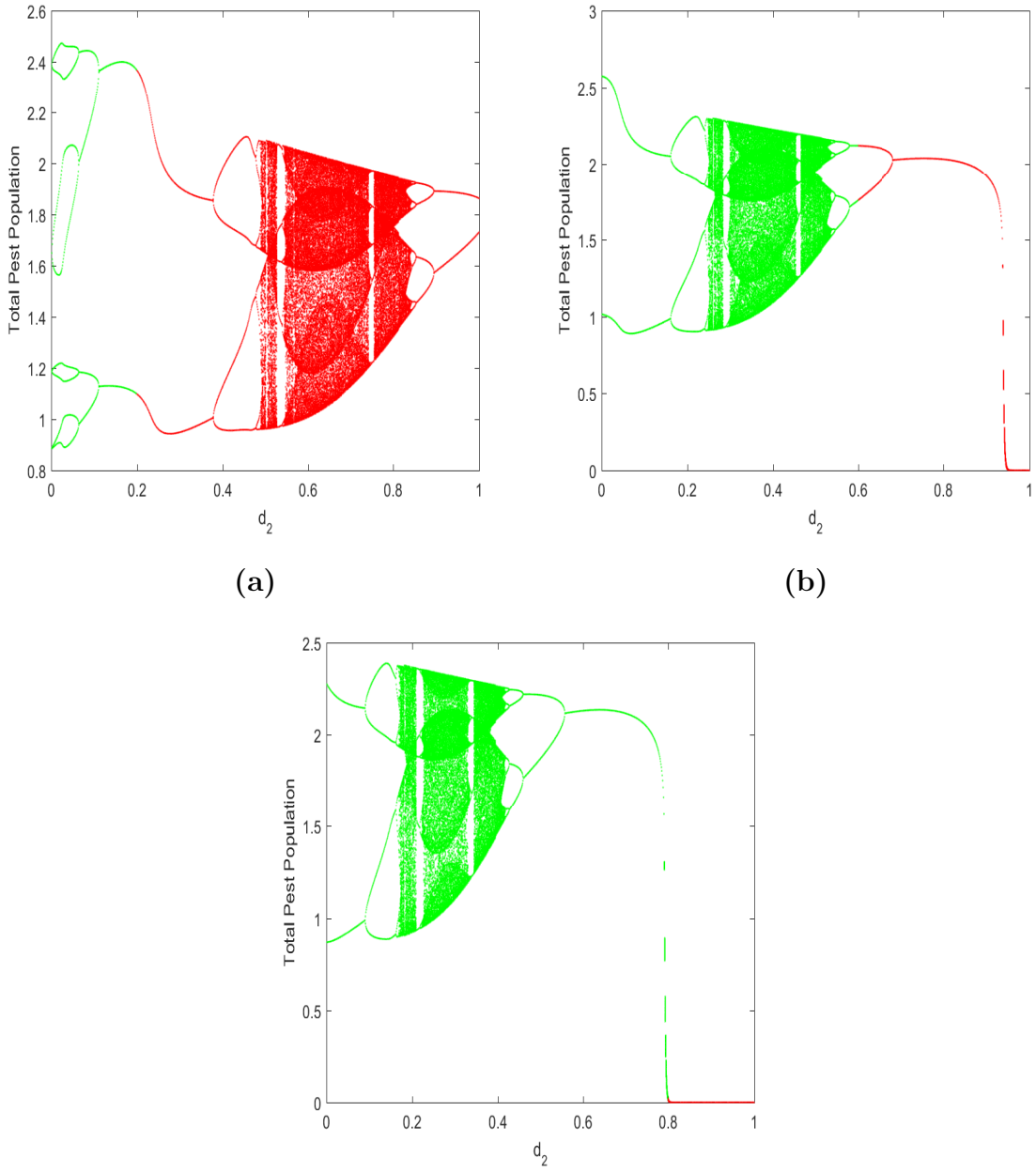

Figure 5.18: Bifurcation diagrams of the map (5.2.6) for total pest population with respect to d_2 at $p = 3$ (a) $d_1 = 0.2$ (b) $d_1 = 0.6$ (c) $d_1 = 0.8$.

Bifurcation diagram is plotted with respect to d_2 for $p = 3$ in Fig. 5.18, keeping other parameters as in (5.3.1). In all cases, the stable periodic solution will settle down to complex dynamical behavior, including periodic windows, quasi-periodic/chaotic

behaviors are observed. The green with green color shows $d_1 > d_2$ and red color region depicts $d_1 < d_2$. No chaos is observed when $d_2 > d_1$ in Fig. 5.18(b) and Fig. 5.18(c).

5.4 Model II: Dynamic Complexities in an Integrated Pest Management Model with Birth Pulse and Asynchronous Pulses

In this section, the dynamics of a stage-structured system with birth pulse subjected to time-dependent impulsive control strategy is investigated with asynchronous pulses. The impulsive system considers the presence of two different control strategies, namely chemical control and mechanical control. Pesticide spray is taken impulsively at a fixed time. Mechanical control is applied continuously. The selective harvesting of immature and mature pest is considered. The following assumptions are made to formulate the model:

- The pesticide is sprayed on the pest impulsively at $t = (m + l - 1)T$, $0 < l < 1$. Both immature and mature pest are instantaneously affected by pesticide spray at the fixed time $t = (m+l-1)T$, $0 < l < 1, m = 1, 2, ...$ impulsively at different killing rates,$0 < \beta < 1$ and $0 < \alpha < 1$ respectively

$$\left.\begin{aligned} x((m+l-1)T)^+ &= (1-\beta)x(m+l-1), \\ y((m+l-1)T)^+ &= (1-\alpha)y(m+l-1), \end{aligned}\right\} t = (m+l-1)T.$$

- To control the pest density, harvesting effort E is applied to both immature and mature pest.

- The birth function $B(N)$ is assumed to be of Beverton-Holt type [42]:

$$B(N) \;=\; p(c + (x(t) + y(t))^{-n}.$$

The above assumptions led to the following impulsive stage-structured system with birth pulse and integrated pest management strategies:

$$\left.\begin{aligned} \frac{dx}{dt} &= -(d + a + E)x(t), \\ \frac{dy}{dt} &= ax(t) - (d + E)y(t), \end{aligned}\right\} t \neq (m + l - 1)T, t \neq mT, \tag{5.4.1}$$

$$\left.\begin{aligned} x((m+l-1)T)^+ &= (1-\beta)x(m+l-1), \\ y((m+l-1)T)^+ &= (1-\alpha)y(m+l-1), \end{aligned}\right\} t=(m+l-1)T, \tag{5.4.2}$$

$$\left.\begin{aligned} x(mT)^+ &= x(mT)+B(N(mT))y(mT), \\ y(mT)^+ &= y(mT), \end{aligned}\right\} t=mT, \tag{5.4.3}$$

$$x(0)=x_0>0, \quad y(0)=y_0>0. \tag{5.4.4}$$

The model is defined on the set $\Re^2_+ = \{(x_1,x_2)\in\Re^2 \mid x\geq 0, y\geq 0\}$. All model parameters are assumed to be positive. The model is associated with the non-negative initial immature and mature pest densities x_0 and y_0 respectively.

5.4.1 Preliminary Analysis

Theorem 5.4.1. *The system* (5.4.1) − (5.4.4) *has ultimately bounded solution.*

Proof. Define a positive definite continuous function

$$L(t)=x(t)+y(t).$$

Let $D^+V(t,X)$ denotes Dini's derivative [120]. Using (5.4.1), it is computed as:

$$D^+L(t,X)+d_1L(t,X) \;=\; -(d+E)(x(t)+y(t)) \leq d_1(x(t)+y(t)).$$

When $t=(m+l-1)T$, Using condition (5.4.2) and choosing $\gamma=\min\{\beta,\alpha\}$ gives:

$$\begin{aligned} L((m+l-1)T^+) &= (1-\beta)x_1((m+l-1)T)+(1-\alpha)y((m+l-1)T) \\ &\leq \gamma L((m+l-1)T). \end{aligned}$$

When $t=mT$, applying birth pulses (5.4.3):

$$L(mT^+) \;=\; x(mT)+\frac{p}{c+(x(mT)+y(mT))^n}y(mT)+y(mT)\leq L(mT)+\frac{pM_1}{2}.$$

Therefore, Using Lemma 2.5 in [8]. For as $t\to\infty$, it can be concluded that

$$\begin{aligned} L(t) \leq L(0^+)e^{-(d+E)t}+M_1(1-e^{-(d+E)t})+p\frac{e^{-d(t-T)}}{1-e^{-(d+E)T}}+p\frac{e^{(d+E)T}}{e^{(d+E)T}-1} \\ \to \frac{M_1}{(d+E)T}+p\frac{e^{(d+E)T}}{e^{(d+E)T}-1}. \end{aligned}$$

Since $\exists$ a constant $M_1>0$, $x(t)\leq M_1/2$ and $y(t)\leq M_1/2$ for each solution $(x(t),y(t))$ of the system (5.4.1) − (5.4.4) for all large value of t. Therefore, $V(t)$ is uniformly bounded. □

5.4.2 Model Analysis

Let $x = x_{m-1}$ and $y = y_{m-1}$ be the initial density of immature and mature pest respectively at $t = (m-1)T$. The analytical solution of differential equations (5.4.1) between the pulses can be written as:

$$\begin{aligned} x(t) &= x_{m-1}e^{-(a+d+E)(t-(m-1)T)}, \qquad (m-1)T \le t < (m+l-1)T, \\ y(t) &= e^{-(d+E)(t-(m-1)T)}[y_{m-1} + x_{m-1}(1-e^{-a(t-(m-1)T)})]. \end{aligned}$$

$$\begin{aligned} x(t) &= (1-\beta)x_{m-1}e^{-(a+d+E)(t-(m-1)T)}, \qquad (m+l-1)T \le t < mT, \quad (5.4.5) \\ y(t) &= [(\alpha-\beta)x_{m-1}e^{-(d+a+E)lT} + (1-\alpha)(y_{m-1}+x_{m-1})e^{-(d+E)lT}]e^{-(d+E)(t-(m+l-1)T)} \\ &\quad -(1-\beta)x_{m-1}e^{-(a+d+E)(t-(m-1)T)}. \end{aligned}$$

Applying impulsive condition (5.4.3) with the analytical solution (5.4.5) gives the stroboscopic map of system (5.4.1)−(5.4.4) after each successive birth pulse can be obtained as:

$$\begin{aligned} x_m &= p(c+B^n)^{-1}[B-(1-\beta)x_{m-1}e^{-(d+a+E)T}] + (1-\beta)x_{m-1}e^{-(a+d+E)T}, \\ y_m &= B-(1-\beta)x_{m-1}e^{-(d+E+a)T}, \qquad (5.4.6) \\ B &= (\alpha-\beta)x_{m-1}e^{-(d+al+E)T} + (1-\alpha)(x_{m-1}+y_{m-1})e^{-(d+E)T}. \end{aligned}$$

The difference equations (5.4.6) describe the stroboscopic sampling of immature and mature pest.

It is observed that for positive initial conditions the solution (5.4.6) of the system $(5.4.1)-(5.4.4)$ always exists and stay positive if $\alpha > \beta$. Therefore, each x_m and y_m of the map (5.4.6) is positive if $\alpha > \beta$. Further the system is dissipative for $\beta, \alpha \in (0,1)$.

Let us define the intrinsic net reproductive number R_0 as

$$R_0 = \frac{pe^{-(d+E)T}((\alpha-\beta)e^{-alT} + (1-\alpha) - (1-\beta)e^{-aT})}{c(1-(1-\beta)e^{-(d+a+E)T})(1-(1-\alpha)e^{-(d+E)T})} = \frac{p}{p_0}. \qquad (5.4.7)$$

It represents the average number of offspring that a pest produces over the period of its life span.

5.4.3 Existence and Stability Analysis of Fixed Points

The following two equilibrium states will exist for the map (5.4.6) :

The trivial pest-free fixed point $E_0 = (0, 0)$ exists without any parametric restriction.

The non-trivial fixed point $E^* = (x^*, y^*)$ is established if $R_0 > 1$ and is given as:

$$x^* = \frac{(1-(1-\alpha)e^{-(d+E)T})\sqrt[n]{c(R_0-1)}}{e^{-(d+E)T}((\alpha-\beta)e^{-alT}+(1-\alpha)-(1-\alpha)(1-\beta)e^{-(d+a+E)T})},$$

$$y^* = \frac{((\alpha-\beta)e^{-alT}+(1-\alpha)-(1-\beta)e^{-aT})\sqrt[n]{c(R_0-1)}}{(\alpha-\beta)e^{-alT}+(1-\alpha)-(1-\alpha)(1-\beta)e^{-(d+a+E)T}}.$$

The unique interior fixed point is feasible if the birth rate of pest is more than a critical value b_0 which depends upon all model parameters.

The stability analysis of the various fixed points has been performed. For this, the coefficients of the linearized matrix A for the map (5.4.6) about any state $E = (x, y)$ can be computed as:

$$\begin{aligned}
a_{11} &= (1-\beta)e^{-(d+a+E)T} + p(c+B^n)^{-1}e^{-(d+E)T}[(\alpha-\beta)e^{-alT}+(1-\alpha)-(1-\beta)e^{-aT}] \\
&\quad + np((\alpha-\beta)e^{-alT}+(1-\alpha))e^{-(d+E)T}B^{n-1}(c+B^n)^{-2}[B-(1-\beta)xe^{-(d+a+E)T}], \\
a_{12} &= p(c+B^n)^{-1}(1+npB^{n-1}(c+B^n)^{-2} \times [B-(1-\beta)xe^{-(d+a_+E)T}](1-\alpha)e^{-(d+E)T}), \\
a_{21} &= [(\alpha-\beta)e^{-alT}+(1-\alpha)-(1-\beta)e^{-aT}]e^{-(d+E)T}, \quad a_{22} = (1-\alpha)e^{-(d+E)T}.
\end{aligned}$$

Theorem 5.4.2. *The pest-free state is locally asymptotically stable if $R_0 < 1$ and unstable for $R_0 > 1$.*

Proof. For small perturbation about E_0, coefficients of matrix $A[E_0]$ are computed. It is observed that conditions $1 + Tr + Det > 0$ and $1 - Det > 0$ are always satisfied. However, for stability, Jury's condition $1 - Tr + Det > 0$ must also be satisfied. On simplification, it yields condition $R_0 < 1$ establishing the local stability of E_0. □

Accordingly, the pest-free point E_0 is locally asymptotically stable for $p \in (0, p_0)$. The trajectories in the neighborhood of $(0, 0)$ tend to origin and pest will extinct. Thus, the pest eradication is possible when $R_0 < 1$. The existence of non-trivial fixed point is overruled in this case. However, for $R_0 > 1$, one of the Jury's condition does not satisfy. Hence the pest-free fixed point will be unstable for $R_0 > 1$.

It is found that $1 - Tr - Det = 0$ at $R_0 = 1$ and one of the eigenvalues is 1. Therefore, the pest-free state E_0 becomes non-hyperbolic at $R_0 = 1$. So, there is a

possibility of transcritical bifurcation. Also, at $R_0 = 1$ pest-eradication point collides with E^*.

Theorem 5.4.3. *Let us define constants C and F as*

$$\begin{aligned} F &= 2((\alpha-\beta)e^{-alT} + (1-\alpha) - (1-\alpha)(1-\beta)e^{-(d+a+E)T}) \\ &\quad \times(1 + (1-\beta)(1-\alpha)e^{-(2d+a+2E)T}), \\ C &= n(1-(1-\beta)e^{-(d+a+E)T})(1-(1-\alpha)e^{-(d+E)T})((\alpha-\beta)e^{-alT} + (1-\alpha) \\ &\quad +(1-\alpha)(1-\beta)e^{-(d+a+E)T}). \end{aligned}$$

The non-trivial fixed point $E^* = (x^*, y^*)$ is locally asymptotically stable provided

$$p_0 < p < p_0 \frac{C}{C-F} (= p_c). \tag{5.4.8}$$

Proof. The matrix A is computed around (x^*, y^*). It is easily seen that inequalities $1 - Tr + Det > 0$ and $1 - Det > 0$ are always satisfied. The stability condition $p < p_c$ is obtained from condition $1 + Tr + Det > 0$ after rearranging the model parameters. Hence, if $p \in (p_0, p_c)$ then $E^* = (x^*, y^*)$ is locally asymptotically stable. □

Accordingly, when $p \in (p_0, p_c)$, E^* is locally asymptotically stable. The trajectories of system (5.4.1) − (5.4.4) tend to asymptotically stable period-1 solution $(x_e(t), y_e(t))$:

$$\begin{aligned} x_e(t) &= x^* e^{-(a+d+E)(t-(m-1)T)}, \qquad (m-1)T \le t < (m+l-1)T, \\ y_e(t) &= e^{-(d+E)(t-(m-1)T)}[y^* + x^*(1 - e^{-a(t-(m-1)T)})]. \end{aligned}$$

$$\begin{aligned} x_e(t) &= (1-\beta)x^* e^{-(a+d+E)(t-(m-1)T)}, \qquad (m+l-1)T \le t < mT, \\ y_e(t) &= [(\alpha-\beta)x^* e^{-alT} + (1-\alpha)(x^*+y^*) - (1-\beta)x^* e^{-aT}]e^{-(d+E)(t-(m-1)T)}. \end{aligned}$$

It can be easily concluded that if there is a small increase in p beyond the critical value p_0, the system (5.4.1) − (5.4.4) has a positive period-1 solution $(x_e(t), y_e(t))$. The period-doubling can occur at $p = p_c$. Further, increasing the parameter value $p > p_c$, E^* losses its stability and the system may exhibit complex dynamics which will be shown in a later section.

Theorem 5.4.4. *The locally asymptotically stable pest-free point E_0 is globally asymptotically stable in the interior of positive quadrant of $x-y$ plane for the map* (5.4.6).

Proof. Consider the positive definite function

$$V_1(x_m, y_m) \;=\; \mid x_m \mid + \mid y_m \mid .$$

Now, computing ΔV_1 and its simplification gives

$$\begin{aligned}\Delta V_1(x_m, y_m) \;=\;& \mid (\alpha-\beta)x_m e^{-(d+al)T} + (1-\alpha)(y_m+x_m)e^{-dT} - (1-\beta)x_m e^{-(d+a)T} \mid \\ & + \mid pe^{-dT}[(\alpha-\beta)x_m e^{-alT} + (1-\alpha)(y_m+x_m) - (1-\beta)x_m e^{-aT}] \\ & \times(c+B^n)^{-1} + (1-\beta)x_m e^{-(a+d)T} \mid - \mid x_m \mid - \mid y_m \mid .\end{aligned}$$

Further simplification of ΔV_1 yields:

$$\begin{aligned}\Delta V_1 \;\leq\;& \mid p[(\alpha-\beta)e^{-(d+al)T} + (1-\alpha)e^{-dT} - (1-\beta)e^{-(d+a)T}] + (\alpha-\beta)e^{-(d+al)T} \\ & +(1-\alpha)e^{-dT} - 1 \mid x_m + \mid p(1-\alpha)e^{-dT} + (1-\alpha)e^{-dT} - 1 \mid y_m, \\ \Delta V_1 \;<\;& -(1-R_0)V_1(x_m, y_m).\end{aligned}$$

Thus, V_1 is a Lyapunov function and the pest-free fixed point $E_0 = (0,0)$ is globally asymptotically stable. □

Theorem 5.4.5. *The local asymptotically stable positive interior fixed point E^* of the map* (5.4.6) *is globally asymptotically stable.*

Proof. Define the positive definite function

$$V_2(x_m, y_m) \;=\; \mid x_m - x^* \mid + \mid y_m - y^* \mid .$$

Computing ΔV_2 on the same lines as in Theorem 5.4.4 proves that V_2 is a Lyapunov function. This proves the theorem. □

5.4.4 Numerical Explorations

To illustrate the stability of the pest-free state and interior fixed point, the numerical experiments of the map (5.4.6) are performed for the following data given as:

$$a = 0.8, c = 1, d = 0.6, l = 0.5, n = 7, \alpha = 0.6, \beta = 0.4. \tag{5.4.9}$$

Considering $T = 1.0$ and $E = 0.5$, the critical value p_0 is computed as $p_0 = 8.9632$ for parameter set (5.4.9). For the above data set and $p = 7$, $R_0 = 0.7810 < 1$ and the pest-free state is locally asymptotically stable. Taking $p = 10$, the pest-free fixed point becomes unstable and E^* exists. It is given as the non-trivial fixed point $E^* = (3.8413, 0.3901)$ is locally asymptotically stable as $p_0 < p < 13.1858$.

Fig. 5.19 shows the variation of R_0 with impulsive period T for parameter set (5.4.9) when $E = 0.5$. The non-monotonic behavior of R_0 with respect to T is observed. The maximum value of threshold R_0 is 1.6289 at $T = 0.3614$. The basic reproduction number R_0 is less than 1 for $T \in (0, 0.09) \cup (1.1268, 3)$. The pest-free solution is possible in this range and pest outbreak can occur for $T \in (0.09, 1.1268)$.

Fig. 5.19(b) shows the variation of R_0 with respect to harvesting effort. It is observed that threshold R_0 decreases with increase in E. Pest eradication is possible for $0.5883 < E < 5$.

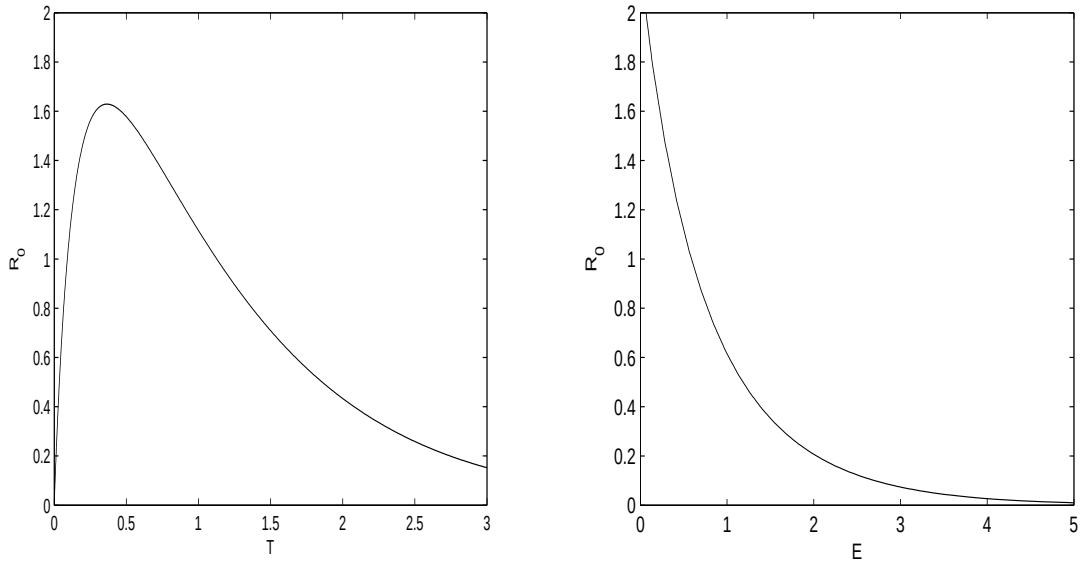

(a) **(b)**

Figure 5.19: Two-parameter bifurcation diagram in (a) $T - R_0$ plane at $E = 0.5$ (b) $E - R_0$ plane at $T = 1$.

Two-parameter bifurcation diagram in the $E - p$ plane is shown in Fig. 5.20. For sufficiently lower birth rate pest will be eradicated for all values of harvesting effort. With an increase in birth rate p, the pest may survive with the harvesting effort. The

chaotic dynamics is evident in a region of $E - p$ plane. The periodic doubling leads to chaos for higher birth rates.

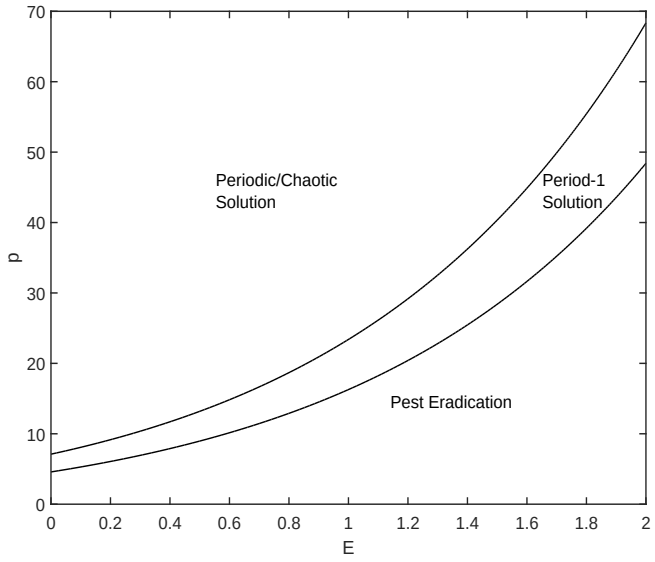

Figure 5.20: Two-parameter bifurcation diagram in $E - p$ plane.

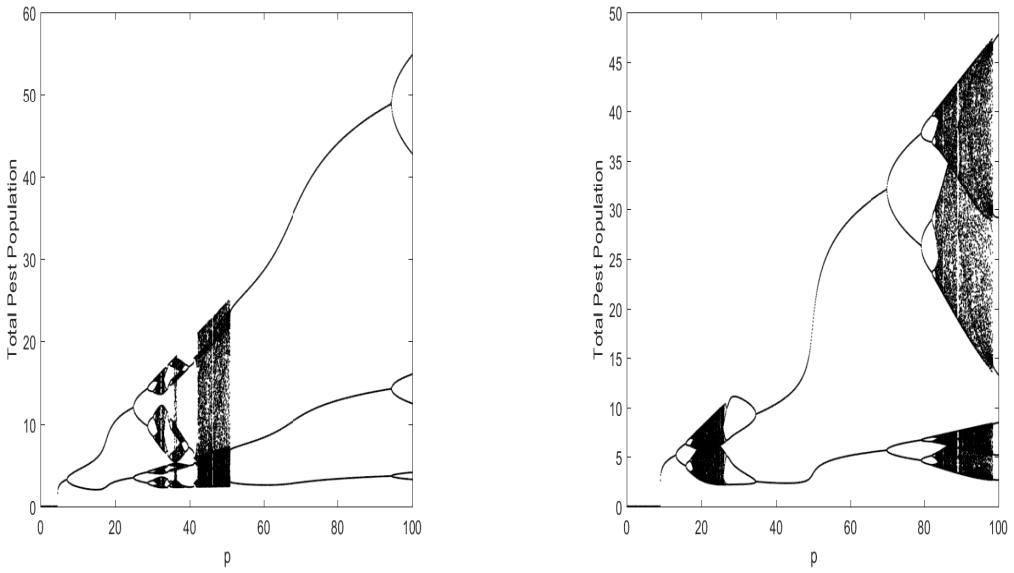

(a) **(b)**

Figure 5.21: Bifurcation diagrams of the map (5.4.6) for total pest population with respect to p at (a) $E = 0$ (b) $E = 0.5$.

Typical bifurcation diagrams are drawn in Fig. 5.21 for $E = 0$ and $E = 0.5$ with respect to critical parameter p. The bifurcation diagram shows the existence of chaos

through period-doubling route. The critical values for period-doubling bifurcation parameter are $p_c = 7$ and $p_c = 13$ is confirmed from Fig. 5.21(a) and Fig. 5.21(b) respectively. The period-1 solution occurs in range $p \in (8.9632, 13)$ for $E = 0.5$.

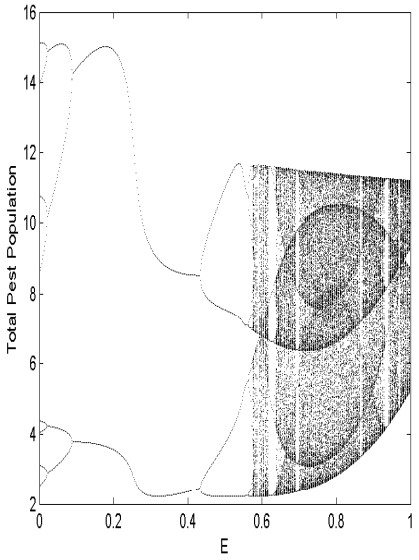

Figure 5.22: Bifurcation diagram of the map (5.4.6) for total pest population with respect to E at $p = 30$.

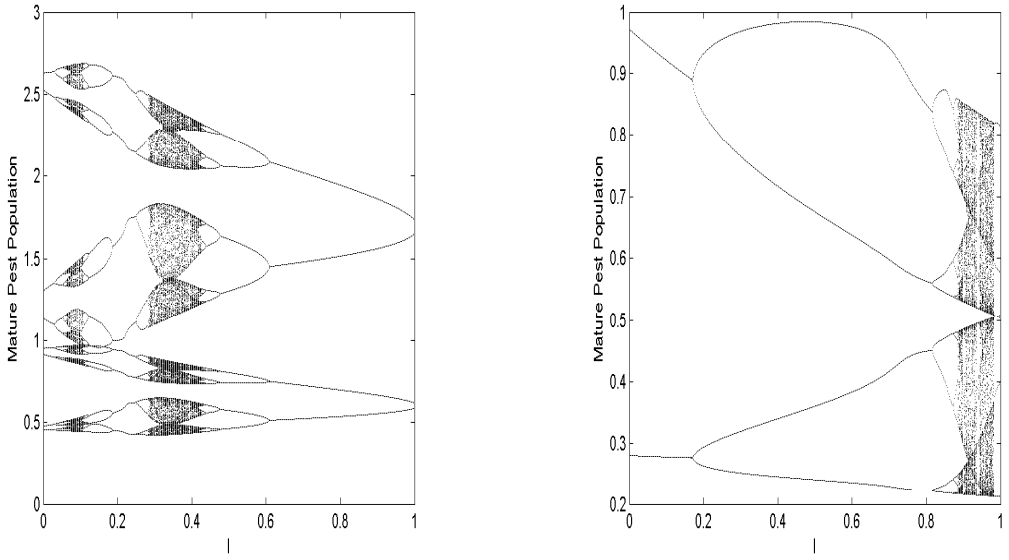

(a) **(b)**

Figure 5.23: Bifurcation diagrams of the map (5.4.6) for total pest population with respect to l (a) $E = 0$ (b) $E = 0.5$ at $p = 30$.

To see the complex dynamical behavior with the variation in the harvesting effort E, bifurcation diagram is drawn in Fig. 5.22 by keeping all parameters fixed as mentioned above in (5.4.9) and $p = 30$. Initially, periodic halving behavior occurs. As the harvesting effort parameter value increases chaotic behavior occurs.

Fig. 5.23 shows bifurcation diagrams with respect to the pesticide spray timing $l \in (0, 1)$ with $p = 30$. The map (5.4.6) depicts the very complex dynamical behavior if no harvesting effort is applied. Also, the pesticide is sprayed just after the birth pulse. As parameter l increases, chaotic behavior is followed by a period-halving bifurcation. If the harvesting effort is taken, then complexity reduces.

5.5 Discussion

An impulsive stage-structured model with birth pulse at fixed time has been formulated. The system incorporates impulsive applications of chemical as well as mechanical control to control the pest. Only the mechanical control is assumed to be continuous. It is assumed that some proportion of the pest population is reduced periodically by pesticide spray. The combination of both strategies decreases the use of chemicals. The two equilibrium states are obtained. For $R_0 < 1$, only the pest-free state will exist and is also found to be globally stable. At $R_0 = 1$, one of the eigenvalues of the Jacobian matrix about the pest-free state becomes one. The period- 1 solution of stroboscopic map is obtained. Some dynamical results such as boundedness, existence and stability of fixed points are analyzed. The sufficient condition for the stability of positive interior fixed point and flip bifurcation are also investigated. The effects of pesticide spray timing and harvesting on the density of pest are investigated. Through numerical analysis, various dynamical aspects including a chaotic behavior have been shown. The system with Beverton-Holt function shows a very complex dynamical behavior. As parameter l increases, there exist, period-halving bifurcations followed by chaotic behavior.

Chapter 6

A Stage-structured Pest Control Model

6.1 Introduction

One of the significant roles of mathematics in pest management is to predict the effectiveness of control tactics. Integrated pest management in agriculture fields is considerably more effective than single tactics [58, 226]. Since pest triggers serious agricultural problems, the first line of action is to control the pest using pesticides. However, the pest develops resistance to the pesticides very quickly and then they are no more effective. Another efficient way to combat the pest is the use of cultural/mechanical control.

Many IPM models used single impulsive strategy [88, 126, 138, 216, 223]. Some impulsive models have also been investigated incorporating multiple pulses [63, 102, 132, 137]. However, they have neglected stage-structure and birth pulses. Few mathematical models with stage-structure and birth pulses have been investigated incorporating single pulse [144, 218] and two pulses [149]. Several stage-structured pest control model with the birth pulse and impulsive harvesting have been discussed [29, 96]. But, they have considered only single tactic for pest control.

This chapter is devoted to multiple pulses impulsive stage-structured pest management system. Integrated pest management strategy is used impulsively by applying two strategies (chemical/mechanical control) at two different fixed times. The model

incorporates stage structure and birth pulse. The focus is on the effectiveness of combining mechanical and chemical control. It is shown that mechanical control reduces the pesticide use.

6.2 Formulation of the Model

In this section, the impulsive model for pest control has been developed considering periodic harvesting and pesticide spray asynchronous with birth pulses. To formulate the model following assumptions have been made:

- For simplicity, mortality rates of immature and mature pest is assumed to be the same, i.e. $d_1 = d_2 = d$.
- The immature transforms to the mature pest with constant maturation rate a.
- The mature pest reproduces periodically and the birth occurs in pulses at an interval T at the time $t = mT$, $m = 1, 2, 3....$
- Let the pesticide be sprayed periodically after each birth pulse with a delay $\tau_2 = l_2 T$, l_2 being a constant lying between 0 and 1. The pesticide is ineffective against the immature pest. Considering $0 < \alpha < 1$ is the instantaneous killing efficiency of the pesticide with which it kills the mature pest. The impulsive conditions at $t = \tau_{m2} = (m-1)T + \tau_2$ are:
$$\left.\begin{aligned} x(\tau_{m2})^+ &= x(\tau_{m2}), \\ y(\tau_{m2})^+ &= (1-\alpha)y(\tau_{m2}), \end{aligned}\right\} t = \tau_{m2}.$$
- The pesticide has no residual effect.
- The mechanical control is applied periodically after each birth pulse with a delay $\tau_1 = l_1 T$, $0 < l_1 < 1$, where l_1 is a constant. The mechanical control is applied before chemical control, thereby $0 < \tau_1 < \tau_2 < 1$. Considering the constant harvesting effort $0 < E < 1$ is applied to capture immature pest only. The impulsive conditions at $t = \tau_{m1} = (m-1)T + \tau_1$ are:
$$\left.\begin{aligned} x(\tau_{m1})^+ &= (1-E)x(\tau_{m1}), \\ y(\tau_{m1})^+ &= y(\tau_{m1}), \end{aligned}\right\} t = \tau_{m1}.$$

Using these assumptions, the impulsive stage-structured pest control model with multiple pulses is written as:

$$\left.\begin{aligned}\frac{dx}{dt} &= -(d+a)x(t),\\ \frac{dy}{dt} &= ax(t) - dy(t),\end{aligned}\right\} t \neq \tau_{m1}, \quad t \neq \tau_{m2}, \quad t \neq mT, \tag{6.2.1}$$

$$\left.\begin{aligned}x(\tau_{m1})^+ &= (1-E)x(\tau_{m1}),\\ y(\tau_{m1})^+ &= y(\tau_{m1}),\end{aligned}\right\} t = \tau_{m_1}, \tag{6.2.2}$$

$$\left.\begin{aligned}x(\tau_{m2})^+ &= x(\tau_{m2}),\\ y(\tau_{m2})^+ &= (1-\alpha)y(\tau_{m2}),\end{aligned}\right\} t = \tau_{m_2}, \tag{6.2.3}$$

$$\left.\begin{aligned}x(mT)^+ &= x(mT) + B(N(mT))y(mT),\\ y(mT)^+ &= y(mT),\end{aligned}\right\} t = mT, \tag{6.2.4}$$

$$x(0) = x_0 > 0, y(0) = y_0 > 0. \tag{6.2.5}$$

The biomass of the immature and mature pest just after the m^{th} birth pulse are $x(mT)^+$ and $y(mT)^+$ respectively. All model parameters are assumed to be positive. The initial densities of the immature and mature pest are x_0 and y_0 respectively. Equations (6.2.2), (6.2.3) and (6.2.4) represent the asynchronous harvesting and pesticide spray with birth pulse at times $t = \tau_{m1}$, $t = \tau_{m2}$ and $t = mT$ respectively, T being the periodicity of pulses. The birth function $B(N(t))$ is considered of Ricker type.

The dynamics of the system (6.2.1) − (6.2.5) is defined on the set

$$\Re^2_+ \quad = \quad \{(x,y) \in \Re^2 \mid x \geq 0, y \geq 0\}.$$

6.3 Analysis of the Model

Let the immature and mature pest density at $t = (m-1)T$ be $x = x_{m-1}$ and $y = y_{m-1}$ respectively. The analytical solution of the differential equations (6.2.1) between the pulses $(m-1)T \leq t < \tau_{m1}$ can be written as:

$$\left.\begin{aligned}x(t) &= e^{-(a+d)(t-(m-1)T)}x_{m-1},\\ y(t) &= e^{-d(t-(m-1)T)}[y_{m-1} + (1 - e^{-a(t-(m-1)T)})x_{m-1}],\end{aligned}\right\}. \tag{6.3.1}$$

Similarly, the analytical solution of differential equations (6.2.1) with the impulsive condition (6.2.2) between the harvesting and chemical pulses (say $\tau_{m1} \leq t < \tau_{m2}$) is obtained as:

$$\left.\begin{aligned} x(t) &= (1-E)e^{-(a+d)(t-(m-1)T)}x_{m-1}, \\ y(t) &= [(1-Ee^{-a\tau_1}-(1-E)e^{-a(t-(m-1)T)})x_{m-1}+y_{m-1}]e^{-d(t-(m-1)T)}, \end{aligned}\right\}. \quad (6.3.2)$$

Further, solving the system (6.2.1) with the impulsive condition (6.2.3) after the chemical control pulses $\tau_{m2} \leq t < mT$, yields:

$$\left.\begin{aligned} x(t) &= (1-E)e^{-(a+d)(t-(m-1)T)}x_{m-1}, \\ y(t) &= e^{-d(t-(m-1)T)}[O_1+(1-E)\{e^{-a\tau_2}-e^{-a(t-(m-1)T)}\}x_{m-1}], \\ O_1 &= (1-\alpha)[\{1-Ee^{-a\tau_1}-(1-E)e^{-a\tau_2}\}x_{m-1}+y_{m-1}], \end{aligned}\right\}. \quad (6.3.3)$$

After the chemical pulses, apply impulsive condition (6.2.4) with (6.3.3), gives the map of the system (6.2.1) – (6.2.5) after each successive birth pulse.

$$\begin{aligned} x_m &= (1-E)e^{-(a+d)T}x_{m-1}+be^{-O_2}[O_2-(1-E)e^{-(d+a)T}x_{m-1}], \\ y_m &= O_2-(1-E)e^{-(d+a)T}x_{m-1}, \\ O_2 &= [(1-E)e^{-a\tau_2}x_{m-1}+O_1]e^{-dT}. \end{aligned} \quad (6.3.4)$$

The map (6.3.4) constitutes the difference equations. These equations describe the densities of the immature and mature pest at m^{th} pulse in terms of values at previous pulse. This is a stroboscopic sampling at the time when birth pulse occurs. For the Ricker Function, the dynamical behavior of the system (6.2.1) – (6.2.5) will be given by the dynamical behavior of the map (6.3.4) associated with the system (6.3.3).

It is observed that for positive initial conditions the solution (6.3.3) of the system (6.2.1) – (6.2.5) always exists and stay positive. Therefore, each x_m and y_m of the map (6.3.4) are positive.

Let R_0 be the intrinsic net reproductive number denoting the average number of offspring that an individual produces over the period of its lifetime. It is computed as:

$$R_0 = \frac{be^{-dT}(O_3-(1-E)e^{-aT})}{(1-(1-E)e^{-(d+a)T})(1-(1-\alpha)e^{-dT})} = \frac{b}{b_0}, \quad (6.3.5)$$

$$O_3 = [(1-E)e^{-a\tau_2}+(1-\alpha)(-Ee^{-a\tau_1}+1-(1-E)e^{-a\tau_2})].$$

Remark 6.3.1. For $0 < \tau_1 < 1$, $0 < \tau_2 < 1$, $0 < E < 1$ and $0 < \alpha < 1$, R_0 will be positive under the condition $O_3 - (1-E)e^{-aT} > 0$.

Two fixed points of the map (6.3.4) can be obtained as:

- There exists a unique pest-free fixed point $E_0 = (0, 0)$ without any parametric restriction.

- The non-trivial fixed point $E^* = (x^*, y^*)$ is obtained as:

$$\begin{aligned} x^* &= \frac{(1-(1-\alpha)e^{-dT})\log R_0}{(O_3-(1-\alpha)(1-E)e^{-(d+a)T})e^{-dT}}, \\ y^* &= \frac{(O_3-(1-E)e^{-aT})\log R_0}{(O_3-(1-\alpha)(1-E)e^{-(d+a)T})}. \end{aligned}$$

The necessary condition for the coexistence of immature and mature pest is $R_0 > 1$. The interior fixed point is feasible if the birth rate of the pest is more than a critical value b_0 which depends upon all model parameters.

Remark 6.3.2. The derivative of equilibrium mature pest density y^* with respect to τ_2 is obtained as:

$$\begin{aligned} \frac{dy^*}{d\tau_2} &= -\frac{a\alpha(1-E)^2e^{-a(\tau_2+T)}(1-(1-\alpha)e^{-dT+\theta})\log(R_0)}{(O_3-(1-\alpha)(1-E)e^{-(d+a)T}))^2} \\ &\quad -\frac{a\alpha(1-E)e^{-a\tau_2}}{(O_3-(1-\alpha)(1-E)e^{-(d+a)T})} < 0. \end{aligned}$$

The equilibrium density of mature pest is a decreasing function with respect to delay parameter τ_2. Accordingly, the mature pest density at equilibrium reduces with increase in time delay τ_2 of chemical control.

Similarly, it can be proved that the equilibrium density of immature pest is a monotonic function with respect to parameter τ_1.

The local stability analysis of the biological feasible fixed point is discussed in the next subsection.

6.3.1 Stability Analysis of the Fixed Points

Let $X = (x, y)$ be any arbitrary fixed point. The linearized system about the arbitrary fixed point $X = (x, y)$ is given as:

$$X_m = AX_{m-1}. \tag{6.3.6}$$

The coefficients of the matrix $A = (a_{ij})_{2\times 2}$ are evaluated as:

$$\left.\begin{aligned} a_{11} &= (1-E)e^{-(d+a)T} + be^{-dT-O_4e^{-dT}}[O_3 - (1-E)e^{-aT} \\ &\quad - \{O_4 - (1-E)e^{-aT}x\}O_3e^{-dT}], \\ a_{12} &= b(1-\alpha)e^{-dT-O_4e^{-dT}}[1 - \{O_4 - (1-E)e^{-aT}x\}e^{-dT}], \\ a_{21} &= (O_3 - (1-E)e^{-aT})e^{-dT}, \qquad a_{22} = (1-\alpha)e^{-dT}, \\ O_4 &= (\alpha(1-E)xe^{-a\tau_2} + (1-\alpha)\{(x+y) - Exe^{-a\tau_1}\}, \end{aligned}\right\}. \tag{6.3.7}$$

Theorem 6.3.1. *The pest-free fixed point $E_0 = (0,0)$ of the map (6.3.4) is locally asymptotically stable provided*

$$R_0 < 1. \tag{6.3.8}$$

Proof. Using (6.3.7), the linearized matrix $A_{E_0} = (a_{ij})_{2\times 2}$ is evaluated about the pest-free state $(0,0)$ as:

$$A_{E_0} = \begin{pmatrix} (1-E)e^{-(d+a)T} + be^{-dT}[O_3 - (1-E)e^{-aT}] & (b(1-\alpha)e^{-dT} \\ O_3 - (1-E)e^{-aT})e^{-dT} & (1-\alpha)e^{-dT} \end{pmatrix}. \tag{6.3.9}$$

The characteristic equation corresponding to (6.3.9) is:

$$\lambda^2 - e^{-dT}[(1-E)e^{-aT} + b[O_3 - (1-E)e^{-aT} + 1 - \alpha]\lambda + (1-E)(1-\alpha)e^{-(2d+a)T} = 0.$$

The eigenvalues are computed as:

$$\begin{aligned} \lambda_1 &= \frac{X_1e^{-dT} + e^{-dT}\sqrt{X_1^2 - 4(1-E)(1-\alpha)e^{-aT}}}{2}, \\ \lambda_2 &= \frac{X_1e^{-dT} - e^{-dT}\sqrt{X_1^2 - 4(1-E)(1-\alpha)e^{-aT}}}{2}, \\ X_1 &= (1-E)e^{-aT} + b[O_3 - (1-E)e^{-aT}] + (1-\alpha). \end{aligned}$$

The eigenvalues λ_1 and λ_2 will lie in the unit circle (i.e. $\mid \lambda_1 \mid < 1$ and $\mid \lambda_2 \mid < 1$) if

$$b < \frac{(1-(1-E)e^{-(d+a)T})(1-(1-\alpha)e^{-dT})}{e^{-dT}[O_3 - (1-E)e^{-aT}]} = b_0. \tag{6.3.10}$$

Using (6.3.5) and (6.3.10), the stability condition (6.3.8) for the pest-free state E_0 is obtained. □

Accordingly, the pest-free fixed point $(0,0)$ is locally asymptotically stable for $b \in (0, b_0)$. The trajectories in the neighborhood of $(0,0)$ tend to origin and pest population will be eradicated. Thus, the pest eradication is possible when $R_0 < 1$. When $R_0 > 1$, the pest-free state is unstable. Biologically, the pest will survive in future time. Hence, the pest will persist if $R_0 > 1$.

Remark 6.3.3. The first order derivative of R_0 with respect to killing rate α is found to be negative:

$$\begin{aligned}\frac{dR_0}{d\alpha} &= -be^{-dT}\frac{\{1-(1-E)e^{-a\tau_2}-Ee^{a\tau_1}\}}{(1-(1-\alpha)e^{-dT})(1-(1-E)e^{-(d+a)T})} \\ &\quad -be^{-dT}\frac{(O_3-(1-E)e^{-aT})e^{-dT}}{(1-(1-\alpha)e^{-dT})^2(1-(1-E)e^{-(d+a)T})} < 0.\end{aligned}$$

Accordingly, the killing (or poisoning) rateα reduces the threshold value R_0. Therefore, increase in the killing rate of mature pest α will be able to establish the pest-free state, once R_0 becomes less than unity.

Remark 6.3.4. The expression of R_0 involves harvesting effort E. The first order derivative with respect to E is obtained as:

$$\begin{aligned}\frac{dR_0}{dE} &= -be^{-dT}\frac{(1-\alpha)(e^{-a\tau_2}-e^{-a\tau_1})-e^{-a\tau_2}+e^{-aT}}{(1-(1-E)e^{-(d+a)T})(1-(1-\alpha)e^{-dT})} \\ &\quad -be^{-dT}\frac{(O_3-(1-E)e^{-aT})}{(1-(1-E)e^{-(d+a)T})^2(1-(1-\alpha)e^{-dT})} < 0.\end{aligned}$$

The threshold R_0 is monotonic decreasing function with respect to E. It can be concluded that still pest-free state can be obtained if the harvesting rate gets higher from critical value E_c provided $R_0 < 1$.

Remark 6.3.5. The pest-free fixed point of the map (6.3.4) become non-hyperbolic at $R_0 = 1$ and one of the eigenvalues becomes 1. Further, the map (6.3.4) admits transcritical bifurcation corresponding to the eigenvalue 1 if $R_0 = 1$. A threshold parametric value with respect to other parameter for transcritical bifurcation is:

$$\alpha = 1-\frac{be^{-dT}(1-E)e^{-a\tau_2}+(1-E)e^{-(d+a)T}-1}{e^{-dT}(1-(1-E)e^{-(d+a)T})-be^{-dT}(1-Ee^{-a\tau_1}-(1-E)e^{-a\tau_2})}.$$

Remark 6.3.6. When $R_0 > 1$, the non-trivial fixed point E^* of the map (6.3.4) exists in this case. This means that the pest population can not eradicate completely and may occur in a periodic manner.

Further, stability analysis for interior fixed point E^* is carried in the next section.

Theorem 6.3.2. *Let us denote*

$$\begin{aligned}C &= 2(O_3-(1-E)e^{-(d+a)T})(1+(1-E)e^{-2(d+a)T}), \\ F &= (1-(1-E)e^{-(d+a)T})(1-(1-\alpha))e^{-dT})(O_3+(1-E)e^{-(d+a)T}).\end{aligned}$$

The non-trivial fixed point $E^* = (x^*, y^*)$ *of the map* (6.3.4) *is locally asymptotically stable provided*

$$b_0 < b < b_0 exp(CF^{-1}) (= b_c). \tag{6.3.11}$$

Proof. Using (6.3.7), coefficients of the linearized matrix $A_{E^*} = (a_{ij})_{2\times 2}$ are evaluated about interior fixed point (x^*, y^*) as:

$$\left.\begin{aligned}
a_{11} &= (1-E)e^{-(d+a)T} + b\ exp(-dT - O_5e^{-dT})\ [O_3 - (1-E)e^{-aT} \\
&\quad - \{O_5 - (1-E)e^{-aT}x^*\}O_3e^{-dT}], \\
a_{12} &= b(1-\alpha)exp(-dT - O_5e^{-dT})[1 - \{O_5 - (1-E)e^{-aT}x^*\}e^{-dT}], \\
a_{21} &= (O_3 - (1-E)e^{-aT})e^{-dT}, \\
a_{22} &= (1-\alpha)e^{-dT}, \\
O_5 &= \alpha(1-E)x^*e^{-a\tau_2} + (1-\alpha)\{(x^*+y^*) - Ex^*e^{-a\tau_1}\},
\end{aligned}\right\}. \tag{6.3.12}$$

Accordingly, the trace Tr and determinant Det are computed as:

$$\begin{aligned}
Tr &= (1-E)e^{-(d+a)T} + b\ exp(-dT - O_5e^{-dT})\ [O_3 - (1-E)e^{-aT} \\
&\quad -\{O_5 - (1-E)e^{-aT}x^*\}O_3e^{-dT}] + (1-\alpha)e^{-dT}, \\
Det &= (1-\alpha)(1-E)e^{-(2d+a)T}[1 - b_0y^*].
\end{aligned}$$

It is easily seen that (1.4.11) and (1.4.13) are always satisfied. The Jury's condition (1.4.12), $1 + Tr + Det > 0$ if

$$R_0 < exp\left(\frac{2(O_3 - (1-E)e^{-(d+a)T})(1 + (1-E)e^{-2(d+a)T})}{(1-(1-E)e^{-(d+a)T})(1-(1-\alpha)e^{-dT})(O_3 + (1-E)e^{-(d+a)T})}\right). \tag{6.3.13}$$

The stability condition (6.3.11) is obtained from (6.3.13) and the existence condition $b_0 < b$. Hence, if $b \in (b_0, b_c)$ then the interior fixed point $E^* = (x^*, y^*)$ of the map (6.3.4) is locally asymptotically stable. □

Accordingly, when $b \in (b_0, b_c)$, the interior fixed point E^* of the map (6.3.4) is locally asymptotically stable. The trajectories of the system (6.2.1) − (6.2.5) tend to asymptotically stable period-1 solution $(x_e(t), y_e(t))$:

$$\begin{cases}
x_e(t) = e^{-(a+d)(t-(m-1)T)}x^*, & (m-1)T \le t < \tau_{m1}, \\
\quad = (1-E)e^{-(a+d)(t-mT)}x^*, & \tau_{m1} \le t < mT,
\end{cases} \tag{6.3.14}$$

$$\begin{cases} y_e(t) = e^{-d(t-(m-1)T)}[y^* + (1-e^{-a(t-(m-1)T)})x^*], \\ \qquad\qquad\qquad\qquad\qquad\qquad (m-1)T \le t < \tau_{m1}, \\ \qquad = [(1-Ee^{-a\tau_1} - (1-E)e^{-a(t-(m-1)T)})x^* + y^*]e^{-d(t-(m-1)T)}, \\ \qquad\qquad\qquad\qquad\qquad\qquad \tau_{m1} \le t < \tau_{m2}, \\ \qquad = [(1-E)\{e^{-a\tau_2} - e^{-a(t-mT)}\}x^* + (1-\alpha)O_6] \times e^{-d(t-mT)}, \\ \qquad\qquad\qquad\qquad\qquad\qquad \tau_{m2} \le t < mT, \\ O_6 = \{1 - Ee^{-a\tau_1} - (1-E)e^{-a\tau_2}\}x^* + y^*. \end{cases} \tag{6.3.15}$$

Remark 6.3.7. Since the interior fixed point E^* of the map (6.3.4) is locally stable, the period-1 solution (6.3.14) – (6.3.15) of the system (6.2.1) – (6.2.5) is locally stable in the range $b_0 < b < b_c$. This would mean that after the increase in the critical birth rate beyond b_0, the pest population will vary periodically.

Further, increasing the parameter value $b > b_c$, the interior fixed point E^* of the map (6.3.4) losses its stability and the map (6.3.4) may exhibit complex dynamics. This implies that the pest population may occur in regular/irregular periodic manner when birth rate increase beyond the critical value b_c. The complex dynamical behavior will be discussed later.

6.3.2 Bifurcation Analysis

The pest-eradication point $E_0 = (0, 0)$ of the map (6.3.4) becomes non-hyperbolic at $b = b_0$ as one of the eigenvalues becomes 1. Note that when $R_0 = 1$, then $E^* = (0, 0)$. It is observed that at $b = b_0$, the fixed points $E_0 = (0, 0)$ and $E^* = (x^*, y^*)$ exchange their stability.

Theorem 6.3.3. *The map* (6.3.4) *undergoes a transcritical bifurcation at* $b = b_0$.

Proof. Consider the map

$$\begin{pmatrix} x \\ y \end{pmatrix} \to \begin{pmatrix} (1-E)e^{-(a+d)T}x + be^{-O_4}[O_4 - (1-E)e^{-(d+a)T}x] \\ (O_4 - (1-E)e^{-(d+a)T}x \end{pmatrix}. \tag{6.3.16}$$

Let $x = u, y = v, b = b_1 + b_0$. The fixed point E_0 of the map (6.3.16) is transformed to (u, v). Now, the map (6.3.16) becomes:

$$\begin{pmatrix} u \\ v \end{pmatrix} \to \begin{pmatrix} (1-E)e^{-(a+d)T}u + be^{-O_7}[O_7 - (1-E)e^{-(d+a)T}u] \\ (O_7 - (1-E)e^{-(d+a)T}u \end{pmatrix}, \tag{6.3.17}$$

where, $O_7 = \alpha(1-E)ue^{-a\tau_2} + (1-\alpha)\{(1-E)(u+v) - Eue^{-a\tau_1}\}$. The map (6.3.17) can be rewritten as:

$$\begin{pmatrix} u \\ v \end{pmatrix} \to M \begin{pmatrix} u \\ v \end{pmatrix} + \begin{pmatrix} c_{11}u^2 + c_{12}uv + c_{13}v^2 + c_{14}b_1u + c_{15}b_1v \\ 0 \end{pmatrix}. \quad (6.3.18)$$

The coefficients of the matrix $M = m_{ij_{2\times 2}}$ and coefficients $c_{ij_{1\times 5}}$ are obtained as:

$$\begin{aligned}
m_{11} &= (1-E)e^{-(d+a)T} + b_0(O_3 - (1-E)e^{-aT})e^{-dT}, \quad m_{12} = b_0(1-\alpha)e^{-dT}, \\
m_{21} &= (O_3 - (1-E)e^{-aT})e^{-dT}, \quad m_{22} = (1-\alpha)e^{-dT}, \\
c_{11} &= -b_0e^{-2dT}(O_3^2 - O_3(1-\alpha)e^{-aT}), \quad c_{12} = b_0(1-\alpha)e^{-(a+2d)T}(2O_3 - (1-E)e^{-aT}), \\
c_{13} &= -b_0(1-\alpha)^2e^{-2dT}, \quad c_{14} = (O_3 - (1-E)e^{-aT})e^{-dT}, \quad c_{15} = (1-\alpha)e^{-dT}.
\end{aligned}$$

The eigenvalues of M are 1 and $(1-\alpha)(1-E)e^{-(a+2d)T}$.

The corresponding eigenvectors O_8 and O_9 are $\{o_8, 1\}^T$ and $\{o_9, 1\}^T$ respectively where $o_8 = \dfrac{1-(1-\alpha)e^{-dT+\theta}}{(O_3-(1-E)e^{-aT})e^{-dT+\theta}}$, $o_9 = \dfrac{(1-\alpha)((1-E)e^{-(d+a)T+\theta}-1)}{(O_3-(1-E)e^{-aT})e^{-dT+\theta}}$.
Consider the transformation

$$\begin{pmatrix} u \\ v \end{pmatrix} = J \begin{pmatrix} \bar{x} \\ \bar{y} \end{pmatrix}, \qquad J = (O_8 \;\; O_9). \quad (6.3.19)$$

Now, the map (6.3.18) can be written as:

$$\begin{pmatrix} \bar{x} \\ \bar{y} \end{pmatrix} \to \begin{pmatrix} 1 & 0 \\ 0 & (1-\alpha)(1-E)e^{-(a+2d)T} \end{pmatrix} \begin{pmatrix} \bar{x} \\ \bar{y} \end{pmatrix} + \begin{pmatrix} f_1(\bar{x}, \bar{y}, b_1) \\ f_2(\bar{x}, \bar{y}, b_1) \end{pmatrix} \quad (6.3.20)$$

$$\begin{aligned}
f_1(\bar{x}, \bar{y}, b_1) &= d_1b_1\bar{x} + d_2b_1\bar{y} + d_3\bar{x}\bar{y} + d_4\bar{x}^2 + d_5\bar{y}^2, \\
f_2(\bar{x}, \bar{y}, b_1) &= -f_1(\bar{x}, \bar{y}, b_1), \\
d_1 &= \left[c_{14}(1-(1-\alpha)e^{-dT})(O_3-(1-E)e^{-aT})^{-1}e^{dT} + c_{15}\right]\kappa^{-1}, \\
d_2 &= \left[c_{14}((1-\alpha)(1-E)e^{-(d+a)T}-1)(O_3-(1-E)e^{-aT})^{-1}e^{dT} + c_{15}\right]\kappa^{-1}, \\
d_3 &= \left[2c_{13} + 2c_{11}\frac{(1-(1-\alpha)e^{-dT})(1-\alpha)((1-E)e^{-(d+a)T-1})}{(O_3-(1-E)e^{-aT})^2e^{-2dT}}\kappa^{-1}\right. \\
&\quad \left. + c_{12}\frac{(1-2(1-\alpha)e^{-dT}) + (1-\alpha)(1-E)e^{-(d+a)T}}{(O_3-(1-E)e^{-aT})e^{-dT}}\right]\kappa^{-1}, \\
d_4 &= \left[c_{11}\left(\frac{(1-(1-\alpha)e^{-dT})}{(O_3-(1-E)e^{-aT})e^{-dT}}\right)^2 + c_{12}\frac{(1-(1-\alpha)e^{-dT})}{(O_3-(1-E)e^{-aT})e^{-dT}} + c_{13}\right]\kappa^{-1}, \\
d_5 &= [c_{13} + c_{11}\left(((1-\alpha)((1-E)e^{-(d+a)T}-1))(O_3-(1-E)e^{-aT})^{-2}e^{2dT}\right) \\
&\quad + c_{12}(1-\alpha)((1-E)e^{-(d+a)T}-1)(O_3-(1-E)e^{-aT})^{-1}e^{dT}]\kappa^{-1}, \\
\kappa &= (1-(1-\alpha)(1-E)e^{-(d+a)T})((O_3-(1-E)e^{-aT})e^{-dT})^{-1}.
\end{aligned}$$

The center manifold $w^c(0)$ for the map (6.3.16) can be represented as:

$$w^c(0) = \{(\bar{x}, \bar{y}, b_1) \in \Re^3 | \bar{y} = f(\bar{x}, b_1), f(0,0) = 0, Df(0,0) = 0\}.$$

Let $\bar{y} = f(\bar{x}, b_1) = B_0 b_1 + B_1 b_1 \bar{x} + B_2 \bar{x}^2 + O(|b_1|^2 + |b_1 \bar{x}^2| + |\bar{x}|^3)$. The coefficients in $\bar{y}$ can be computed as:

$$B_0 = 0, \quad B_1 = \frac{-d_1}{(1-(1-\alpha)(1-E)e^{-(a+2d)T})}, \quad B_2 = \frac{-d_4}{1-(1-\alpha)(1-E)e^{-(a+2d)T}}.$$

The map restricted to the center manifold is given by:

$$\begin{aligned} \bar{f} &: \bar{x} \to \bar{x} + f_1(\bar{x}, \bar{y}, b_1) = \bar{x} + d_1 b_1 \bar{x} + d_2 b_1 \bar{y} + d_3 \bar{x}\bar{y} + d_4 \bar{x}^2 + d_5 \bar{y}^2 \\ &= \bar{x} + d_1 b_1 \bar{x} + d_3 \frac{d_4}{(1-\alpha)(1-E)e^{-(a+2d)T} - 1} \bar{x}^3 + d_4 \bar{x}^2 + O(|b_1|^2 + |b_1 \bar{x}^2| + |\bar{x}|^4). \end{aligned}$$

Using Theorem 1.4.3, it can be calculated that

$$\frac{\partial \bar{f}(0,0)}{\partial b_1} = 0, \frac{\partial^2 \bar{f}(0,0)}{\partial x \partial b_1} = d_1 \neq 0, \frac{\partial^2 \bar{f}(0,0)}{\partial^2 x} = 2d_4 \neq 0.$$

Note that, all the conditions of the Theorem 1.4.3 are satisfied at $(\bar{x}, b_1) = (0,0)$. Further, E^* becomes E_0 as $b = b_0$. Hence the map (6.3.4) undergoes to transcritical bifurcation between $E_0 = (0,0)$ and $E^* = (x^*, y^*)$ at $b = b_0$. □

The following theorem characterizes the flip bifurcation at $b = b_c$.

Theorem 6.3.4. *The map* (6.3.4) *undergoes a flip bifurcation about* $E^* = (x^*, y^*)$ *at* $b = b_c$. *Moreover, if* $\bar{a} > 0$*(resp.* $\bar{a} < 0$*), then period−2 solutions that bifurcate from this fixed point are stable (resp. unstable).*

Proof. Proof is omitted here. It is on the same lines as in previous chapters. □

There exist a series of bifurcations that lead to chaotic dynamic when b increases from b_c. This will be explored through numerical simulation in the next section.

6.4 Numerical Simulations

In the previous sections, birth rate parameter is considered as the control parameters to diagnose chaotic behavior. To detect chaos, bifurcation diagrams, Lyapunov exponents and Lyapunov dimension have been analyzed numerically. Extensive numerical

simulations are carried out to illustrate the analytical findings. Consider the following parameter set

$$a = 0.4, d = 0.2, E = 0.4, \alpha = 0.6, \tau_1 = 0.21, \tau_2 = 0.6. \tag{6.4.1}$$

Bifurcation diagram is plotted with respect to control parameter b for the fixed parameters (6.4.1). The maxima of the pest population is plotted as a function of birth rate parameter b. The bifurcation diagram in Fig. 6.1 exhibits variety of dynamical behaviors of the map (6.3.4) as the parameter b changes.

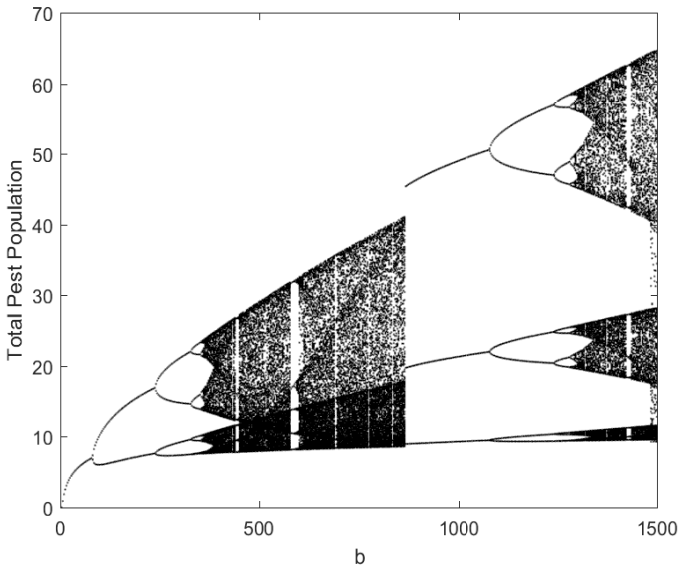

Figure 6.1: Bifurcation diagram of the map (6.3.4) for total pest population with respect to parameter b.

Table 6.1: Study of the map (6.3.4) for the data set (6.4.1) about E_0.

Parameter varied	Analytical behavior	Numerical behavior
$b \in (0, 4.1)$	E_0 stable	Stable Pest-free State
$b = 4.1 = b_0$	E_0 non-hyperbolic	Transcritical Bifucartion
$b > 4.1$	E_0 unstable E^* exists	Pest will Persist Periodic/Chaotic behavior

In Fig. 6.2(a), magnified part of the Fig. 6.1 has been drawn between $0 < b \leq 10$.

The pest will die out for $b < 4.1$ ($\approx b_0$), confirming the result obtained in Theorem 6.3.1. The Fig. 6.2(a) shows that birth rate should be small to eliminate the pest. The system dynamics about the trivial fixed point can be summarized in Table 6.1.

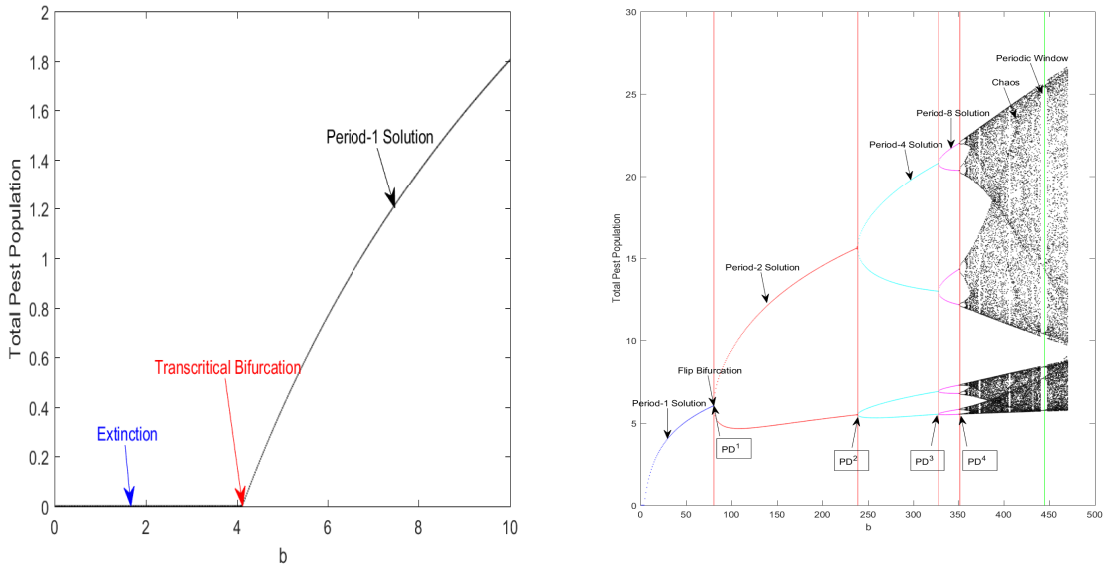

(a) **(b)**

Figure 6.2: (a) Transcritical Bifurcation (b) Period-doubling phenomena for the data set (6.4.1).

Table 6.2: Behavior of impulsive system about interior fixed points.

Parameter varied	Analytical Behavior	Numerical behavior	
$4.1 < b < 79.105$	E^* stable	Period-1 Solution	Blue Curve
$b = 79.105 = b_c$	E^* non-hyperbolic	Flip Bifurcation	Red Line (PD^1)
$3.1226 < b < 236.5$	E^* unstable	Period-2 solution	Red Curve
$b = 236.5$		Second Period-doubling	Red Line (PD^2)
$236.5 < b < 327.5$		Period-4 solution	Cyan Color
$b = 327.5$		Third Period-doubling	Red Line (PD^3)
$327.5 < b < 351.15$		Period-8 solution	Magenta Color
$b = 351.15$		Fourth Period-doubling	Red Line (PD^4)
$357.42 < b < 470$		Chaotic solution	Black Color
$440 < b < 447.9$		Periodic Window	Green Line

Fig. 6.2(b) is the blown up bifurcation diagram of Fig. 6.1 in the range $0 < b \leq 470$, shows successive period doubling leading to chaos. The region of stability, periodic and chaotic behavior are clearly visible. The system exhibits complex dynamical behavior, including chaos. Very narrow periodic window can be observed in this figure. The dynamics of the system is further explored by different values of b while other parameter are fixed. The observations are summarized in the Table 6.2.

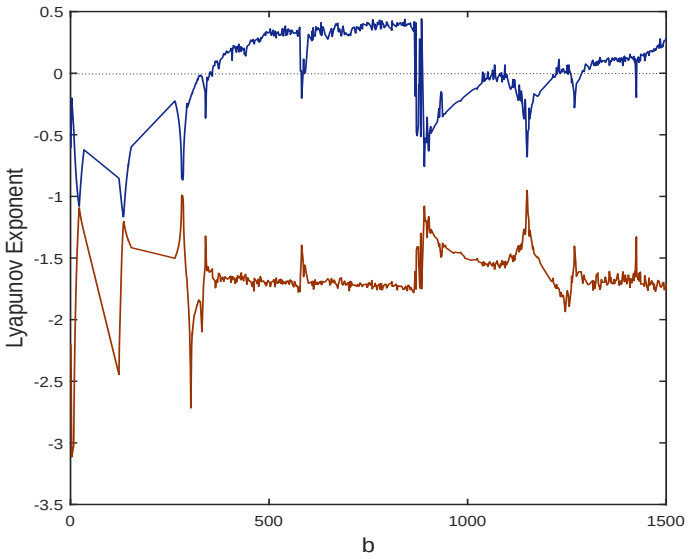

Figure 6.3: Lyapunov exponents of the map (6.3.4) with respect to b.

Table 6.3: Behavior of impulsive system about fixed points.

Parameter varied	Parameter Value	Lyapunov exponent	D_L	Dynamical behavior
$b \in (4.1, 351.15]$	$b = 200$	LE_1=-0.438503997, LE_2=-1.452704796	0	Stable Periodic Solution
$b \in (351.15, 357.42]$	$b = 357.42$	LE_1=0, LE_2=-1.619674207	1	Quasi-Periodic Solution/Torus
$b \in (357.42, 868.59]$	$b = 420$	LE_1=0.207510507, LE_2=-1.667962525	1.1244	Strange attractor/ Chaos

The Lyapunov exponents with respect to parameter b have been shown in Fig. 6.3. The Blue color shows the largest Lyapunov exponent (say LE_1) and red color shows the smallest Lyapunov exponent(say LE_2). It can be easily observed that LE_2 is always negative. Further, LE_1 is zero for some values of b. Therefore, the map (6.3.4) is dissipative. The results for system dynamics are summarized in Table 6.3. For $b = 420$, the sum of two Lyapunov exponents is negative (say $LE_1 + LE_2 = 0.207510507 - 1.667962525 = -1.4604552018 < 0$). The Lyapunov dimension D_L for $b = 420$ is $0 < D_L = 1.1244 < 2$ and there exists strange attractor.

Fig. 6.4 shows the variation of R_0 with impulsive period T for $b = 6$. E_0 is stable in the range $0 < T < 0.388 \cup 4.24 < T < 1$. The non-monotonic behavior of R_0 with respect to pulse period T is observed. As the value of T increases, R_0 first increases and attains a peak at critical value $T = 1.44$ and then it decreases with increase in T. It can be easily observed that pest will survive in the domain $T \in [0.388, 4.24]$.

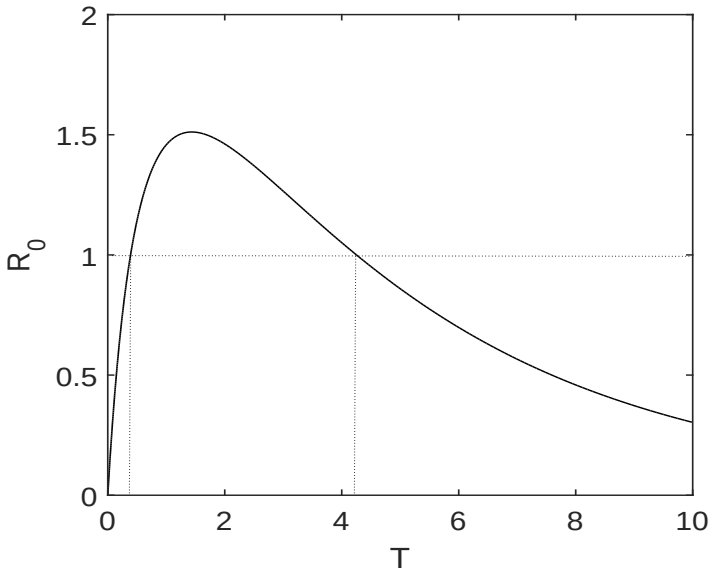

Figure 6.4: Plot of R_0 with respect to parameter T.

The bifurcation diagram is plotted with respect to the maturation rate a with $b = 350$ in the Fig. 6.5. With the increase in maturation rate, the periodic solution settles down to a chaotic solution. In this case too, a number of periodic-doubling cascades can be observed. Very narrow and wide periodic windows will appear in this figure. A Period-5 period window will appear at $a = 0.79$.

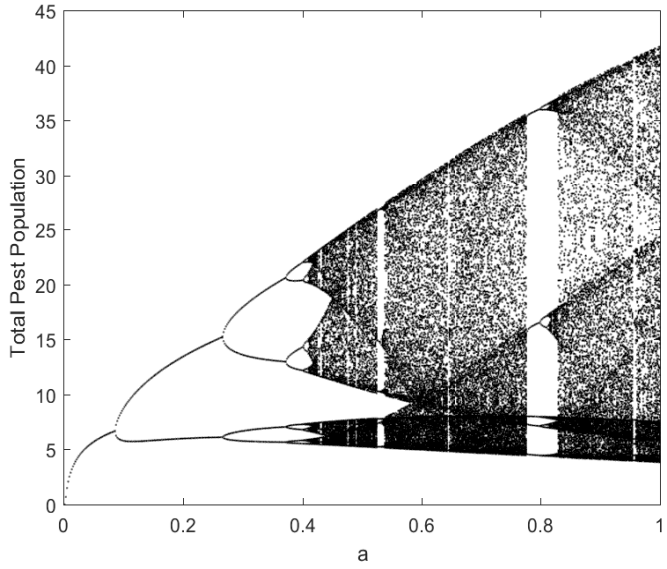

Figure 6.5: Bifurcation diagram of the map (6.3.4) for total pest population with respect to the parameter a.

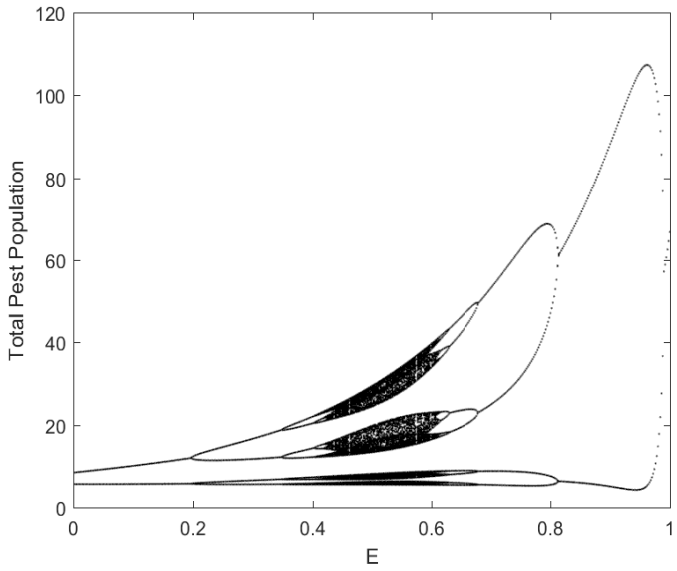

Figure 6.6: Bifurcation diagram of the map (6.3.4) for total pest population with respect to the parameter E.

The bifurcation diagram has been plotted with respect to E in Fig. 6.6 taking $b = 350$ while other parameters are fixed as in data set (6.4.1). For this figure, it can

be easily observed that complexity increases with increase of parameter E. A period doubling and period halving cascade can be seen with the chaotic region in between. Initially, the stable periodic solution becomes unstable and there exist complex behavior after a critical value of E. Further, the complex solutions become stable after a certain choice of parameter E. The chaotic behavior will occur for $E \in (0.405, 0.615)$.

Similarly, bifurcation diagram has been plotted with respect to the killing rates α in the Fig. 6.7. Initially, periodic behavior can be observed. As the parameter, α increase, the periodic solution will lead to chaotic behavior. Further, the increasing killing rate due to chemical spray, the chaotic behavior will settle down to periodic behavior. Also, there exists period-doubling and period-halving behavior with the occurrence of the chaotic region in between. Very narrow and wide periodic windows can also be observed.

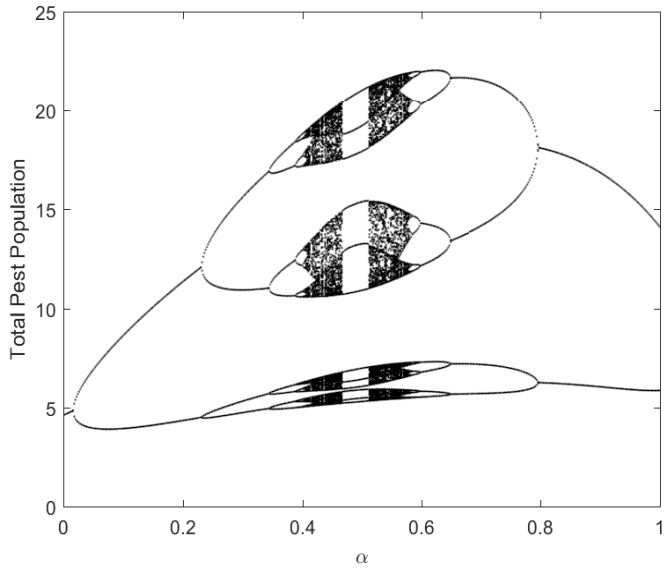

Figure 6.7: Bifurcation diagram of the map (6.3.4) for total pest population with respect to the parameter α.

For the data set (6.4.1), the bifurcation diagram has been plotted with respect to the parameter τ_1 with $b = 350$ in Fig. 6.8. It can be observed that overall complexity increases with increase in parameter τ_1. Initially, the solution settles down to periodic behavior which required eliminating pest. Further, with an increase in pesticide spray timing, chaotic behavior will occur. In this case too, a number of periodic doubling

cascades can be observed.

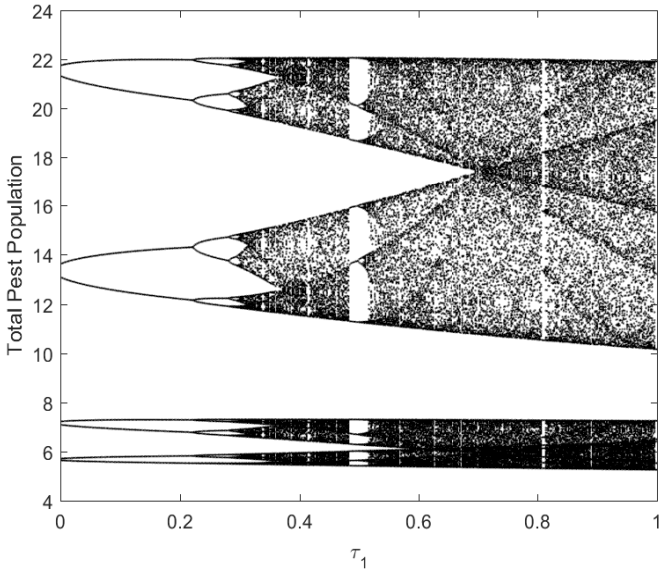

Figure 6.8: Bifurcation diagram of the map (6.3.4) for total pest population with respect to to the parameter τ_1.

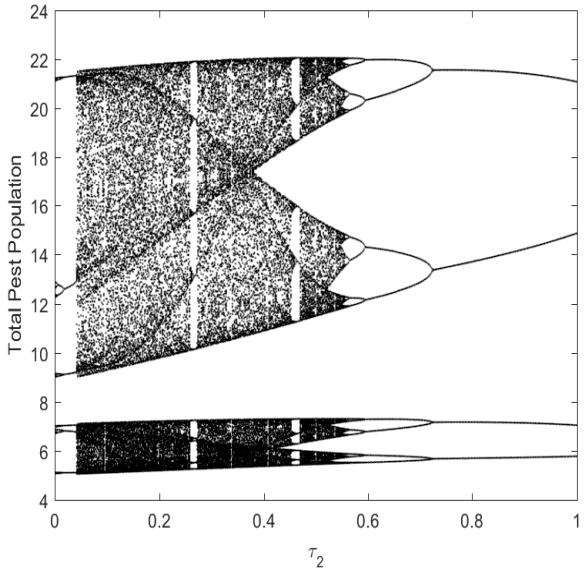

Figure 6.9: Bifurcation diagram of the map (6.3.4) for total pest population with respect to the parameter τ_2.

The bifurcation diagram has been plotted with the time of impulsive harvesting

in Fig. 6.9 for $b = 350$. Here, the chaotic regions are predominant and as τ_2 increase, the chaotic solution will settle down to periodic behavior. Various periodic windows can be observed in Fig. 6.9. The figure shows that for higher values of delay in harvesting reduces the complexity of the system. Also, in this case too, a number of periodic halving cascades can be observed.

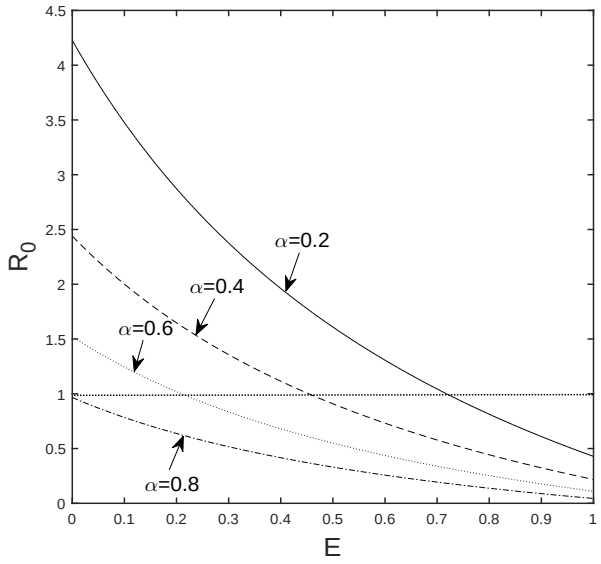

Figure 6.10: Plot of R_0 with respect to parameter E.

The Fig. 6.10 is drawn to show the variation of R_0 with respect to harvesting rate E in the range $0 < E < 1$ and for fixed values of $\alpha = 0.2(2)0.8$ with $b = 3$. For $\alpha = 0.8$, R_0 remains less than one for all values of E. Accordingly, the pest-free state is stable and pest eradication will be possible. For $\alpha = 0.6$, the pest-free state E_0 stabilizes when the harvesting rate parameter E exceeds beyond 0.21. However, for $\alpha = 0.4$, the pest-free state remains stable for $E > 0.45375$. Accordingly, sufficient amount of harvesting rate and killing efficiency rate are needed to achieve the pest-free state.

6.5 Discussion

The impulsive pest control model has been formulated and analyzed for studying the effects of chemical and mechanical control. The threshold R_0 is obtained which is the

basic reproduction number for the pest-free state. When the threshold R_0 is less than unity, the local stability of the pest-free state has been established. Accordingly, pest eradication can be possible. The combined effects of chemical control and mechanical control are required to control the pest. These effects enhance the stability of pest-free state and interior fixed point.

Numerical simulations have been carried out for the resulting system reveal that the impulsive system can have a variety of complex dynamical properties including complex dynamical behavior. The bifurcation diagram with respect to birth rate parameter shows that for $b < b_0$ pest can be eradicated successfully. It can be concluded that for $b > b_c$, the pest will oscillate in regular/irregular periodic manner for the interior fixed point E^* which shows the unstable behavior of the interior fixed point. Further, Lyapunov exponent and Lyapunov dimension are obtained confirming the existence of chaos.

Chapter 7

A Stage-structured Pest Control Model with Birth Pulse, Impulsive Harvesting, and Pesticide that have Residual Effects

7.1 Introduction

The study in chapter 5 and chapter 6 incorporated instantaneous effect of the pesticide on the pest. However, chemical pesticides may have long-term residual as well as delayed effects. Delayed response occurs due to repeated exposure to pesticides over long time [228]. Due to a delayed response, the adverse effects may not appear immediately after the pesticide spray. Such a lack of immediate responses by pests to a pesticide application means that the pest density increase for a time even after a pesticide application has been made [205, 209]. This delayed response is important from the pest control point of view. Some pest does not succumb after being pesticide spray for several weeks, months or years. For example, Mycopesticide Metarhizium Acridum takes 1-4 weeks to kill pest population of grasshoppers and locusts [114, 195].

An IPM strategy must consider the residual effect and delayed response to achieve successful pest control. It can be described by continuous or piecewise-continuous periodic functions which affect the growth rate of the pest [172, 174]. Tang et al.

developed an impulsive pest-natural enemy model using the residual effect of pesticides on pest and threshold dynamical analysis has been discussed in different cases [221]. An IPM model for pest control has been discussed incorporating delayed response to the pesticide application [126]. The IPM model with dose-response effect with a delayed response of pesticides has been discussed by [103].

In this chapter, an impulsive stage-structured pest control model is proposed to incorporate IPM strategies (chemical and mechanical control). The model incorporates residual effects and delayed response of pesticide. The mechanical control is applied impulsively. The effects of delayed response and residual effect of pesticide on pest and the threshold condition have also been addressed. Using the center manifold theorem, bifurcation analysis has been performed.

7.2 Model Formulation

In this section, an impulsive stage-structure pest control with the birth pulse and integrated pest management is discussed using asynchronous pulses. However, in this chapter, the timing of mechanical control and birth pulse are not synchronized. Further to formulate the model following assumption has been made:

- The mortality rates of the immature and mature pest are assumed to be constant d.
- The maturation rate of immature pest is constant a.
- Birth pulses take place periodically at $t = mT$, $m = 1, 2, 3...$ where T being the periodicity of the pulses. The birth function $B(N(t))$ is considered of Ricker type. Accordingly,

$$\left.\begin{aligned} x(mT)^+ &= x(mT) + B(N(mT))y(mT), \\ y(mT)^+ &= y(mT), \end{aligned}\right\} t = mT. \tag{7.2.1}$$

- The pest population is controlled using chemical and mechanical methods applied periodically with period T.
- The instantaneous effects of the pesticides are ignored.

- Its residual effect with delayed response on immature and mature pest can be described by the kill functions [221] $k_1(t)$ and $k_2(t)$ respectively. Let m_1 be the killing efficiency, a_1 be its decay rate and $c_1 > a_1$ be the delayed response rate. The kill functions $k_1(t)$ and $k_2(t)$ between two successive pulses can be written as:

$$\left.\begin{aligned} k_1(t) &= m_1(e^{-a_1(t-(m-1)T)} - e^{-c_1(t-(m-1)T)})x(t), \\ k_2(t) &= m_1(e^{-a_1(t-(m-1)T)} - e^{-c_1(t-(m-1)T)})y(t), \end{aligned}\right\} (m-1)T < t < mT. \tag{7.2.2}$$

- The mechanical control (harvesting effort) is applied periodically after each birth pulse with a delay $\tau_3 = l_3 T$, l_3 being a constant lying between 0 and 1. The immature and mature pest are harvested with constant harvesting rates E_1 and E_2, $0 < E_1, E_2 < 1$ respectively. The impulsive conditions at $\tau_m = (m-1)T + \tau_3$ are:

$$\left.\begin{aligned} x(\tau_m)^+ &= (1-E_1)x(\tau_m), \\ y(\tau_m)^+ &= (1-E_2)y(\tau_m), \end{aligned}\right\} t = \tau_m. \tag{7.2.3}$$

Using these assumptions, the dynamics of impulsive system incorporating residual effect with delayed response of pesticides (7.2.2), harvesting (7.2.3) and birth pulses (7.2.1) is written as:

$$\left.\begin{aligned} \frac{dx}{dt} &= -dx(t) - ax(t) - k_1(t), \\ \frac{dy}{dt} &= ax(t) - dy(t) - k_2(t), \end{aligned}\right\} t \neq \tau_m T, t \neq mT, \tag{7.2.4}$$

$$\left.\begin{aligned} x(\tau_m)^+ &= (1-E_1)x(\tau_m), \\ y(\tau_m)^+ &= (1-E_2)y(\tau_m), \end{aligned}\right\} t = \tau_m, \tag{7.2.5}$$

$$\left.\begin{aligned} x(mT)^+ &= x(mT) + B(N(mT))y(mT), \\ y(mT)^+ &= y(mT), \end{aligned}\right\} t = mT, \tag{7.2.6}$$

$$x(0) = x_0 > 0, y(0) = y_0 > 0. \tag{7.2.7}$$

All model parameters are assumed to be constant and positive. Here, $x(mT)^+$ and $y(mT)^+$ be the biomass of the immature and mature pest after the m^{th} birth pulse.

All parameters of the model are assumed to be positive. Let x_0 and y_0 be the initial densities of immature and mature pest respectively. Equations (7.2.5) and (7.2.6) represent the asynchronous harvesting with birth pulse at times $t = \tau_m$ and $t = mT$. The dynamics of stage-structured impulsive pest control system (7.2.4)-(7.2.7) is defined on the set:

$$\Re^2_+ = \{(x, y) \in \Re^2 \mid x \geq 0, y \geq 0\}.$$

7.3 Model Analysis

In the next subsection, the stroboscopic map is described which is used as a tool to discuss the dynamics of the system (7.2.4)-(7.2.7).

7.3.1 Stroboscopic Map

Let, the immature and mature pest densities be $x = x_{m-1}$ and $y = y_{m-1}$ at $t = (m-1)T$ respectively. The analytical solution of the differential equations (7.2.4) before mechanical control $(m-1)T \leq t < \tau_m$ is obtained as:

$$\begin{aligned} x(t) &= x_{m-1}e^{-(a+d)(t-(m-1)T)+\phi}, \\ y(t) &= e^{-d(t-(m-1)T)+\phi}[y_{m-1} + x_{m-1}(1 - e^{-a(t-(m-1)T)})], \qquad (m-1)T \leq t < \tau_m, \\ \phi &= m_1\left(\frac{e^{-a_1(t-(m-1)T)} - 1}{a_1} - \frac{e^{-c_1(t-(m-1)T)} - 1}{c_1}\right). \end{aligned}$$

Furthermore, the analytical solution of differential equations (7.2.4) with the impulsive conditions (7.2.5) between the pulses $\tau_m \leq t < mT$ is obtained as:

$$\begin{aligned} x(t) &= (1 - E_1)x_{m-1}e^{-(a+d)(t-(m-1)T)+\phi}, \\ y(t) &= [C_1x_{m-1} + (1 - E_2)y_{m-1}]e^{-d(t-(m-1)T)+\phi}, \qquad \tau_m \leq t < mT, \\ C_1 &= (E_2 - E_1)e^{-a\tau_3} + (1 - E_2) - (1 - E_1)e^{-a(t-(m-1)T)}. \end{aligned} \tag{7.3.1}$$

After the mechanical control, the solution (7.3.1) of the system (7.2.4)-(7.2.7) at the initial point (x_{m-1}, y_{m-1}) jumps to the point (x_m, y_m) with the effect of impulsive

conditions (7.2.6). Now the map after each successive birth pulse at $t = mT$ is:

$$\begin{aligned} x_m &= (1-E_1)x_{m-1}e^{-(a+d)T+\theta} + bexp[-(Cx_{m-1}+(1-E_2)y_{m-1})e^{-dT+\theta}] \\ &\quad \times[(Cx_{m-1}+(1-E_2)y_{m-1})e^{-dT+\theta}], \qquad (7.3.2) \\ y_m &= (Cx_{m-1}+(1-E_2)y_{m-1})e^{-dT+\theta}, \\ \theta &= m_1\left(\frac{(e^{-a_1T}-1)}{a_1} - \frac{(e^{-c_1T}-1)}{c_1}\right) < 0, \\ C &= (E_2-E_1)e^{-a\tau_3} + (1-E_2) - (1-E_1)e^{-aT}. \end{aligned}$$

The system (7.3.2) constitutes the difference equations. These equations describe the numbers of the immature and mature pest at m^{th} pulse in terms of values at previous pulse. This is stroboscopic sampling at the time when birth pulse occurs. For the Ricker Function, the dynamical behavior of the system (7.2.4)-(7.2.7) will be given by the dynamical behavior of the system (7.3.2) coupled with system (7.3.1).

7.3.2 Basic Reproduction Number

Let R_0 be the intrinsic net reproductive number denoting the average number of offspring that an individual produces over the period of its lifetime. Define

$$b_0 = \frac{(1-(1-E_1)e^{-(d+a)T+\theta})(1-(1-E_2)e^{-dT+\theta})}{e^{-dT+\theta}(A-(1-E_1)e^{-aT})}, \qquad (7.3.3)$$

$$R_0 = bb_0^{-1}, \qquad (7.3.4)$$

$$A = (E_2-E_1)e^{-a\tau_3} + (1-E_2).$$

Remark 7.3.1. R_0 is positive whenever $A-(1-E_1)e^{-aT} > 0$.

Remark 7.3.2. In the absence of delayed response, $\theta = m_1\left(\frac{(e^{-a_1T}-1)}{a_1}\right) = \theta_0$,

$$R_0^R = \frac{be^{-dT+\theta_0}(A-(1-E_1)e^{-aT})}{(1-(1-E_1)e^{-(d+a)T+\theta_0})(1-(1-E_2)e^{-dT+\theta_0})}.$$

When only the decay rate of residual pesticide is considered then the threshold R_0 reduces to R_0^R. Observe that, $R_0 < R_0^R$. Therefore, inclusion of delayed response of residual pesticides is more effective to reduce the threshold value.

7.3.3 Existence of Fixed Points

Two fixed points are obtained for the map (7.3.2):

1. The pest-free state $E_0 = (0, 0)$ exists for all set of parameters.

2. The expressions for the non-trivial fixed point $E^* = (x^*, y^*)$ are obtained as:

$$\begin{aligned} x^* &= \frac{(1-(1-E_2)e^{-dT+\theta})\log(R_0)}{e^{-dT+\theta}(A-(1-E_2)(1-E_1)e^{-(d+a)T+\theta})}, \\ y^* &= \frac{(A-(1-E_1)e^{-aT})\log(R_0)}{(A-(1-E_2)(1-E_1)e^{-(d+a)T+\theta})}. \end{aligned}$$

Introducing $b > b_0$, the existence condition for E^* becomes

$$R_0 > 1. \tag{7.3.5}$$

Remark 7.3.3. For,

$$\tau_{3c} = \frac{1}{a}\ln\left[\frac{be^{-dT+\theta}(E_2-E_1)}{(1-(1-E_1)e^{-(d+a)T+\theta})(1-(1-E_2)e^{-dT+\theta})+be^{-dT+\theta}[(1-E_1)e^{-aT}-1+E_2]}\right].$$

the existence condition for E^* is $\tau_3 < \tau_{3c}$. Thus, for $R_0 > 1$, there is the critical value for delay in harvesting over which pest will persist.

7.4 Stability Analysis about Fixed Points

Now for the stability analysis, the linearized matrix A for the map (7.3.2) about any arbitrary fixed point (x, y) is computed as:

$$A = \begin{pmatrix} a_{11} & a_{12} \\ a_{21} & a_{22} \end{pmatrix}.$$

The coefficients of the matrix $A = (a_{ij})_{2\times 2}$ are evaluated as :

$$\begin{aligned} a_{11} &= (1-E_1)e^{-(d+a)T+\theta} + bexp[-dT+\theta-(Ax+(1-E_2)y)e^{-dT+\theta}] \\ &\quad \times(C-(Cx+(1-E_2)y)Ae^{-dT+\theta}), \qquad (7.4.1) \\ a_{12} &= b(1-E_2)exp[-dT+\theta-(Ax+(1-E_2)y)e^{-dT+\theta}](1-((1-E_2)y+Cx)e^{-dT+\theta}), \\ a_{21} &= (A-(1-E_1)e^{-aT})e^{-dT+\theta}, \quad a_{22} = 1-E_2)e^{-dT+\theta}. \end{aligned}$$

7.4.1 Local Stability Analysis of Pest-free State (E_0)

For the stability of pest-free state, the following theorem is established:

Theorem 7.4.1. *The pest- free state $E_0 = (0, 0)$ is locally asymptotically stable for*

$$R_0 < 1. \tag{7.4.2}$$

Proof. Using (7.4.1), the coefficients of the linearized matrix A_{E_0} at the pest-free fixed point are evaluated as:

$$\begin{aligned} a_{11} &= (1-E_1)e^{-(d+a)T+\theta} + bCe^{-dT+\theta}, \qquad a_{21} = Ce^{-dT+\theta}, \\ a_{12} &= b(1-E_2)e^{-dT+\theta}, \qquad a_{22} = (1-E_2)e^{-dT+\theta}. \end{aligned}$$

Accordingly, the trace Tr and determinant Det are computed as:

$$\begin{aligned} Tr &= (1-E_1)e^{-(d+a)T+\theta} + bCe^{-dT+\theta} + (1-E_2)e^{-dT+\theta}, \\ Det &= (1-E_1)(1-E_2)e^{-(2d+a)T+2\theta}. \end{aligned}$$

Note that, the Jury's conditions (1.4.12) and (1.4.13) are always satisfied:

$$\begin{aligned} 1+Tr+Det &= 1+(1-E_1)e^{-(d+a)T+\theta} + bCe^{-dT+\theta} + (1-E_2)e^{-dT+\theta} \\ &\quad +(1-E_1)(1-E_2)e^{-(2d+a)T+2\theta} > 0, \\ 1-Det &= 1-(1-E_1)(1-E_2)e^{-(2d+a)T+2\theta} > 0. \end{aligned}$$

The expression $1 - Tr + Det$ simplifies to:

$$\begin{aligned} 1-Tr+Det &= 1-(1-E_1)e^{-(d+a)T+\theta} - be^{-dT+\theta}[(1-E_2) + (E_2-E_1)e^{-alT} \\ &\quad -(1-E_1)e^{-aT}] + (1-E_2)e^{-dT+\theta} + (1-E_1)(1-E_2)e^{-(2d+a)T+2\theta} \\ &= (1-(1-\beta)e^{-(d+a)T+\theta})(1-(1-E_2)e^{-dT+\theta}) \\ &\quad -b[(1-E_2)e^{-dT+\theta} + (E_2-E_1)e^{-(dT+a\tau_3)+\theta} - (1-E_1)e^{-(d+a)T+\theta}]. \end{aligned}$$

Accordingly, the Jury's condition (1.4.11), that is $1 - Tr + Det > 0$ gives:

$$(1-(1-E_1)e^{-(d+a)T+\theta})(1-(1-E_2)e^{-dT+\theta}) > be^{-dT+\theta}[A-(1-E_1)e^{-aT}],$$

i.e.

$$b < \frac{(1-(1-E_1)e^{-(d+a)T+\theta})(1-(1-E_2)e^{-dT+\theta})}{e^{-dT+\theta}((1-E_2)+(E_2-\beta)e^{-a\tau_3}-(1-E_1)e^{-aT})} = b_0. \tag{7.4.3}$$

Using (7.3.4) and (7.4.3), the stability condition (7.4.2) is obtained. □

Accordingly, the pest-free state is locally asymptotically stable for $b \in (0, b_0)$. When $R_0 < 1$, all the eigenvalues will lie in unit circle and therefore the pest eradication is possible. The trajectories in the neighborhood of $(0, 0)$ tend to origin.

When $R_0 > 1$, then one eigenvalue lies outside the unit circle provided

$$b > \frac{(1-(1-E_1)e^{-(d+a)T+\theta})(1-(1-E_2)e^{-dT+\theta})}{e^{-dT+\theta}((1-E_2)+(E_2-\beta)e^{-a\tau_3}-(1-E_1)e^{-aT})} = b_0. \tag{7.4.4}$$

Thus, for $R_0 > 1$, there is a critical level for birth rate over which pest will persist and the pest-free state E_0 will be unstable. This means that the birth rate b is the crucial parameter that affects the dynamics of pest-free state.

Remark 7.4.1. When threshold R_0 is independent of delayed response as well as residual effect, i.e. $m_1 = 0$, $\theta = 0$, the threshold condition is obtained as:

$$R_0^D = \frac{be^{-dT}((E_2-E_1)e^{-a\tau_3}+(1-E_2)-(1-E_1)e^{-aT})}{(1-(1-E_1)e^{-(d+a)T})(1-(1-E_2)e^{-dT})}. \tag{7.4.5}$$

In the absence of residual effect, it can be observed that $R_0 < R_0^D$. If single tactic (only mechanical control) will be used, the threshold value will increase, which is not effective for pest control. Therefore, inclusion of residual effects (combination of two strategies) may transfer unstable pest-free state to a stable state.

The pest-free state E_0 is stable if $R_0 < 1$. Since E_0 is only fixed point and it is locally stable if $R_0 < 1$. It is possible that it may be globally stable. The next theorem proves its global stability.

7.4.2 Global Stability Analysis about Pest-free State

Theorem 7.4.2. *The locally asymptotically stable pest-free point E_0 is globally asymptotically stable in the interior of positive quadrant of $x - y$ plane for the map* (7.3.2) *if* $R_0 < 1$.

Proof. Consider the positive definite function

$$V_1(x_m, y_m) = x_m + y_m.$$

Now, computation of ΔV_1 and its simplification gives

$$\begin{aligned}
\Delta V_1(x_m, y_m) &= f(x_m, y_m) + g(x_m, y_m) - x_m - y_m \\
&= (1-E_1)e^{-(d+a)T+\theta}x_m + be^{-dT+\theta}[(E_2-E_1)e^{-a\tau_3}x_m + (1-E_2)y_m \\
&\quad +(1-E_2)x_m - (1-E_1)e^{-aT}x_m]exp[-e^{-dT+\theta}(Ax_m - (1-E_2)y_m)] \\
&\quad +[Ax_m + (1-E_2)y_m - (1-E_1)e^{-aT}x_m]e^{-dT+\theta} - x_m - y_m \\
&\leq [\{(1-E_1)e^{-aT} + b\{A-(1-E_1)e^{-aT}\} + (1-E_1)e^{-aT} + (1-E_2) \\
&\quad -(E_2-E_1)e^{-a\tau_3}\}e^{-dT+\theta} - 1]x_m + [(1-E_2)\{b+1\}e^{-dT+\theta} - 1]y_m.
\end{aligned}$$

Further simplification of ΔV_1 yields:

$$\Delta V_1(x_m, y_m) < -(1-R_0)V_1(x_m, y_m) < 0.$$

Further, $\Delta V_1(0,0) = 0$. Therefore, $V_1(x_m, y_m)$ is negative definite when $R_0 < 1$. Thus, $V_1(x_m, y_m)$ is a Lyapunov function and pest-free point E_0 is globally asymptotically stable in the positive quadrant of $x - y$ plane. □

Remark 7.4.2. The point E_0 collides with E^*. The pest-free fixed point become non-hyperbolic at $R_0 = 1$ and one of the eigenvalues becomes 1. Further, the map (7.3.2) may admit transcritical bifurcation about E_0 with respect to birth rate parameter $b = b_0(R_0 = 1)$.

When the pest-free fixed point is unstable then the interior fixed point exists. In the next subsection, stability for interior fixed point E^* will be analyzed. The next theorem establishes the local stability of E^*.

7.4.3 Local Stability Analysis about E^*

Theorem 7.4.3. *Let us assume the constants P and Q as:*

$$\begin{aligned}
P &= 2(A-(1-E_2)(1-E_1)e^{-(d+a)T+\theta})(1+(1-E_2)(1-E_1)e^{-(2d+a)T+2\theta}), \\
Q &= (1-(1-E_2)e^{-dT+\theta})(A+(1-E_1)(1-E_2)e^{-(d+a)T+\theta})(1-(1-E_1)e^{-(d+a)T+\theta}).
\end{aligned}$$

The non-trivial interior fixed point $E^* = (x^*, y^*)$ of the system (7.3.2) is locally asymptotically stable provided

$$b_0 < b < b_0 exp(PQ^{-1})(= b_c). \tag{7.4.6}$$

Proof. Using (7.4.1), coefficients of linearized matrix $A_{[E^*]}$ are computed around E^* as:

$$\begin{aligned}
a_{11} &= b[A-(1-E_1)e^{-aT}-\{C_2-(1-E_1)e^{-aT}x^*\}Ae^{-dT+\theta}] \\
&\quad \times exp[-dT+\theta-C_2e^{-dT+\theta}]+(1-E_1)e^{-(d+a)T+\theta}, \\
a_{12} &= bexp[-dT+\theta-C_2e^{-dT+\theta}][1-\{C_2-(1-E_1)e^{-aT}x^*\}e^{-dT+\theta}]\times(1-E_2), \\
a_{21} &= (A-(1-E_1)e^{-aT})e^{-dT+\theta}, \qquad a_{22}=(1-E_2)e^{-dT+\theta}, \\
C_2 &= (E_2-E_1)(x^*e^{-a\tau_3}+(1-E_2)(x^*+y^*).
\end{aligned}$$

The trace Tr and determinant Det are computed as:

$$\begin{aligned}
Tr &= be^{-dT+\theta}[A-(1-E_1)e^{-aT}-\{C_2-(1-E_1)e^{-aT}x^*\}Ae^{-dT+\theta}] \\
&\quad \times exp[-C_2e^{-dT+\theta}]+\{(1-E_1)e^{-aT}+(1-E_2)\}e^{-dT+\theta}, \\
Det &= (1-E_1)(1-E_2)e^{-(2d+a)T+2\theta}[1-b_0y^*].
\end{aligned}$$

It is observed that condition (1.4.11) and (1.4.13) are always satisfied:

$$\begin{aligned}
1-Tr+Det &= 1-bexp[-dT+\theta-C_2e^{-dT+\theta}][A-(1-E_1)e^{-aT} \\
&\quad -\{C_2-(1-E_1)e^{-aT}x^*\}Ae^{-dT+\theta}]-(1-E_2)e^{-dT+\theta} \\
&\quad +(1-E_1)(1-E_2)e^{-(2d+a)T+2\theta}[1-b_0y^*]-(1-E_1)e^{-(d+a)T+\theta} \\
&= (1-(1-E_1)e^{-(d+a)T+\theta})(1-(1-E_2)e^{-dT+\theta})\log R_0>0, \\
1-Det &= 1-(1-E_1)(1-E_2)e^{-(2d+a)T+2\theta}[1-b_0y^*]>0.
\end{aligned}$$

The expression $1+Tr+Det$ simplifies to:

$$\begin{aligned}
1+Tr+Det &= 1+(1-E_1)e^{-(d+a)T+\theta}+b_0[A-(1-E_1)e^{-aT}-Ay^*] \\
&\quad +(1-E_2)e^{-dT+\theta}+(1-E_1)(1-E_2)e^{-(2d+a)T+2\theta}\times[1-b_0y^*] \\
&= (1+(1-E_1e^{-(d+a)T+\theta})(1+(1-E_2)e^{-dT+\theta}) \\
&\quad +b_0[A-(1-E_1)e^{-aT}-Ay^*+(1-E_1)(1-E_2)e^{-(2d+a)T+2\theta}y^*] \\
&= (1+(1-E_1e^{-(d+a)T+\theta})(1+(1-E_2)e^{-dT+\theta}) \\
&\quad +(1-(1-E_1e^{-(d+a)T+\theta})(1-(1-E_2)e^{-dT+\theta}) \\
&\quad \times\left[1-\frac{A+(1-E_1)(1-E_2)e^{-(d+a)T+\theta}}{A-(1-E_1)(1-E_2)e^{-(d+a)T+\theta}}\log(R_0)\right].
\end{aligned}$$

Accordingly, Jury's condition (1.4.12), that is $1 + Tr + Det > 0$, gives

$$R_0 < exp\left(\frac{2(A-(1-E_2)(1-E_1)e^{-(d+a)T+\theta})(1+(1-E_2)(1-E_1)e^{-(2d+a)T+2\theta})}{(1-(1-E_2)e^{-dT+\theta})(A+(1-E_1)(1-E_2)e^{-(d+a)T+\theta})(1-(1-E_1)e^{-(d+a)T+\theta})}\right). \tag{7.4.7}$$

Therefore, using (7.4.7) with the existence condition $b_0 < b$ gives the required condition (7.4.6). □

The next theorem establishes the global stability analysis about E^*.

7.4.4 Global Stability Analysis about E^*

Theorem 7.4.4. *The locally asymptotically stable positive interior fixed point E^* of the map* (7.3.2) *is globally asymptotically stable.*

Proof. Consider the positive definite function:

$$V_2(x_m, y_m) \;=\; \mid x_m - x^* \mid + \mid y_m - y^* \mid .$$

Computing ΔV_2 on the same lines as in Theorem 7.4.2 proves that V_2 is a Lyapunov function. This proves the theorem. □

Accordingly, when $b \in (b_0, b_c)$, the fixed point E^* is locally asymptotically stable. Accordingly, when $b \in (b_0, b_c)$, the fixed point E^* is locally asymptotically stable. The trajectories of the system (7.2.4)-(7.2.7) tend to asymptotically stable period-1 solution $(x_e(t), y_e(t))$:

$$\begin{aligned} x_e(t) &= x^* e^{-(a+d)(t-(m-1)T)+\theta}, \qquad (m-1)T \le t < \tau_m \\ y_e(t) &= e^{-d(t-(m-1)T)+\phi}[y^* + x^*(1-e^{-a(t-(m-1)T)})]. \end{aligned}$$

$$\begin{aligned} x_e(t) &= (1-E_1)x^* e^{-(a+d)(t-(m-1)T)+\phi}, \qquad \tau_m \le t < mT, \\ y_e(t) &= [(E_2-E_1)x^* e^{-(d+a)\tau_3} + (1-E_2)(y^*+x^*)e^{-d\tau_3}]e^{-d(t-\tau_m)+\phi} \\ &- (1-E_1)x^* e^{-(a+d)(t-(m-1)T)+\phi}. \end{aligned}$$

As b increases beyond b_0, E^* remains stable until it reaches to the point $b = b_c$.

It may be observed that violation of condition (7.4.6) will lead to instability of interior fixed point. From the above, it can be concluded that the trajectories of the system (7.2.4)-(7.2.7) tends to positive period-1 solution in the range $b \in (b_0, b_c)$.

The period-1 solution, period-2 solution or flip bifurcation and complex dynamical behavior occurs for the conditions $b < b_c$, $b = b_c$ and $b > b_c$ respectively. Further, increasing the parameter value $b > b_c$, the fixed point E^* losses its stability and the system may exhibit complex dynamics.

7.5 Bifurcation Analysis

To analyze the behavior of bifurcation about E_0 following theorem is established:

7.5.1 Transcritical Bifurcation Analysis

Theorem 7.5.1. [Transcritical Bifurcation] *The map* (7.3.2) *undergoes a transcritical bifurcation at* $b = b_0$.

Proof. Consider the map

$$\begin{pmatrix} x \\ \\ y \end{pmatrix} \to \begin{pmatrix} (1-E_1)xe^{-(a+d)T+\theta} + bexp[-(Ax+(1-E_2)y)e^{-dT+\theta}] \\ \times[(Cx+(1-E_2)y)e^{-dT+\theta}] \\ (Cx+(1-E_2)y)e^{-dT+\theta} \end{pmatrix}. \quad (7.5.1)$$

Let $x = u$, $y = v$, $b = b_1 + b_0$, $b_0 = \dfrac{(1-(1-E_1)e^{-(d+a)T+\theta})(1-(1-E_2)e^{-dT+\theta})}{e^{-dT+\theta}(A-(1-E_1)e^{-aT})}$.
The pest-free point E_0 of the map (7.3.2) is transformed to (u, v) and the map (7.5.1) becomes:

$$\begin{pmatrix} u \\ v \end{pmatrix} \to \begin{pmatrix} (b_1+b_0)\wp(Cu+(1-E_2)v)e^{-dT+\theta} + (1-E_1)e^{-(a+d)T}u \\ Cu+(1-E_2)ve^{-dT+\theta} \end{pmatrix}. \quad (7.5.2)$$

where $\wp = exp[-(E_2-E_1)ue^{-(d+al)T+\theta} - (1-E_2)(v+u)e^{-dT+\theta}]$.
The map (7.5.2) can be rewritten as:

$$\begin{pmatrix} u \\ v \end{pmatrix} \to M \begin{pmatrix} u \\ v \end{pmatrix} + \begin{pmatrix} c_{11}u^2 + c_{12}uv + c_{13}v^2 + c_{14}b_1u + c_{15}b_1v \\ 0 \end{pmatrix},$$

The coefficients of the matrix $M = m_{ij_{2\times 2}}$ and coefficients $c_{ij_{1\times 5}}$ are obtained as:

$$\begin{aligned}
m_{11} &= (1-E_1)e^{-(d+a)T+\theta} + Cb_0e^{-dT+\theta}, \quad m_{12} = b_0(1-E_2)e^{-dT+\theta},\\
m_{21} &= (A-(1-E_1)e^{-aT})e^{-dT+\theta}, \quad m_{22} = (1-E_2)e^{-dT+\theta},\\
c_{11} &= -b_0e^{-2dT+2\theta}(A^2 - A(1-E_2)e^{-aT}),\\
c_{12} &= -b_0(1-E_2)e^{-2dT+2\theta}((1-E_1)e^{-aT} - 2A), \quad c_{13} = -b_0(1-E_2)^2e^{-2(dT+\theta)},\\
c_{14} &= (A-(1-E_1)e^{-aT} + (1-E_2)e^{-dT+\theta}, \quad c_{15} = (1-E_2)e^{-dT+\theta}.
\end{aligned}$$

The eigenvalues of M are 1 and $(1-E_1)(1-E_2)e^{-(a+2d)T+2\theta}$. .

The corresponding eigenvectors V_{25} and V_{26} are $\{v_{25}, 1\}^T$ and $\{v_{26}, 1\}^T$ respectively where $v_{25} = \dfrac{e^{dT-\theta}(1-(1-E_2)e^{-dT+\theta})}{(A-(1-E_1)e^{-aT})}$ and $v_{26} = \dfrac{(1-E_2)((1-E_1)e^{-(d+a)T+\theta}-1)}{(A-(1-E_1)e^{-aT})}$.
Consider the transformation

$$\begin{pmatrix} u \\ v \end{pmatrix} = J \begin{pmatrix} \bar{x} \\ \bar{y} \end{pmatrix}, \quad J' = (V_9 \;\; V_{10}). \tag{7.5.3}$$

Using the translation (7.5.3), the map (7.5.1) becomes:

$$\begin{pmatrix} \bar{x} \\ \bar{y} \end{pmatrix} \to \begin{pmatrix} 1 & 0 \\ 0 & \lambda \end{pmatrix} \begin{pmatrix} \bar{x} \\ \bar{y} \end{pmatrix} + \begin{pmatrix} f_1(\bar{x}, \bar{y}, b_1) \\ f_2(\bar{x}, \bar{y}, b_1) \end{pmatrix}, \tag{7.5.4}$$

where

$$\begin{aligned}
f_1(\bar{x}, \bar{y}, b_1) &= d_1b_1\bar{x} + d_2b_1\bar{y} + d_3\bar{x}\bar{y} + d_4\bar{x}^2 + d_5\bar{y}^2,\\
f_2(\bar{x}, \bar{y}, b_1) &= -f_1(\bar{x}, \bar{y}, b_1),
\end{aligned}$$

$$\begin{aligned}
d_1 &= (1-(1-E_1)(1-E_2)e^{-(a+2d)T+2\theta})C^{-1}e^{dT-\theta},\\
d_2 &= (1-E_1)(1-E_2)e^{-(a+d)T+\theta}[1-(1-E_1)(1-E_2)e^{-(a+2d)T+2\theta}]C^{-1},\\
d_3 &= [2c_{13} + 2c_{11}(1-E_2)((1-E_1)e^{-(d+a)T+\theta}-1)(1-(1-E_2)e^{-dT+\theta})C^{-2}e^{dT-\theta}\\
&\quad +c_{12}(1-2(1-E_2)e^{-dT+\theta} + (1-E_2)((1-E_1)e^{-(d+a)T+\theta})e^{-dT+\theta})]C^{-1}e^{dT-\theta}\\
&\quad \times(1-(1-E_1)(1-E_2)e^{-(a+2d)T+2\theta})e^{dT-\theta}C^{-1},\\
d_4 &= [c_{11}C^{-1}(1-(1-E_2)e^{-dT+\theta})^2e^{-dT+\theta} + c_{12}C^{-1}(1-(1-E_2)e^{-dT+\theta})e^{-dT+\theta} + c_{13},\\
d_5 &= (1-(1-E_1)(1-E_2)e^{-(a+2d)T+2\theta})[c_{12}(1-E_2)((1-E_1)e^{-(d+a)T+\theta}-1)C^{-1}e^{-dT+\theta}\\
&\quad +c_{11}(1-E_2)^2((1-E_1)e^{-(d+a)T+\theta}-1)^2Cn^{-2}e^{-2dT+2\theta} + c_{13}]C^{-1}.
\end{aligned}$$

The center manifold theorem [69] is used to determine the nature of bifurcation about E_0 at $b_1 = 0$. The center manifold for the map (7.5.1) can be represented as:

$$w^c(0) = \{(\bar{x}, \bar{y}, b_1) \in \Re^3 | \bar{y} = f(\bar{x}, b_1), f(0,0) = 0, Df(0,0) = 0\}.$$

Let $\bar{y} = f(\bar{x}, b_1) = B_0 b_1 + B_1 b_1 \bar{x} + B_2 \bar{x}^2 + O(|b_1|^2 + |b_1 \bar{x}^2| + |\bar{x}|^3)$. The coefficients in $\bar{y}$ can be computed as:

$$\begin{aligned} B_0 &= 0, \qquad B_1 = \frac{-d_1}{(1-(1-E_1)(1-E_2)e^{-(a+2d)T+2\theta)}}, \\ B_2 &= \frac{d_4}{1-(1-E_1)(1-E_2)e^{-(a+2d)T+2\theta}}. \end{aligned}$$

The map restricted to the center manifold is given by:

$$\bar{f} : \bar{x} \to \bar{x} + f_1(\bar{x}, \bar{y}, b_1) = \bar{x} + d_1 b_1 \bar{x} + d_2 b_1 \bar{y} + d_3 \bar{x}\bar{y} + d_4 \bar{x}^2 + d_5 \bar{y}^2$$

$$= \bar{x} + d_1 b_1 \bar{x} + d_3 \frac{d_4}{(1-E_1)(1-E_2)e^{-(a+2d)T+2\theta} - 1} \bar{x}^3 + d_4 \bar{x}^2 + O(|b_1|^2 + |b_1 \bar{x}^2| + |\bar{x}|^4).$$

Using Theorem 1.4.3, it can be calculated that

$$\frac{\partial \bar{f}(0,0)}{\partial b_1} = 0, \qquad \frac{\partial^2 \bar{f}(0,0)}{\partial x \partial b_1} = d_1 \neq 0, \qquad \frac{\partial^2 \bar{f}(0,0)}{\partial^2 x} = 2d_4 \neq 0.$$

Note that, all conditions of transcritical bifurcation are satisfied at $(\bar{x}, b_1) = (0,0)$. Further, E^* becomes E_0 as $b = b_0$. Hence the map (7.3.2) undergoes to a transcritical bifurcation between $E_0 = (0,0)$ and $E^* = (x^*, y^*)$ at $b = b_0$. □

The interior fixed point become non-hyperbolic at $b = b_c$ and one of the eigenvalues becomes -1. So, there is a possibility of flip bifurcation. To characterize the nature of the fixed point E^* at $b = b_c$, following theorem is concluded.

7.5.2 Flip Bifurcation Analysis

Theorem 7.5.2. [*Flip Bifurcation] The system* (7.3.2) *undergoes a flip bifurcation about* $E^* = (x^*, y^*)$ *at* $b = b_c$. *Moreover, if* $\bar{a} > 0$*(resp.* $\bar{a} < 0$*), then period-2 solutions that bifurcate from this fixed point are stable (resp. unstable).*

Proof. Proof is omitted here. It is on the same lines as in previous chapters. □

7.6 Effect of Pesticide Residual Effects with Delayed Response

The threshold value R_0 is

$$\begin{aligned} R_0 &= \frac{be^{-dT+\theta}((E_2-E_1)e^{-a\tau_3}+(1-E_2)-(1-E_1)e^{-aT})}{(1-(1-E_1)e^{-(d+a)T+\theta})(1-(1-E_2)e^{-dT+\theta})}, \\ \theta &= m_1\left(\frac{(e^{-a_1T}-1)}{a_1}-\frac{(e^{-c_1T}-1)}{c_1}\right)<0. \end{aligned}$$

The long-term effect of delayed response rate:

$$\begin{aligned} \lim_{c_1\to\infty} R_0 &= \frac{be^{-dT+\theta_0}((E_2-E_1)e^{-a\tau_3}+(1-E_2)-(1-E_1)e^{-aT})}{(1-(1-E_1)e^{-(d+a)T+\theta_0})(1-(1-E_2)e^{-dT+\theta_0})}=R_0^R, \\ \theta_0 &= m_1\left(\frac{e^{-a_1T}-1}{a_1}\right)<0. \end{aligned}$$

This would mean that the larger delayed response gives smaller threshold value. Therefore, the pest population can be controlled more effectively. Further, the delayed response c_1 affects the threshold R_0. The effects of delayed response on threshold R_0 will be analyzed by taking first order derivatives of the threshold R_0 with respect to c_1:

$$\begin{aligned} \frac{dR_0}{dc_1} &= -\frac{bm_1e^{-dT+\theta}((E_2-E_1)e^{-a\tau_3}+(1-E_2)-(1-E_1)e^{-aT})}{(1-(1-E_2)e^{-dT+\theta})^2(1-(1-E_1)e^{-(d+a)T+\theta})^2} \\ &\times (1+(1-E_1)(1-E_2)e^{-(2d+a)T+2\theta})e^{-c_1T}(e^{c_1T}-1-c_1T)c_1^{-2}<0. \end{aligned}$$

This would mean that after the increase in critical delayed response, the pest density will be eradicated otherwise it will vary periodically.

The threshold R_0 depends on decay rate a_1. The derivatives of R_0 with respect to a_1 is computed:

$$\begin{aligned} \frac{dR_0}{da_1} &= \frac{bm_1e^{-dT+\theta}((E_2-E_1)e^{-a\tau_3}+(1-E_2)-(1-E_1)e^{-aT})}{(1-(1-E_2)e^{-dT+\theta})^2(1-(1-E_1)e^{-(d+a)T+\theta})^2} \\ &\times (1+(1-E_1)(1-E_2)e^{-(2d+a)T+2\theta})e^{-a_1T}(e^{a_1T}-1-a_1T)a_1^{-2}>0. \end{aligned}$$

It is noted that an increase in decay rate will enhance the threshold R_0. Therefore, as a_1 increase, the threshold R_0 goes above unity and pest density will vary periodically. Therefore, pest eradication is difficult. However, increasing decay rate in sufficient amount may destabilize the pest-free state. The model parameters m_1 is involved in

the threshold R_0. The first order derivatives of the threshold R_0 with respect to m_1 is computed as:

$$\begin{aligned}\frac{dR_0}{dm_1} &= \frac{be^{-dT+\theta}(1+(1-E_1)(1-E_2)e^{-(2d+a)T+2\theta})}{(1-(1-E_2)e^{-dT+\theta})^2(1-(1-E_1)e^{-(d+a)T+\theta})^2}\left(\frac{e^{-a_1T}-1}{a_1}-\frac{e^{-c_1T}-1}{c_1}\right)\\ &\times \ ((E_2-E_1)e^{-a\tau_3}+(1-E_2)-(1-E_1)e^{-aT})<0.\end{aligned}$$

This indicates that R_0 is monotonic decreasing function with respect to m_1. Sufficient increase in the killing efficiency rate m_1 may stabilize the pest-free state. Therefore, the threshold R_0 become less than unity and the pest can be eradicated successfully. This is due to the stability of the pest-free state (see Theorem 7.4.1).

7.7 Effect of Mechanical Control

The expression of R_0 involves E_1 and E_2. The first derivatives of R_0 with respect to E_1 and E_2 are found to be negative:

$$\begin{aligned}\frac{dR_0}{dE_1} &= -\frac{be^{-dT+\theta}((1-E_2)e^{-(d+a)T+\theta}(1-e^{-a_1lT})+e^{-aT}-e^{-alT})}{(1-(1-E_2)e^{-dT+\theta})(1-(1-E_1)e^{-(d+a)T+\theta})^2}<0,\\ \frac{dR_0}{dE_2} &= -\frac{be^{-dT+\theta}((1-E_1)e^{-dT+\theta}(e^{-aT}-e^{-a_1lT})+1-e^{-alT})}{(1-(1-E_2)e^{-dT+\theta})^2(1-(1-E_1)e^{-(d+a)T+\theta})}<0.\end{aligned}$$

R_0 is monotonic decreasing function with respect to E_1 and E_2. Accordingly, harvesting effort E_1 and E_2 reduces the threshold R_0. Once $R_0<1$, pest can be eradicated successfully.

7.8 Effect of Harvesting Timing τ_3

It is necessary that mechanical control will be selected suitably to achieve successful pest control. The first order derivative of the threshold R_0 with respect to harvesting timing:

$$\frac{dR_0}{d\tau_3} = -\frac{baT(E_2-E_1)e^{-dT-a\tau_3+\theta}}{(1-(1-E_2)e^{-dT+\theta})(1-(1-E_1)e^{-(d+a)T+\theta})}.$$

Accordingly, the threshold R_0 is a monotonic decreasing function with respect to harvesting time τ_3, when $E_2>E_1$ and monotonic increasing function when $E_2<E_1$. That is, if harvesting timing increase from critical $t>\tau_{3c}$,

$$\tau_{3c}=\frac{1}{a}\ln\left[\frac{be^{-dT+\theta}(E_2-E_1)}{(1-(1-E_1)e^{-(d+a)T+\theta})(1-(1-E_2)e^{-dT+\theta})+be^{-dT+\theta}[(1-E_1)e^{-aT}-1+E_2]}\right].$$

then pest eradication will occur for $E_2 > E_1$. Otherwise, for $t < \tau_{3c}$ may destabilize the pest-free state.

The derivative of y^* with respect to τ_3 is obtained as

$$\begin{aligned}\frac{dy^*}{d\tau_3} &= -\frac{aT(E_2-E_1)(1-E_1)e^{-a(\tau_3+T)}(1-(1-E_2)(1-\alpha)e^{-dT+\theta}))\log(R_0)}{(A-(1-E_2)(1-E_1)e^{-(d+a)T+\theta})^2} \\ &\quad -\frac{aT(1-\alpha)(E_2-E_1)e^{-a\tau_3}}{(A-(1-E_2)(1-E_1)e^{-(d+a)T+\theta})}.\end{aligned}$$

The equilibrium density of mature pest is a decreasing function with respect to parameter l if the harvesting rate of mature pest is greater than the immature pest. Therefore, $\frac{dy^*}{d\tau_3} < 0$ provided $E_2 > E_1$. Accordingly, the mature pest density at equilibrium reduces with increase in time delay τ_3 of mechanical control.

7.9 Numerical Simulations

In the foregoing sections, the analytical results have been established and qualitative analysis of the system has been carried out using analytical tools. In this section, extensive numerical simulations are carried out to illustrate the analytical findings. To study the effect of delayed response and mechanical control in the model dynamics, the following data set has been chosen:

$$a = 0.4, d = 0.2, \tau_3 = 0.6, a_1 = 0.2, c_1 = 0.5, m_1 = 3, E_1 = 0.6, E_2 = 0.8. \quad (7.9.1)$$

In the Table 7.1, for different values of harvesting time τ_3, the thresholds R_0 and R_0^D(in the absence of residual effect) are computed which are responsible for the stability and existence of fixed points E_0 and E^*. For $\tau_3 < 1$, in the absence of residual effect, the condition (7.4.5) for stability of the pest-free state is violated while interior fixed points exist. Therefore, pest eradication is not possible when chemical control is not applied. The threshold reduces below less than one by applying chemical control. From the Table 7.1, it can be observed that the pest-free state stabilizes when $m_1 \neq 0$. The condition (7.3.4) for the pest-eradication will be satisfied as $R_0 < 1$. Therefore, the pest will extinct.

τ_3	0.2	0.4	0.6	0.8	1
R_0	0.9781	0.8589	0.7589	0.6474	0.5536
R_0^D	1.6075	1.4116	1.2308	1.0639	0.7444

Table 7.1: Numerical simulation for effectiveness of residual effect of pesticide.

τ_3	x^*	y^*	b_0	b_c	R_0	Analytical behavior	Numerical Behavior
0.0	1.4374	0.1471	9.9398	107.0264	1.4092	E^* stable	Period-1 Solution
0.1	1.2061	0.1203	10.5630	112.9629	1.3254	E^* stable	Period-1 Solution
0.2	0.9577	0.0948	11.2461	119.3825	1.2449	E^* stable	Period-1 Solution
0.3	0.6913	0.0705	11.9913	126.3835	1.1675	E^* stable	Period-1 Solution
0.4	0.4059	0.0476	12.8066	134.0040	1.0932	E^* stable	Period-1 Solution
0.5	0.1001	0.0260	13.7016	142.3428	1.0218	E^* stable	Period-1 Solution
0.6	-	-	14.6879	-	0.9532	E_0 stable	Pest-free Solution
0.7	-	-	15.7791	-	0.8872	E_0 stable	Pest-free Solution
0.8	-	-	16.9921	-	0.8239	E_0 stable	Pest-free Solution
0.9	-	-	18.3472	-	0.7631	E_0 stable	Pest-free Solution
1	-	-	19.8696	-	0.7046	E_0 stable	Pest-free Solution

Table 7.2: Effect of harvesting timing on pest density and stability of pest-free state for $b = 14$.

In the Table 7.2, considering $\tau_3 = 0.6$, the constant b_0 is found as $b_0 \approx 14.6879$. For $b = 14$, the basic reproduction number is computed as $R_0 = 0.9532$. Accordingly, the pest-free state of the map (7.3.2) is locally asymptotically stable as $R_0 < 1 (b < b_0)$ (see Theorem 7.4.1) and interior fixed point does not exist. For $b > b_0 \approx 14.6879$, the pest-free state becomes unstable as $R_0 > 1$ and interior fixed point E^* exists.

The bifurcation diagram drawn in Fig. 7.1 verifies the local stability of E_0 and existence of E^*. The diagram has two different color lines. When $b < 14.6879$, the blue line shows stable pest-free state and the red line shows that the interior fixed point does not exists. For $b > 14.6879$, the blue line shows E^* will exists and the red line

shows that line of unstable pest-free state. It is observed that transcritical bifurcation occurs at $b \approx 14.6879$.

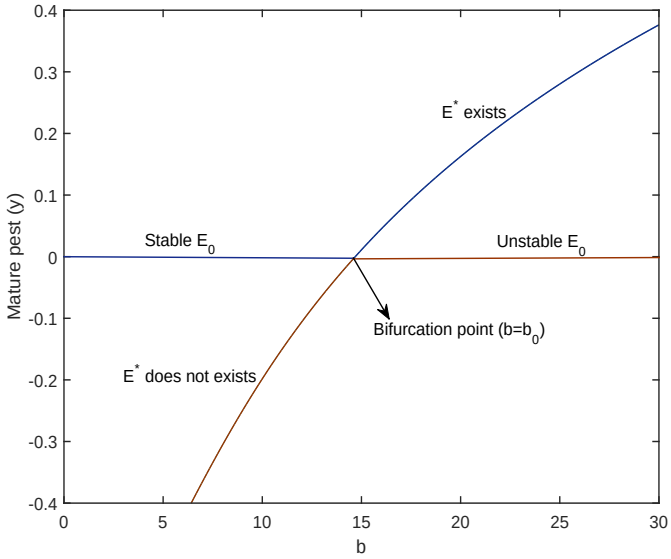

Figure 7.1: Variation of mature pest density versus b.

In Table 7.3, it can be observed that the threshold R_0 is greater than 1 for $b = 20$ and data set (7.9.1). In other words, the pest-free state is unstable for higher birth rates. The interior fixed point is found as $E^* = (1.4626, 0.0843)$ for $\tau_3 = 0.6$. According to Theorem 7.4.3., the interior fixed point is locally asymptotically stable for $b > b_0$. The flip bifurcation will occur at $b_c \approx 151.5037$. Therefore, the period-1 solution will occur in $14.6879 < b < 151.5037$.

From Table 7.3, it can be observed that the increase in time delay of harvesting τ_3 reduces the immature/mature pest density and the threshold R_0. If the time delay is harvesting is very small i.e. $\tau_3 = 0.1$, the reduction in immature and mature pest densities are 6.78% and 12.31% respectively. When the harvesting effort is applied just before the birth pulse (i.e. $l = 0.9$) The reduction is 85.26% and 92.02% of mature and mature pest densities respectively. The maximum reduction in the immature and mature pest is 98.86% and 99.43% if the time delay is the same with that of birth pulse ($l = 1$). Therefore, the best time of harvesting is just before the births.

τ_3	x^*	y^*	b_0	b_c	R_0	Decrease in x(in %)	Decrease in y(in %)
0.0	2.9320	0.2498	9.9398	107.0264	2.0131	-	-
0.1	2.7331	0.2190	10.5630	112.9629	1.8934	6.78	12.31
0.2	2.5172	0.1895	11.2461	119.3825	1.7782	14.15	24.14
0.3	2.2834	0.1612	11.9913	126.3835	1.6679	22.12	35.47
0.4	2.0305	0.1342	12.8066	134.0040	1.5617	30.75	46.27
0.5	1.7574	0.1086	13.7016	142.3428	1.4597	40.06	56.53
0.6	1.4626	0.0843	14.6879	151.5037	1.3617	50.12	66.25
0.7	1.1447	0.0614	15.7791	161.6112	1.2675	60.96	75.41
0.8	0.8019	0.0400	16.9921	172.8162	1.1770	72.65	84.011
0.9	0.4322	0.0199	18.3472	185.3035	1.0901	85.26	92.02
1	0.0334	0.0014	19.8696	199.3012	1.0066	98.86	99.43

Table 7.3: Effect of harvesting timing on pest density and stability of interior fixed point for $b = 20$.

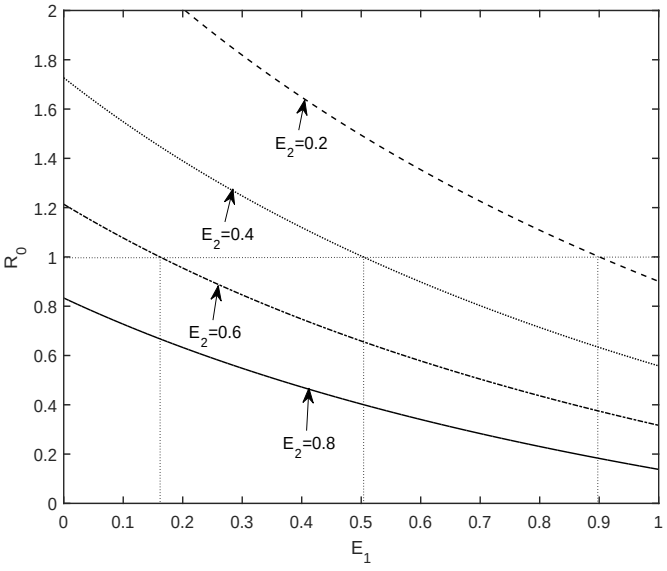

Figure 7.2: Variation of R_0 versus E_1.

The Fig. 7.2 is drawn to show the variations of the threshold R_0 with E_1 in the range $0 < E_1 < 1$ and for fixed values of $E_2 = 0.2(2)0.8$. For $E_2 = 0.8$, the

threshold R_0 is less than one. Accordingly, the pest-free state is stable for all values of E_1. Further, choices of E_1 and E_2, the threshold R_0 will remain less than one. The pest-eradication is possible for $E_1 > E_{1c}$ for a choice of harvesting effort E_2 (i.e. for $E_2 = 0.4$, $R_0 < 1$ when $E_1 > 0.16 = E_{1c}$). Accordingly, the harvesting effort E_1 can stabilize the pest-free state. For $E_2 = 0.6$, the state E_0 is unstable if $E_1 < 0.505 = E_{1c}$ and survival state will exist.

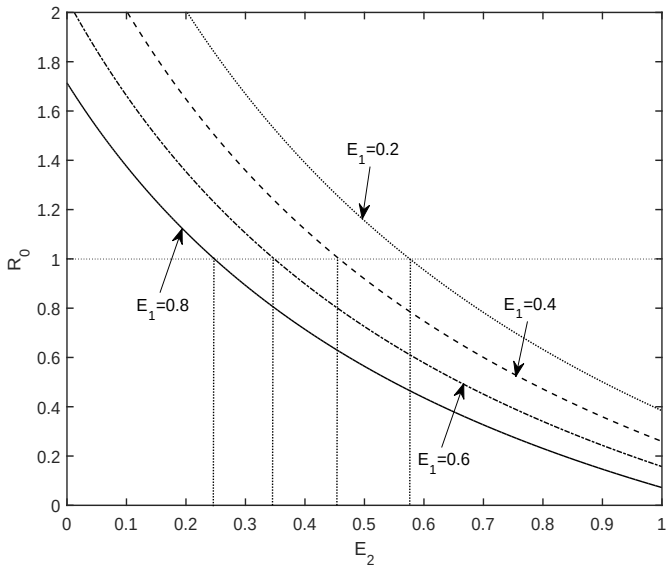

Figure 7.3: Variation of R_0 versus E_2.

Similarly, in the Fig.7.3, variation of R_0 with the harvesting effort E_2 in the range $0 < E_2 < 1$ for fixed values of $E_1 = 0.2(2)0.8$. For $E_1 = 0.2$, the pest-free state E_0 is stable for $E_2 > 0.58$ as R_0 is less than one and the state E^* does not exist. Further, the state E^* is expected to be locally stable for $E_1 = 0.4$ in the range $E_2 > 0.458$ as $R_0 > 1$. However, E_0 is stable for the range $E_2 < 0.458$ while E^* does not exist. Further, the pest-free state E_0 stabilizes when the harvesting effort of mature pest E_2 exceeds beyond 0.458. Accordingly, the combination of harvesting effort of immature and mature pest is needed to control the pest. For $E_1 = 0.6$, the threshold R_0 is less than 1 for $E_2 > 0.347$. Further, R_0 remains greater than 1 for $E_2 < 0.347$. Accordingly, pest will eradicated for $E_2 > 0.347$ while the states E^* does not exist in this range. It is concluded that the sufficient amount of harvesting efforts of mature and immature pest are needed to achieve the pest-free state. At $R_0 = 1$, E_0 become the non hyperbolic

fixed points and the fixed points E_0 and E^* collide. Transcritical bifurcation occurs along the line $R_0 = 1$ as the states E_0 and E^* exchange their stability along this line.

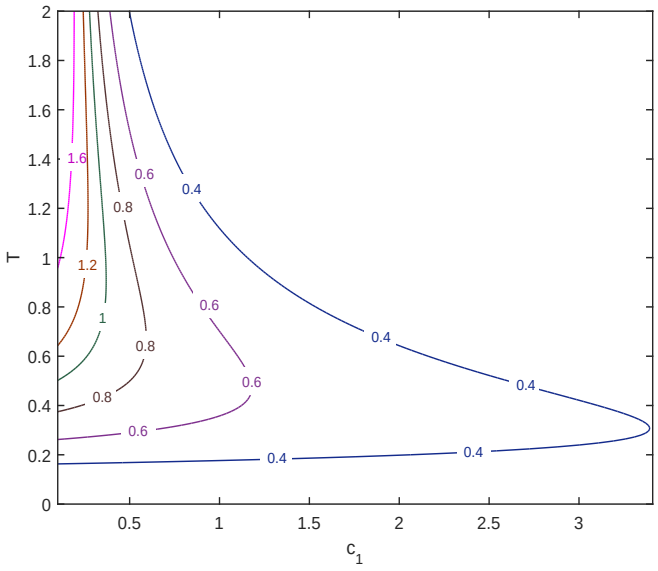

Figure 7.4: Variation of delayed response and pulse period in $T - c_1$ plane.

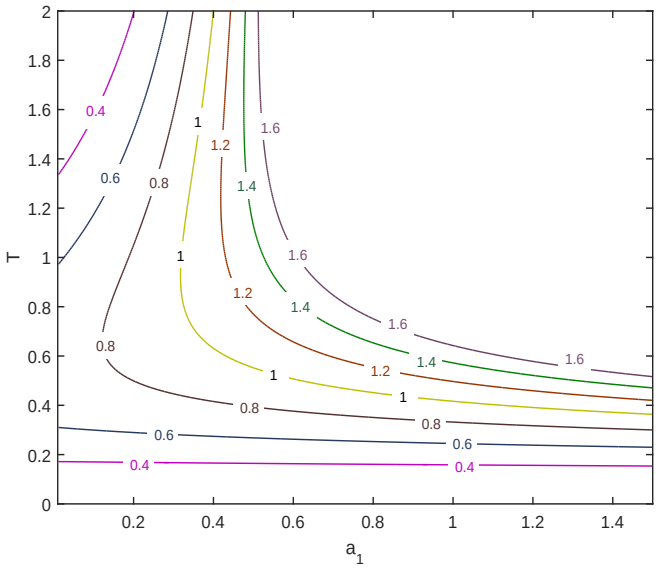

Figure 7.5: Variation of decay rate and pulses period in $T - a_1$ plane.

In Fig. 7.4, the variation of the threshold R_0 with respect to the delayed response of pesticide c_1 and pulse period T is drawn on $T - c_1$ plane keeping other parameters fixed as in (7.9.1). The green color curve is drawn corresponding to the equation $R_0 = 1$

in (7.3.4) which bifurcates the $T - c_1$ domain into pest eradication state and survival state. It can be observed that for larger delayed response c_1, the threshold R_0 will be less than unity. It is apparent from the Fig. 7.4 that for $c_1 > 0.36$, $R_0 < 1$ for all values of T and pest can be eradicated successfully. If the delayed rate is sufficiently small (i.e. $c_1 < 0.36$), pest eradication is possible irrespective of pulse period T. This emphasizes that the combination of the pulse period and delayed response rate is useful in reducing the pest load and ultimately to eradicate the pest density.

Similarly, in Fig. 7.5, the effect of decay rate a_1 and pulse period T on the threshold R_0 is drawn in $T - a_1$ plane, keeping other parameters fixed as in (7.9.1). It is evident from the figure that the threshold R_0 reduces when the decay rate becomes smaller irrespective of T. For a fixed value of pulse period, the corresponding decay rate $a_1 < a_{1c}$ is needed to eradicate the pest population. The stable and unstable regions of pest-free state E_0 is divided by the yellow curve($R_0 = 1$). For $a_1 < 0.318$, the pest-free state will be stable for all values of pulse period T. Otherwise, for $a_1 > 0.318$, pest population will vary periodically irrespective of T and R_0 becomes greater than one. Therefore, pest eradication will not possible. Hence, pest eradication is possible for different combinations of decay rate and pulse period.

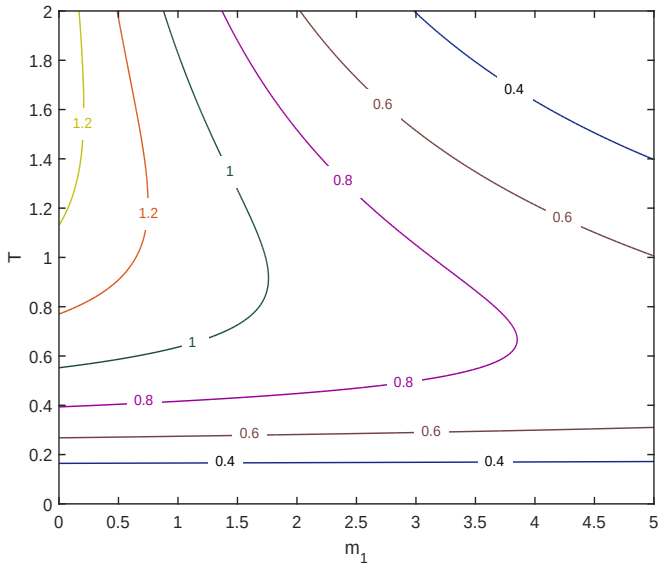

Figure 7.6: Variation of killing efficiency and pulses period in $T - m_1$ plane.

Again in Fig. 7.6, the influence of the parameters T and m_1 on the stability

of the pest-free state E_0 has been shown. Clearly, the region in left side of the green line corresponds to $R_0 > 1$. It is the region of instability of E_0. Beyond this, the pest-free state will become stable and pest will be eradicated. The threshold R_0 will become smaller when killing rate is high for all values of T. This implies that the pest population can be minimized by making the threshold less than one. For $m_1 < 1.761$, the system may admit periodic solution or more complex dynamical behavior irrespective of T. Therefore, sufficient amount of killing rate $m_1 > 1.761$ will be required for pest control.

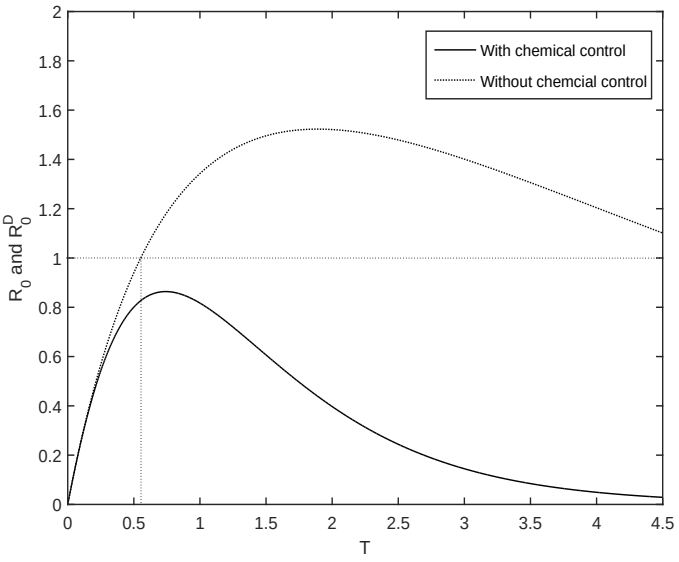

Figure 7.7: Effect of chemical control in $T - R_0$ plane.

In Fig. 7.7, variation of R_0 and R_0^D with pulse period T in the range $0 < T < 4.5$. For $m_1 = 0$, the pest-free state remains stable for $T < 0.5524$ while it become globally stable for $T > 0.5524$. Further, when $m_1 \neq 0$, the pest-free state E_0 stabilizes for all values of pulse period T as $R_0 < 1$. Also, the state E^* does not exist when the chemical control is applied. It is observed that in the absence of chemical control (i.e. $m_1 = 0$), for the data set (7.9.1), the threshold for pest eradication increases than that has been obtained by the chemical control.

A set of the bifurcation diagrams has been plotted with the delayed response rate c_1 in Fig. 7.8 *a-d* taking $b = 20, 60, 180, 540$, while other parameters are fixed as in (7.9.1). From these figures, it can be easily observed that complexity increases

with the increase of birth rate parameter b. The pest-free state becomes stable after a certain value of c_1, say c_{1k} in Fig. 7.8(a). In this figure, the pest will be eradicated for $c_1 > 0.747 = c_{1k}$, confirming the result obtained in Theorem 7.4.1. Thereby indicating a critical value of delayed response pest can be effectively controlled. A period halving cascade can be observed in Fig. 7.8(d). These observations suggest that delayed response can play a crucial role in eliminating the pest from the field.

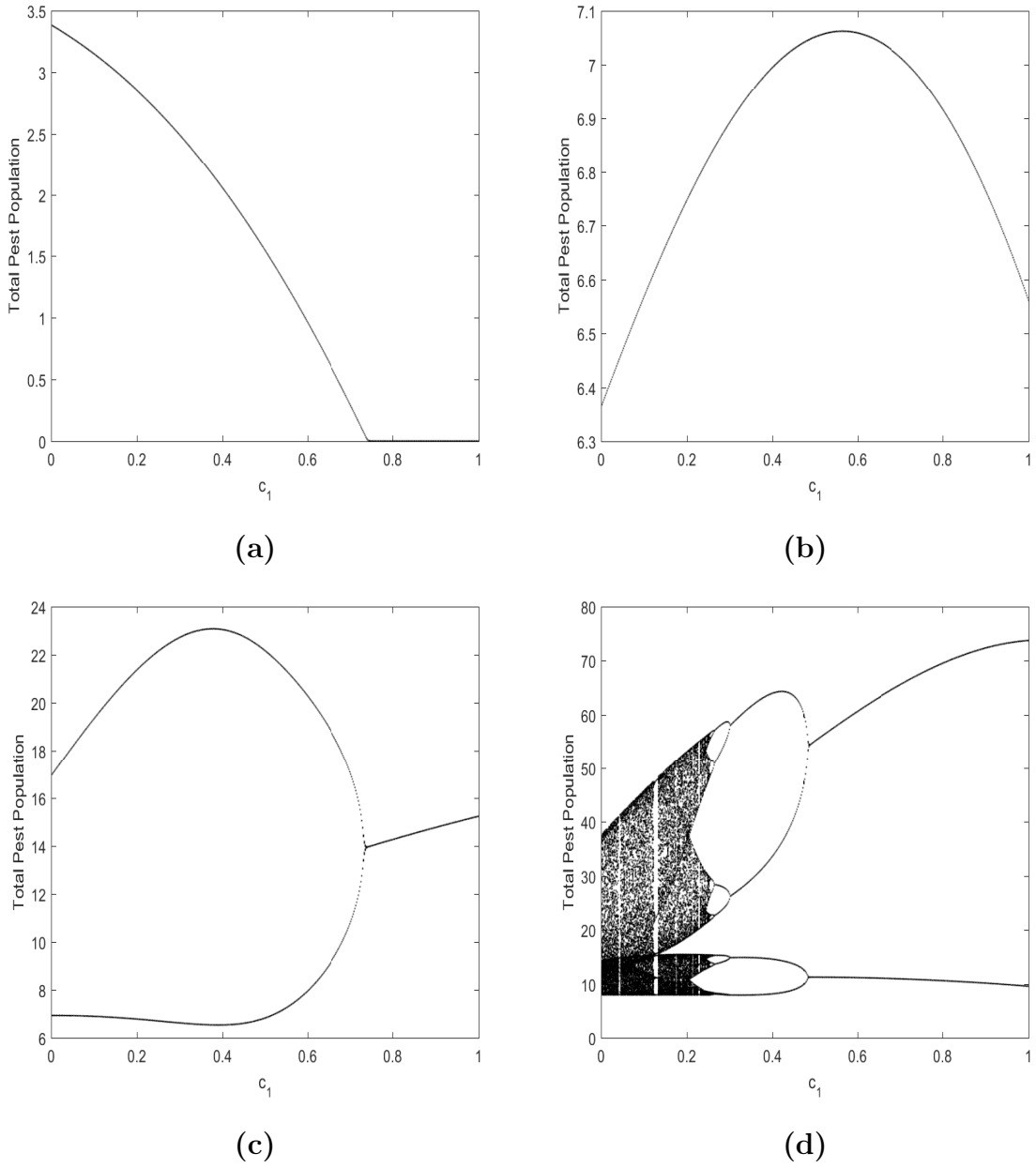

Figure 7.8: Bifurcation diagrams of the map (7.3.2) for total pest population with respect to c_1 at (a) $b = 20$ (b) $b = 60$ (c) $b = 180$ (d) $b = 540$.

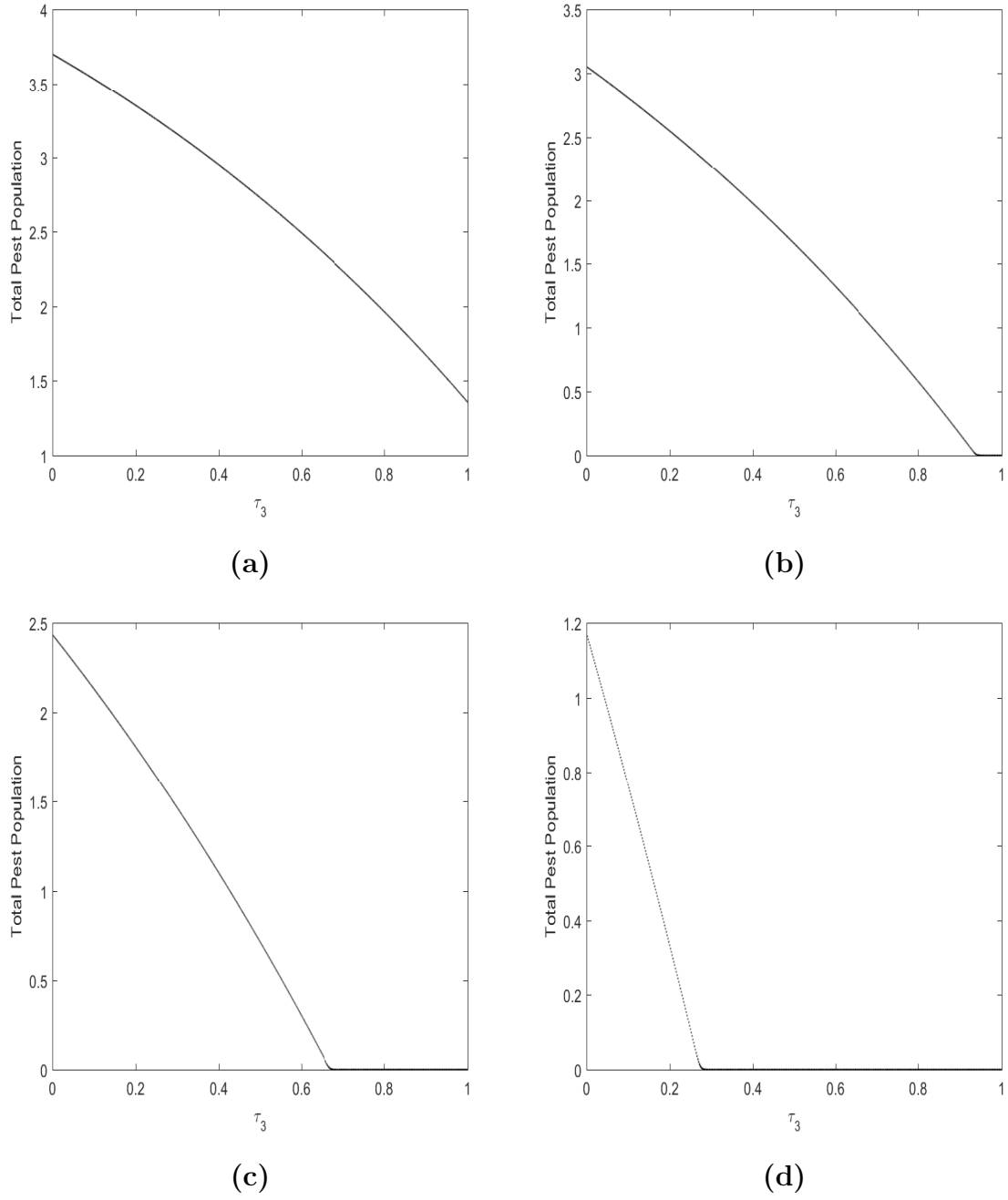

Figure 7.9: Bifurcation diagrams of the map (7.3.2) for total pest population with respect to τ_3 at (a) $c_1 = 0.3$ (b) $c_1 = 0.54$ (c) $c_1 = 0.7$ (d) $c_1 = 0.95$.

Another set of bifurcation diagrams has been plotted with the parameter τ_3 in Fig. 7.9 for $c_1 = 0.3, 0.54, 0.7, 0.95$ and other parameters are fixed as in the data set (7.9.1). No chaotic behavior is observed in these figures. The threshold for pest-free state decreases with increase of parameter c_1, the delayed response rate of pesticide in Fig. 7.9(a), the delayed response rate would be not enough to eliminate the pest.

In other figures, the increase in delayed response rate decreases the harvesting time required to eliminate the pest. This occurs due to the long-term effectiveness of the residual effect. Further, delay in harvesting, the period-1 solution will lead to stable pest-free state where pest can be eliminated after a certain value of τ_3 say τ_{3k}. Further, τ_{3k} decreases with increase in c_1. The pest will be eradicated when $\tau_3 > 0.954 \approx \tau_{3c}$.

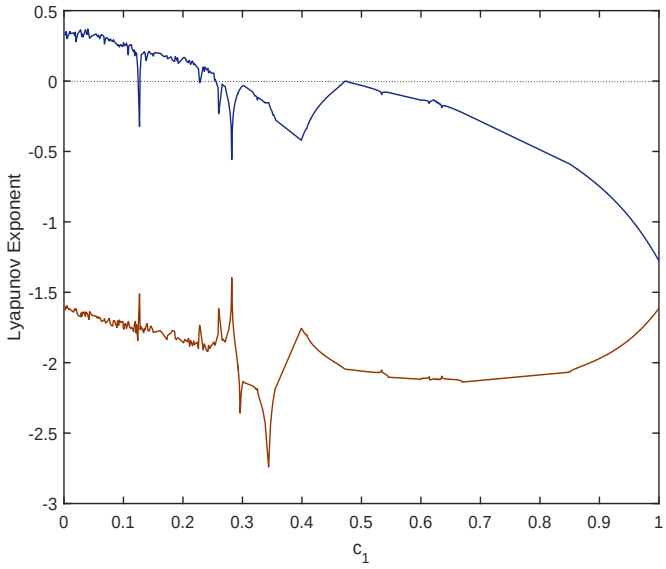

Figure 7.10: Lyapunov exponents of the map (7.3.2) with respect to c_1 for $b = 540$.

The Lyapunov exponents with respect to delayed response rate c_1 have been shown in Fig. 7.10 for $b = 540$ and other parameters are fixed as in the data set (7.9.1). The Blue color shows the largest Lyapunov exponent (say LE_1) and red color shows the smallest Lyapunov exponent(say LE_2). It can be easily observed that LE_2 is always negative. Further, LE_1 is zero for some values of c_1. Therefore, the map (7.3.2) is dissipative.

Further, the Lyapunov dimension of chaotic attractor obtained in the map (7.3.2) is computed by the formula of Kaplan and Yorke [104] as:

$$D_L = j + \frac{1}{|\lambda_{j+1}|}\sum_{i=1}^{j}\lambda_i. \tag{7.9.2}$$

The results for the system dynamics are summarized in Table 7.4.

Table 7.4: Lyapunov exponents and behavior of the system (7.3.2)

.

Parameter varied	Parameter Value	Lyapunov exponent	D_L	Dynamical behavior
$c_1 \in (0, 0.2554]$	$c_1 = 0.1$	LE_1=0.27203, LE_2=-1.75619	1.1549	Strange attractor/ Chaos
$c_1 \in (0.125, 0.128)$	$c_1 = 0.126$	LE_1=-0.18675, LE_2=-1.66242	0	Periodic window
$c_1 \in (0.2554, 1]$	$c_1 = 0.474$	LE_1=0, LE_2=-2.04691	1	Quasi-Periodic Solution/Torus
	$c_1 = 0.8$	LE_1=-4.87948, LE_2=-2.08672	0	Stable Periodic Solution

A set of the bifurcation diagrams has been plotted in the Fig. 7.11 with respect to the parameter E_2 for $b = 15, b = 45, b = 135, b = 405$ while other parameters are fixed as in the data set (7.9.1). In these figures it is observed that the complexity of the system increase with an increase in birth rate. In the Fig. 7.11(b)-Fig. 7.11(d), increases in the birth rate increases the threshold for pest-free solution and therefore, pest eradication is not possible. This happens due to the fact that more and more pest are produced with an increase in birth rate b. In the Fig. 7.11(a), for the smaller birth rate $b = 15$, pest can be controlled for higher harvesting rate. The pest can be eliminated for a critical level of harvesting effort $E_2 > 0.805$.

The bifurcation diagrams are plotted in the Fig. 7.12 with respect to the pulse period T for $b = 540, b = 740, b = 940, b = 1040$ while other parameters are fixed as in the data set (7.9.1). In these figures, it can be noted that the threshold for pest eradication increases, with the increase in the birth rate parameter b. The regular/irregular behavior will lead to stable pest-free state after a critical value of pulse period T say T_k. As b increase, critical level for pest eradication T_k increase. If the pulse period exceeds beyond $T > T_k$, then the pest can be effectively controlled. The pest-free state stabilizes for $T > 5.4 \approx T_k$ when $b = 1040$. Further, with an increase in birth rate, the complexity of the system increases. In this case, too, periodic doubling and periodic

halving cascade can be observed.

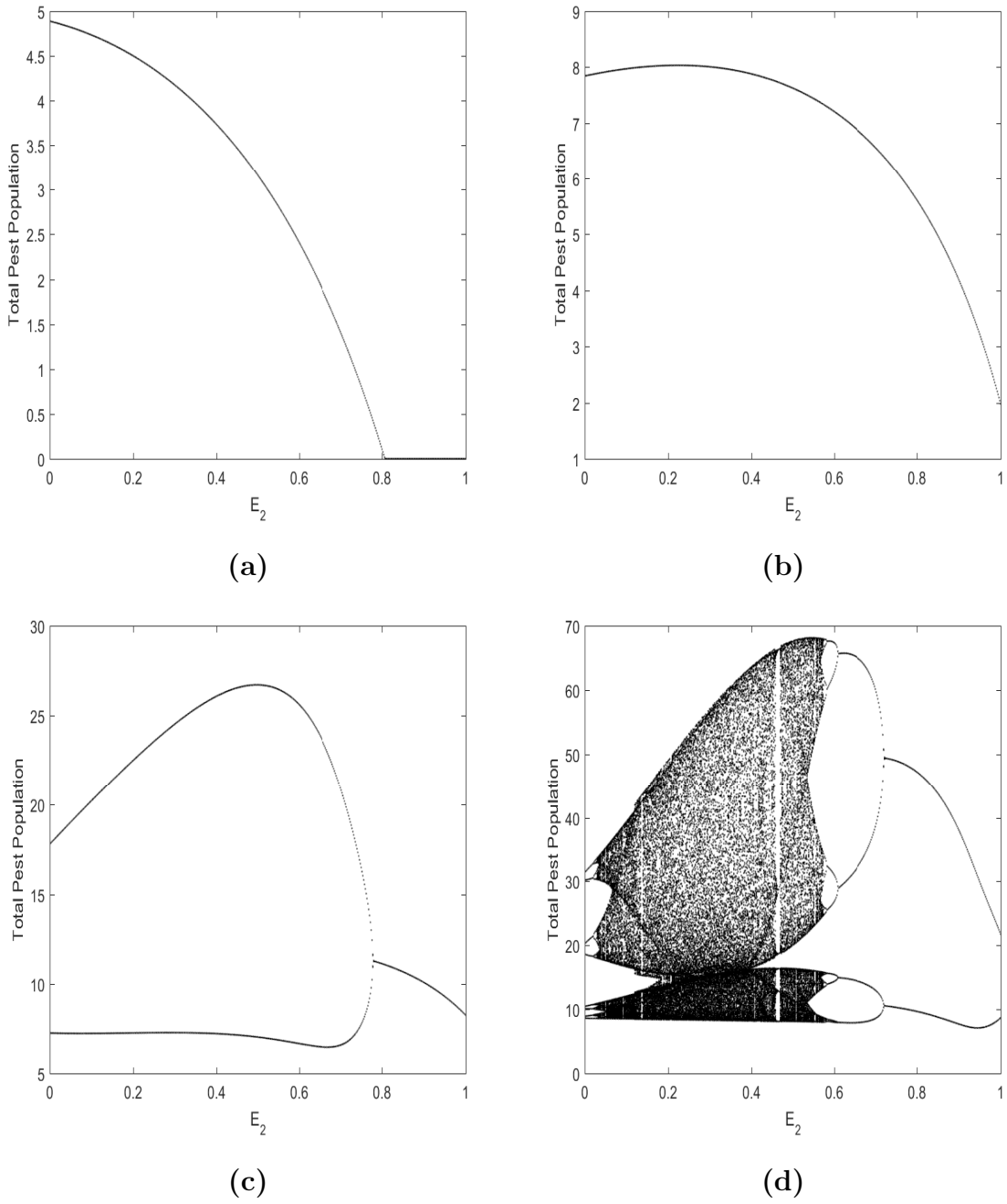

Figure 7.11: Bifurcation diagrams of the map (7.3.2) for total pest population with respect to E_2 at (a) $b = 15$ (b) $b = 45$ (c) $b = 135$ (d) $b = 405$.

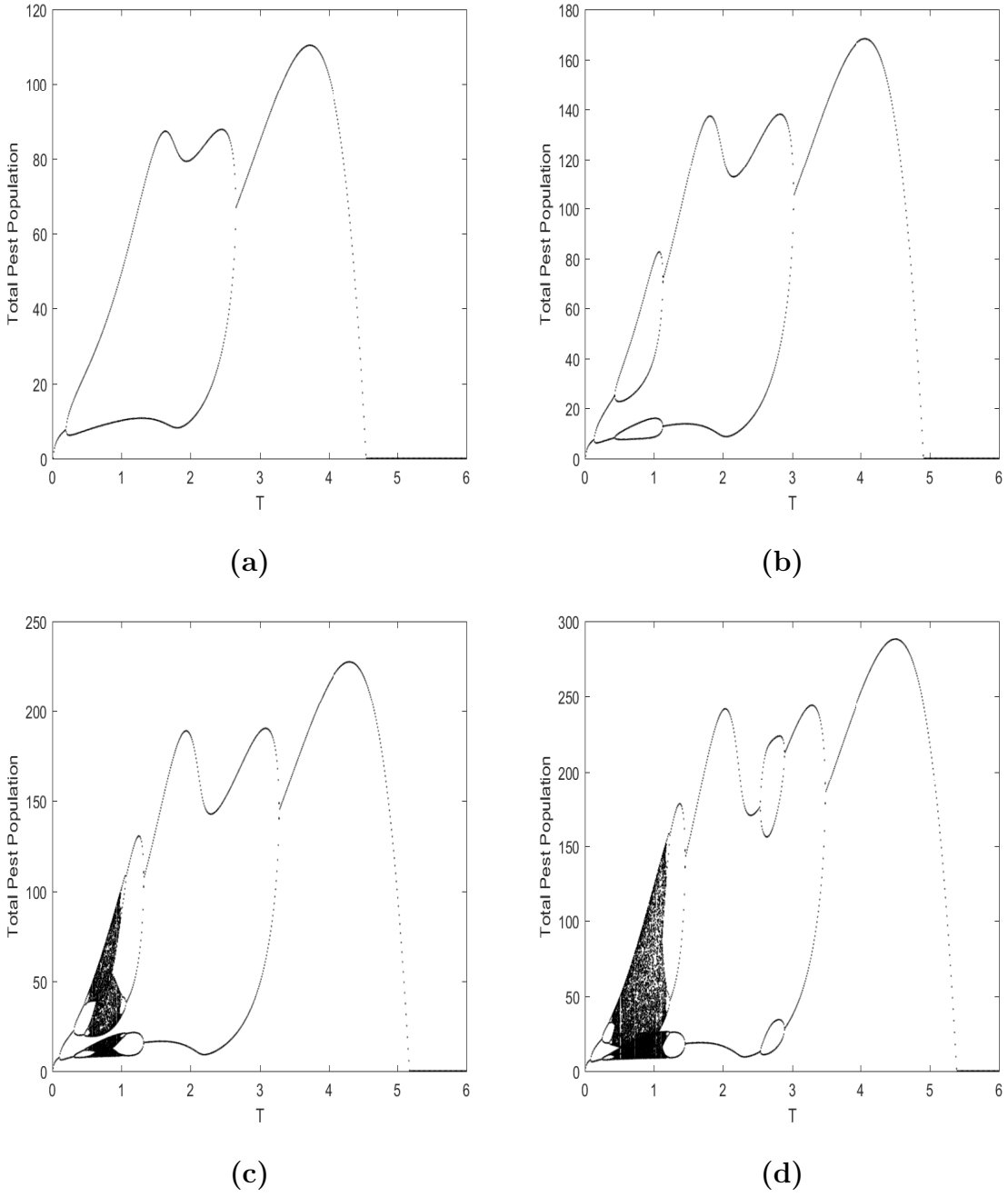

Figure 7.12: Bifurcation diagrams of the map (7.3.2) for total pest population with respect to pulse period T at (a) $b = 540$ (b) $b = 740$ (c) $b = 940$ (d) $b = 1040$.

7.10 Discussion

In this chapter, the dynamics of stage-structured pest control model with birth pulses has been formulated and analyzed through the impulsive system. A time-dependent

the impulsive control strategy for chemical control is used. The model incorporates the residual effect with the delayed response of pesticide. The existence condition for periodic solution and stability conditions for two fixed points have been obtained. The critical level of time delay in harvesting τ_3 has been obtained which is found to be responsible for pest extinction. It is also found that large value of time delay stabilizes the pest-free state. Further bifurcation plots for relevant parameters have been drawn to analyze the stable and the unstable domain of the pest-free state. It is concluded that the pest-free state can be obtained if $R_0 < 1$ provided birth rate gets lower than a critical level.

The pest-free state stabilizes when time delay exceeds beyond a critical level. Otherwise, pest density varies periodically. This implies that when $\tau_3 < \tau_{3c}$ the pest could not be eradicated and may occur in a periodic manner. This may happen due to early harvesting of the pest population. It is observed from numerical simulations that increasing delayed response to a sufficient level stabilizes the pest-free state.

On the other hand, when the decay rate is greater than a critical level, the interior fixed point exists. However, the state E_0 is unstable. Further, it is found that increasing harvesting effort of mature pest reduces the complexity of the system and pest can be eradicated completely. By numerical simulation, it is found that there exists transcritical bifurcation, flip bifurcation, period-halving bifurcation and chaotic behavior.

Chapter 8

Integrated Pest Management Strategy in a Birth Pulse Pest Control Model with Impulsive Toxin Input

8.1 Introduction

Many single or multiple populations models have been developed and studied extensively assuming continuous input of toxicant [76, 197, 198, 200]. Some population models have been investigated incorporating impulsive input of toxicant [128, 136]. Few mathematical models incorporate the effects of pollutants from industry/ households/ other sources on the biological species as well as on the environment [85, 98]. The effect of impulsive toxin input on a predator-prey system in a polluted environment has been investigated by X. Yang et al. [235]. The effect of pulse toxicant input into a polluted environment on a two-species competition system has been discussed by B. Liu et al. [135]. B. Liu et al. investigated the effects of impulsive toxicant input on two-species Lotka-Volterra system [128]. S. Cai discussed the effect on a stage-structured single species model with pulse input into a polluted environment [25]. The pesticides not only kill the pest instantaneously, but it has long time effects on the pest as well as on the environment. The mathematical models for the polluting effect

of the pesticide have been developed and analyzed [31, 133]. It can be pointed that the effects of the toxicant on the biological species are impulsive while the pest growth is continuous in these models. The effect of continuous toxin input with birth-pulse single-species model and pulse harvesting was studied by Y. Ma et al. [148]. But, the effect of toxin input is continuous, not impulsive.

In this chapter, a mathematical model for controlling the pest with pesticide spray is developed combining the effect of pesticide present in the environment as well as the pesticide uptake by the pest. The presence of toxin in the environment reduces the growth rate of the pest. The reduction in the growth rate of the pest may affect the dynamics of the system. The model has been analyzed mathematically as well as numerical simulations have been carried out to study the complex dynamical behaviors.

8.2 Model Formulation

A pest control model with toxin(pesticide) input due to pesticide spray in the environment is formulated under the following assumptions:

- $x(t)$, $C_0(t)$ and $C_E(t)$ represent the pest density, the concentration of toxicant in the pest and the concentration of toxicant in the environment at the time t respectively,

- Due to uptake of the toxicant from the environment, the pest density declines at a constant rate r which depends upon $x(t)$ as well as $C_0(t)$. Let constant d be the natural death rate of the pest. The pest density is controlled by its harvesting at the rate $E > 0$,

- $kC_E(t)$ represents the absorbing rate of the toxicant by the pest from the environment. The excretion and depuration rates of the toxicant from the pest are $gC_0(t)$ and $cC_0(t)$ respectively,

- The depletion rate of toxicant from the environment is $hC_E(t)$,

- The toxicant entered into the environment impulsively by the constant rate μ at the time $t = mT$, $m = 1, 2, 3...$,

- The growth rate $B(x(t))$ of the pest occurs in pulses. It is assumed that the pest reproduce in pulses periodically with period T at different fixed times $t = mT$,
- Birth pulse and impulsive toxical input are synchronized at time $t = mT$,
- All model parameters are positive constants.

The dynamics of a pest control system with impulsive toxin input and birth pulse is writhen as:

$$\left.\begin{aligned} \frac{dx}{dt} &= -rC_0(t)x(t) - dx(t) - Ex(t), \\ \frac{dC_0(t)}{dt} &= kC_E(t) - gC_0(t) - cC_0(t), \\ \frac{dC_E(t)}{dt} &= -hC_E(t), \end{aligned}\right\} t \neq mT, \tag{8.2.1}$$

$$\left.\begin{aligned} x(mT)^+ &= x(mT) + B(x(mT))x(mT), \\ C_0(mT)^+ &= C_0(mT), \\ C_E(mT)^+ &= C_E(mT) + \mu \end{aligned}\right\} t = mT. \tag{8.2.2}$$

Here, $x(mT)^+$, $C_0(mT)^+$ and $C_E(mT)^+$ are the biomass of the population just after the birth pulse. Equation (8.2.2) represents the synchronous birth pulse and toxin input at time $t = mT$. The period of the exogenous input of the toxicant and periodic birth is T. The initial distribution of state variables at the time $t = 0$ associated with the system (8.2.1) − (8.2.2) are:

$$x(0) = x_i > 0, \quad C_0(0) = C_{0i} > 0, \quad C_E(0) = C_{Ei} > 0. \tag{8.2.3}$$

The birth function $B(N)$ is assumed to be of Ricker type [186] as:

$$B(x) = be^{-x}. \tag{8.2.4}$$

The dynamics of impulsive pest control system is defined on the set:

$$\Re^3_+ = \{(x, C_0, C_E) \in \Re^3 \mid x \geq 0, C_0 \geq 0\, C_E \geq 0\}.$$

Remark 8.2.1. For $0 \leq C_0(t), C_E(t) \leq 1$, it is compulsory that

$$g \leq k \leq g + c.$$

The detailed analysis can be found in [85].

8.3 Model Analysis

Let $x(t) = x_{m-1}$, $C_0(t) = C_{0m-1}$, $C_E(t) = C_{Em-1}$ be the pest density, toxicant concentration in the pest and toxicant concentration in the environment at $t = (m-1)T$ respectively. The analytical solution of the differential equations of system (8.2.1) between the pulses $(m-1)T \leq t < mT$ is obtained as:

$$\begin{aligned}
x(t) &= x_{m-1}e^{D}, \\
C_0(t) &= C_{0m-1}e^{-(g+c)(t-(m-1)T)} + \frac{kC_{Em-1}(e^{(-h(t-(m-1)T))} - e^{-(g+c)(t-(m-1)T)})}{(g+c-h)}, \\
C_E(t) &= C_{Em-1}e^{(-h(t-(m-1)T))}, \qquad (m-1)T \leq t < mT, \\
D &= -\frac{krC_{Em-1}}{g+c-h}\left(\frac{1-e^{-h(t-(m-1)T)}}{h} - \frac{1-e^{-(g+c)(t-(m-1)T)}}{g+c}\right), \\
&\quad -(d+E)(t-(m-1)T) - \frac{rC_{0m-1T}(1-e^{-(g+c)(t-(m-1)T)})}{g+c}.
\end{aligned} \tag{8.3.1}$$

The following map can be obtained from (8.3.1) by applying impulsive conditions (8.2.2):

$$\begin{aligned}
x_{mT} &= x_{m-1}e^{D_1}(1+be^{-x_{(m-1)T}e^{D_1}}) = f(x_{m-1}, C_{0m-1}, C_{E(m-1)}), \\
C_{0mT} &= C_{0m-1}e^{-(g+c)T} + \frac{kC_{Em-1}(e^{-hT} - e^{-(g+c)T})}{(g+c-h)} = g(x_{m-1}, C_{0m-1}, C_{Em-1}), \\
C_{EmT} &= C_{Em-1}e^{-hT} + \mu = \psi(x_{m-1}, C_{0m-1}, C_{Em-1}), \\
D_1 &= -\frac{rC_{0m-1}(1-e^{-(g+c)T})}{g+c} - \frac{krC_{Em-1}}{g+c-h}\left(\frac{1-e^{-hT}}{h} - \frac{1-e^{-(g+c)T}}{g+c}\right) \\
&\quad -(d+E)T.
\end{aligned} \tag{8.3.2}$$

The map (8.3.2) constitutes the difference equations. These equations describe the pest density, toxicant concentration in the pest and toxicant concentration in the environment at m^{th} pulse in terms of values at previous pulse. This is stroboscopic sampling at the time when birth pulse and toxin input in the environment occurs. For the Ricker Function, the dynamical behavior of the system (8.2.1) – (8.2.2) will be given by the dynamical behavior of the map (8.3.2) coupled with system (8.3.1).

The intrinsic net reproductive number R_0 denotes the average number of offspring that a pest produces over the period of its life span. Define:

$$R_0 = \frac{b}{exp\left[dT + ET + \frac{kr\mu}{h(g+c)}\right] - 1} = \frac{b}{b_0}. \tag{8.3.3}$$

8.3.1 Existence of Fixed Points

The fixed points of the map (8.3.2) are obtained by solving the system

$$x = f(x, C_0, C_E), \quad C_0 = g(x, C_0, C_E), \quad C_E = g\psi(x, C_0, C_E).$$

Accordingly, the fixed points can be obtained as follows:

1. The pest-free state $E_0 = (0, C_0, C_E)$ is obtained as:

$$\begin{aligned} C_0 &= \frac{k\mu(e^{-hT} - e^{-(g+c)T})}{(1 - e^{-hT})(g + c - h)(1 - e^{-(g+c)T})}, \\ C_E &= \frac{\mu}{1 - e^{-hT}}. \end{aligned}$$

2. The non-trivial interior fixed point $E^* = (x^*, C_0, C_E)$ is obtained as:

$$x^* = exp\left[dT + ET + \frac{kr\mu}{h(g + c)}\right] \log(R_0).$$

Remark 8.3.1. The interior fixed point E^* exists for $R_0 > 1$, for biological feasible choices of parameters.

Remark 8.3.2. If $R_0 = 1$ then positive interior fixed point collides with the pest-free fixed point, i.e. $E^* = E_0$.

8.3.2 Local Stability Analysis of Fixed Points

Let $X = (x, C_0, C_E)$ be any arbitrary fixed point. The local stability about the feasible fixed points is based upon the standard linearization technique corresponding to (8.3.2) about $X = (x, C_0, C_E)$ is given by:

$$X_m = AX_{m-1}. \tag{8.3.4}$$

where A is the linearized matrix. The fixed point of the system is stable if the eigenvalues $\lambda_i, i = 1, 2, 3$ are less than 1 in magnitude.

Theorem 8.3.1. *The pest-free state $E_0 = (0, C_0, C_E)$ is locally asymptotically stable provided*

$$b < exp\left[dT + ET + \frac{kr\mu}{h(g + c)}\right] - 1 (= b_0) (\text{or} R_0 < 1). \tag{8.3.5}$$

Proof. The coefficients of linearized matrix A are evaluated about the pest-free point $E_0 = (0, C_0, C_E)$ as:

$$a_{11} = \frac{(1+b)}{exp\left[dT + ET + \frac{kr\mu}{h(g+c)}\right]}, \qquad a_{22} = e^{-(g+c)T},$$

$$a_{23} = \frac{k(e^{-hT} - e^{-(g+c)T})}{g+c-h}, \qquad a_{21} = 0, \qquad a_{31} = 0, \qquad a_{32} = 0, \qquad a_{33} = e^{-hT}.$$

Also, the linearized matrix A is the triangular matrix therefore there is no need to find other terms. The eigenvalues of the matrix A are

$$\lambda_1 = (1+b)exp\left[-dT - ET - \frac{kr\mu}{h(g+c)}\right], \qquad \lambda_2 = e^{-gT}, \qquad \lambda_3 = e^{-hT}.$$

It can be easily concluded that $\lambda_2 < 1$ and $\lambda_3 < 1$. The fixed point is stable if all the absolute eigenvalues are less than one. Therefore, the pest-free state E_0 is stable if the condition (8.3.5) is satisfied. □

Accordingly, the pest-free fixed point E_0 is locally stable for $b \in (0, b_0)$. The trajectories in the neighborhood of E_0 tend to $C_0 - C_E$ plane and the pest will be eradicated. Thus, the pest eradication is possible when $R_0 < 1$. However, when the condition $R_0 < 1$ is not satisfied, the pest-free state is locally unstable.

Remark 8.3.3. The stability condition of pest-free state E_0 guarantees the non-existence of E^*.

Remark 8.3.4. The pest-free state will become non-hyperbolic at $b = b_0(R_0 = 1)$. There is a possibility of transcritical bifurcation. Also, at this point E_0 collides with E^*.

Remark 8.3.5. The condition (8.3.5) can be re-written in terms of a threshold E_c on the harvesting rate:

$$E > \frac{1}{T}(\log(b+1) - dT - \frac{kr\mu}{h(g+c)}) = E_c. \tag{8.3.6}$$

The next theorem analyzes the stability of interior fixed point:

Theorem 8.3.2. *The non-trivial fixed point $E^* = (x^*, C_0^*, C_E^*)$ is locally asymptotically stable provided*

$$b_0 < b < b_0 exp\left[2exp\left(dT + ET + \frac{k\mu r}{h(g+c)}\right)b_0^{-1}\right] = b_c. \tag{8.3.7}$$

Proof. The coefficients of the linearized matrix A of the map (8.3.2) around the fixed point $E^* = (x^*, C_0^*, C_E^*)$ are computed as:

$$a_{11} = 1 - \left(1 - exp\left[-dT - ET - \frac{kr\mu}{h(g+c)}\right]\right)\log(R_0), \qquad a_{22} = e^{-(g+c)T},$$

$$a_{23} = \frac{k(e^{-hT} - e^{-(g+c)T})}{g+c-h}, \qquad a_{21} = 0, \qquad a_{31} = 0, \qquad a_{32} = 0, \qquad a_{33} = e^{-hT}.$$

The linearized matrix A is again a triangular matrix. Its eigenvalues are

$$\lambda_1 = 1 - \left(1 - exp\left[-dT - ET - \frac{kr\mu}{h(g+c)}\right]\right)\log(R_0), \quad \lambda_2 = e^{-gT-cT}, \quad \lambda_3 = e^{-hT}.$$

It can be easily concluded that $\lambda_2 < 1$ and $\lambda_3 < 1$. The fixed point is stable if all the absolute eigenvalues are less than one. Therefore, the stability condition of the positive interior fixed point is obtained as (8.3.7). Further, the threshold condition for stability is $b_0 < b < b_c$. □

Also, when $b_0 < b < b_c$, the trajectories of the system (8.2.1) − (8.2.2) tends to asymptotically stable period-1 solution (x_e, C_{0e}, C_{Ee})

$$\begin{aligned}
x_e(t) &= x^* e^{D_2}, \\
C_{0e}(t) &= C_0^* e^{-g(t-mT)} + \frac{kC_E^*(e^{(-h(t-mT))} - e^{-(g+c)(t-mT)})}{(g+c-h)}, \\
C_{Ee}(t) &= C_E^* e^{(-h(t-mT))}, \\
D_2 &= -(d+E)(t-mT) - \frac{rC_0^*(1-e^{-g(t-mT)})}{g+c} \\
&\quad - \frac{krC_E^*}{g+c-h}\left(\frac{1-e^{-h(t-mT)}}{h} - \frac{1-e^{-(g+c)(t-mT)}}{g+c}\right),
\end{aligned}$$

If $b > b_c$, E^* is unstable and a small density of the pest population will be increased from E^*. Further, increasing the parameter value b, the non-trivial fixed point E^* losses its stability and the system may exhibit complex dynamics.

Remark 8.3.6. The interior fixed point will become non-hyperbolic at $b = b_c$ and there exists a flip bifurcation. As, at this point $b = b_c$, when one of the eigenvalues becomes -1.

8.4 Numerical Simulations

The numerical simulations have been carried out in the system (8.2.1) − (8.2.2). The possibility of existence of the periodic solutions and chaotic solutions of the systems

has been explored. Consider the following parameter set:

$$c = .2, d = 0.4, g = 1, h = 1.5, k = 1, r = 2, E = 0.5, \mu = 0.25. \tag{8.4.1}$$

Considering $T = 1.0$ and parameter set (8.4.1), the constant b_0 is computed as $b_0 = 2.2472$. The necessary condition (8.3.5) for the stability of pest-free state is satisfied for $b < 2.2472$. According to Theorem 8.3.1, the pest free fixed point $E_0 = (0, 0.11978, 0.3218)$ of the map (8.3.2) is locally asymptotically stable for $b < 2.2472$.

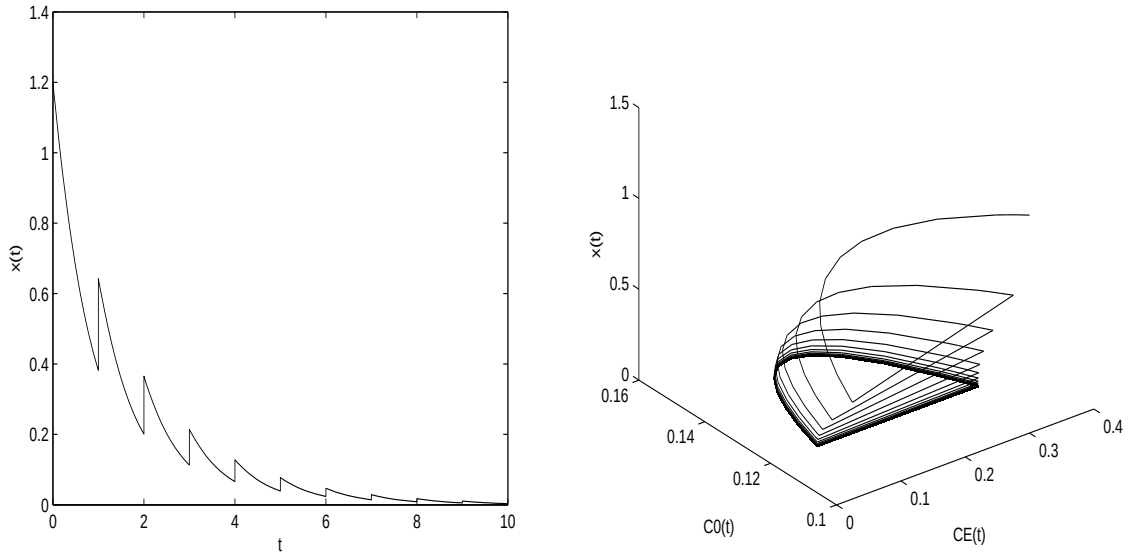

(a) **(b)**

Figure 8.1: (a) Time series (b) Phase plane showing stability of pest-free state of the system (8.2.1) − (8.2.2) at $b = 1$.

Fig. 8.1 displays the stable dynamics of the system (8.2.1) − (8.2.2). The solution converges to the origin showing the pest-extinction. This means that the system (8.2.1) − (8.2.2) is locally asymptotically stable around the pest-free state.

Considering $b = 10$, in this case, the basic reproduction number is obtained as $R_0 = 4.44998 > 1$. According to the Theorem 8.3.1, the pest-free state of the map (8.3.2) is unstable as $b > b_0$ $(R_0 > 1)$. Further, the map (8.3.2) admits a locally stable non-trivial fixed point $E^* = (2.1053, 0.11978, 0.3218)$ for $2.2472 < b < 40.4344$ (Theorem 8.3.2). The transcritical bifurcation occurs at $b = 2.2472$. The system (8.2.1) − (8.2.2) has stable period-1 solution (see Fig. 8.2).

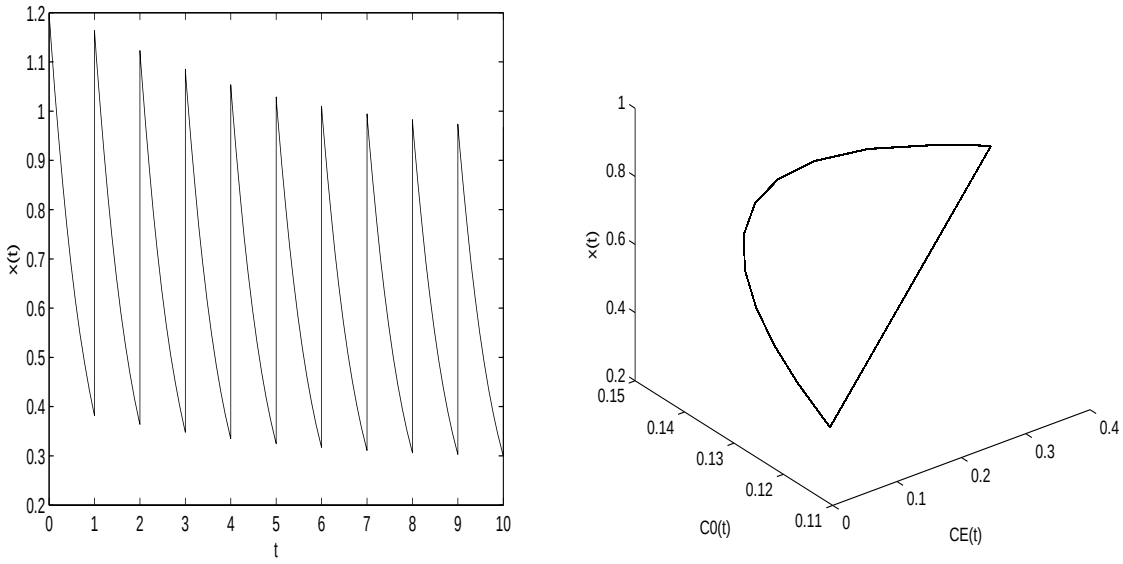

(a) **(a)**

Figure 8.2: (a) Time series (b) Phase plane showing stability of period-1 solution of the system $(8.2.1) - (8.2.2)$ at $b = 3$.

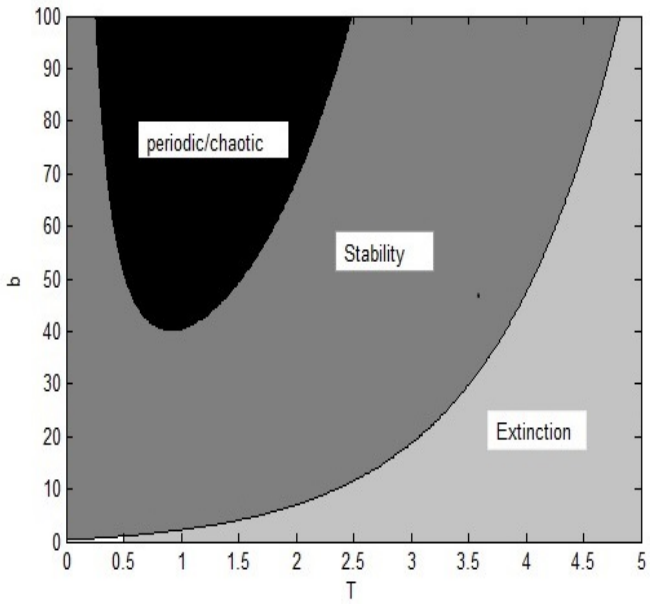

Figure 8.3: Variation of b with T.

In Fig. 8.3, the curve $b = b_0$ and $b = b_c$ corresponding to equation (8.3.3) and (8.3.7) respectively, are drawn on $T - b$ plane, keeping other parameters as in (8.4.1).

This curve bifurcates $T - b$ domain into pest eradication, stable period-1 solution and periodic/chaos regions. In this figure, region of periodic solutions/chaos is shown in black color, while the region of stability is shown by dark-grey color. Due to lower birth, the pest population goes into extinction. This is observed in the region shown in light-grey.

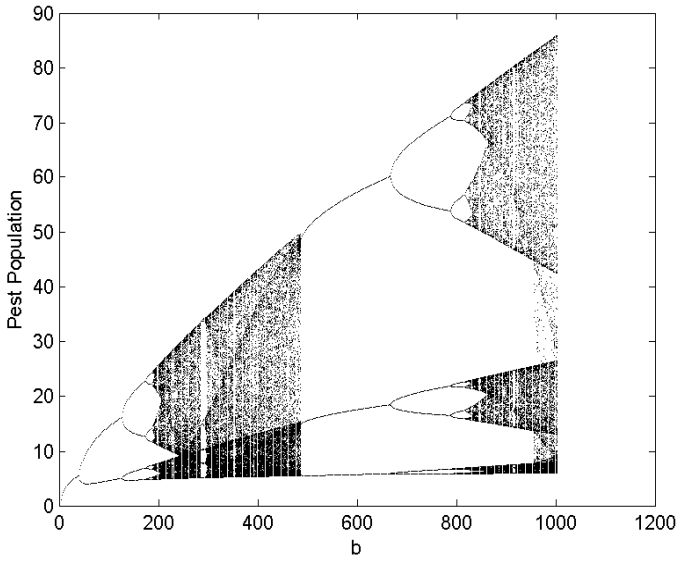

Figure 8.4: Bifurcation diagram of the map (8.3.2) versus pest population with respect to the parameter b.

Table 8.1: Behavior of the impulsive system (8.2.1) − (8.2.2).

Parameter varied	Parameter Value	Dynamical behavior	Figure
$b < 2.2472$	$b = 1$	Pest-free Solution	Fig. 8.1
$b \in (2.2472, 40.4344)$	$b = 3$	Period-1 Solution	Fig. 8.2
$b \in (40.4344, 125.6)$	$b = 50$	Period-2 solution	Fig. 8.5
$b \in (125.6, 174.59)$	$b = 150$	Period-4 solution	Fig. 8.6
$b \in (174.59, 186.41)$	$b = 180$	Period-8 solution	Fig. 8.7
$b \in (186.41, 285.13)$	$b = 250$	Chaotic attractor	Fig. 8.8

To study the complex dynamical behavior, the typical bifurcation diagram is drawn for the pest with respect to critical parameter b in Fig. 8.4. The diagram shows

the existence of chaos through period doubling route. The chaotic region is followed by a region of the period-3 solution in the interval $b \in (487.29, 666.1)$ which again becomes chaotic through period-doubling.

Variety of dynamical behaviors, including periodic solution/chaotic attractor will appear for different values of b. The observations are summarized in Table 8.1. The cascades of period-doubling are observed in the bifurcation diagram which is the route to chaos in the system.

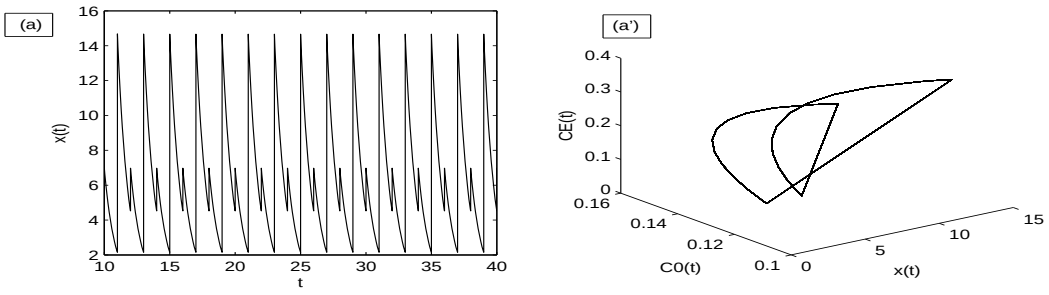

Figure 8.5: (a) Time series (a') Phase portrait showing Period-2 solution of the system (8.2.1) – (8.2.2) at $b = 50$.

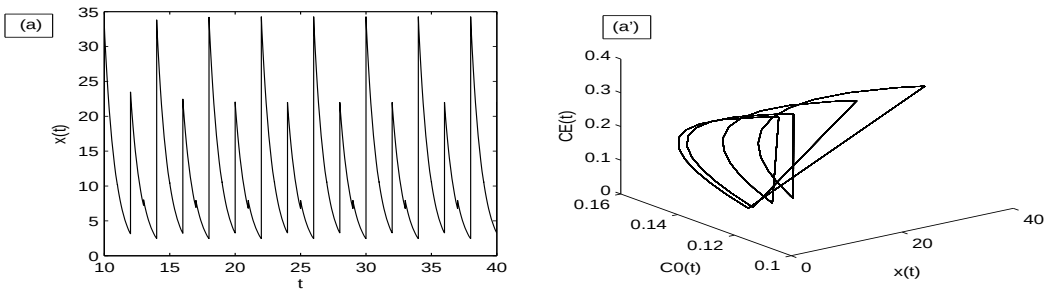

Figure 8.6: (a) Time series (a') Phase portrait showing Period-4 solution of the system (8.2.1) – (8.2.2) at $b = 150$.

The chaotic regions of Fig. 8.4 are separately blown up in Fig. 8.9. The rich dynamical behavior is clearly visible, including stability, period-doubling, narrow and wide periodic windows, crises and chaos. Accordingly, the attractors are drawn in Fig. 8.10 at $b = 400$ and $b = 950$ are strange attractors. The crises are shown in the neighborhood of $b = 300$ in Fig. 8.11.

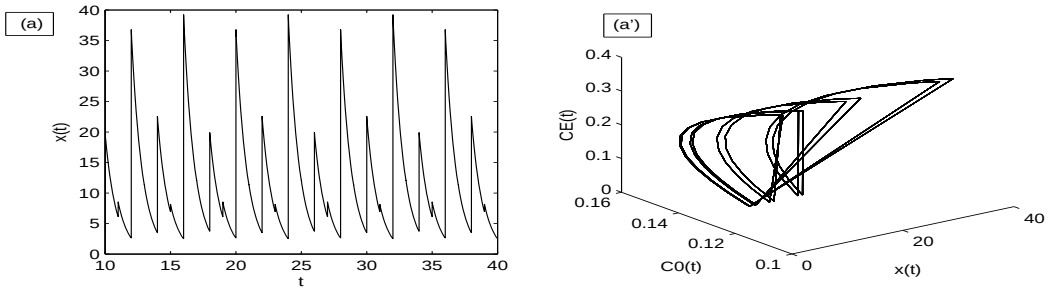

Figure 8.7: (a) Time series (a') Phase portrait showing Period-8 solution of the system (8.2.1) − (8.2.2) at $b = 180$.

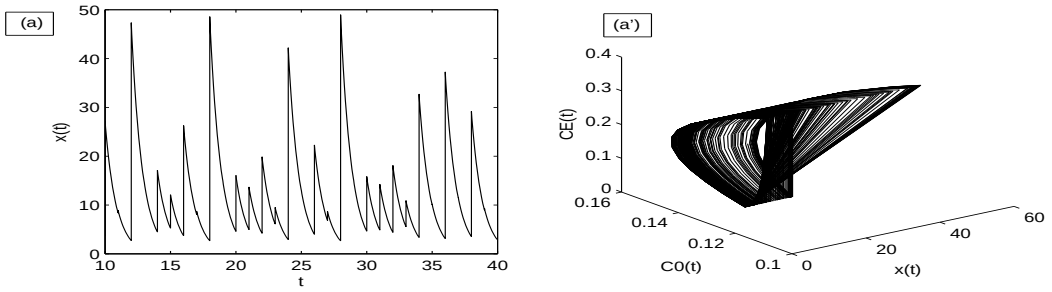

Figure 8.8: (a) Time series (a') Phase portrait showing chaotic attractor of the system (8.2.1) − (8.2.2) at $b = 250$.

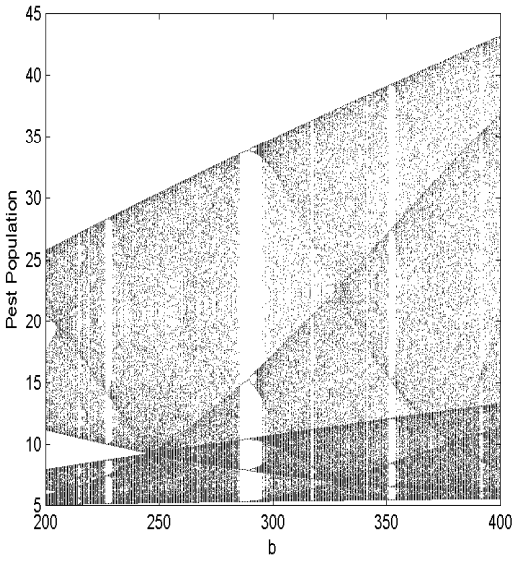

Figure 8.9: The magnified parts of the bifurcation diagram 8.4 in $b \in (200, 400)$.

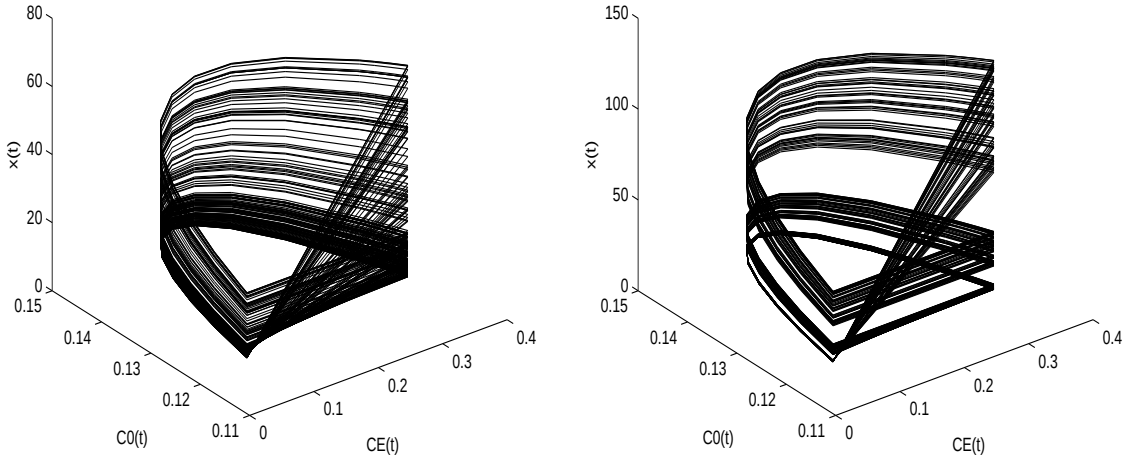

(a) **(b)**

Figure 8.10: Chaotic attractors of the system (8.2.1)−(8.2.2) at (a) $b = 400$ (b) $b = 950$.

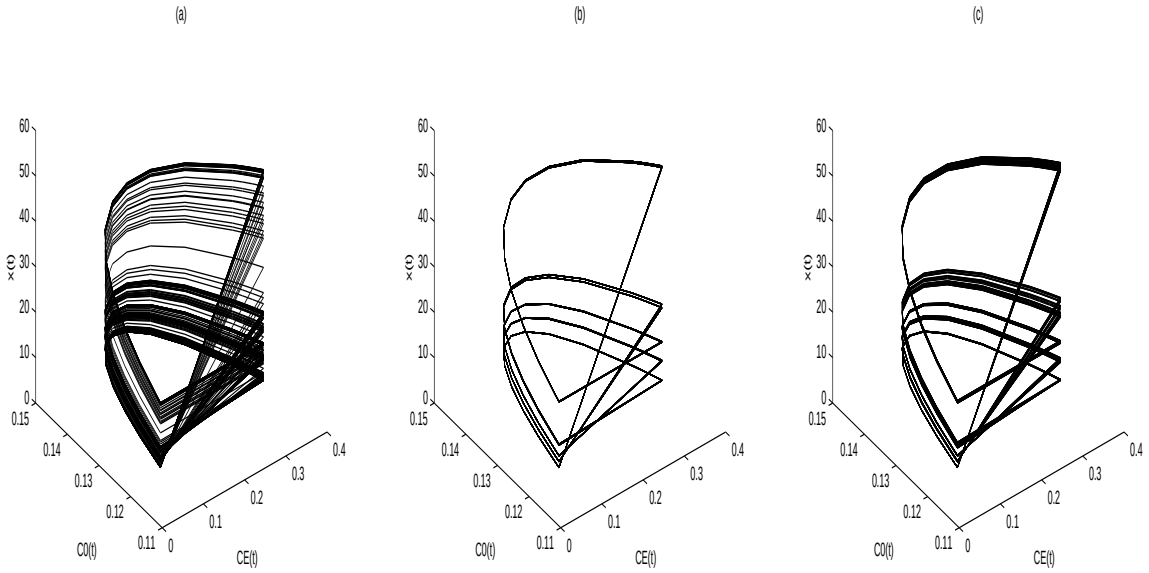

Figure 8.11: Emergence of crises of the system (8.2.1) − (8.2.2) at (a) $b = 285$ (b) $b = 290$ (c) $b = 295$.

Fig. 8.12 depicts the bifurcation diagrams with respect to E for a range of values of b keeping other parameters fixed as mentioned in (8.4.1). It can be observed from these figures that overall complexity increase with an increase in birth rate b. The appearance of period-doubling and period-halving cascade can be observed. For $b = 50$,

$b = 150$, $b = 180$, $b = 182$, periodic solutions occurs while the chaotic behavior does not appear. Period of oscillatory solution increases with the increase in the parameter value of b. For $b = 185$, Fig. 8.12(e) shows the appearance of chaos in a range value of E. For $b = 200$, a chaotic solution may arise for bigger range of harvesting rate of E see Fig. 8.12(f). Very narrow periodic windows can be observed in Fig. 8.12(e) and Fig. 8.12(f). These figures imply that the harvesting rate should be low/high enough to control the pest. Also, it can be observed that the higher birth rate is responsible for the pest outbreak.

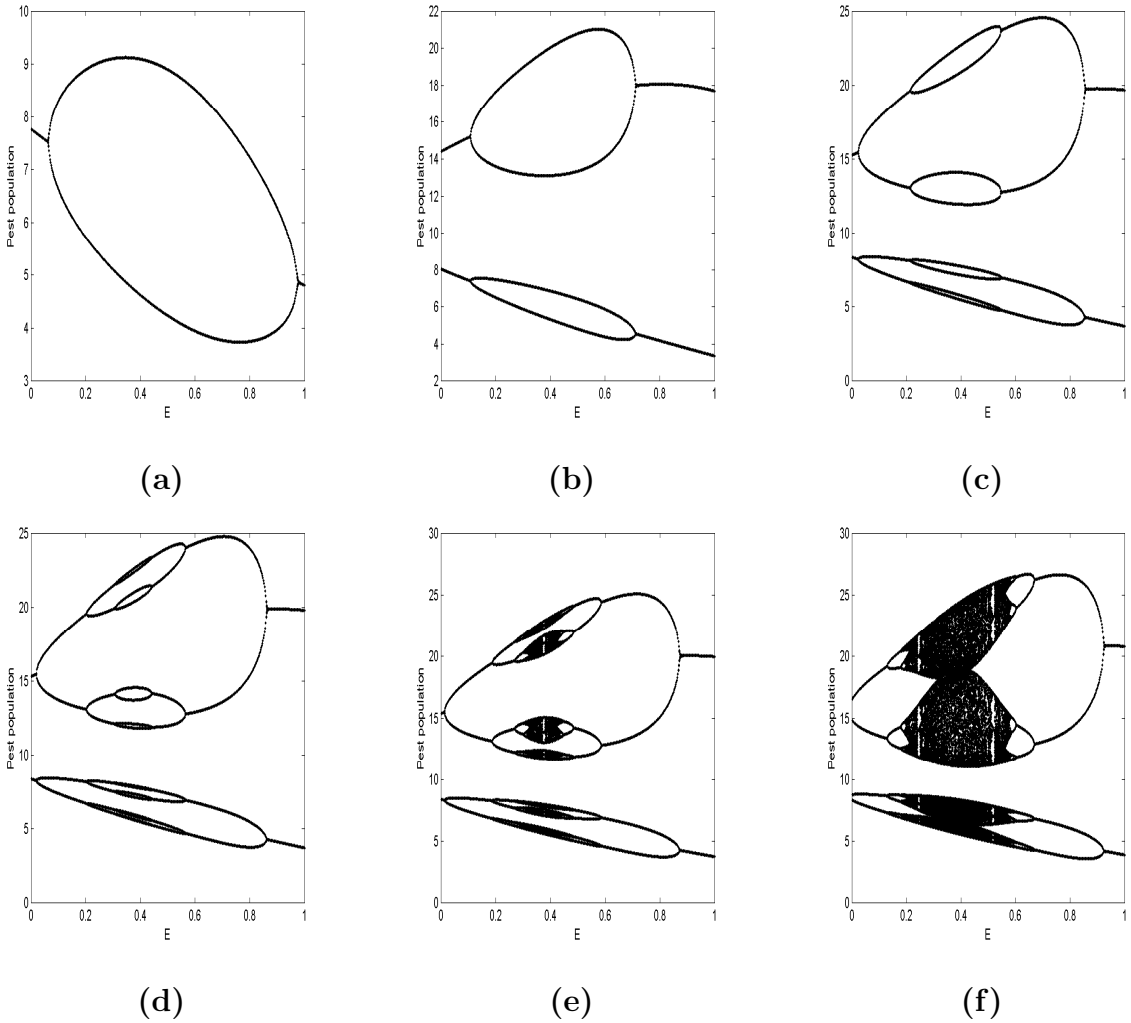

Figure 8.12: Bifurcation diagrams of the map (8.3.2) versus pest population with respect to E at (a) $b = 50$ (b) $b = 150$ (c) $b = 180$ (d) $b = 182$ (e) $b = 185$ (f) $b = 200$.

Now, the effect of impulsive toxicant input in the environment has been explored. In Fig. 8.13, bifurcation diagram is drawn with respect to key parameter μ for the

choice of the parameters as in (8.4.1). Initially, the solution is chaotic. The sensitivity of the solution to initial condition is checked for the range $0 < \mu < 0.32$. The solution is observed to be sensitive. The sensitivity to initial conditions shows the system is chaotic. Further, the periodic nature of the solution is evident in the range $0.34 < \mu < 0.41$ and when $0.32 < \mu < 0.34$ multi-periodicity can be observed. Also, periodic halving behavior can be observed. It may be observed that for a lower input rate of toxicant, the pest will persist. But as the toxicant rate increases, the system is well behaved.

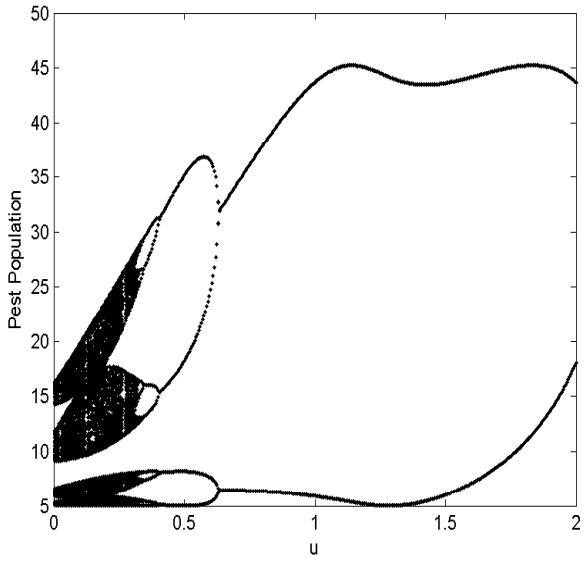

Figure 8.13: Bifurcation diagram of the map (8.3.2) versus pest population with respect to impulsive toxin input μ at $b = 250$.

In Fig. 8.14, bifurcation diagram of the pest population against parameter h is drawn in the interval $0 < h < 1$ with $b = 250$ while all parameters are fixed as in (8.4.1). From, this figure, it can be easily observed that complexity increases with increase in parameter h. A period-doubling cascade can be observed. The periodic solution becomes chaotic after a certain value of h, say h_c. Further, the pest will extinct for $h < 0.1\ (\approx h_k) < h_c$ confirming the result as obtained in Theorem 8.3.1. The sufficiently small toxicant removal from the environment may eradicate the pest successfully. Therefore, indicating a critical value for toxicant removal from the environment may responsible for the pest elimination. These observations suggest that the

rate of change of toxicant from the environment can play a crucial role in eliminating the pest.

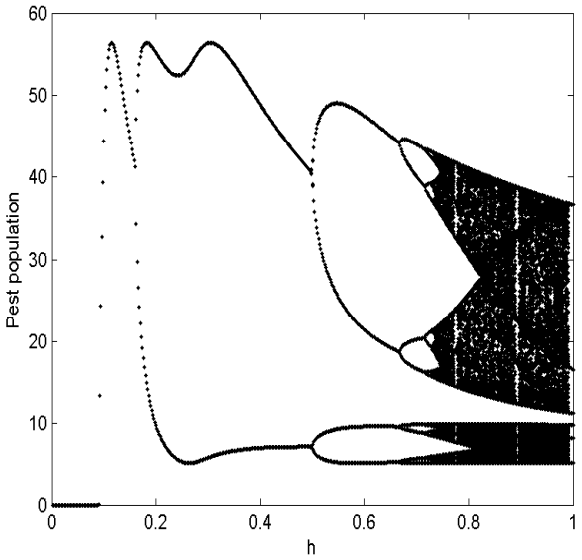

Figure 8.14: Bifurcation diagram of the map (8.3.2) versus pest population with respect to h at $b = 250$.

8.5 Discussion

In this chapter, an impulsive differential model for pest control has been formulated and analyzed. It is also assumed that a constant amount of toxicant enters from the environment at a specific interval of time. The critical values of birth rate b_0 and b_c are obtained. It can be concluded that $b < b_0$ the pest can be effectively controlled. When the harvesting effort increases beyond the critical value E_c then the pest will be eradicated. Numerical simulations have been carried out for resulting impulsive system which reveals that the impulsive system have a variety of dynamical properties including complex dynamical behavior. It can be concluded from the numerical simulation that for $h < h_k$ and $b < b_0$, the pest can be eradicated. Further, for birth rate b and removal rate of toxicant h satisfying $b > b_0$ and $h > h_k$ respectively, the pest will persist.

Chapter 9

Dynamics of Integrated Pest Management System with State Dependent Control

9.1 Introduction

Many impulsive models that incorporate various IPM strategies have been discussed [64, 137, 147, 178, 216, 217, 233]. These strategies include periodic spraying of pesticides [125] and/or release of natural enemies of pest [158, 170, 185]. These are applied at predetermined times, irrespective of the state of the system at that time. In recent years, several researchers have started paying attention to another control measure based on the state feedback control strategy in which control tactics are applied when the population reaches a threshold level [91, 92, 94, 95]. The state-dependent methods are more effective and economical for pest control [169, 237, 244]. However, state-dependent impulses have been relatively less studied due to underlying difficulties in analyzing state dependent control systems [12, 202]. Dynamics of impulsive pest control models incorporating state-dependent strategy have been addressed in [214, 229].

When biological control is applied delay differential equations are formulated to incorporate discrete time delay due to the gestation/maturation time of natural enemy. Very few models are available incorporating delay and state-dependent impulses

[43, 44]. Due to the time delay in the non-autonomous delay differential equations, a stable equilibrium can become unstable and have complex dynamics [36, 60, 143]. It is an important component in pest management systems. Anuraj et al. have discussed State-dependent impulsive control of a prey-predator system with gestation delay [203].

In this chapter, an integrated pest control model with state-dependent feedback control is considered. It is assumed that the natural enemy is introduced to annihilate the pest. Chemical control is also applied affecting pest as well as a natural enemy. Control is applied when the pest density reaches a critical level. The problem is formulated as a state-dependent impulsive pest-natural enemy system. The model also incorporates a delay due to maturation of natural enemy. The dynamic of the underlying model is analyzed and numerical simulations are performed.

9.2 The Mathematical Model

Let $x(t)$ and $y(t)$ be the respective densities of prey and predator at the time t. The predator is taking food from the prey. The predator-prey model is considered with Holling type II functional response and maturation delay in predator dynamics. The mortality rate of the predator in the absence of prey is assumed to be constant. Assuming logistically growing prey, the predator-prey dynamics is governed by the following system of equations:

$$\begin{aligned} \frac{dx}{dt} &= x(1-x) - \frac{ax(t)y(t-\tau)}{x(t)+k}, \\ \frac{dy}{dt} &= \frac{rx(t)y(t-\tau)}{x(t)+k}) - dy(t). \end{aligned} \tag{9.2.1}$$

The above system is subjected to the initial conditions

$$\begin{aligned} &x(\theta) = \phi_1(\theta), \qquad y(\theta) = \phi_2(\theta) \qquad \forall \qquad \theta \in [-\tau, 0], \\ &(\phi_1, \phi_2) \in C([-\tau, 0], \Re^2_+), \qquad \phi_i(0) \geq 0, \quad i = 1, 2.. \end{aligned}$$

All model parameters have usual meaning and assumed to be positive.

Many investigations have been made on the model (9.2.1). The delay model (9.2.1) has equilibrium point $(0, 0)$ which is saddle [55]. Also, the complex dynamical behavior has been observed due to delay. In the scenario of pest management, for the

system (9.2.1), there is no stable pest-eradication solution and such types of approaches are not effective for pest control. The model (9.2.1) is modified with state-dependent impulsive strategies and integrated pest management. The chemical, as well as biological control, are applied. The model formulation considers following assumptions:

- Pest is controlled by poisoning (or catching) pest population and releasing its natural enemy. The control is applied when the pest population reached at threshold value l at the time $t_i(l)$, $i = 1, 2, 3, \ldots$. At such times, a constant fraction μ of natural enemies are released increasing its density instantaneously.

- The pesticide spray instantaneously kills a portion of pest and natural enemy. No residual effect is considered for pesticide. Accordingly, the pesticide spray is modeled as impulsive phenomenon. As pesticides affect pest and natural enemy differently, therefore the respective killing rates are α and $\beta <$, $0 < \alpha, \beta < 1$. Chemical and biological control are applied concurrently at $t = t_i(l)$ then the impulsive conditions become:

$$x(t)^+ = (1-\alpha)x(t), \quad y(t)^+ = (1-\beta+\mu)y(t), \quad x(t) = l.$$

The dynamics of the impulsive pest control system with state dependent strategy is defined on the set $\Re^2_+ = \{(x, y) \in \Re^2 \mid x \geq 0, y \geq 0\}$ with positive model parameter. The IPM model with above assumptions is modeled by the following impulsive system:

$$\left.\begin{array}{l} \dfrac{dx}{dt} = x(1-x) - \dfrac{ax(t)y(t-\tau)}{x(t)+k} = F_1(x(t), y(t)), \\ \dfrac{dy}{dt} = \dfrac{rx(t)y(t-\tau)}{x(t)+k}) - dy(t) = F_2(x(t), y(t)), \end{array}\right\} x(t) \neq l, \tag{9.2.2}$$

$$\left.\begin{array}{l} x(t)^+ = (1-\alpha)x(t), \\ y(t)^+ = (1-\beta)y(t) + \mu y(t), \end{array}\right\} x(t) = l. \tag{9.2.3}$$

The dynamical properties for solutions of the system (9.2.2) − (9.2.3) are discussed under the assumptions that μ is a control parameter for fixed α, β and l. In this chapter, it is assumed that $l < 1$ because the maximum carrying capacity of the pest is 1.

9.3 Preliminary Analysis

Some preliminary results are stated to show that the model is well behaved. It may be considered that $F_1(x, y)$ and $F_2(x, y)$ are piecewise continuously differentiable functions then the pest control impulsive system $(9.2.2) - (9.2.3)$ has non-negative initial conditions.

9.3.1 Boundedness

Theorem 9.3.1. *The system* $(9.2.2) - (9.2.3)$ *has an ultimately bounded solution.*

Proof. The first equations of system (9.2.2) and (9.2.3) gives:

$$\begin{aligned} \frac{dx}{dt} &\leq x(t)(1-x(t)), & x(t) \neq l, \\ x(t)^+ &= (1-\alpha)x(t), & x(t) = l. \end{aligned}$$

Let $x = \widehat{x}(t)$ be the solution of the following impulsive differential equation

$$\begin{aligned} \frac{d\widehat{x}(t)}{dt} &= \widehat{x}(t)(1-\widehat{x}(t)), & \widehat{x}(t) \neq l, \\ \widehat{x}(t)^+ &= (1-\alpha)\widehat{x}(t), & \widehat{x}(t) = l, \\ \widehat{x}(0) &= \phi_1(0). \end{aligned}$$

Solving the above system between $t_k \leq t \leq t_{k+1}, k = 1, 2, 3, 4, ...$

$$\widehat{x}(t) = \frac{(1-\alpha)le^{(t-t_k)}}{1-(1-\alpha)l+(1-\alpha)le^{(t-t_k)}} < 1.$$

The pest population just after $(k+1)^{th}$ pulse becomes

$$\widehat{x}(t_{k+1}) = \frac{(1-\alpha)}{\dfrac{1-(1-\alpha)lb}{(1-\alpha)le^{(t_{k+1}-t_k)}}+b} < 1-\alpha < 1.$$

Hence, it can be observed $\widehat{x}(t) < 1$. The standard comparison theorem of impulsive differential equation [12] yields:

$$\limsup_{t\to\infty} x(t) \leq 1.$$

Hence, $x(t)$ of the system $(9.2.2) - (9.2.3)$ is bounded for $t \to \infty$. The second equation of the system (9.2.2) and impulsive condition (9.2.3) gives:

$$\begin{aligned} \frac{dy}{dt} &= \frac{rx(t)y(t-\tau)}{x(t)+k}) - dy(t), & x(t) \neq l, \\ y(t)^+ &= (1-\beta)y(t) + \mu y(t), & x(t) = l. \end{aligned}$$

Let $\widehat{y}(t)$ be the solution of the above impulsive differential equation and for $x(t) \leq 1$:

$$\frac{d\widehat{y}(t)}{dt} < \frac{ry(t-\tau)}{1+k}) - dy(t).$$

On simplification,it yields

$$\widehat{y}(t) < e^{-dt} \int_0^t e^{ds} \frac{ry(s-\tau)}{1+k}) ds + C_0 e^{-dt}.$$

Solving, between the pulse $t_{k+1}^+ \leq t \leq t_{k+1} + \tau,\ k = 1, 2, 3, ...$

$$\widehat{y}(t) < (1 - \beta + \mu) y(t_k^+) e^{-d(t-t_k^+)} + \mu.$$

By continuity of y in $t_{k+1}^+ \leq t \leq t_{k+1} + \tau$

$$\widehat{y}(t) \to 0 \quad \text{as} \quad t \to \infty.$$

Using comparison theorem of impulsive differential equation for $t \to \infty$.

$$\limsup_{t \to \infty} y(t) = 0.$$

and $y(t)$ is bounded. Therefore, the solutions of the system (9.2.2) – (9.2.3) are ultimately bounded. □

9.3.2 Poincare Map

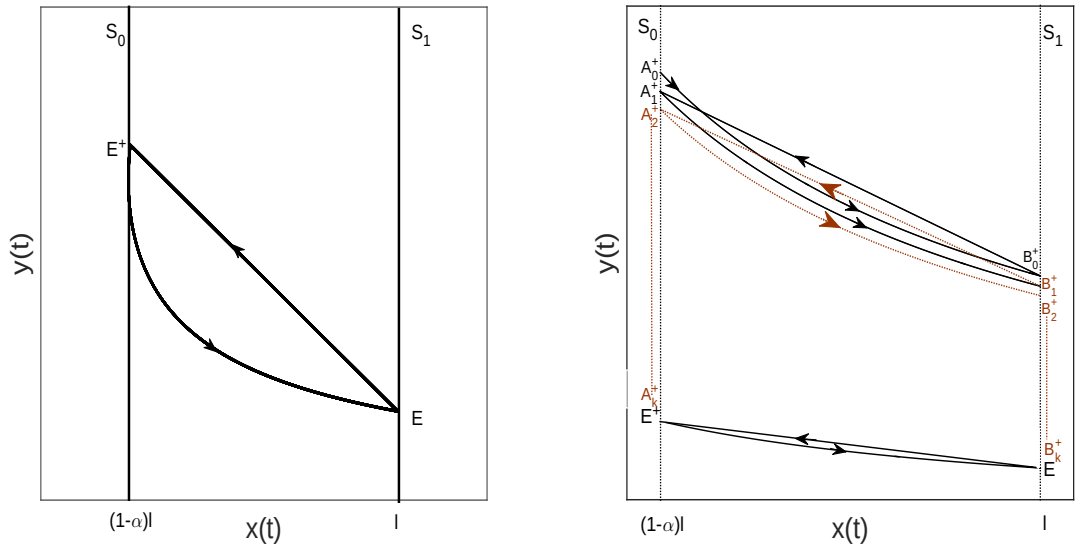

Figure 9.1: (a) Period-1 solution (b) Distributed solution with periodic solution of the system (9.2.2) – (9.2.3).

In this section, the Poincare map is described which is used as a tool to discuss the dynamics of the system (9.2.2) – (9.2.3).

Let us consider the sections S_0 and S_1 of the $x-y$ phase plane as:

$$\begin{aligned} S_0 &= \{(x,y) : x = (1-\alpha)l, y_0 \geq 0\}, \\ S_1 &= \{(x,y) : x = l, y_0 \geq 0\}. \end{aligned}$$

An approximate formula will be used to establish the Poincare map of S_1. Consider that the system (9.2.2) – (9.2.3) has a positive period-1 solution $(\xi(t), \eta(t))$ with period T. The periodic trajectory with the initial point $p_0 = E^+ = ((1-\alpha)l, y_0)$ on S_0 intersects the Poincare section S_1 at the point $E = (l, y_1)$. After that it jumps to the point $E^+ = ((1-\alpha)l, y_0)$ on the Poincare section S_0 due to the impulsive effects (9.2.3) with $x(t^+) = (1-\alpha)x(t)$ and $y(t^+) = (1-\beta+\mu)y(t)$ (See Fig. 9.1). Thus

$$\xi(0) = (1-\alpha)l, \quad \eta(0) = y_0, \quad \xi(T) = l, \quad \eta(T) = \frac{y_0}{(1-\beta+\mu)} = y_1.$$

Now, consider another solution $(\bar{\xi}(t), \bar{\eta}(t))$ with slightly perturbed initial values $\bar{\xi}(0) = (1-\alpha)l$ and $\bar{\eta}(0) = y_0 + \delta y_0$ on S_0. The disturbed trajectory starting from the point $A_0^+((1-\alpha)l, y_0 + \delta y_0)$,where ($\delta y_0$ is very small) first intersects the Poincare section S_1 at the point $B_0^+(l, \bar{y_1})$ when $t = T + \delta t$. After that, it jumps to the point $A_1^+((1-\alpha)l, \bar{y})$ on S_0. Therefore,

$$\bar{\xi}(0) = (1-\alpha)l, \quad \bar{\eta}(0) = y_0 + \delta y_0, \quad \bar{\xi}(T+\delta t) = l, \quad \bar{\eta}(T+\delta t) = \bar{y_1}.$$

Now, difference between the undisturbed $(\xi(t), \eta(t))$ and disturbed $(\bar{\xi}(t), \bar{\eta}(t))$ trajectories are denoted by $(\delta x, \delta y)$ where $\delta x = \bar{\xi}(t) - \xi(t)$ and $\delta y = \bar{\eta}(t) - \eta(t)$. Therefore,

$$\delta x(0) = x_0 = \bar{\xi}(0) - \xi(0), \quad \delta y(0) = \delta y_0 = \bar{\eta}(0) - \eta(0) = \mid \overline{A_0^+ E^+} \mid .$$

Consider $\delta y_1 = \mid \overline{A_1^+ E^+} \mid = \bar{y_2} - y_0$ and $\delta y_0^* = \bar{y_1} - y_1 = \mid \overline{B_0^+ E} \mid$. Now the relation between δy_0 and δy_1 will be calculated. It is known that, for $0 < t < T$, the variables δx and δy are described by the relation

$$\begin{pmatrix} \delta x(t) \\ \delta y(t) \end{pmatrix} = M(t) \begin{pmatrix} \delta x_0 \\ \delta y_0 \end{pmatrix} + O(\delta x_0^2 + \delta y_0^2) \simeq M(t) \begin{pmatrix} 0 \\ \delta y_0 \end{pmatrix} + O \begin{pmatrix} 0 \\ \delta y_0^2 \end{pmatrix} \quad (9.3.1)$$

Here, the fundamental solution matrix $M(t)$ satisfies the variational matrix equation

$$\frac{dM(t)}{dt} = A(t) * M(t), \quad M(0) = I_2(\text{identity matrix}). \quad (9.3.2)$$

The coefficients of the variational matrix $A(t)$ are calculated along the periodic trajectory $(\xi(t), \eta(t))$ corresponding to the system (9.2.2) – (9.2.3)

$$A(t) = \begin{pmatrix} \frac{\partial F_1}{\partial x} & \frac{\partial F_1}{\partial y} \\ \frac{\partial F_2}{\partial x} & \frac{\partial F_2}{\partial y} \end{pmatrix}. \tag{9.3.3}$$

Let

$$\begin{aligned} F_1(\xi(t), \eta(t)) &= \xi(t)\left(1 - \xi(t) - \frac{a\eta(t-\tau)}{\xi(t)+k}\right), \\ F_2(\xi(t), \eta(t)) &= \frac{r\eta(t-\tau)\xi(t)}{(1-p)\xi(t)+k} - d\eta(t). \end{aligned}$$

The disturbed trajectory $(\bar{\xi}(t), \bar{\eta}(t))$ in a first-order Taylor's expansion for $t = T + \delta t$ can be expressed as:

$$\bar{\xi}(T+\delta t) \approx \xi(T) + \delta x(T) + F_1(\xi(T), \eta(T))\delta t. \tag{9.3.4}$$

$$\bar{\eta}(T+\delta t) \approx \eta(T) + \delta y(T) + F_2(\xi(T), \eta(T))\delta t. \tag{9.3.5}$$

As $\bar{\xi}(T+\delta t) = \xi(T) = l$, from (9.3.4)

$$\delta t = -\frac{\delta x(T)}{F_1(T)}. \tag{9.3.6}$$

It follows from (9.3.5)

$$\delta y_0^* = \bar{y_1} - y_1 = \mid \overline{B_0 E} \mid = \delta y(T) + F_2(T)\delta t. \tag{9.3.7}$$

Hence,

$$\delta y_0^* = \delta y(T) - \frac{F_2(T)\delta x(T)}{F_1 T}. \tag{9.3.8}$$

As $\bar{y_2} = (1 - \beta + \mu)\bar{y_1}$, it is concluded that $\delta y_1 = \bar{y_2} - y_0 = (1 - \beta + \mu)(\bar{y_1} - y_1)$. Thus $\delta y_1 = (1 - \beta + \mu)\delta y_0^*$. Substituting the value of δy_0^* from (9.3.8) , the Poincare map f of S_0 can be constructed as follows:

$$\delta y_1^* = f(\beta, \delta y_0) = (1 - \beta + \mu)\left[\delta y(T) - \frac{F_2(T)\delta x(T)}{F_1 T}\right]. \tag{9.3.9}$$

where, $\delta x(T)$ and $\delta y(T)$ are calculated from (9.3.1).

Now, another type of Poincare maps will be considered. Suppose that, the point $B_k^+(l, y_k)$ is on the Poincare section S_1. Then $A_k^+((1-\alpha)l, (1-\beta+\mu)y_k)$ is on Poincare

map S_0 due to the impulsive effects (9.2.3). The trajectory with initial point A_k^+ intersects Poincare section S_1 at the point $B_{k+1}^+(l, y_{k+1})$ where y_{k+1} is calculated by y_k and the parameters β and μ. Thus Poincare map F can be obtained as follows:

$$y_{k+1} = f(\beta, \mu, y_k). \tag{9.3.10}$$

The function f is continuous on β, μ and y_k because solutions are dependent on the initial conditions. It can be observed that for each fixed point of the map f (9.3.10) there is an associated periodic solution of the system (9.2.2) − (9.2.3), and vice versa.

9.4 Existence of Semi-trivial Periodic Solution and Its Stability

The existence of a semi periodic solution is established in the following theorem.

Theorem 9.4.1. *The system* (9.2.2) − (9.2.3) *admits semi-trivial periodic solution* $(\xi(t), \eta(t))$*:*

$$\left.\begin{aligned} \xi(t) &= \frac{(1-\alpha)le^{(t-(k-1)T)}}{1-(1-\alpha)l+(1-\alpha)le^{(t-(k-1)T)}}, \\ \eta(t) &= 0, \end{aligned}\right\} (k-1)T \le t \le kT, \tag{9.4.1}$$

with the pulse period

$$T = \ln \frac{1-(1-\alpha)l}{(1-\alpha)(1-l)}.$$

Proof. Consider $y(t) = 0$ in the system (9.2.2) − (9.2.3) for $t \in (0, \infty)$ to calculate a semi-trivial periodic solution for the system:

$$\begin{aligned} \dot{x}(t) &= x(1-x), & x \neq l, \\ x(t)^+ &= (1-\alpha)x, & x = l. \end{aligned} \tag{9.4.2}$$

Setting the initial value as $x_0 = x(0) = (1-\alpha)l$, the solution of the equation $\dfrac{dx}{dt} = x(t)(1-x(t))$ is

$$x(t) = \frac{Ce^t}{1+Ce^t}. \tag{9.4.3}$$

The arbitrary constant can be computed as $C = \dfrac{(1-\alpha)l}{1-(1-\alpha)l}$.

Now, assume that $x(0) = x((k-1)T) = (1-\alpha)l$. Then at $t = (k-1)T$,

$$x(t) = \frac{(1-\alpha)le^{t-(k-1)T}}{1-(1-\alpha)l+(1-\alpha)le^{t-(k-1)T}}. \tag{9.4.4}$$

When $x(T) = l$ and $x(T)^+ = x_0$, the pulse period $T = \ln \dfrac{1-(1-\alpha)l}{(1-\alpha)((1-l)}$.

Hence, the system (9.2.2)−(9.2.3) admits the semi-trivial periodic solution (9.4.1) with period T for $(k-1)T \leq t \leq kT$. □

The stability of the periodic semi-trivial solution (9.4.1) of the system (9.2.2) − (9.2.3) is obtained with the help of Poincare map (9.3.9).

Suppose that delay $\tau > 0$ is sufficiently small so that the natural enemy density does not vary rapidly and $y(t)$ can be approximated as $y(t-\tau) = y(t) - \tau\dot{y}(t)$. The system (9.2.2) − (9.2.3) can be rewritten as:

$$\left.\begin{aligned} \frac{dx}{dt} &= x(t)(1-x(t)) - \frac{ax(t)(y(t)-\tau\dot{y}(t))}{x(t)+k}, \\ \frac{dy}{dt} &= \frac{rx(t)(y(t)-\tau\dot{y}(t))}{x(t)+k} - dy(t), \end{aligned}\right\} x(t) \neq l, \tag{9.4.5}$$

$$\left.\begin{aligned} x(t)^+ &= (1-\alpha)x(t), \\ y(t)^+ &= (1-\beta)y(t) + \mu y(t), \end{aligned}\right\} x(t) = l. \tag{9.4.6}$$

With this approximation, after rearranging the terms in the system (9.4.5) − (9.4.6), the model (9.2.2) − (9.2.3) can be rewritten as:

$$\left.\begin{aligned} \frac{dx}{dt} &= x(t)(1-x(t)) - \frac{a(1+d\tau)x(t)y(t)}{(1+r\tau)x(t)+k} = G_1(x,y), \\ \frac{dy}{dt} &= \frac{r(1+\tau d)x(t)y(t)}{(1+r\tau)x(t)+k} - dy(t) = G_2(x,y), \end{aligned}\right\} x(t) \neq l, \tag{9.4.7}$$

$$\left.\begin{aligned} x(t)^+ &= (1-\alpha)x(t), \\ y(t)^+ &= (1-\beta)y(t) + \mu y(t), \end{aligned}\right\} x(t) = l. \tag{9.4.8}$$

Theorem 9.4.2. *The semi-trivial periodic solution* $(\xi(t), 0)$ *of the system* (9.2.2) − (9.2.3) *is stable provided*

$$0 < \mu < \mu_0, \tag{9.4.9}$$

where

$$\mu_0 = \left[\frac{[(1+r\tau)l + k(1-l) + l](1-(1-\alpha)l)}{[(1+r\tau)(1-\alpha)l + k](1-l)}\right]^{\frac{-r(1+\tau d)}{(1+r\tau)+k}} \left[\frac{(1-\alpha)(1-l)}{1-(1-\alpha)l}\right]^{-d} - 1 + \beta.$$

Proof. Using (9.3.2) with the linearized matrix of the delayed system (9.4.7) − (9.4.8) about the semi-trivial periodic solution $(\xi(t), 0)$, the matrix $M = (m_{ij})_{2\times 2}$ is given by:

$$\frac{dM(t)}{dt} = \begin{pmatrix} 1-2\xi(t) & -\dfrac{a(1+d\tau)\xi}{(1+r\tau)\xi(t)+k} \\ 0 & \dfrac{r(1+\tau d)\xi(t)}{(1+r\tau)\xi(t)+k} - d \end{pmatrix} * M(t), \quad M(0) = I_2. \tag{9.4.10}$$

Let

$$M(t) = \begin{pmatrix} m_{11} & m_{12} \\ m_{21} & m_{22} \end{pmatrix}. \tag{9.4.11}$$

For $0 < t < T$, using (9.4.10) and (9.4.11):

$$\begin{cases} \dot{m_{11}}(t) = (1-2\xi(t))m_{11}(t) - \dfrac{a(1+d\tau)\xi}{(1+r\tau)\xi(t)+k} m_{21}(t), \\ \dot{m_{12}}(t) = (1-2\xi(t))m_{12}(t) - \dfrac{a(1+d\tau)\xi}{(1+r\tau)\xi(t)+k} m_{22}(t), \\ \dot{m_{21}}(t) = \left(\dfrac{r(1+\tau d)\xi(t)}{(1+r\tau)\xi(t)+k} - d\right) m_{21}(t), \\ \dot{m_{22}}(t) = \left(\dfrac{r(1+\tau d)\xi(t)}{(1+r\tau)\xi(t)+k} - d\right) m_{22}(t), \end{cases} \tag{9.4.12}$$

where,

$$M(0) = \begin{pmatrix} 1 & 0 \\ 0 & 1 \end{pmatrix}.$$

For $0 < t < T$, observe that, $\delta x(0) = 0 = \delta x_0$ and

$$G_2(t) = \left(\frac{r\xi(t)}{\xi(t)+k} - d\right) \times 0 = 0,$$

then

$$\delta y_1 = f(\beta, \mu, \delta y_0) = (1-\beta+\mu)\left(\delta y(T) - \frac{G_2(T)\delta x(T)}{G_1 T}\right) = (1-\beta+\mu)\delta y(T)$$

$$= (1-\beta+\mu)(m_{21}(T)\delta x_0 + m_{22}(T)\delta y_0) = (1-\beta+\mu)m_{22}(T)\delta y_0.$$

Now, it is only necessary to calculate $m_{22}(t)$. From the fourth equation of (9.4.12), it can be obtained that

$$m_{22}(t) = Aexp\left(\int \left(\frac{r(1+\tau d)\xi(t)}{(1+r\tau)\xi(t)+k} - d\right)dt\right)$$

$$= Aexp\left(\int \left(\frac{r(1+\tau d)ce^t}{[(1+r\tau)c+c]e^t+k} - d\right)dt\right)$$

$$= A[((1+r\tau)c+c)e^t+k]^{\frac{r(1+\tau d)}{(1+r\tau)+k}}.e^{-dt}.$$

For $t = 0$,

$$m_{22}(0) = A[((1 + r\tau)c + c) + k]^{\frac{r(1+\tau d)}{(1+r\tau)+k}} = 1,$$

then

$$A = [((1 + r\tau)c + c) + k]^{\frac{-r(1+\tau d)}{(1+r\tau)+k}}.$$

Now,

$$m_{22}(t) = [((1 + r\tau)c + c) + k]^{\frac{-r(1+\tau d)}{(1+r\tau)+k}}[((1 + r\tau)c + c)e^t + k]^{\frac{r(1+\tau d)}{(1+r\tau)+k}}.e^{-dt}$$

$$= \frac{[((1 + r\tau)c + c)e^t + k]}{[((1 + r\tau)c + c) + k]}^{\frac{r(1+\tau d)}{(1+r\tau)+k}} e^{-dt}.$$

Since

$$T = \ln \frac{1 - (1 - \alpha)l}{(1 - \alpha)(1 - l)}, \quad e^T = \frac{1 - (1 - \alpha)l}{(1 - \alpha)(1 - l)}, \quad C = \frac{(1 - \alpha)l}{1 - (1 - \alpha)l}.$$

Therefore,

$$m_{22}(T) = \left[\frac{[(1 + r\tau)l + k(1 - l) + l](1 - (1 - \alpha)l)}{[(1 + r\tau)(1 - \alpha)l + k](1 - l)}\right]^{\frac{r(1+\tau d)}{(1+r\tau)+k}} \left[\frac{(1 - \alpha)(1 - l)}{1 - (1 - \alpha)l}\right]^d.$$

Now,

$$\delta y_1 = (1-\beta+\mu)\left[\frac{[(1 + r\tau)l + k(1 - l) + l](1 - l(1 - \alpha))}{[l(1 + r\tau)(1 - \alpha) + k](1 - l)}\right]^{\frac{r(1+\tau d)}{(1+r\tau)+k}} \left[\frac{(1 - \alpha)(1 - l)}{1 - (1 - \alpha)l}\right]^d \delta y_0.$$

Observe that, $\delta y_0 = 0$ is a fixed point of $f(\beta, \mu, \delta y_0)$ and

$$D_{\delta y_0} f(\beta, \mu, 0) = (1 - \beta + \mu)m_{22}(T)$$

$$= (1 - \beta + \mu)\left[\frac{[(1 + r\tau)l + k(1 - l) + l](1 - (1 - \alpha)l)}{[(1 + r\tau)(1 - \alpha)l + k](1 - l)}\right]^{\frac{r(1+\tau d)}{(1-p)(1+r\tau)+k}} \left[\frac{(1 - \alpha)(1 - l)}{1 - (1 - \alpha)l}\right]^d.$$

The system will be stable when $0 < D_{\delta y_0} f(\beta, 0) < 1$ with $l < 1$. That is,

$$0 < \mu < \mu_0.$$

Hence, the system (9.2.2) – (9.2.3) has a stable semi-trivial periodic solution under the condition (9.4.9). □

Remark 9.4.1. For small delay, the semi-trivial periodic solution of the system (9.2.2)– (9.2.3) is unstable if $\mu > \mu_0$.

Remark 9.4.2. Let

$$\mu_0 = \left[\frac{[(1 + r\tau)l + k(1 - l) + l](1 - (1 - \alpha)l)}{[(1 + r\tau)(1 - \alpha)l + k](1 - l)}\right]^{\frac{-r(1+\tau d)}{(1+r\tau)+k}} \left(\frac{(1 - \alpha)(1 - l)}{1 - (1 - \alpha)l}\right)^{-d} - 1 + \beta.$$

A bifurcation occurs at $\mu = \mu_0$ since $D_{\delta y_0} f(\beta, \mu, 0) = 1$.

9.5 Existence of Positive Period-1 Solution and Its Stability

In this section, existence of periodic solution of the system (9.2.2) − (9.2.3) and its stability will be carried out for $\mu > \mu_0$.

The semi-trivial periodic solution passing through the points $A((1-\alpha)l, 0)$ and $B(l, 0)$ is stable if$\mu > \mu_0$. Define, $Z(x) = f(\mu, 0, \epsilon)$ where f is the Poincare map.

Now, it can be proved that there exist two positive numbers ϵ and ω_0 such that $Z(\epsilon) > 0$ and $Z(\omega_0) \leq 0$ as follows: First, it will be proven that for $\epsilon > 0$,

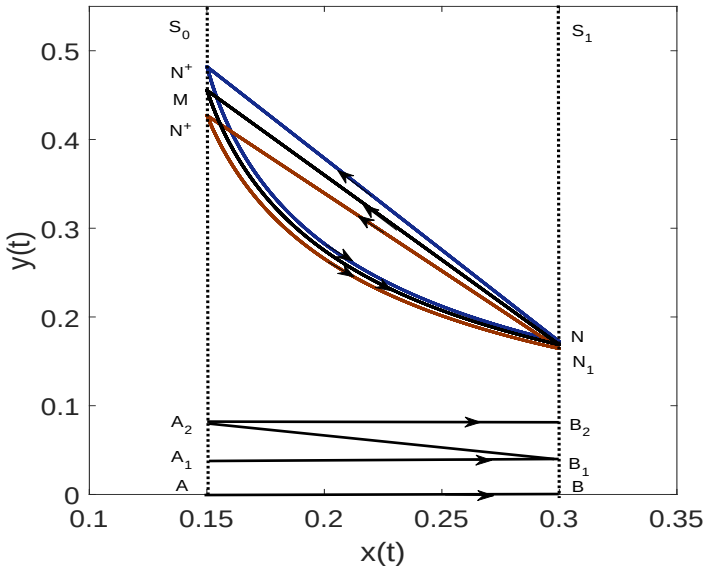

Figure 9.2: Location of positive periodic solution of the system (9.2.2) − (9.2.3).

$Z(\epsilon) > 0$. Let $A_1((1-\alpha)l, \epsilon)$ where $\epsilon > 0$ is sufficiently small. From Fig. 9.2, it can be observed that trajectory starting from the initial point A_1 at Poincare section S_0 intersects the Poincare section S_1 at the point $B_1(l, \bar{\epsilon})$. After that it jumps to the point $A_2((1-\alpha)l, (1-\beta+\mu)\epsilon_1)$ and goes to the point $B_2(l, \epsilon_1)$ on the Poincare section S_1 again. Since $(1-\beta+\mu)\bar{\epsilon} > \epsilon$, the point A_2 is above the point A_1 on the Poincare section S_0 and then the point B_2 is above the point B_1 on the Poincare section S_1. Thus, observe that $\epsilon_1 > \bar{\epsilon}$. From (9.3.10), it can be obtained that $\epsilon_1 = f(\beta, \mu, \bar{\epsilon})$. So,

$$\bar{\epsilon} - f(\beta, \mu, \bar{\epsilon}) = \bar{\epsilon} - \epsilon_1 < 0. \tag{9.5.1}$$

Now, consider that the line

$$w : 1 - x(t) - \frac{a(1+d\tau)y(t)}{(1+r\tau)x(t)+k} = 0,$$

intersects the Poincare section S_0 at the point

$$M\bigg((1-\alpha)l, \frac{(1-(1-\alpha)l)((1+r\tau)(1-\alpha)l+k)}{a(1+d\tau)}\bigg).$$

The trajectory from the initial point M intersects the Poincare section S_1 at the point $N(l, \eta_0)$. After that it jumps to the point $N^+((1-\alpha)l, (1-\beta+\mu)\eta_0)$ on Poincare section S_0 and again meets the Poincare section S_1 at the point $N_1(l, \bar{\eta_0})$. Consider that there exists some $\mu_0 > 0$ such that

$$(1-\beta+\mu_0)\eta_0 = \frac{(1-(1-\alpha)l)((1+r\tau)(1-\alpha)l+k)}{a(1+d\tau)},$$

then the point N^+ is just the point M for $\mu = \mu_0$. Observe that, the point N^+ is above the point M for $\mu > \mu_0$, while it is under the point M for $\mu < \mu_0$. Note that, the location of the point (i.e. above the point M, under the point M or just M) depends on the different values of parameter μ. However, for any $\mu > \mu_0$, the point N_1 is not above the point N in view of the vector field of the system (9.2.2) – (9.2.3). Then $\bar{\eta_0} \leq \eta_0$.

(a) If $\bar{\eta_0} = \eta_0$, then the system (9.2.2) – (9.2.3) has period-1 solution given by the cycle NMN.

(b) If $\bar{\eta_0} < \eta_0$, then

$$\eta_0 - f(\beta, \mu, \eta_0) = \eta_0 - \bar{\eta_0} > 0. \tag{9.5.2}$$

From (9.5.1) and (9.5.2) it can be observed that the Poincare map (9.3.10) has a fixed point corresponds to positive period-1 solution of the system (9.2.2) – (9.2.3) for $\mu > \mu_0 + \bar{\epsilon}$.

Remark 9.5.1. From the Theorem 9.4.2, it can be observed that the semi-trivial periodic solution of the system (9.2.2) – (9.2.3) is stable when $0 < \mu < \mu_0$. The positive period-1 solution exist for $\mu > \mu_0 + \bar{\epsilon}$. Since $D_{\delta y_0} f(\mu_0, 0) = 1$, a transcritical bifurcation will occurs at $\mu = \mu_0$. Furthermore, the system (9.2.2) – (9.2.3) has a

positive period-1 solution $(\xi(t), \eta(t))$ passing through the point $((1-\alpha)l, (1-\beta+\mu)\eta_0)$ and (l, η_0) which satisfies the condition

$$\frac{(1-(1-\alpha)l)((1+r\tau)(1-\alpha)l+k)}{a(1+d\tau)} = (1-\beta+\mu_1)\eta_0,$$

for some $\mu_1 > \mu_0$.

Now, with the help of Analogue of the Poincare criterion, the stability analysis of positive period-1 solution of the system (9.2.2) – (9.2.3) will be carried out for smaller delay

Theorem 9.5.1. *The positive periodic solution* $(\xi(t), \eta(t))$ *of the system* (9.2.2) – (9.2.3) *is locally asymptotically stable if*

$$\mu_0 < \mu < \mu_1, \tag{9.5.3}$$

where

$$g(\mu) = \Delta_1 e^{\int_0^T G(t)dt}, \quad g(\mu_1) = -1.$$

Proof. Consider the period-1 solution $(\xi(t), \eta(t))$ of the system (9.2.2) – (9.2.3) passes through the points $E^+((1-\alpha)l, (1-\beta+\mu)\eta_0)$ and $E(l, \eta_0)$. The stability of positive period-1 solution $(\xi(t), \eta(t))$ of the system (9.4.7)−(9.4.8) will be discussed by Analogue of the Poincare criterion [202].

$$G_1(x,y) = x(t)(1-x(t)) - \frac{a(1+d\tau)x(t)y(t)}{(1+r\tau)x(t)+k},$$

$$G_2(x,y) = \frac{r(1+\tau d)x(t)y(t)}{(1+r\tau)x(t)+k} - dy(t),$$

and

$$\alpha_1(x,y) = -\alpha x,\ \beta_1(x,y) = -\beta y + \mu y,\ \Theta(x,y) = x - l,$$

Then,

$$\begin{aligned}
\frac{\partial G_1}{\partial x} &= 1 - 2x(t) - \frac{ak(1+d\tau)y(t)}{((1+r\tau)x(t)+k)^2}, \\
\frac{\partial G_2}{\partial y} &= \frac{r(1+\tau d)x(t)}{(1+r\tau)x(t)+k} - d, \\
\frac{\partial \alpha_1}{\partial y} &= 0, \quad \frac{\partial \alpha_1}{\partial x} = -\alpha, \quad \frac{\partial \beta_1}{\partial y} = -\beta+\mu, \quad \frac{\partial \beta_1}{\partial x} = 0, \quad \frac{\partial \Phi}{\partial x} = 1, \quad \frac{\partial \Phi}{\partial y} = 0.
\end{aligned}$$

Note that

$$(\xi(T),\eta(T))=(l,\eta_0),\quad (\xi(T^+),\eta(T^+))=((1-\alpha)l,(1-\beta+\mu)\eta_0).$$

Now,

$$\Delta_1=\frac{G_{1+}\left(\frac{\partial\beta_1}{\partial y}\frac{\partial\Theta}{\partial x}-\frac{\partial\beta_1}{\partial x}\frac{\partial\Theta}{\partial y}+\frac{\partial\Theta}{\partial x}\right)+G_{2+}\left(\frac{\partial\alpha_1}{\partial x}\frac{\partial\Theta}{\partial y}-\frac{\partial\alpha_1}{\partial y}\frac{\partial\Theta}{\partial x}+\frac{\partial\Theta}{\partial y}\right)}{G_1\frac{\partial\xi}{\partial x}+G_2\frac{\partial\eta}{\partial y}}.$$

$$\Delta_1=\frac{(1-\beta+\mu)G_{1+}(\xi(T^+),\eta(T^+))}{G_1(\xi(T),\eta(T))}.$$

$$\begin{aligned}\Delta_1 &= \frac{(1-\beta+\mu)(1-\alpha)l\left[1-(1-\alpha)l-\frac{a(1+d\tau)(1-\beta+\mu)\eta_0}{(1+r\tau)(1-\alpha)l+k}\right]}{l(1-l)-\frac{a(1+d\tau)l\eta_0}{(1-p)(1+r\tau)l+k}}\\ &= \frac{(1-\beta+\mu)(1-\alpha)\left[1-(1-\alpha)l-\frac{a(1+d\tau)(1-\beta+\mu)\eta_0}{(1+r\tau)(1-\alpha)l+k}\right]}{(1-l)-\frac{a(1+d\tau)\eta_0}{(1+r\tau)l+k}}.\end{aligned}$$

Consider

$$\Psi(t)=\frac{\partial G_1}{\partial x}(\xi(t),\eta(t))+\frac{\partial G_2}{\partial y}(\xi(t),\eta(t),$$

then

$$\lambda=g(\mu)=\Delta_1 e^{\int_0^T\Psi(t)dt},$$

$$\lambda=\frac{(1-\beta+\mu)(1-\alpha)\left[1-(1-\alpha)l-\frac{a(1+d\tau)(1-\beta+\mu)\eta_0}{(1+r\tau)(1-\alpha)l+k}\right]}{(1-l)-\frac{a(1+d\tau)\eta_0}{(1+r\tau)l+k}}e^{\int_0^T\Psi(t)dt}.$$

It can be concluded that $\frac{d\lambda}{d\mu}<0$ for $\mu>\mu_0$. Also, it can be observed that λ is strictly decreasing on μ for $\mu\in(\mu_0,\infty)$.

Now, as mentioned above, consider that the point $M^+((1-\alpha)l,(1-\beta+\mu)m_0)$ is similar to the point

$$N\left((1-\alpha)l,\frac{(1-(1-\alpha)l)((1+r\tau)(1-\alpha)l+k)}{a(1+d\tau)}\right),$$

for $\mu=\mu_1$, $\mu_0<\mu_1$, then

$$(1-\beta+\mu_0)m_0=\frac{(1-(1-\alpha)l)((1+r\tau)(1-\alpha)l+k)}{al(1+d\tau)},$$

and

$$\lambda = \frac{0}{(1-l) - \dfrac{a(1+d\tau)\eta_0}{(1+r\tau)l+k}} e^{\int_0^T G(t)dt} = 0.$$

Since

$$\mid \lambda \mid = 0 < 1, \ \mu = \mu_1, \tag{9.5.4}$$

then the periodic solution is stable.

For $\mu_0 < \mu < \mu_1$, the point M^+ is just below the point N. Therefore, the point E^+ is below the point N and

$$(1-\beta+\mu_0)m_0 < \frac{(1-(1-\alpha)l)((1+r\tau)(1-\alpha)l+k)}{a(1+d\tau)},$$

which results in

$$[1-(1-\alpha)l - \frac{a(1+d\tau)(1-\beta+\mu)\eta_0}{(1+r\tau)(1-\alpha)l+k}] > 0.$$

Since, $e^{\int_0^T \Psi(t)dt} > 0$ and $\left[1-l-\dfrac{a(1+d\tau)\eta_0}{(1+r\tau)l+k}\right] > 0$ then $\lambda > 0$ for $0 < \mu < \mu_1$.
Note that, at the bifurcation point of transcritical bifurcation, $\mu = \mu_0$ for $\eta_0 = 0$, $T = \ln \dfrac{1-(1-\alpha)l}{(1-\alpha)(1-l)}$,

$$\lambda = 1, \mu = \mu_0. \tag{9.5.5}$$

which substantiates the result of the periodic semi-trivial solution in the previous section.

From (9.5) and (9.5.5)

$$0 < \lambda < 1, \mu_0 < \mu < \mu_1. \tag{9.5.6}$$

For $\mu > \mu_1$, M^+ is above the point N and

$$(1-\beta+\mu_0)m_0 > \frac{(1-(1-\alpha)l)((1+r\tau)(1-\alpha)l+k)}{a(1+d\tau)},$$

$$[1-(1-\alpha)l - \frac{a(1+d\tau)(1-\beta+\mu)\eta_0}{(1+r\tau)(1-\alpha)l+k}] < 0.$$

It can be observed that $\lambda < 0$ for $\mu_2 > \mu_1$. If $\mid \lambda \mid < 1$

$$\mid \frac{(1-\beta+\mu)(1-\alpha)[1-(1-\alpha)l - \dfrac{a(1+d\tau)(1-\beta+\mu)\eta_0}{(1+r\tau)(1-\alpha)l+k}]}{(1-l) - \dfrac{a(1+d\tau)\eta_0}{(1+r\tau)l+k}} e^{\int_0^T G(t)dt} \mid < 1.$$

Therefore, it can be found that $\mu_2 > \mu_1$ such that $\lambda = g(\mu_2) = -1$, then $\mid \lambda \mid = 0 < 1$ for $\mu \in (\mu_0, \mu_2)$. Then the positive periodic solution is stable. □

Remark 9.5.2. If there exists $\mu_2 > \mu_1$ such that $\lambda = -1$, the positive period-1 solution losses its stability and a flip bifurcation may occur at $\mu = \mu_2$. If a flip bifurcation occurs, $\exists$ a stable positive period-2 solution of the system (9.2.2) − (9.2.3) for $\mu > \mu_2$, which may also loss its stability with increasing the parameter μ.

Remark 9.5.3. For small values of delay, the system (9.2.2) − (9.2.3) has a positive period-1 solution. Moreover, for the system (9.2.2)−(9.2.3), there exist a stable periodic semi-trivial solution for $0 < \mu < \mu_0$ and a stable positive period-1 solution for $\mu_0 < \mu < \mu_2$. The transcritical bifurcation occurs at $\mu = \mu_0$ and flip bifurcation can occur at $\mu = \mu_2$. It is also possible that the system (9.2.2) − (9.2.3) has chaotic solution.

9.6 Bifurcation analysis

In this section, bifurcation of semi-trivial periodic solution of the system (9.2.2)−(9.2.3) about $\mu = \mu_0$ will be discussed. Consider the Poincare map $y_k^+ = (1 - \beta + \mu)f(y_{k-1}^+)$. Put $\Omega = y_k^+$ and $\Omega \geq 0$ to be very small. In terms of a new variable, the Poincare map can be written as:

$$\Omega \to (1 - \beta + \mu)f(\Omega) = G_3(\Omega, \mu). \tag{9.6.1}$$

Now, $g(0) = 0$ because the uniqueness of the solution. Therefore, the semi-trivial periodic solution which is discussed in the above section is associated with the fixed point zero of this map. Since the solution depends on the initial conditions, the function $G_3(u, \mu)$ is continuously differentiable with respect to u and μ. Therefore, $\lim_{u\to 0^+} f(u) = f(0) = 0$. To discuss the bifurcation of the map (9.6.1), Theorem 1.4.3 and following lemma will be required.

Lemma 9.6.1. For the map (9.6.1), $f'(u) \neq 0$ and $f''(u) \neq 0$.

Proof. Any trajectory through the initial point $((1 - \alpha)l, u)$ where $0 \leq u \leq y_0 = u_0$ intersects the Poincare section S_1 at the point $(l, f(u))$. The system (9.4.7) − (9.4.8) can be written as follows:

$$\frac{dy}{dx} = \frac{G_2(x, y)}{G_1(x, y)}. \tag{9.6.2}$$

Let(x, y) be an point of the system (9.6.2). Assume that $x_0 = (1 - \alpha)l$ and $y_0 = u$. Then

$$y(x, u) = y(x; (1 - \alpha)l, u), \quad 0 < u \leq u_0, \quad (1 - \alpha)l \leq x \leq l. \tag{9.6.3}$$

Therefore, with the help of (9.6.3)

$$\frac{\partial y(x,u)}{\partial u} = exp\Big[\int_{(1-\alpha)l}^{l} \frac{\partial}{\partial y}\Big(\frac{G_2(\omega,y(\omega,u))}{G_1(\omega,y(\omega,u))}\Big)d\omega\Big] > 0.$$

$$\frac{\partial^2 y(x,u)}{\partial u^2} = \frac{\partial y(x,u)}{\partial u} exp\Big[\int_{(1-\alpha)l}^{l} \frac{\partial^2}{\partial y^2}\Big(\frac{G_2(\omega,y(\omega,u))}{G_1(\omega,y(\omega,u))}\Big)\frac{\partial y(\omega,u)}{\partial u}d\omega\Big].$$

Now,

$$f'(0) = \frac{\partial y(l,0)}{\partial u} = exp\Big[\int_{(1-\alpha)l}^{l} \frac{\partial}{\partial y}\Big(\frac{G_2(\omega,y(\omega,0))}{G_1(\omega,y(\omega,0))}\Big)d\omega\Big] \tag{9.6.4}$$

$$= \frac{[(1+r\tau)l + k(1-l) + l](1-(1-\alpha)l)}{[(1+r\tau)(1-\alpha)l + k](1-l)}^{\frac{r(1+\tau d)}{(1+r\tau)+k}} \Big(\frac{(1-\alpha)(1-l)}{1-(1-\alpha)l}\Big)^d.$$

Therefore,

$$f''(0) = f'(0)exp\Big[\int_{(1-\alpha l)}^{l} z(s)\frac{\partial y(\omega,0)}{\partial u}\Big]d\omega,$$

where

$$z(s) = \frac{\partial^2}{\partial y^2}\Big(\frac{G_2(\omega,y(\omega,0))}{G_1(\omega,y(\omega,0))}\Big)d\omega = -2\Big(\frac{a(1+\tau d)s}{(1+r\tau)s+k}\Big)\Big(\frac{r(1+\tau d)s}{(1+r\tau)s+k}) - d\Big) < 0.$$

Because x_1 is the smaller zero point of the function $f(x)$. Observe that $f(x)$ is monotonically decreasing in the interval $[0, x_1]$. It shows that $f(s) > 0$ when $s \in [0, x_1)$ for $h \leq x_1$. Therefore $g''(0) < 0$. □

Now, Lemma 9.5.1 is applied to the one parameter map (9.4.10) for proving the following theorem:

Theorem 9.6.2. *The transcritical bifurcation will occur at $\mu = \mu_0$.*

Proof. The system (9.2.2)−(9.2.3) has a transcritical bifurcation if following conditions will be satisfied.

1. $G_3(0,\mu) = (1-\beta+\mu)f(0) = 0$,
2. $\frac{\partial G_3(0,\mu)}{\partial u} = (1-\beta+\mu)f'(0)$
   $= (1-\beta+\mu)\Big[\frac{[(1-p)(1+r\tau)l + k(1-l)+l](1-(1-\alpha)l)}{[(1-p)(1+r\tau)(1-\alpha)l+k](1-l)}\Big]^{\frac{r(1-p)(1+\tau d)}{(1-p)(1+r\tau)+k}}\Big[\frac{(1-\alpha)(1-l)}{1-(1-\alpha)l}\Big]^d$,
   Now it can be calculated that $\frac{\partial G_3(0,\mu_0)}{\partial u} = 1$. Hence, $(0,\mu_0)$ is a fixed point with the eigenvalue 1.
3. $\frac{\partial G_3(0,\mu)}{\partial \mu} = f(0) = 0$,

4. $\dfrac{\partial^2 G_3(0,\mu_0)}{\partial u \partial \mu} = f'(0) > 0,$

5. $\dfrac{\partial^2 G_3(0,\mu_0)}{\partial u^2} = (1-\beta+\mu)f''(0) < 0.$

Hence, all the conditions of the Theorem 1.4.3 have been satisfied and there exists transcritical bifurcation at $\mu = \mu_0$. □

9.7 Numerical Simulations

In this section, some numerical results are explored to carried out the dynamical aspects of the system (9.2.2) − (9.2.3). To illustrate analytical findings following set of parameters is chosen:

$$a = 2.814, d = 0.8, k = 2, l = 0.2, r = 2, \alpha = 0.5, \beta = 0.2. \tag{9.7.1}$$

The system (9.2.2) − (9.2.3) admits a positive equilibrium point $(1.333, 0.3949)$. Considering $\tau = 0.001$ and data set (9.7.1), with the initial value $(0.15, 0.03)$, the solution of the system (9.2.2) − (9.2.3) tends to periodic solution E^+EE^+ for $\mu = 3.2$. This solution is stable if $0 < \beta < \beta_0$ for $\mu > 0$ see Fig. 9.3.

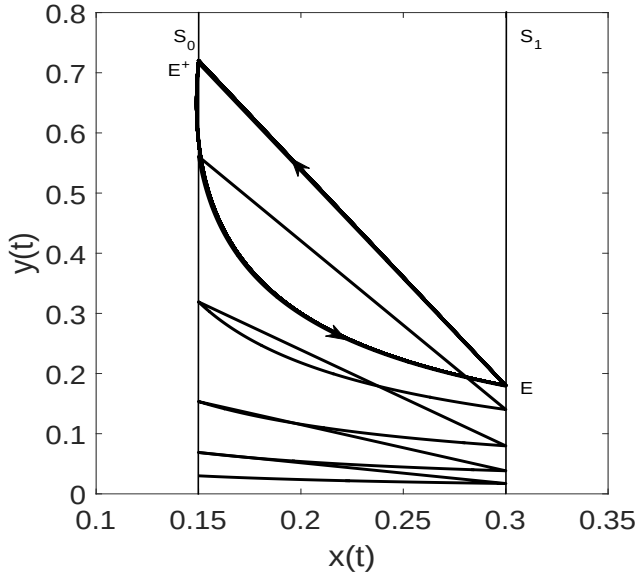

Figure 9.3: Phase portrait of the system (9.2.2) − (9.2.3).

The two cross-sections of the system (9.2.2) − (9.2.3) are:

$$\begin{aligned} S_0 &= \{(x,y) : x = 0.15, y_0 \geq 0\} \\ S_1 &= \{(x,y) : x = 0.30, y_0 \geq 0\} \end{aligned}$$

From Theorem 9.4.2.

$$\mu_0 = \left[\frac{[(1.002)0.3 + 2(1-0.3) + 0.3]0.85}{[(1.002)0.15 + 2]0.7}\right]^{\frac{-2(1+0.001\times 0.8)}{3.002}} \left[\frac{0.15}{0.85}\right]^{-0.8} - 1 + 0.2 \approx 0.92$$

For $\mu = 0.6$, the semi-trivial solution of the system (9.2.2) − (9.2.3) is shown in Fig. 9.4. The solution of the system (9.2.2) − (9.2.3) with the initial point $(0.15, 0.03)$ tends to the semi-trivial solution as t increase. It shows that the semi-trivial solution of the system (9.2.2) − (9.2.3) is stable.

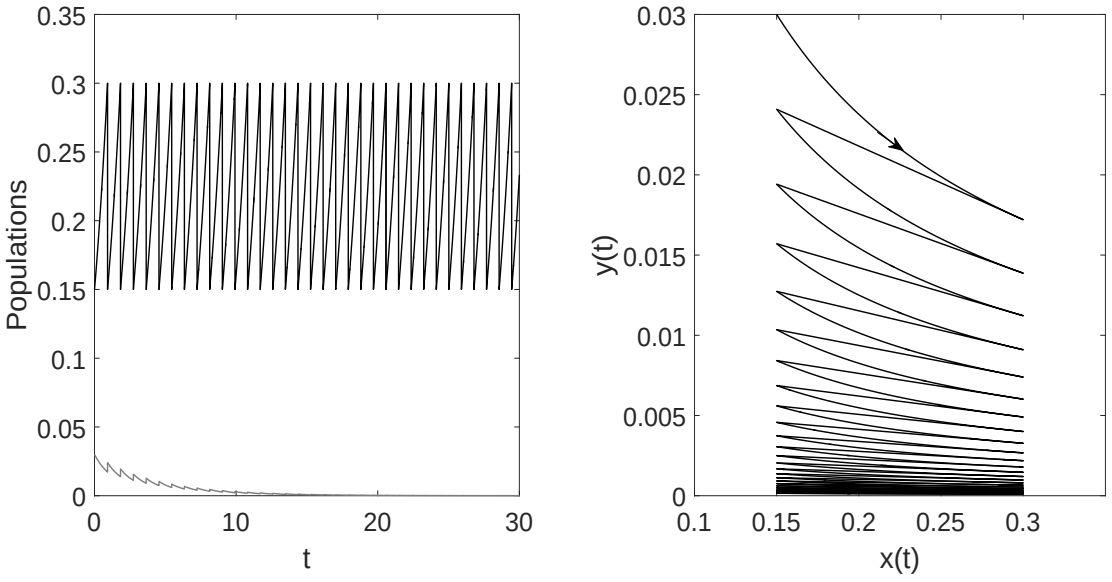

Figure 9.4: (a) Time series (b) Phase portrait showing the stability of semi-trivial solution of the system (9.2.2) − (9.2.3) at $\mu = 0.6$.

Consider $\mu = 6.2$, the system (9.2.2) − (9.2.3) displays a stable positive period-1 solution see Fig. 9.5. Further releasing more natural enemies to $\mu = 8.7$, the system (9.2.2) − (9.2.3) exhibits a stable positive period-2 solution see Fig. 9.6(a). As the parameter μ increases repeated period-doubling leads to chaos. The period-4 solution will appear at $\mu = 16.7$ see Fig. 9.6(b).

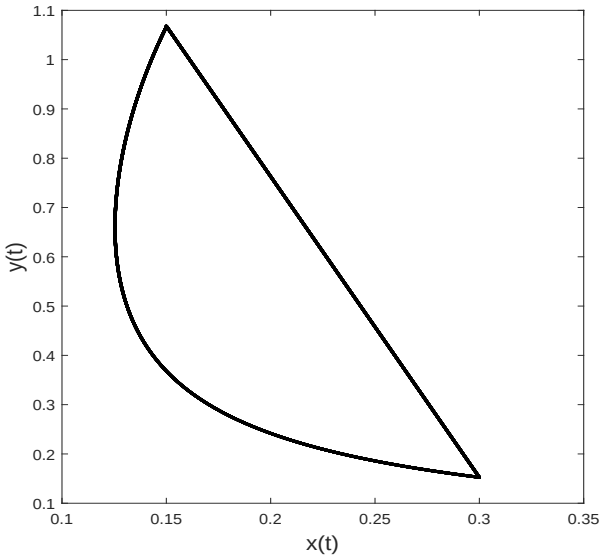

Figure 9.5: Phase portrait showing stability of positive period-1 solution of the system (9.2.2) – (9.2.3) at $\mu = 6.2$.

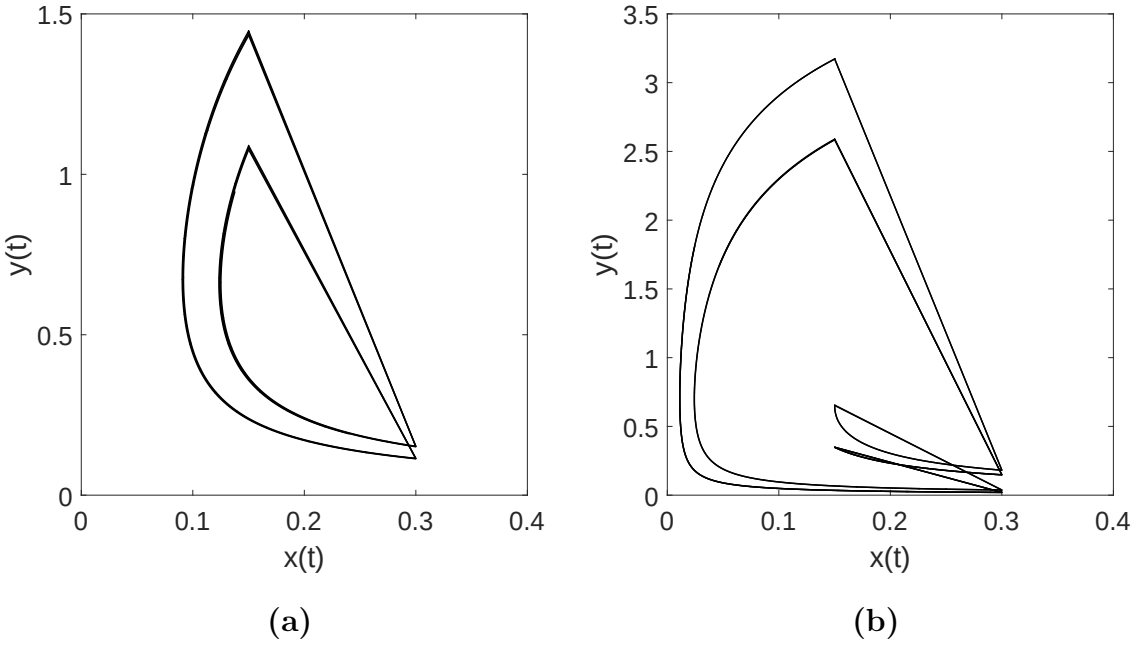

(a) **(b)**

Figure 9.6: Positive periodic solution of the system (9.2.2) – (9.2.3) (a) Period-2 at $\mu = 8.7$ (b) Period-4 at $\mu = 16.7$.

Further increasing parameter μ, period-8 solution can be observed in Fig. 9.7(a) at $\mu = 18.4$. As parameter μ increases, the chaotic solution at $\mu = 25.7$ is shown Fig.

9.7(b). It is observed that there exists a cascade of period-doubling bifurcation which results in the chaotic solutions.

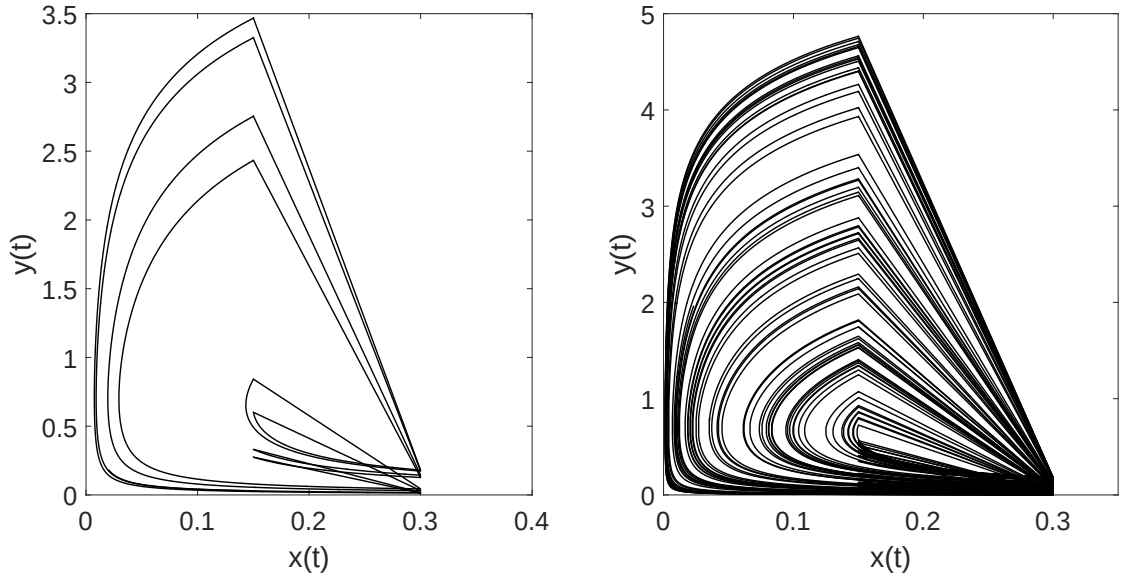

(a) **(b)**

Figure 9.7: (a) Period-8 solution at $\mu = 18.4$ (b) Chaotic solution at $\mu = 25.7$ of the system $(9.2.2) - (9.2.3)$.

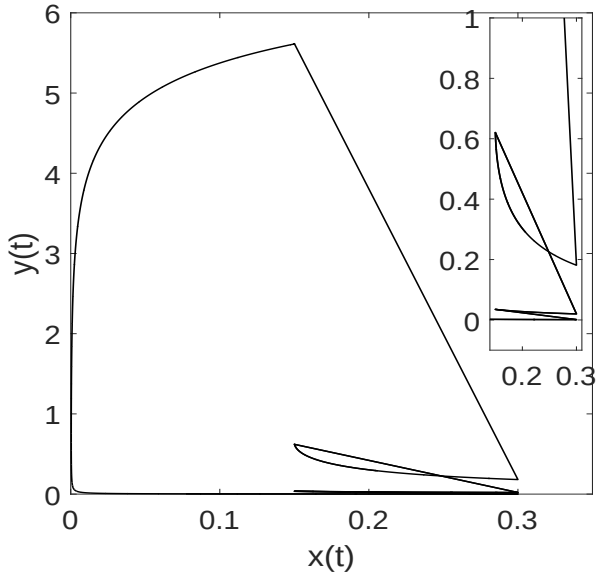

Figure 9.8: Period-3 solution of the system $(9.2.2) - (9.2.3)$ at $\mu = 30.2$.

To show the existence of chaos, a period-3 solution of the system $(9.2.2) - (9.2.3)$

is drawn in Fig. 9.8 at $\mu = 30.2$. For more clarity, it's magnified part is also drawn in Fig. 9.8.

Above numerical results are computed for small delay $\tau = 0.001$ but time delay has the advantage to make the dynamical systems more complex. Now, phase trajectory is drawn for large value of delay $\tau = 0.9$ at $\mu = 6.2$. Observe that, there exists a multi-periodic solution in Fig. 9.9. Hence, on comparing the Fig. 9.5 and Fig. 9.9, more complex dynamical behavior occurs for large value of delay.

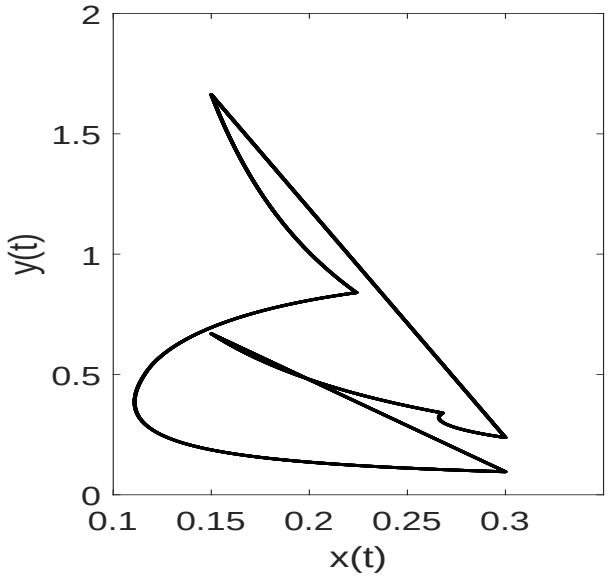

Figure 9.9: Multi-periodic solution of the system (9.2.2) − (9.2.3) at $\tau = 0.9$ and $\mu = 6.2$.

9.8 Discussion

A delayed pest-natural enemy model with impulsive state feedback is analyzed to control the pest. It is observed that the system (9.2.2) − (9.2.3) is bounded. For small delay, there exists a semi-trivial periodic and positive period-1 solution. The stability of semi-trivial periodic solution and period-1 solutions are analyzed. The conditions for flip bifurcation and transcritical bifurcation are also investigated. The numerical simulations exhibit the existence of chaotic behavior. The various diagrams indicate the rich dynamics, including stable, periodic and chaotic solutions. It can be proved that when the pest density reaches a given threshold, the pest density can be reduced

below a certain level with the help of an impulsive state feedback strategy. Moreover, qualitative analysis for the system (9.2.2) – (9.2.3) with the large delay has been analyzed which shows the more complex dynamical behavior.

Chapter 10

Conclusions and Future Scope

In this chapter, the main results of the thesis have been wrapped and further, research directions for future research work have been provided.

10.1 Conclusions

In this thesis, some mathematical models have been developed for pest control with impulsive time-dependent and state-dependent strategies. The factors responsible for pest eradication and a variety of complex dynamical behaviors in impulsive pest management systems ranging from order to chaos have been investigated. Such a study is important since the ecological systems have all the necessary ingredients to control the pest or to support chaos. The objective is either pest eradication or reduces its density below the threshold level. Efforts have been made to explore the different mechanism that may control the pest below the injury level. To understand the effect of pest management strategies in pest dynamics, the stage-structured pest control models have been proposed and analyzed. In particular, the conclusions of this work are presented as below:

- The synchronous pesticide application with birth pulses may reduce the threshold below unity. It is required for successful pest control. A critical level of the birth rate parameter is obtained, below which the pest can be successfully eliminated. If the birth rate goes beyond this critical level, then the pest density oscillates in regular/irregular manner. Center manifold theorem is used to establish the

existence of bifurcation. Other factors which affect the dynamics of the system are mortality rates, killing rates of immature/mature pest and pulse period.

- Further, in case of asynchronous pulses, the delay in pesticide spray timing reduces the threshold and the equilibrium level of mature pest density. The pest-free state stabilizes and complexity of the system reduces. It is found that higher killing rates of mature pest than that of the immature pest may lead to pest eradication.

- The presence of residual effect of pesticide further reduces the threshold for pest eradication. The threshold depends upon the pulse period, decay rate and killing efficiency of residual pesticide.

- It is found that only impulsive chemical control or continuous mechanical control (harvesting) would not be sufficient to control the pest. The combinations of chemical and mechanical control are more effective in controlling the pest. Also, use of pesticides can be lowered by introducing mechanical control which is environment friendly. Both the synchronous and asynchronous cases are considered and the latter case is found to be more effective for pest control.

- Threshold for pest eradication is obtained for multiple pulses IPM model. The effects of time delays in chemical and mechanical control are investigated. For effective pest control, it is suggested that harvesting delay should be reduced while pesticide spray can be delayed.

- The delayed response of residual pesticide has been considered in another model. The critical value of the delayed response rate and pulse period has been computed to control the pest. It is concluded that if only mechanical control is applied, then the threshold level may be greater than one and the pest may persist. Further, combining mechanical control with chemical control reduces the threshold and pest eradication is possible.

- An IPM model incorporating toxic effects of the pesticides on the environment has also been considered. The pest can be eradicated, but the toxicant persists in the environment and in the pest. The critical level of harvesting effort is obtained

to stabilize the pest-free state. The harvesting may reduce the toxicant in the environment.

- Another IPM model using chemicals as well as biological control is studied with state-dependent feedback control strategy. The motivation is to maintain the pest below an economic threshold level. While releasing more natural enemies, the pest density remains below the given threshold even though the complexity of the system increases. From a biological point of view, the state-dependent strategy is more effective to control the pest.

10.2 Future Scope

In future, this research work can be extended in the following directions:

- To reduce pest load, apart from chemical/mechanical control other strategies can be incorporated.

- To account for patch system, Network models can be developed for the patchy system.

- The idea of optimal control can be applied to find out the optimal timing for the pesticide applications which can suppress the pest most effectively. Optimum use of pesticide and an optimum rate for release of natural enemies, calls for new efforts and endeavors for the future investigation.

- In this thesis, state-dependent feedback control strategy has been discussed for a pest-natural enemy model for the small delay. Qualitative analysis of the system with state-dependent impulses and large delay is an interesting problem to be investigated in the future. The global stability and bifurcation analysis of impulsive models using state-dependent feedback control strategy, which is not covered in this thesis, is advisable in order to get more appropriate results into the realistic models.

Bibliography

[1] Agrawal, T. and Saleem, M., Complex dynamics in a ratio-dependent two-predator one-prey model, Computational and Applied Mathematics, **34(1)** (2015), 265–274.

[2] Agur, Z., Cojocaru, L., Mazor, G., Anderson, R. M. and Danon, Y. L., Pulse mass measles vaccination across age cohorts, Proceedings of the National Academy of Sciences, **90(24)**(1993), 11698–11702.

[3] Aiello, W. G. and Freedman, H. I., A time-delay model of single-species growth with stage structure, Mathematical Biosciences, **101(2)**(1990), 139–153.

[4] Aiello, W. G., Freedman, H. I. and Wu, J., Analysis of a model representing stage-structured population growth with state-dependent time delay, SIAM Journal on Applied Mathematics, **52(3)**(1992), 855–869.

[5] Aihara, K., Matsumoto, G. and Ichikawa, M., An alternating periodic-chaotic sequence observed in neural oscillators, Physics Letters A, **111(5)**(1985), 251–255.

[6] Alligood, K. T., Sauer, T. D. and Yorke, J. A., *Chaos: An Introduction to Dynamical Systems*, Springer-Verlag, New York, 1996.

[7] Baek, H. K., Qualitative analysis of Beddington-DeAngelis type impulsive predator–prey models, Nonlinear Analysis: Real World Applications, **11(3)**(2010), 1312–1322.

[8] Baek, H. K., Kim, S. D. and Kim, P., Permanence and stability of an Ivlev-type predator–prey system with impulsive control strategies, Mathematical and Computer Modelling, **50(9-10)**(2009), 1385–1393.

[9] Baek, H. and Lim, Y., Dynamics of an impulsively controlled Michaelis-Menten type predator–prey system, Communications in Nonlinear Science and Numerical Simulation, **16(4)**(2011), 2041–2053.

[10] Baer, S. M., Kooi, B. W., Kuznetsov, Y. A. and Thieme, H. R., Multiparametric bifurcation analysis of a basic two-stage population model, SIAM Journal on Applied Mathematics, **66(4)**(2006), 1339–1365.

[11] Bainov, D. D., and Simeonov, P. S., *Systems with Impulse Effect: Stability, Theory and Applications*, Chichester [England]: Ellis Horwood, 1989.

[12] Bainov, D. and Simeonov, P., *Impulsive Differential Equations: Periodic Solutions and Applications*, Longman Scientific and Technical, New York, CRC Press, **66**, 1993.

[13] Baker, G. L. and Gollub, J. P., *Chaotic Dynamics: An Introduction*, Cambridge University Press, New york, 1996.

[14] Barclay, H. J., Models for pest control using predator release, habitat management and pesticide release in combination, Journal of Applied Ecology, **19(2)**(1982), 337–348.

[15] Basir, F. A., Venturino, E. and Roy, P. K., Effects of awareness program for controlling mosaic disease in Jatropha curcas plantations, Mathematical Methods in the Applied Sciences, **40(7)**(2017), 2441–2453.

[16] Bence, J. R. and Nisbet, R. M., Space-limited recruitment in open systems: the importance of time delays, **70(5)**(1989), 1434–1441.

[17] Bergh, O. and Getz, W. M., Stability of discrete age-structured and aggregated delay-difference population models, Journal of Mathematical Biology, **26(5)**(1988), 551–581.

[18] Bernard, O. and Gouze, J. L., Transient behaviour of biological loop models with application to the Droop model, Mathematical Biosciences, **127(1)**(1995), 19–43.

[19] Bernard, O. and Souissi, S., Qualitative behavior of stage-structured populations: application to structural validation, Journal of Mathematical Biology, **37(4)**(1998), 291–308.

[20] Bhattacharya, D. K., Toxicity in plants and optimal growth under fertilizer, Journal of Applied Mathematics and Computing, **16(1-2)**(2004), 355–369.

[21] Bhattacharya, D. K. and Begum, S., Bionomic equilibrium of two-species system, I, Mathematical Biosciences, **135(2)**(1996), 111–127.

[22] Biswas, D., Kesh, D. K., Datta, A., Chatterjee, A. N. and Roy, P. K., A mathematical approach to control cutaneous leishmaniasis through insecticide spraying, Sop Transactions On Applied Mathematics, **1(2)**(2014), 44–54.

[23] Bor, Y. J., Optimal pest management and economic threshold, Agricultural Systems, **49(2)**(1995), 113–133.

[24] Botsford, L. W., Further analysis of Clark's delayed recruitment model, Bulletin of Mathematical Biology, **54(2-3)**(1992), 275–293.

[25] Cai, S., A stage-structured single species model with pulse input in a polluted environment, Nonlinear Dynamics, **57(3)**(2009), 375–382.

[26] Carr, J., *Applications of Centre Manifold Theory*, Springer, New York, NY, USA, **35**, 2012.

[27] Carroll, J. E. and Lamberson, R. H., The Owl's Odessey: A continuous model for the dispersal of a territorial species, SIAM Journal on Applied Mathematics, **53(1)**(1993), 205–218.

[28] Caughley, G., *Analysis of Vertebrate Populations*, John Wiley and Sons, New York, NY, USA, 1977.

[29] Changguo, L., Dynamics of stage-structured population models with harvesting pulses, WSEAS Transactions on Mathematics, **11(1)**(2012), 74–82.

[30] Chatterjee, S., Isaia, M. and Venturino, E., Effects of spiders predational delays in intensive agroecosystems, Nonlinear Analysis: Real World Applications, **10(5)**(2009), 3045–3058.

[31] Chen, Y., Liu, Z. and Qin, W., Modelling and analysis of a pest-control pollution model with integrated control tactics, Discrete Dynamics in Nature and Society, **2010**(2010), Article ID 962639.

[32] Chowdhury, S. and Roy, P. K., Mathematical modelling of enfuvirtide and protease inhibitors as combination therapy for HIV, International Journal of Nonlinear Sciences and Numerical Simulation, **17(6)**(2016), 259–275.

[33] Cui, J. A. and Takeuchi, Y., Permanence, extinction and periodic solution of predator–prey system with Beddington-DeAngelis functional response, Journal of Mathematical Analysis and Applications, **317(2)**(2006), 464–474.

[34] Cushing, J. M., Predator–prey interactions with time delays, Journal of Mathematical Biology, **3(3-4)**(1976), 369–380.

[35] Cushing, J. M., *Integrodifferential Equations and Delay Model in Population Dynamics*, Springer, Heidelberg, 1977.

[36] Cushing, J. M., Periodic time-dependent predator–prey systems, SIAM Journal on Applied Mathematics, **32(1)**(1977), 82–95.

[37] Cushing, J. M., Two species competition in a periodic environment, Journal of Mathematical Biology, **10(4)**(1980), 385–400.

[38] Cushing, J. M., Costantino, R. F., Dennis, B., Desharnais, R. A. and Henson, S. M., *Chaos in Ecology: Experimental Nonlinear Dynamics*, Academic Press, London, Elsevier, **(1)**2002.

[39] Cushing, J. M., Henson, S. M., Desharnais, R. A., Dennis, B., Costantino, R., F. and King, A., A chaotic attractor in ecology: theory and experimental data, Chaos, Solitons and Fractals, **12(2)**(2001), 219–234.

[40] DeBach, P., *Biological Control of Insect Pests and Weeds*, Biological control of insect pests and weeds, London, Chapman and Hall Ltd., 1964.

[41] DeBach, P. and Rosen, D., *Biological Control by Natural Enemies*, 2nd ed., Cambridge University Press, Cambridge, 1991.

[42] De la Sen, M. and Alonso-Quesada, S., A control theory point of view on Beverton-Holt equation in population dynamics and some of its generalizations, Applied Mathematics and Computation, **199(2)**(2008), 464–481.

[43] Domoshnitsky, A., Drakhlin, M. and Litsyn E., On positivity of solutions of delayed differential equation with state-dependent impulses, International Conference on Parallel Processing and Applied Mathematics, Springer, (2001), 870–876.

[44] Domoshnitsky, A., Drakhlin, M. and Litsyn, E., Nonoscillation and positivity of solutions to first order state-dependent differential equations with impulses in variable moments, Journal of Differential Equations, **228(1)**(2006), 39–48.

[45] d'Onofrio, A., Pulse vaccination strategy in the SIR epidemic model: global asymptotic stable eradication in presence of vaccine failures, Mathematical and Computer Modelling, **36(4-5)**(2002), 473–489.

[46] Dubey, B., A prey–predator model with a reserved area, Nonlinear Analysis: Modelling and Control, **12(4**)(2007), 479–494.

[47] Dubey, B., Chandra, P. and Sinha, P., A model for fishery resource with reserve area, Nonlinear Analysis: Real World Applications, **4(4)**(2003), 625–637.

[48] Dubey, B., Shukla, J. B., Sharma, S., Agarwal, A. K. and Sinha, P., A mathematical model for chemical defense mechanism of two competing species, Nonlinear Analysis: Real World Applications, **11(2**)(2010), 1143–1158.

[49] Dubey, B. and Upadhyay, R. K., Persistence and extinction of one-prey and two-predators system, Nonlinear Analysis: Modelling and Control, **9(4)**(2004), 307–329.

[50] Eckmann, J. P., *Routes to chaos with special emphasis on period doubling*, Chaotic behaviour of deterministic systems, Amsterdam: Elsevier North- Holland, 1983.

[51] Elaydi, S., *An Introduction to Difference Equations*, Springer, New York, (2nd Edition), 1999.

[52] Elaydi, S. N., *Discrete Chaos: with Applications in Science and Engineering*, CRC Press, 2007.

[53] Elaydi, S. and Sacker, R. J., Periodic difference equations, population biology and the Cushing-Henson conjectures, Mathematical Biosciences, **201(1-2)**(2006), 195–207.

[54] Epstein, I. R., Oscillations and chaos in chemical systems, Physica D: Nonlinear Phenomena, **7(1-3)**(1983), 47–56.

[55] Faro, J. and Velasco, S., An approximation for prey–predator models with time delay, Physica D: Nonlinear Phenomena, **110(3-4)**(1997), 313–322.

[56] Feng, J. W. and Chen, S. H., Global asymptotic behavior for the competing predators of the Ivlev types, Mathematica Applicata, **13(4)**(2000), 85–88.

[57] Ferriere, R. and Fox, G. A., Chaos and evolution, Trends in Ecology and Evolution, **10(12)**(1995), 480–485.

[58] Flint, M. L., Integrated pest management for walnuts, University of California Statewide Integrated Pest Management Project, Division of Agriculture and Natural Resources, 2nd edn, publication, University of California, Oakland, CA, **3270**(1987).

[59] Franco, D., Liz, E., Nieto, J. J. and Rogovchenko, Y. V., A contribution to the study of functional differential equations with impulses, Mathematische Nachrichten, **218(1)**(2000), 49–60.

[60] Freedman, H. L. and Rao, V. S. H., The trade-off between mutual interference and time lags in predator–prey systems, Bulletin of Mathematical Biology, **45(6)**(1983), 991–1004.

[61] Gao, S. and Chen, L., Dynamic complexities in a single-species discrete population model with stage structure and birth pulses, Chaos, Solitons and Fractals, **23(2)**(2005), 519–527.

[62] Gao, S., Chen, L., Nieto, J. J. and Torres, A., Analysis of a delayed epidemic model with pulse vaccination and saturation incidence, Vaccine, **24(35-36)**(2006), 6037–6045.

[63] Georgescu, P. and Morosanu, G., Pest regulation by means of impulsive controls, Applied Mathematics and Computation, **190(1)**(2007), 790–803.

[64] Georgescu, P. and Zhang, H., An impulsively controlled predator-pest model with disease in the pest, Nonlinear Analysis: Real World Applications, **11(1)**(2010), 270–287.

[65] Georgescu, P., Zhang, H. and Chen, L., Bifurcation of nontrivial periodic solutions for an impulsively controlled pest management model, Applied Mathematics and Computation, **202(2)**(2008), 675–687.

[66] Ghosh, M., Chandra, P. and Sinha, P., A mathematical model to study the effect of toxic chemicals on a prey–predator type fishery, Journal of Biological Systems, **10(2)**(2002), 97–105.

[67] Grantham, W. J. and Lee, B., A chaotic limit cycle paradox, Dynamics and Control, **3(2)**(1993), 159–173.

[68] Greathead, D. J., Natural enemies of tropical locusts and grasshoppers: their impact and potential as biological control agents, In Biological Control of Locusts and Grasshoppers: proceedings of a workshop held at the International Institute of Tropical Agriculture, Cotonou, Republic of Benin, C.A.B. International, Wallingford, UK, (1991), 105–121.

[69] Guckenheimer, J. and Holmes, P., *Nonlinear Oscillations, Dynamical Systems and Bifurcations of Vector Fields*, Springer Science and Business Media, **42**(2013).

[70] Guckenheimer, J., Oster, G. and Ipaktchi, A., The dynamics of density dependent population models, Journal of Mathematical Biology, **4(2)**(1977), 101–147.

[71] Gupta, R. P., Banerjee, M. and Chandra, P., Bifurcation analysis and control of Leslie-Gower predator–prey model with Michaelis-Menten type prey-harvesting, Differential Equations and Dynamical Systems, **20(3)**(2012), 339–366.

[72] Gupta, R. and Chandra, P., Bifurcation analysis of modified Leslie-Gower predator–prey model with Michaelis-Menten type prey harvesting, Journal of Mathematical Analysis and Applications, **398(1)**(2013), 278–295.

[73] Gupta, R. P., Chandra, P. and Banerjee, M., Dynamical complexity of a prey–predator model with nonlinear predator harvesting, Discete and Continuous Dynamical Systems-Series B, **20(2)**(2015), 423–443.

[74] Hale, J. K., *Ordinary differenential equations*, New York, Wiley-Interscience, 1969.

[75] Hallam, T. G., Clark, C. E. and Jordan, G. S., Effects of toxicants on populations: a qualitative approach 11, First order kinetics, Journal of Mathematical Biology, **18(1)**(1983), 25–37.

[76] Hallam, T. G., Clark, C. E. and Lassiter, R. R., Effects of toxicants on populations: a qualitative approach 1, Equilibrium environmental exposure, Ecological Modelling, **18(3-4)**(1983), 291–304.

[77] Hallam, T. G. and De Luna, J. T., Effects of toxicants on populations: a qualitative approach, 111, Environmental and food chain pathways, Journal of Theoretical Biology, **109(3)**(1984), 411–429.

[78] Hastings, A., Age-dependent predation is not a simple process I: Continuous time models, Theoretical Population Biology, **23(3)**(1983), 347–362.

[79] Hastings, A. and Higgins, K., Persistence of transients in spatially structured ecological models, Science, **263(5150)**(1994), 1133–1136.

[80] He, X. Z. and Ruan, S., Global stability in chemostat-type plankton models with delayed nutrient recycling, Journal of Mathematical Biology, **37(3)**(1998), 253–271.

[81] Hoffmann, M. P. and Frodsham, A. C., Natural Enemies of Vegetable Insect Pests, Cooperative Extension, Cornell University, Ithaca, NY, USA, 1993.

[82] Holling, C. S., The functional response of predators to prey density and its role in mimicry and population regulations, The Memoirs of the Entomological Society of Canada, **97(S45)**(1965), 5–60.

[83] Hsu, S. B. and Huang, T. W., Global stability for a class of predator–prey systems, SIAM Journal on Applied Mathematics, **55(3)**(1995), 763–783.

[84] Huang, M., Song, X. and Li, J., Modelling and analysis of impulsive releases of sterile mosquitoes, Journal of Biological Dynamics, **11(1)**(2017), 147–171.

[85] Huaping, L. and Zhien, M., The threshold of survival for system of two species in a polluted environment, Journal of Mathematical Biology, **30(1)**(1991), 49–61.

[86] Hui, J. and Chen, L. S., Dynamic complexities in ratio-dependent predator–prey ecosystem models with birth pulse and pesticide pulse, International Journal of Bifurcation and Chaos, **14(08)**(2004), 2893–2903.

[87] Hui, J. and Chen, L. S., Impulsive vaccination of SIR epidemic models with nonlinear incidence rates, Discrete and Continuous Dynamical Systems-B, **4(3)**(2004), 595–605.

[88] Hui, J. and Zhu, D., Dynamic complexities for prey-dependent consumption integrated pest management models with impulsive effects, Chaos, Solitons and Fractals, **29(1)**(2006), 233–251.

[89] Hung, Y. F., Yen, T. C. and Chern, J. L., Observation of period-adding in an optogalvanic circuit, Physics Letters A, **199(1-2)**(1995), 70–74.

[90] Hwang, T. W., Uniqueness of limit cycles of the predator–prey system with Beddington-DeAngelis functional response, Journal of Mathematical Analysis and Applications, **290(1)**(2004), 113–122.

[91] Jiang, G. and Lu, Q., The dynamics of a prey–predator model with impulsive state feedback control, Discrete and Continuous Dynamical System-B, **6(6)**(2006), 1301–1320.

[92] Jiang, G. and Lu, Q., Impulsive state feedback control of a predator–prey model, Journal of Computational and Applied Mathematics, **200(1)**(2007), 193–207.

[93] Jiang, G., Lu, Q. and Peng, L., Impulsive ecological control of stage-structured pest management system, Mathematical Biosciences and Engineering: MBE, **2(2)**(2005), 329–344.

[94] Jiang, G., Lu, Q. and Qian, L., Chaos and its control in an impulsive differential system, Chaos, Solitons and Fractals, **34(4)**(2007), 1135–1147.

[95] Jiang, G., Lu, Q. and Qian, L., Complex dynamics of a Holling type II prey–predator system with state feedback control, Chaos, Solitons and Fractals, **31(2)**(2007), 448–461.

[96] Jiao, J., Cai, S. and Chen, L., Analysis of a stage-structured perdator-prey system with birth pulse and impulsive harvesting at different moments, Nonlinear Analysis: Real World Applications, **12(4)**(2011), 2232–2244.

[97] Jiao, J. J., Chen, L. S. and Cai, S. H., Impulsive control strategy of a pest management SI model with nonlinear incidence rate, Applied Mathematical Modelling, **33(1)**(2009), 555–563.

[98] Jiao, J., Long, W. and Chen, L., A single stage-structured population model with mature individuals in a polluted environment and pulse input of environmental toxin, Nonlinear Analysis: Real World Applications, **10(5)**(2009), 3073–3081.

[99] Jury, E. I., *Inners and stability of dynamic systems*, New york, Wiley, 1974.

[100] Kaneko, K., On the period-adding phenomena at the frequency locking in a one-dimensional mapping, Progress of Theoretical Physics, **68(2)**(1982), 669–672.

[101] Kaneko, K., Similarity structure and scaling property of the period-adding phenomena, Progress of Theoretical Physics, **69(2)**(1983), 403–414.

[102] Kang, B. He, M. and Liu, B., Optimal control policies of pests for hybrid dynamical systems, In Abstract and Applied Analysis, **2013**(2013), Article ID 574541, Hindawi.

[103] Kang, B., Liu, B. and Tao, F., An integrated pest management model with dose-response effect of pesticides, Journal of Biological Systems, **26(01)**(2018), 59-86.

[104] Kaplan, J. L. and Yorke, J., Chaotic behavior of multidimensional difference equations, In functional differential equations and approximations of fixed points, Springer, Berlin, Heidelberg, **730**(1979), 204–227.

[105] Kawczynski, A. L. and Misiurewicz, M., Period adding phenomenon in 1D return maps, eitschrift fr Physikalische Chemie, **271(1)**(1990), 1037–1046.

[106] Khan, Q. J. A. and Al-Lawatia, M., Effect of the intensity of predator switching on the stability, Advances in Mathematical Sciences and Applications, **19(1)**(2009), 51–70.

[107] Khan, Q. J. A., Balakrishnan, E. and Wake, G. C., Analysis of a predator–prey system with predator switching, Bulletin of Mathematical Biology, **66(1)**(2004), 109–123.

[108] Khan, Q. J. A., Bhatt, B. S. and Jaju, R. P., Stability of a switching model with two habitats and a predator, Journal of the Physical society of Japan, **63(5)**(1994), 1995–2001.

[109] Khan, Q. J. A., Bhatt, B. S. and Jaju, R. P., Hopf bifurcation analysis of a predator–prey system involving switching, Journal of the Physical Society of Japan, **65(3)**(1996), 864–867.

[110] Khan, Q. J. A., Bhatt, B. S. and Jaju, R. P., Switching model with two habitats and a predator involving group defence, Journal of Nonlinear Mathematical Physics, **5(2)**(1998), 212–223.

[111] Khan, Q. J. A. and Jaju, R. P., Comparative study of two prey–predator switching models, Journal of the Physical Society of Japan, **68(4)**(1999), 1430–1435.

[112] Khan, Q. J. A., Krishnan, E. V. and Balakrishnan, E., Two-predator and two-prey species group defence model with switching effect, International Journal of Computational Bioscience, **1(1)**(2010), 69–78.

[113] Kocic, V. L., A note on the nonautonomous Beverton-Holt model, Journal of Difference Equations and Applications, **11(4-5)**(2005), 415–422.

[114] Kooyman, C., Bateman, R. P., Jrgen, L., Lomer, C. J., Ouambama, Z. and Thomas, M. B., Operational-scale application of entomopathogenic fungi for control of sahelian grasshoppers, Proceedings of the Royal Society of London B: Biological Sciences, **264(1381)**(1997), 541–546.

[115] KostoVa, T., Li. J. and Friedman, M., Two models for competition between age classes, Mathematical Biosciences, **157(1-2)**(1999), 65–89.

[116] Kot, M., *Elements of Mathematical Ecology*, Cambridge University Press, Cambridge, 2001.

[117] Kuznetsov, Y. A., *Elements of Applied Bifurcation Theory*, Springer Science and Business Media, **112**, 2013.

[118] Lakmeche, A. and Arino, O., Bifurcation of non trivial periodic solutions of impulsive differential equations arising chemotherapeutic treatment, Dynamics of continuous, Discrete and impulsive systems, **7(2)**(2000), 265–287.

[119] Lakshmanan, M. and Rajasekar, S., *Nonlinear Dynamics: Integrability, Chaos and Patterns*, Springer Science and Business Media, 2002.

[120] Laksmikantham, V., Bainov, D. D. and Simeonov, P. S., *Theory Of Impulsive Differential Equations*, World Scientific, Singapore, **6**, 1989.

[121] Lamberson, R. H., Persistence of structured populations, Natural Resource Modeling, **12(1)**(1999), 1–4.

[122] Lamberson, R. H., McKelvey, R., Noon, B. R. and Voss, C., A dynamic analysis of northern spotted owl viability in a fragmented forest landscape, Conservation Biology, **6(4)**(1992), 505–512.

[123] Li, B., Liu, S., Cui, J. A. and Li, J., A simple predator–prey population model with rich dynamics, Applied Sciences, **6(5)**(2016), 151.

[124] Li, J., Cai, L. and Li, Y., Stage-structured wild and sterile mosquito population models and their dynamics, Journal of Biological Dynamics, **11(1)**(2017), 70–101.

[125] Liang, J. H. and Tang, S. Y., Optimal dosage and economic threshold of multiple pesticide applications for pest control, Mathematical and Computer Modelling, **51(5-6)**(2010), 487–503.

[126] Liang, J., Tang, S. and Cheke, R. A., An integrated pest management model with delayed responses to pesticide applications and its threshold dynamics, Nonlinear Analysis: Real World Applications, **13(5)**(2012), 2352–2374.

[127] Liapounoff, A. M., *Probleme General de la Stabilite du Mouvement*, Annals of Mathematics Studies, **17**(1947).

[128] Liu, B., Chen, L. S. and Zhang, Y. J., The effects of impulsive toxicant input on a population in a polluted environment, Journal of Biological Systems, **11(03)**(2003), 265–274.

[129] Liu, B., Chen, L., and Zhang, Y., The dynamics of a prey-dependent consumption model concerning impulsive control strategy, Applied Mathematics and Computation, **169(1)**(2005), 305-320.

[130] Liu, B., Duan, Y. and Luan, S., Dynamics of an SI epidemic model with external effects in a polluted environment, Nonlinear Analysis: Real World Applications, **13(1)**(2012), 27–38.

[131] Liu, B. and Teng, Z., The effect of impulsive spraying pesticide on stage-structured population models with birth pulse, Journal of Biological Systems, **13(1)**(2005), 31–44.

[132] Liu, B., Teng, Z. and Chen, L., Analysis of a predator–prey model with Holling II functional response concerning impulsive control strategy, Journal of Computational and Applied Mathematics, **193(1)**(2006), 347–362.

[133] Liu, B., Xu, L. and Kang, B., Dynamics of a stage-structured pest control model in a polluted environment with pulse pollution input, Journal of Applied Mathematics, **2013**(2013), Article ID 678762.

[134] Liu, B., Zhang, L. and Zhang, Q., The effects of a single stage-structured population model with impulsive toxin input and time delays in a polluted environment, Applicable Analysis, **88(8)**(2009), 1143–1155.

[135] Liu, B. and Zhang, Q. L., Dynamics of a two-species Lotka–Volterra competition system in a polluted environment with pulse toxicant input, Applied Mathematics and Computation, **214(1)**(2009), 155–162.

[136] Liu, B., Zhang, Q. and Gao, Y., The dynamics of pest control pollution model with age structure and time delay, Applied Mathematics and Computation, **216(10)**(2010), 2814–2823.

[137] Liu, B., Zhang, Y. J. and Chen, L. S., Dynamics complexities of a Holling I predator–prey model concerning periodic biological and chemical control, Chaos, Solitons and Fractals, **22(1)**(2004), 123–134.

[138] Liu, B., Zhang, Y. and Chen, L., The dynamical behaviors of a Lotka–Volterra predator–prey model concerning integrated pest management, Nonlinear Analysis: Real World Applications, **6(2)**(2005), 227–243.

[139] Liu, C., Liu, T., Liu, L. and Liu, K., A new chaotic attractor, Chaos, Solitons and Fractals, **22(5)**(2004), 1031–1038.

[140] Liu, X. and Stechlinski, P., Pulse and constant control schemes for epidemic models with seasonality, Nonlinear Analaysis: Real World Applications, **12(2)**(2011), 931–946.

[141] Liu, X. and Wang Q., The method of Lyapunov functionals and exponential stability of impulsive systems with time delay, Nonlinear Analysis: Theory, Methods and Applications, **66(7)**(2007), 1465–1484.

[142] Liu, X. N. and Chen L. S., Complex dynamics of Holling type II Lotka–Volterra predator–prey system with impulsive perturbations on the predator, Chaos, Solitons and Fractals, **16(2)**(2003), 311–320.

[143] Liu, X. Z. and Ballinger, G., Continuous dependence on initial values for impulsive delay differential equations, Applied Mathematical Letters, **17(4)**(2004), 483–490.

[144] Liu, Z. and Chen, L., Periodic solution of a two-species competitive system with toxicant and birth pules, Chaos, Solitons and Fractals, **32(5)**(2007), 1703–1712.

[145] Liu, Z. and Tan, R., Impulsive harvesting and stocking in a Monod-Haldane functional response predatorprey system, Chaos, Solitons and Fractals, **34(2)**(2007), 454–464.

[146] Lou, J., Lou, Y. and Wu, J., Threshold virus dynamics with impulsive antiretroviral drug effects, Journal of Mathematical Biology, **65(4)**(2012), 623–652.

[147] Lu, Z. H., Chi, X. B. and Chen, L. S., Impulsive control strategies in biological control of pesticide, Theoretical Population Biology, **64(1)**(2003), 39–47.

[148] Ma, Yi, Liu, B. and Feng, W., Dynamics of a birth-pulse single-species model with restricted toxin input and pulse harvesting, Discrete Dynamics in Nature and Society, **2010**(2010), 1–20.

[149] Ma, Z., Yang, J. and Jiang, G., Impulsive control in a stage structure population model with birth pulses, Applied Mathematics and Computation, **217(7)**(2010), 3453–3460.

[150] May, R. M., Biological populations with nonoverlapping generations: stable points, stable cycles and chaos, Science, **186(4164)**(1974), 645–647.

[151] May, R. M., *Stability and Complexity in Model Ecosystems*, New Jersey Princeton University Press, Princeton, 1974.

[152] May, R. M. and Oster, G. F., Bifurcations and dynamic complexity in simple ecological models, The American Naturalist, **110(974)**(1976), 573–599.

[153] Mehrotra, K. N., Use of DDT and its environmental effects in India, In Proc Indian Natl Sci Acad B, **51**(1985), 169–184.

[154] Meng, X. and Chen, L., A stage-structured SI eco-epidemiological model with time delay and impulsive controlling, Journal of Systems Science and Complexity, **21(3)**(2008), 427–440.

[155] Meng, X., Chen, L. and Wu, B., A delay SIR epidemic model with pulse vaccination and incubation times, Nonlinear Analysis: Real World Applications, **11(1)**(2010), 88–98.

[156] Meng, X. and Li, Z., The dynamics of plant disease models with continuous and impulsive cultural control strategies, Journal of Theoretical Biology, **266(1)**(2010), 29–40.

[157] Metz, J. A. J. and Diekmann, O., *The Dynamics of Physiologically Structured Populations*, Lecture Notes in Biomathematics, Springer, Berlin, Heidelberg, New York, **68**, 1986.

[158] Mills, N. J. and Getz, W. M., Modelling the biological control of insect pests: a review of host-parasitoid models, Ecological Modelling, **92(2-3)**(1996), 121–143.

[159] Milman, V. D. and Myshkis, A. D., On the stability of motion in the presence of impulses, Sibirskii Mathematical Journal, **1(2)**(1960), 233–237.

[160] Minorsky, N., *Nonlinear Oscillations*, Princeton: Van Nostand, 1962.

[161] Misra, A. and Dubey, B., A ratio-dependent predator–prey model with delay and harvesting, Journal of Biological Systems, **18(2)**(2010), 437–453.

[162] Moussaoui, A., Effect of a toxicant on the dynamics of a spatial fishery, African Diaspora Journal of Mathematics, New Series, **10(2)**(2010), 122–134.

[163] Moussaoui, A., Bassaid, S., and Dads, E. H. A., The impact of water level fluctuations on a delayed prey–predator model, Nonlinear Analysis: Real World Applications, **21**(2015), 170–184.

[164] Moussaoui, A., Doanh, N. N. and Auger P., Analysis of a model describing stage-structured population dynamics using Hawk-Dove tactics, Africaine de la Recherche en Informatique et Mathematiques Appliquees, **20**(2015), 127–143.

[165] Murray, J. D., Lectures on nonlinear-differential-equation models in biology, Clarendon Press, Walton Street, Oxford, 1977.

[166] Murray, J. D., *Mathematical Biology I. An Introduction*, Springer-Verlag, NewYork, 2002.

[167] Myrberg, P. J., Sur l'iteration des polynomes reels quadratique, Journal de Mathematiques Pures et Appliquees, **41(9)**(1962), 339–351.

[168] Myrberg, P. J., Iteration der reellen polynome zweiten grades III, Annales Academia Scientiarum Fennica, **336(3)**(1963), 1–10.

[169] Nie, L., Peng, J., Teng, Z. and Hu, L., Existence and stability of periodic solution of a Lotka–Volterra predator–prey model with state dependent impulsive effects, Journal of Computational and Applied Mathematics, **224(2)**(2009), 544–555.

[170] Nundloll, S., Mailleret, L. and Grognard, F., Two models of interfering predators in impulsive biological control, Journal of Biological Dynamics, **4(1)**(2010), 102–114.

[171] Nusse, H. E. and York, J. A., *Dynamics: Numerical Explorations*, Springer Science and Business Media, Springer-Verlag, New York, **101**(1998).

[172] Panetta, J. C., A logistic model of periodic chemotherapy, Applied Mathematics Letters, **8(4)**(1995), 83–86.

[173] Panetta, J. C., A logistic model of periodic chemotherapy with drug resistance, Applied Mathematics Letters, **10(1)**(1996), 123–127.

[174] Panetta, J. C., A mathematical model of periodically pulsed chemotherapy: tumor recurrence and metastasis in a competition environment, Bulletion of Mathematical Biology, **58(3)**(1996), 425–447.

[175] Pang, G., Wang, F. and Chen, L., Extinction and permanence in delayed stage-structure predator–prey system with impulsive effects, Chaos, Solitons and Fractals, **39(5)**(2009), 2216–2224.

[176] Parker, F. D., Management of pest populations by manipulating densities of both host and parasites through periodic releases, In Biological Control, Springer, Boston, MA, (1971), 365–376.

[177] Parker, T. S. and Chua, L. O., *Practical Numerical Algorithms for Chaotic Systems*, Springer-Verlag, Newyork, 1989.

[178] Pei, Y., Ji, X. and Li, C., Pest regulation by means of continuous and impulsive nonlinear controls, Mathematical and Computer Modelling, **51(5-6)**(2010), 810–822.

[179] Pei, Y., Li, C., Chen, L. and Wang, C., Complex dynamics of one-prey multi-predator system with defensive ability of prey and impulsive biological control on predators, Advances in Complex Systems, **8(4)**(2005), 483–495.

[180] Perko, L., *Differential Equations and Dynamical System*, Springer Science and Business Media, **7**, 2013.

[181] Pimentel, D., Amounts of pesticides reaching target pests: environmental impacts and ethics, Journal of Agricultural and Environmental Ethics, **8(1)**(1995), 17–29.

[182] Pimentel, D., Estimated annual world pesticide use, in Facts and Figures, Rockefeller Foundation, New York, NY, USA, 1990.

[183] Qi, J. and Fu, X., Existence of limit cycles of impulsive differential equations with impulses at variable times, Nonlinear Analysis: Theory, Methods and Applications, **4(3)**(2001), 345–353.

[184] Rafikov, M., Balthazar, J. M. and Von Bremen, H. F., Mathematical modeling and control of population systems: application in biological pest control, Applied Mathematics and Computation, **200(2)**(2008), 557–573.

[185] Rafikov, M. and de Holanda Limeira, E., Mathematical modelling of the biological pest control of the sugarcane borer, International Journal of Computer Mathematics, **89(3)**(2012), 390–401.

[186] Ricker, W. E., *Handbook of Computation for Biological Statistics of Fish Populations*, Bulletin of the Fisheries Resource Board, Canada, Ottawa, **119**, 1958.

[187] Roberts, M. G. and Kao, R. R., The dynamics of an infectious disease in a population with birth pulses, Mathematical Biosciences, **149(1)**(1998), 23–36.

[188] Robinson, C., *Dynamical Systems: Stability, Symbolic Dynamics and Chaos.*, CRC Press, Boca Raton, 1995.

[189] Roy, P. K., Li, X. Z., Basiri, F. A., Datta, A. and Chowdhury, J., Effect of insecticide spraying on jatropha curcas plant to control mosaic virus: a mathematical study, Communications in Mathematical Biology and Neuroscience, **2015**(2015), 2052–2541.

[190] Ruberson, J., Nemoto, H. and Hirose, Y., Pesticides and conservation of natural enemies in pest management, In Conservation biological control, (1998), 207–220.

[191] Saleem, M. and Pandey, R. K., Switching in a stage structured predator–prey model: Unpredictable behavior of species, In Applications and Teaching of Mathematics for Engineers and Scientists (p.1 45), Allied New Delhi, 2002.

[192] Saleem, M., Sadiyal, A. H., Edi, P. and Arora, P. R., Evolutionarily stable strategies for defensive switching, Applied Mathematics and Computation, **177(2)**(2006), 697–713.

[193] Saleem, M., Tripathi, A. K. and Sadiyal, A. H., Coexistence of species in a defensive switching model, Mathematical Biosciences, **181(2)**(2003), 145–164.

[194] Samoilenko, A. M. and Perestyuk, N. A., *Impulsive Differential Equations*, World Scientific, Singapore, 1995.

[195] Scanlan, J. C., Grant, W. E., Hunter, D. M. and Milner R. J., Habitat and

environmental factors influencing the control of migratory locusts (Locusta migratoria) with an entomopathogenic fungus (Metarhizium anisopliae), Ecological Modelling, **136(2-3)** (2001), 223–236.

[196] Shi, R. and Chen, L., Staged-structured Lotka–Volterra predator–prey models for pest management, Applied Mathematics and Computation, **203(1)**(2008), 258–265.

[197] Shukla, J. B., Agrawal, A. K., Dubey, B. and Sinha, P., Existence and survival of two competing species in a polluted environment: A mathematical model, Journal of Biological Systems, **9(2)**(2001), 89–103.

[198] Shukla, J. B., Agrawal, A., Sinha, P. and Dubey, B., Modeling effects of primary and secondary toxicants on renewable resources, Natural Resource Modeling, **16(1)**(2003), 99–120.

[199] Shukla, J. B., Dubey, B. and Freedman, H. I., Effect of changing habitat on survival of species, Ecological Modelling, **87(1-3)**(1996), 205–216.

[200] Shukla, J. B., Sharma, S., Dubey, B. and Sinha, P., Modeling the Survival of a resource-dependent population: Effects of toxicants (pollutants) emitted from external sources as well as formed by its precursor, Nonlinear Analysis: Real World Applications, **10(1)**(2009), 54–70.

[201] Shulgin, B., Stone, L. and Agur, Z., Pulse vaccination strategy in the SIR epidemic model, Bulletin of Mathematical Biology, **60(6)**(1998), 1123–1148.

[202] Simeonov, P. S. and Bainov, D. D., Orbital stability of periodic solutions of autonomous systems with impulse effect, International Journal of Systems Science, **19(12)**(1988), 2561–2585.

[203] Singh, A. and Gakkhar, S., State-dependent impulsive control of a delayed prey–predator system, Dynamics of Continuous, Discrete and Impulsive Systems (Waterloo Press), **18** (2012), 231–249.

[204] Song, X., Hao, M. and Meng, X., A stage-structured predator–prey model with disturbing pulse and time delays, Applied Mathematical Modelling, **33(1)**(2009), 211–223.

[205] Speight, M. R., Kelly, P. M., Sterling, P. H. and Entwistle, P. F., Field application of a nuclear polyhedrosis virus against the Brown-tail moth, Euproctis chrysorrhoea (L.) (Lep., Lymantriidae), Journal of Applied Entomology, **113(1-5)**(1992), 295–306.

[206] Srinivasu P. D. V., Prasad, B. S. R. V. and Venkatesulu, M., Biological control through provision of additional food to predators: a theoretical study, Theoretical Population Biology, **72(1)**(2007), 111–120.

[207] Stern, V. M., Economic Thresholds, Annual review of entomology, **18(1)**(1973), 259–280.

[208] Sugie, J., Two-parameter bifurcation in a predator–prey system of Ivlev type, Journal of Mathematical Analysis and Applications, **217(2)**(1998), 349–371.

[209] Suttman, C. E. and Barrett, G. W., Effects of sevin on arthropods in an agricultural and an old-field plant community, Ecology, **60(3)**(1979), 628–641.

[210] Takeuchi, Y., *Global Dynamical Properties of Lotka-Voltera Systems*, World Scientific, Singapore, 1996.

[211] Takeuchi, Y. and Adachi, N., The existence of globally stable equilibria of ecosystems of the generalized Volterra type, Journal of Mathematical Biology, **10(4)**(1980), 401–415.

[212] Takeuchi, Y. and Adachi, N., Existence and bifurcation of stable equilibrium in two prey, one-predator communities, Bulletin of Mathematical Biology, **45(6)**(1983), 877–900.

[213] Takeuchi, Y., Adachi, N. and Tokumaru, H., Global stability of ecosystems of the generalized Volterra type, Mathematical Biosciences, **42(1-2)**(1978), 119–136.

[214] Tang, S. and Cheke, R. A., State-dependent impulsive models of integrated pest management (IPM) strategies and their dynamic consequences, Journal of Mathematical Biology, **50(3)**(2005), 257–292.

[215] Tang, S., Cheke, R. A. and Xiao, Y., Optimal implusive harvesting on non-autonomous Beverton-Holt difference equations, Nonlinear Analysis: Theory, Methods and Applications, **65(12)**(2006), 2311–2341.

[216] Tang, S. and Cheke, R. A., Models for integrated pest control and their biological implications, Mathematical Biosciences, **215(1)**(2008), 115–125.

[217] Tang, S. Y., Cheke, R. A. and Xiao Y. N., Effects of predator and prey dispersal on success or failure of biological control, Bulletin of Mathematical Biology, **71(8)**(2009), 2025–2047.

[218] Tang, S. and Chen, L., Density-dependent birth rate, birth pulses and their population dynamic consequences, Journal of Mathematical Biology, **44(2)**(2002), 185–199.

[219] Tang, S. Y. and Chen, L. S., Multiple attractors in stage-structured population models with birth pulses, Bulletin of Mathematical Biology, **65(3)**(2003), 479–495.

[220] Tang, S. Y. and Chen, L. S., The effect of seasonal harvesting on stage-structured population models, Journal of Mathematical Biology, **48(4)**(2004), 357–374.

[221] Tang, S., Liang, J., Tan, Y. and Cheke, R. A., Threshold conditions for integrated pest management models with pesticides that have residual effects, Journal of Mathematical Biology, **66(1-2)**(2013), 1–35.

[222] Tang, S., Tang, G. and Cheke, R. A., Optimum timing for integrated pest management: modelling rates of pesticide application and natural enemy releases, Journal of Theoretical Biology, **264(2)**(2010), 623–638.

[223] Tang, S., Xiao, Y., Chen, L. and Cheke, R. A., Integrated pest management models and their dynamical behaviour, Bulletin of Mathematical Biology, **67(1)**(2005), 115–135.

[224] Van den Bosch, R., *The Pesticide Conspiracy*, Doubleday and co, Garden City, NY, 1978.

[225] Van Lenteren, J. C., *Integrated Pest Management in Protected Crops*, In Integrated Pest Management, Chapman and Hall, London, 1995.

[226] Van Lenteren, J. C., *Environmental Manipulation Advantageous to Natural Enemies of Pests*, In: Delucchi, V.(Ed.), Integrated Pest Management,Parasitis, Geneva, (1987), 123–166.

[227] Van Lenteren, J. C., Success in biological control of arthropods by augmentation of natural enemies, In Biological control: measures of success, Springer, Dordrecht, (2000), 77–103.

[228] Van Lenteren, J. C. and Woets, J. V., Biological and integrated pest control in greenhouses, Annual review of Entomology, **33(1)**(1988), 239–269.

[229] Wang, F., Pang, G. and Chen, L., Qualitative analysis and applications of a kind of state-dependent impulsive differential equations, Journal of Computational and Applied Mathematics, **216(1)**(2008), 279–296.

[230] Ward, D. J. and Wilson, R. E., Pesticide effects on decomposition and recycling of Avena litter in a monoculture ecosystem, American Midland Naturalist, **90**(1973), 266–276.

[231] Wiggins, S., *Introduction to Applied Nonlinear Dynamical Systems and Chaos*, Texts in Applied Mathematics 2, Springer-Verlag, New York, 1990.

[232] Xiao, D., and Ruan, S., Global analysis in a predator–prey system with nonmonotonic functional response, SIAM Journal on Applied Mathematics, **61(4)**(2001), 1445–1472.

[233] Xiao, Y. N. and Van Den Bosch, F., The dynamics of an eco-epidemic model with biological control, Ecological Modelling, **168(1-2)**(2003), 203–214.

[234] Xie, Y., Yuan, Z. and Wang, L., Dynamic analysis of pest control model with population dispersal in two patches and impulsive effect, Journal of Computational Science, **5(5)**(2014), 685–695.

[235] Yang, X., Jin, Z. and Xue, Y., Weak average persistence and extinction of a predator–prey system in a polluted environment with impulsive toxicant input, Chaos, Solitons and Fractals, **31(3)**(2007), 726–735.

[236] Zeng, G. Z., Chen, L. S. and Sun, L. H., Complexity of an SIR epidemic dynamics model with impulsive vaccination control, Chaos, Solitons and Fractals, **26(2)**(2005), 495–505.

[237] Zeng, G., Wang, F. and Nieto, J. J., Complexity of delayed predator–prey model with impulsive harvest and Holling type II functional response, Advances in Complex Systems, **11(01)**(2008), 77–97.

[238] Zhang, H., Chen, L. and Nieto, J. J., A delayed epidemic model with stage-structure and pulses for pest management strategy, Nonlinear Analysis: Real World Applications, **9(4)**(2008), 1714–1726.

[239] Zhang, H., Georgescu, P. and Chen, L., On the impulsive controllability and bifurcation of a predator-pest model of IPM, BioSystems, **93(3)**(2008), 151–171.

[240] Zhang, H., Jiao, J. and Chen, L., Pest management through continuous and impulsive control strategies, Biosystems, **90(2)**(2007), 350–61.

[241] Zhang, T., Meng, X., Song, Y. and Zhang, T., A stage-structured predator–prey SI model with disease in the prey and impulsive effects, Mathematical Modelling and Analysis, **18(4)**(2013), 505–528.

[242] Zhang, W., Discrete Dynamical Systems, Bifurcations and Chaos in Economics, **204**(2006), Elsevier.

[243] Zhao, Z., Zhang, X. and Chen, L., The effect of pulsed harvesting policy on the inshore-offshore fishery model with the impulsive diffusion, Nonlinear Dynamics, **63(4)**(2011), 537–545.

[244] Zhou, J., Xiang, L. and Liu, Z., Synchronization in complex delayed dynamical networks with impulsive effects, Physica A: Statistical Mechanics and Its Applications, **384(2)**(2007), 684–692.

List of Publications

Paper Published in Journal:

1. **Gakkhar, S. and Goel, A.**, An Impulsive Stage-Structured Pest Control Model Using Pesticide Spray Synchronized with Birth Pulse, Dynamics of Continuous, Discrete and Impulsive Systems Series B: Applications and Algorithms, **24**(2017), 309–333.

Papers Presented in International Proceedings:

1. **Goel, A. and Gakkhar, S.**, Dynamic Complexities in A Pest Control Model with Birth Pulse, Chapter in Applied Analysis in Biological and Physical Sciences, Volume 186, Springer Proceedings in Mathematics and Statistics, pp 83-97, Doi:10.1007/978-81-322-3640-5, International Conference on Recent Advances in Mathematical Biology, Application and Analysis (ICMBAA-2015), Aligarh Muslim University.

2. **Goel, A. and Gakkhar, S.**, Dynamic Complexities in A Pest Control Model with Birth Pulse and Harvesting presented, in AIP Conference Proceedings, Volume 1723, Issue 1, DOI 10.1063/1.4945068, Symposium on Biomathematics (SYMOMATH-2015), Institut of Teknologi, Bandung, Indonesia.

3. **Goel, A. and Gakkhar, S.**, A Single Species Model with Birth Pulse and Impulsive Toxin Input, Global Science and Technology Forum (GSTF), ISSN 2251-1911, pp 205-211, DOI: 10.5176/2251-1911 CMCGS16.23, 5th Annual International Conference on Computational Mathematics, Computational Geometry

and Statistics (CMCGS-2016), Singapore.

4. **Goel, A. and Gakkhar, S.**, A Stage-Structured Pest Control Model with Chemical Control that have Residual Effects, 21st International Conference of International Academy of Physical Sciences (CONIAPS XI-2017), Guru Jambheswar University of Science and Technology, Hisar. (submitted)